International PhD program in Cardiovascular Pathophysiology and Therapeutics – CardioPaTh

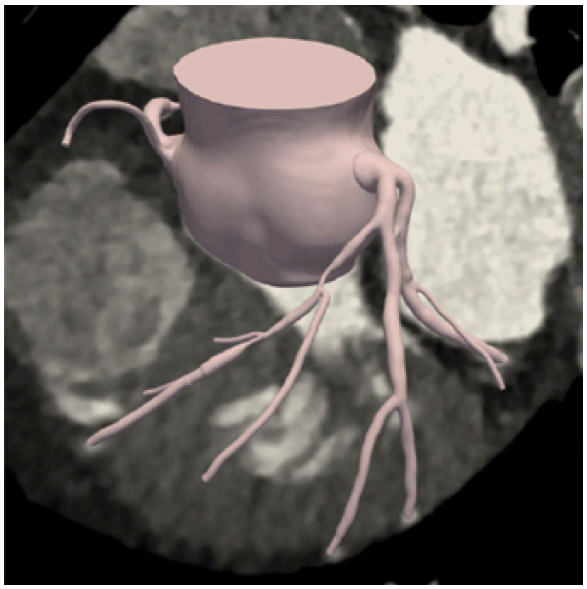

Coronary physiology-guided revascularization: Paving the future for ischemia-driven coronary treatment

PhD Thesis

Jeroen Sonck, MD

Coronary physiology-guided revascularization: Paving the future for ischemia-driven coronary treatment

Jeroen Sonck, MD

28th of May 1978
Dendermonde, Belgium

Promotor: Prof. Emanuele Barbato

Cardiovascular Center OLV Aalst, OLV Clinic, Aalst, Belgium
University Federico II of Naples, Faculty of Medicine, Naples, Italy

Naples, 10 Jan 2022, University Federico II of Naples, Faculty of Medicine, Via Pansini n. 5, 80131 Naples, Italy

Table of content

- Graft patency and progression of coronary artery disease after CABG assessed by angiography-derived fractional flow reserve.
- Vessel Fractional Flow Reserve and Graft Vasculopathy in Heart Transplant Recipients
- Risk of Myocardial Infarction based on Endothelial Shear Stress Analysis Using Coronary Angiography

Chapter 5: Redefining the patterns of coronary artery disease

- Impact of Coronary Remodeling on Fractional Flow Reserve
- Motorized fractional flow reserve pullback: Accuracy and reproducibility
- Measurement of Hyperemic Pullback Pressure Gradients to Characterize Patterns of Coronary Atherosclerosis
- Duration of Hyperemia with Intracoronary Administration of Papaverine
- Development, Validation, and Reproducibility of Pullback Pressure Gradient (PPG) derived from Manual Fractional Flow Reserve Pullbacks
- Hyperemic hemodynamic characteristics of serial coronary lesions assessed by Pullback Pressure Gradients
- Mismatch between the anatomical and functional extent of coronary artery disease
- Invasive Coronary Physiology After Stent Implantation: Another Step Toward Precision Medicine

Chapter 6: FFR_{CT}: Non-invasive Fractional Flow Reserve derived from coronary CT angiography for treatment planning

- Feasibility of planning coronary artery bypass grafting based only on coronary computed tomography angiography and CT-derived fractional flow reserve: a pilot survey of the surgeons involved in the randomized SYNTAX III Revolution trial
- Evaluation of epicardial coronary resistance using computed tomography angiography: A proof of concept
- Rationale and Design of the Precise PCI Plan (P3) Study: Prospective evaluation of a virtual CT-based percutaneous intervention planner
- Clinical Validation of a Virtual Planner for Coronary Interventions Based on Coronary CT Angiography and Blood Flow Simulations
- Expert Recommendations for Assessing Fractional Flow Reserve after Percutaneous Coronary Interventions

Chapter 7: CT-guided percutaneous coronary interventions

- State of the art paper: Implementing coronary computed tomography angiography in the catheterization laboratory
- Pre-procedural Planning of Coronary Revascularization by Cardiac-CT: An Expert Consensus Document of the Society of Cardiovascular Computed Tomography

General introduction and outline of the thesis

Outline of the thesis

Introduction

Until today, the conundrum of a comprehensive and precise diagnosis of the hemodynamic significance of coronary artery disease (CAD) remains intricate despite scientific advances in the non-invasive and invasive evaluation of atherosclerosis. For decades, patients were referred for invasive assessment of presumed CAD following a non-invasive functional assessment. Exercise stress testing, thallium scintigraphy and dobutamine stress echocardiography but also positron electron tomography (PET) has been used to determine the functional impact of CAD as the decision to perform revascularization procedures should be based not only on the coronary anatomy but also on the hemodynamic impact of a lesion[1]. In 1993, the concept of fractional flow reserve (FFR) was introduced by Pijls and De Bruyne[2]. This index performed well as compared with standard non-invasive tests for myocardial ischemia[3]. FFR is defined as the maximal blood flow to the myocardium in the presence of a stenosis in the supplying coronary artery, divided by the normal maximal flow in the same distribution assuming an absence of stenosis. As such, this invasive index represents the fraction of the normal maximal myocardial flow that can be achieved despite the coronary stenosis[4]. Both the DEFER and FAME trials have suggested that using an FFR cut-off of 0.75-0.80 could identify the patient benefiting from percutaneous revascularization[5,6]. The long-term follow-up date of the FAME II trial confirmed that an initial FFR-guided PCI strategy was associated with a significantly lower rate of the primary composite end point of death, myocardial infarction or urgent revascularization at 5 years than medical therapy alone[7]. Nowadays, FFR has been adopted by the guidelines as the gold standard to select patients for revascularization[8].

An FFR measurement comprises a pressure wire introduction in the distal coronary bed and the use of a hyperemic agent, mostly intravenous adenosine. FFR entails a single-point, distal coronary pressure value[9]. The measured pressure losses in the coronary arteries ensue due to viscous friction and flow separation. The contribution of each mechanism is highly dependent on patient-specific coronary geometries. Mild reductions in luminal area modulated by lesion length have shown to reduce coronary pressures distal to an epicardial stenosis. Lesion features affecting laminar flow conditions also contribute to pressure losses[10,11]. As such, 2 comparable FFR values could be the resultant of distinct pressure loss patterns along the coronary vessel, i.e., focal or diffuse pressure gradients. Although not routinely assessed, the

identification of functional focal and diffuse CAD patterns is of utmost importance for decision making about revascularization. Patients with focal disease have a more severe reduction in myocardial perfusion, lower FFR, and higher trans-stenotic gradients[12,13]. These features have also been associated with plaque vulnerability and a worse prognosis[14]. Conversely, patient with diffuse disease have relatively higher FFR values and lower plaque stress[13,14]. Furthermore, treatment options differ in their ability to reestablish epicardial conductance. PCI with stent implantation is a focal treatment and despite the clinical benefit observed with FFR-guided PCI, one-third of the patients remain with a suboptimal post-PCI FFR, which has been associated with major adverse cardiac events[7,15]. Indeed, in focal CAD, PCI has the potential to restore epicardial conductance and relieves ischemia. In contrast, PCI in cases of diffuse CAD results in a minor improvement in epicardial conductance and low post-PCI FFR[16]. As such, the conundrum of a comprehensive and precise diagnosis of the hemodynamic significance of coronary artery disease (CAD) entails a more detailed assessment of the distribution and hemodynamic consequences of atherosclerosis. This thesis aims at enhancing current available technologies and introduces novel tools for ischemia-driven coronary revascularization.

From FFR pullbacks to PPG

Based on coronary angiograms, different definitions have been proposed aiming at differentiating diffuse and focal CAD[17–19]. However, assessing the pattern of atherosclerosis using angiography is often equivocal and has low interobserver reproducibility[19]. Moreover, even in apparent normal coronaries, intravascular ultrasound has demonstrated diffuse atherosclerosis indicating that visual assessment of the severity of CAD is misleading[20].
As such, an alternative approach to assess the severity and functional pattern of CAD could be based on coronary physiology combined with intracoronary pressure pullbacks. Using FFR, this is performed during prolonged adenosine infusions allowing for motorized or manual pressure wire withdraw[9]. These FFR pullback curves depict the distribution of epicardial resistance and expose the functional pattern of CAD. As with the interpretation of DS, the visual interpretation of the computed pullback curves proves often debatable[19]. Consequently, it appeared of interest for the community to develop a metric that objectively quantifies the functional pattern of CAD: focal or diffuse. The Pullback Pressure Gradient (PPG) (chapter 5), derived from FFR pressure pullbacks, describes the spatial contribution of the atherosclerotic process to the overall pressure loss as measured by a single-point, distal FFR. The PPG incorporates the magnitude and extension of pressure losses providing a continuous

metric from 0 to 1; values close to 0 represent diffuse CAD, whereas values close to 1 represent focal CAD. As such, after the confirmation of the hemodynamic significance of the atherosclerosis by single-point distal FFR, the resulting PPG after pressure wire withdraw informs about the appropriateness of PCI. Indeed, PPG has been shown to predict the degree of functional revascularization, bearing the potential to enhance patient selection for PCI and improve clinical outcomes. Higher PPG at baseline results in higher post-PCI FFR. Conversely, PCI in patients with a low PPG results in lower post-PCI FFR (Sonck J, EuroPCR 2020). Furthermore, patients with a high PPG are often free from angina after the procedure, whereas patients with a low PPG have a higher rate of recurrent angina after PCI (Collet C, EuroPCR 2021). Subsequently, it can be hypothesized that patients with a high PPG have a better clinical prognosis than patients with a low PPG. This hypothesis is being tested in the ongoing prospective evaluation of the impact of the PPG index on clinical decision-making and outcomes in the "PPG Global Registry" (NCT04789317).

To start, the PPG concept was investigated and developed using motorized pullbacks using an adapted IVUS pullback machine with a wire withdraw speed of 1 mm per second. For this, we primarily assessed the accuracy and reproducibility of motorized FFR pullbacks (chapter 5). Automated pullback allowed for a standardization of the pressure-length relationship for co-registration purposes. This proved instrumental for later comparison with non-invasive FFR pullbacks derived from coronary computed tomography scan (FFR_{CT}) described in chapter 6.

In conjunction with this groundwork, we focused on 2 additional aspects of the invasive pullback procedure to allow for the potential adoption of the PPG in a non-research setting in the catheterization laboratory (chapter 5). Indeed, motorized pullbacks are cumbersome and time demanding. First, adenosine is associated with patient discomfort and potential adverse effects e.g. transient AV block[21]. Also, during long adenosine infusions unstable hyperemia could hamper correct pressure analysis for FFR and PPG evaluation[22]. We re-introduced the use of intra-coronary papaverine to achieve hyperemia[23,24]. We evaluated the vessel-specific dose–response and steady hyperemic state duration stratified by severity of coronary artery disease during papaverine induced hyperemia. Intracoronary administration of papaverine proved to provide a rapid onset hyperemia with minimal variability and a duration of steady-state sufficient for pullback maneuvers. This allowed for the switch from motorized towards manual FFR pullbacks. For this, the initial PPG equation was adapted to allow for an online PPG calculation derived from manual pullbacks. The accuracy of manual PPG and both intra- and inter-operator reproducibility are described in a separate paper. As a result, the PPG is

now available online in the catheterization laboratory and can be derived from a 20-40 seconds manual FFR pullback.

Concurrently, the feasibility to distinguish focal from diffuse CAD in serial lesions or tandem disease was investigated. This was motivated by the cross-talk between stenoses within the same coronary artery that makes the prediction of the functional contribution of each lesion challenging. We analyzed in tandem disease if FFR pullback tracings with PPG would allow for a quantitative functional evaluation useful to assess the appropriateness of PCI and to guide percutaneous revascularization strategy.

Functional-anatomical mismatch

In the FAME study, more than one-third of lesions with an angiographic 50% to 70% diameter stenosis demonstrated an FFR ≤0.80 whereas one-fifth of lesions with a 71% to 90% angiographic diameter stenosis demonstrated an FFR > 0.80[25]. The uncoupled relationship between anatomy and physiology is widely recognized[26].

We developed another approach to predict the response to PCI by quantifying the extent of functional CAD from FFR pullbacks. With this method, the length of functional disease is computed based on an automated algorithm classifying the FFR curve segments as healthy or diseased. This approach may be less vulnerable to artefacts in the pullback curves compared to the application of a threshold. The difference between the anatomical, herein QCA and OCT, and the functional length of CAD was defined as Functional Anatomical Mismatch (FAM). Two distinct phenotypes are then identified: (1) functional disease circumscribed within the anatomical defined lesion (i.e., FAM > 0), and (2) functional disease extending beyond the anatomical defined lesion (FAM < 0). A positive FAM represents focal CAD where the functional length of disease is restricted to the anatomical length, whereas a negative FAM value identifies the presence of functional disease outside the anatomical lesion. In cases with FAM >0, PCI restores epicardial conductance, results in higher post-PCI FFR, increases the likelihood of relieving patients from angina and is associated with improved clinical outcomes. In contrast, in patients with functional diffuse disease (FAM <0), PCI results in minor improvement in vessel physiology, low post-PCI FFR and higher likelihood of persistent angina[27]. Comparable to PPG, also the FAM concept could aid in enhancing ischemia-driven revascularization. This concept of Functional Anatomical Mismatch is described in chapter 5.

CCTA and FFR_{CT} for diagnosis, decision-making and percutaneous treatment planning

Technological advances in the field of coronary computed tomography angiography (CCTA) have improved the non-invasive evaluation of coronary atherosclerosis. In the SCOT-HEART trial, the use of CCTA to detect CAD has proven to tailor patient management and as such impact on patient outcomes[28,29]. Subsequently, CCTA has evolved from a tool to exclude coronary artery disease to a tool detecting atherosclerosis in an early phase, assessing for the presence of obstructive disease, and risk stratifying patients based on plaque characteristics[30–33]. CCTA has the unique opportunity to provide detailed insights in the anatomical distribution of the pattern of CAD comparable to intra-vascular imaging[34,35]. Meanwhile, fractional flow reserve derived from coronary CT angiography (FFR_{CT}) has proven to correlate well with its non-invasive and invasive counterparts[36,37]. Initially, our research focused on the use of CCTA and FFR_{CT} in the diagnostic process (ADVANCE FFR_{CT} registry in chapter 1) and heart team decision-making between PCI and coronary artery bypass grafting (CABG) in multi-vessel disease (SYNTAX III Revolution trial in chapter 2). Most importantly, the 1-year outcomes from the ADVANCE FFR_{CT} Registry have shown low rates of events, with less revascularization and a trend toward lower MACE and significantly lower cardiovascular death or MI in patients with a negative FFR_{CT} compared with patients with abnormal FFR_{CT} values. In the SYNTAX III trial, in patients with left main or three-vessel coronary artery disease, a heart team treatment decision-making based on coronary CTA showed high agreement with the decision derived from conventional coronary angiography suggesting the potential feasibility of a treatment decision-making and planning based solely on this non-invasive imaging modality and clinical information. These results have encouraged us to explore other potential applications of FFR_{CT} beyond diagnosing lesion significance alone or modulating only the decision between PCI or CABG.

FFR_{CT} applies computational flow dynamics on a patient-specific coronary geometric model[38]. Subsequently, a potential advantage of the FFR_{CT} technology is that a FFR value can be derived at any point of the coronary tree and vessel. As such, FFR_{CT} could be instrumental in providing insights in the assessment of pressure loss distribution when virtual FFR_{CT} pullbacks are reconstructed from the patient-specific hemodynamic map. This could identify CAD patterns, focal or diffuse, non-invasively and comparable to invasive FFR pullbacks. For this, we initially assessed the feasibility to derive virtual pullbacks from the FFR_{CT} model with motorized invasive FFR pullbacks, developed for the PPG (chapter 5) as a reference. Following this step, we expanded our research to a novel FFR_{CT}-based technology that could help in predicting the effect of percutaneous revascularization. The FFR_{CT} Planner

(HeartFlow, Inc., Redwood City, CA) is a tool able to immediately recompute FFR_{CT} values after opening coronary stenoses. The Planner leverages the results of multiple simulations and reduced order modeling to instantly calculate a FFR_{CT} value in the desired lumen configuration[39]. This provides the benefit of anticipating the effect of PCI influencing treatment planning prior to the catheterization laboratory. As such, FFR_{CT} and the Planner could provide hemodynamic cognizance in the pre-catheterization setting, further tailoring decision-making and percutaneous treatment planning without the need for pressure wire interrogation nor hemodynamic evaluation using invasive FFR pullbacks. This could be especially instrumental in simulating PCI in focal vs. diffuse CAD and in tandem disease[39,40]. The FFR_{CT} Planner, was validated in the international prospective, multi-center and core lab controlled Precise PCI trial (P^3 trial). The primary objective was the agreement between the predicted post-PCI FFR by FFR_{CT} Planner and measured post-PCI invasive FFR as a reference. The rationale and results of the Precise PCI trial are described in chapter 6.

FFR_{CT} for surgical treatment planning?

CABG remains the standard-of-care therapy for complex and extensive CAD[41,42]. Moreover, when percutaneous revascularization is expected to result in futile functional restoration of flow (e.g., diffuse CAD), medical therapy or surgical CABG could demonstrate more appropriate. In the SYNTAX III Revolution trial, the addition of FFR_{CT} altered treatment recommendation in 7 percent of cases without the need for a demanding three-vessel FFR interrogation during invasive coronary angiography. In multi-vessel coronary artery disease, the availability of a combined anatomic and comprehensive hemodynamic FFR_{CT} map in all epicardial branches was anticipated to further enhance surgical treatment recommendation and planning. Indeed, FFR_{CT} can identify which vessels should require a bypass and CCTA allows for the identification of a normal, graftable landing zone for CABG. As a result, we studied the theoretical feasibility of surgical decision-making and treatment planning based on non-invasive imaging only. This could render the FFR_{CT} technology a potential game-changer for non-invasive decision-making and treatment planning in complex CAD. Based on our presented analysis, the FAST-TRACK CABG study is currently recruiting patients investigating if CABG based on sole CCTA and FFR_{CT} is feasible and safe[43]. The paper on surgical treatment planning is presented in chapter 6. Our perspective on the use of CT and FFR_{CT} for CABG planning is part of the Expert Consensus Document of the SCCT on "Pre-procedural Planning of Coronary Revascularization by Cardiac-CT" presented in chapter 7.

Coronary plaque assessment by CCTA

Recent developments in CT scan technology have improved its spatial resolution. Previously, it was shown that CCTA could reliably evaluate plaque burden and volume[34,44]. In a first collaboration, we have shown that nowadays improved plaque volume assessment can be achieved with reduced radiation exposure by modern CT scans. Assessment of plaque composition is as important and can influence both the PCI technique as prognosis. Indeed, severe coronary calcifications often lead to stent under-expansions. High calcium volume, thickness, arc and length have been associated with stent under-expansion[45]. We evaluated the degree of concordance upon calcium volume measurement between coronary CTA and OCT in patients undergoing PCI. Both papers addressing the evaluation of coronary plaque by CCTA are bundled in chapter 3.

From plaque to hemodynamics

Plaque composition, severity and extent determine its hemodynamic effect[46]. The identification of the anatomical and functional pattern of CAD by different techniques has renewed interest in resulting trans-lesional pressure gradients, flow phenomena and its association with plaque progression and rupture. Indeed, the risk of plaque rupture is the resultant of plaque resistance, depending on plaque composition, and forces applied on the plaque e.g. wall shear stress and axial plaque stress[10]. In the EMERALD trial, a higher trans-lesional gradient was associated with increased risk for plaque rupture and ACS[14]. In our paper addressing future culprits for myocardial infarction (chapter 4), we investigated the influence of plaque stress on the risk of future ACS. The combination of luminal stenosis, pressure gradients and wall shear stress (WSS) predicted the occurrence of MI. A WSS-based descriptor that accounts for the variation in the contraction and expansion action of shear forces on the endothelium along the cardiac cycle, i.e., TSVI, improved the discrimination of lesions prone to rupture. Novel herein, is the fact that the WSS information is derived from conventional angiography using a QCA-like software. This brings the calculation of WSS closer to clinicians and may increase the feasibility of adopting WSS analysis in routine clinical practice. Comparably, FFR_{CT}, able to discriminate between focal and diffuse CAD, comprises trans-lesional pressure gradients and the forces on the plaque derived from computational flow dynamics. Combined with the identification of adverse plaque characteristics on CCTA, FFR_{CT} has as such the potential to further risk stratify patients[47–49]. This is currently investigated in the EMERALD II trial.

The conundrum of post-PCI FFR

The PPG and HeartFlow Planner have demonstrated to predict the degree of functional revascularization. Higher PPG at baseline results in higher post-PCI FFR (chapter 5). Also, in the Precise PCI Plan trial we validated the HeartFlow Planner that predicts post-PCI FFR (chapter 6). Post-PCI FFR has been proposed as a clinical target to optimize PCI and as a surrogate endpoint of clinical outcomes[15,27,50–55]. Post-PCI FFR measured in the left anterior descending (LAD) artery has been reported to be lower than in non-LAD vessels[56]. This finding was also observed during the P^3 trial where available OCT and FFR pullbacks provided mechanistic insights in the longitudinal FFR decrease in the coronaries. This triggered a systematic review of individual patient-level data obtained from four randomized clinical trials and five observational studies encompassing 2,760 patients and 3,336 vessels with post-PCI FFR measurements. We envisaged to confirm this difference in post-PCI FFR observed between LAD and non-LAD and to assess the predictive power of post-PCI FFR for adverse events. Next, we tried to identify the mechanisms leading to low post-PCI FFR. We studied the hydrostatic effects during pressure wire evaluation of FFR (microtip sensor wire vs. fluid-filled pressure wire) and the effect of myocardial mass and vascular volume (V/M ratio). We suggested also an influence of the pre-PCI pressure pullback pattern (captured by the PPG) and the post-PCI pullback pattern. Indeed, in the PPG and P^3 cohorts, PCI of focal CAD leads to higher functional gain as compared to percutaneous treatment of diffuse CAD. Insufficient data on pullback patterns before PCI are available to unequivocally confirm its contribution to a lower post-PCI FFR. Post-PCI in the LAD, after optimal stent implantation and even in absence of residual atherosclerotic disease, the FFR pullback curve shows a downslope that is statistically different than of non-LAD. In contrast, the pattern of the post-PCI FFR pullback curve in non-LAD vessels exhibits a flat slope profile leading to higher distal FFR values. Currently, there is insufficient information available from OCT and IVUS post-PCI to retain this as a clear-cut explanation for the observed lower post-PCI FFR. For now, only the hydrostatic effect and the volume to mass ratio are considered to influence post-PCI FFR. Minor hydrostatic effect produces both pre- and post-PCI a slightly lower FFR in the LAD. Vessels that supply a larger amount of myocardium will experience greater pressure loss for the same anatomic degree of stenosis, and also greater viscous pressure loss along normal vessel segments inducing lower FFR. These concepts are described in the "Expert Recommendations for Assessing Fractional Flow Reserve after Percutaneous Coronary Interventions" in chapter 6, putting into perspective the interpretation and prediction of post-PCI FFR.

CT-guided PCI

In the last chapter, a novel concept of "CT-guided PCI" is described. There is an increasing awareness of the potential of CCTA to help plan and guide coronary interventions in the catheterization laboratory. The first part of the state-of-the-art paper focusses on diagnostic novelties and CT-based decision-making regarding treatment strategy. For this, we focus on current evidence in luminal assessment, plaque characterization, the evaluation of lesion significance and in treatment planning (PCI vs. CABG) integrating data from chapters 1, 2, 3 and 6. Part two of the paper focuses on the use of CCTA for catheterization laboratory preparation and the most novel part 3 introduces the online PCI guidance.

For this purpose, we developed a novel hardware and software solution to integrate the comprehensive CAD assessment by CCTA in the diagnostics and therapeutic workflow of the invasive coronary angiography and percutaneous coronary interventions. Reconstructions of the coronary circulation derived from CCTA provide a 3D view of the coronary tree and plaque components during conventional angiography procedures. A manufacturer-independent approach was accomplished by attaching an external sensor, called an inertial measurement unit to the C-arm. The inertial measurement unit is connected to a Raspberry Pi, which continuously communicates the sensor's—and therefore, also the C-arm's—orientation with the 3D visualization software. Guidance of PCI based on the CT-guided PCI principles follows the same flow as with intravascular imaging (e.g., IVUS or OCT) including the evaluation of plaque characteristics, composition, and extension[57]. The continuous display of CCTA and invasive angiography allows also the use of anatomic landmarks to visually co-register both modalities. Currently, we are testing this novel approach in a randomized trial: The Precise Procedural PCI Planning trial (P4) should prove that CT-guided PCI is non-inferior compared to IVUS-guided PCI.

Additionally, chapter 7 contains an extract from the chapter written in the "Expert Consensus Document of the SCCT on Pre-procedural Planning of Coronary Revascularization by Cardiac-CT". This document aims to expound the key technical aspects of CCTA and to review the available data that support the role of CCTA, FFR_{CT} and stress myocardial CT-perfusion in the preprocedural and intraprocedural planning and guidance of myocardial revascularization interventions.

Chapter 1: Clinical use of coronary CT angiography and non-invasive Fractional Flow Reserve derived from coronary CT angiography for the diagnosis of coronary artery disease

Chapter introduction

In the first chapter, we focus on the use of FFR_{CT} for the diagnosis of CAD. Following the advent of CT-derived FFR, CTA evolved from a tool to exclude CAD to a test able to identify hemodynamic significant atherosclerosis[38]. Initially, FFR_{CT} was validated against invasive FFR in the DISCOVER-FLOW, DeFACTO and NXT studies[36,58,59]. The Assessing Diagnostic Value of Non-invasive FFR_{CT} in Coronary Care (ADVANCE) registry was designed to observe the 'real-world' utility and impact of using FFR_{CT} in a broad variety of healthcare settings, geographical regions, and patient populations by examining how the incremental information of FFR_{CT} on top of the anatomical information from conventional coronary CT angiography altered diagnosis and clinical decision-making, patient management, clinical outcomes and resource utilization.

The main paper was followed by sub-analyses investigating the 1-year impact on medical practice and clinical outcomes of FFR_{CT}, the temporal changes in FFR_{CT}-guided management of CAD and the clinical utility of FFR_{CT} stratified by age. In the paper on the impact of non-invasive anatomical testing on optimal medical prescription in patients with suspected coronary artery disease, we compared the rate of statins prescription in a patient cohort assessed either with coronary CTA or exercise testing and evaluated the agreement on medication prescriptions. The intensification of preventive therapy, also observed in the SCOT-HEART trial, has the potential to improve patient prognosis.

Real-world Clinical Utility and Impact on Clinical Decision-making of Coronary Computed Tomography Angiography-derived Fractional Flow Reserve: Lessons from the ADVANCE Registry

Coronary CT angiography has emerged as a non-invasive tool for the diagnosis of CAD and treatment planning in patients with suspected coronary artery disease. Initially, the guidelines suggested a pivotal role for coronary CT angiography to exclude the presence of CAD. Recently its role has been expanded to the initial test strategy to diagnose CAD in symptomatic patients in whom obstructive CAD cannot be excluded by clinical assessment alone (Ia)[42]. However, the diagnostic accuracy of coronary CT angiography to discriminate significant from non-flow limiting CAD is limited[60]. Recent evolutions in coronary CT angiography and CT-derived fractional flow reserve (FFR_{CT}) have broadened the use of coronary CT to the assessment of lesion-specific ischemia. The DISCOVER-FLOW, DeFACTO and NXT studies have shown a higher correlation between CT-derived FFR and invasive FFR increasing mostly the specificity of coronary CT angiography to diagnose physiologically significant CAD[36,58,59]. The combined high sensitivity and enhanced specificity of coronary CT angiography and additional CT-derived fractional flow reserve extended the use from the initial binary "CAD vs. no CAD" momentum to the diagnostic and treatment planning indications. The Assessing Diagnostic Value of Non-invasive FFR_{CT} in Coronary Care (ADVANCE) registry was designed to observe the 'real-world' utility and impact of using FFR_{CT} in a broad variety of healthcare settings, geographical regions, and patient populations by examining how the incremental information of FFR_{CT} on top of the anatomical information from conventional coronary CT angiography altered diagnosis and clinical decision-making, patient management, clinical outcomes and resource utilization. 5083 Patients being investigated for clinically suspected CAD with documented atherosclerosis >30% degree stenosis (DS) on CCTA were prospectively enrolled at 38 sites. Demographics, symptom status, CCTA and FFR_{CT} findings, treatment plans, and clinical outcomes through 90 days were recorded. Investigators were asked to report an initial management plan and treatment strategy based on CCTA alone for each subject in accordance with local guidelines for the practice and interpretation of CCTA with optional FFR_{CT} for stenoses in the 30–90% range followed by re-determining the treatment strategy based on the new information of the CCTA combined with the locally interpreted FFR_{CT} result.

Management plan treatment strategies for both site and core laboratory consisted of the following options: (i) optimal medical therapy, (ii) percutaneous coronary intervention (PCI), (iii) coronary artery bypass grafting (CABG) surgery, or (iv) additional diagnostic testing required.

The primary endpoint was the reclassification rate between CCTA alone vs. CCTA and FFR_{CT}-based management plans as determined by the core laboratory. Secondary endpoints included: reclassification rate between CCTA-based and FFR_{CT}-based management plans as determined by the site; incidence of ICA demonstrating absence of obstructive CAD (no coronary stenosis >50%); percutaneous and surgical revascularization rates; and 90 days survival free from all cause or major adverse cardiovascular events (MACE) inclusive of myocardial infarction (MI), all-cause mortality or unplanned hospitalization for Acute Coronary Syndrome (ACS) leading to revascularization.

The primary endpoint of reclassification between core lab CCTA alone and CCTA plus FFR_{CT}-based management plans occurred in 66.9% [confidence interval (CI): 64.8–67.6] of patients. Non-obstructive coronary disease was significantly lower in ICA patients with FFR_{CT} <_0.80 (14.4%) compared to patients with FFR_{CT} >0.80 (43.8%, odds ratio 0.19, CI: 0.15–0.25, P< 0.001). In total, 72.3% of subjects undergoing ICA with FFR_{CT} <_0.80 were revascularized. No death/myocardial infarction (MI) occurred within 90 days in patients with FFR_{CT} >0.80 (n= 1529), whereas 19 (0.6%) MACE [hazard ratio (HR) 19.75, CI: 1.19–326, P = 0.0008] and 14 (0.3%) death/MI (HR 14.68, CI 0.88–246, P= 0.039) occurred in subjects with an FFR_{CT} <_0.80.

In a large international multi-center population, FFR_{CT} modified treatment recommendation in two-thirds of subjects as compared to CCTA alone, was associated with less negative ICA, predicted revascularization, and identified subjects at low risk of adverse events through 90 days.

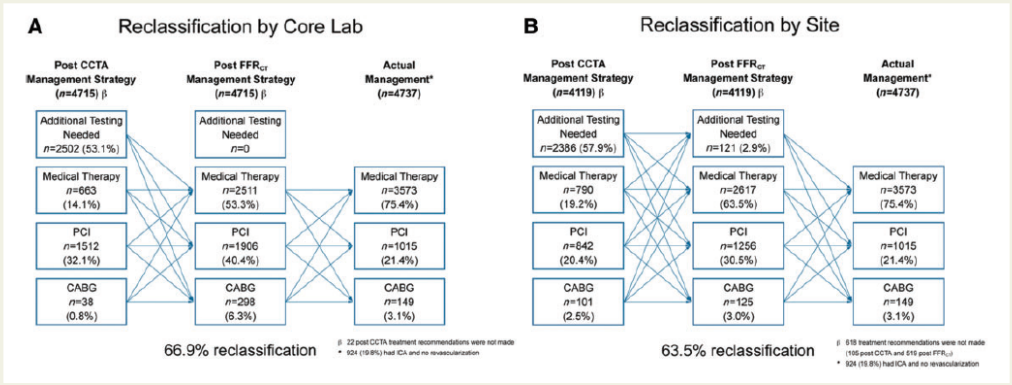

Figure 2 Clinical management strategies and reclassification of post-coronary computed tomography angiography, following coronary computed tomography angiography-derived fractional flow reserve and actual management at 90 days (*A* Core and *B* Site).

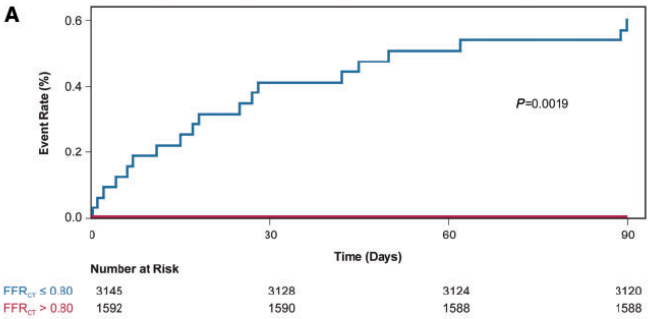

Number at Risk

$FFR_{CT} \leq 0.80$	3145	3128	3124	3120
$FFR_{CT} > 0.80$	1592	1590	1588	1588

Subjects for whom no event was recorded were censored at 90 days post-cCTA unless data was recorded on the Registry Completion CRF page, in which case the subject was censored at the minimum of the date of participation completion or discontinuation and 90 days post-cCTA.

	K-M Event Rate% (standard error)		
	30 Days	60 Days	90 Days
$FFR_{CT} \leq 0.80$	0.41%(0.11%)	0.51%(0.13%)	0.60%(0.14%)
$FFR_{CT} > 0.80$	0.00%(0.00%)	0.00%(0.00%)	0.00%(0.00%)

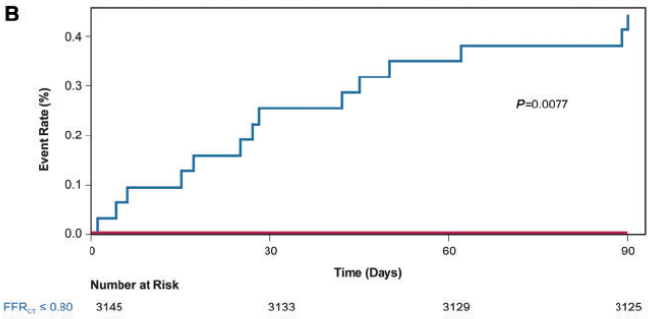

Number at Risk

$FFR_{CT} \leq 0.80$	3145	3133	3129	3125
$FFR_{CT} > 0.80$	1592	1590	1588	1588

Subjects for whom no event was recorded were censored at 90 days post-cCTA unless data was recorded on the Registry Completion CRF page, in which case the subject was censored at the minimum of the date of participation completion or discontinuation and 90 days post-cCTA.

	K-M Event Rate% (standard error)		
	30 Days	60 Days	90 Days
$FFR_{CT} \leq 0.80$	0.25%(0.09%)	0.35%(0.11%)	0.45%(0.12%)
$FFR_{CT} > 0.80$	0.00%(0.00%)	0.00%(0.00%)	0.00%(0.00%)

Figure 5 Major adverse cardiac events (*A*) (all-cause mortality, myocardial infarction, unplanned hospitalization with urgent revascularization) and (*B*) myocardial infarction/all-cause mortality alone at 90 days for coronary computed tomography angiography-derived fractional flow reserve positive (≤0.80) and negative values (>0.80).

1-Year Impact on Medical Practice and Clinical Outcomes of FFR_{CT}: The ADVANCE Registry

Coronary CT angiography was initially a first-line diagnostic tool to exclude the presence of CAD. The randomized SCOT-HEART trial tested a coronary CT angiography based diagnostic approach in a population with low- to intermediate-risk and compared this approach with standard care. CTA increased certainty in the diagnosis of angina due to coronary heart disease (CHD) (relative risk [RR] = 1.79, 95% confidence interval [CI] 1.62-1.96, $p < 0.001$) vs. standard care (exercise electrocardiography and/or stress imaging). Most importantly, the trial confirmed a difference in death or nonfatal myocardial infarction (MI) at 5 years between groups: 2.3% in the CTA group vs. 3.9% in the standard care group ($p = 0.004$)[28]. Although CTA was associated with an increase in invasive therapy and revascularization in the short-term, there was no difference in invasive therapy and revascularization between treatment arms at 5 years. Since there was no difference in overall revascularization rates, long-term benefit from CTA may have been due to lifestyle modification and statin therapy initiated from the early diagnosis of CAD[28].

Also, the PROMISE (Prospective Multicenter Imaging Study for Evaluation of Chest Pain) trial randomized 10,003 low-risk, symptomatic patients to CCTA or stress testing (nuclear 68%, echo 22%, and exercise 10%). At 25 months, there was no difference in the primary composite outcome of death, MI, hospitalization for unstable angina, or major procedural complication (3.3% in CCTA group vs. 3% in stress group, P=0.75). Nevertheless, there were 23% lower odds of MI with the CCTA strategy, but this was not statistically significant (95% confidence interval 0.48-1.23) although the study was underpowered to show differences between groups[61].

As a consequence of these data, suggesting a potential role for coronary CT to improve outcomes, coronary CT angiography emerged as a first-line diagnostic tool in many guidelines[42].

Accordingly, The DISCOVER-FLOW, DeFACTO and NXT studies have shown a high correlation between CT-derived FFR and gold standard invasive FFR[36,58,59]. Invasive Fractional Flow Reserve (FFR) has demonstrated to improve outcomes[7]. FFR_{CT} can be considered the non-invasive counterpart of invasive FFR.

The ADVANCE registry showed FFR_{CT} modified treatment recommendations in a large majority of patients as compared with coronary CTA alone. In addition, a positive FFR_{CT} was

associated with revascularization and less negative invasive coronary angiography (ICA)[62]. Intermediate term clinical utility and outcomes data with an FFR_{CT} had been limited to single-center reports. Using 1-year data from the ADVANCE Registry, we evaluated the relationship of FFR_{CT} with clinical outcomes.

Patients (N=5,083) evaluated for clinically suspected coronary artery disease and in whom atherosclerosis was identified by coronary CTA were prospectively enrolled at 38 international sites from July 15, 2015, to October 20, 2017. Demographics, symptom status, coronary CTA and FFR_{CT} findings and resultant site-based treatment plans, and clinical outcomes through 1 year were recorded and adjudicated by a blinded core laboratory. Major adverse cardiac events (MACE), death, myocardial infarction (MI), and acute coronary syndrome leading to urgent revascularization were captured.

At 1 year, 449 patients did not have follow-up data. Revascularization occurred in 1,208 (38.40%) patients with an FFR_{CT} ≤0.80 and in 89 (5.60%) with an FFR_{CT} >0.80 (relative risk [RR]: 6.87; 95% confidence interval [CI]: 5.59 to 8.45; $p < 0.001$). MACE occurred in 55 patients, 43 events occurred in patients with an FFR_{CT} ≤0.80 and 12 occurred in those with an FFR_{CT} >0.80 (RR: 1.81; 95% CI: 0.96 to 3.43; $p = 0.06$). Time to first event (all-cause death or MI) occurred in 38 (1.20%) patients with an FFR_{CT} ≤0.80 compared with 10 (0.60%) patients with an FFR_{CT} >0.80 (RR: 1.92; 95% CI: 0.96 to 3.85; $p = 0.06$). Time to first event (cardiovascular death or MI) occurred cardiovascular death or MI occurred more in patients with an FFR_{CT} ≤0.80 compared with patients with an FFR_{CT} >0.80 (25 [0.80%] vs. 3 [0.20%]; RR: 4.22; 95% CI: 1.28 to 13.95; $p = 0.01$).

The 1-year outcomes from the ADVANCE FFR_{CT} Registry show low rates of events in all patients, with less revascularization and a trend toward lower MACE and significantly lower cardiovascular death or MI in patients with a negative FFR_{CT} compared with patients with abnormal FFR_{CT} values.

CENTRAL ILLUSTRATION **Kaplan-Meier Event Curves for MACE**

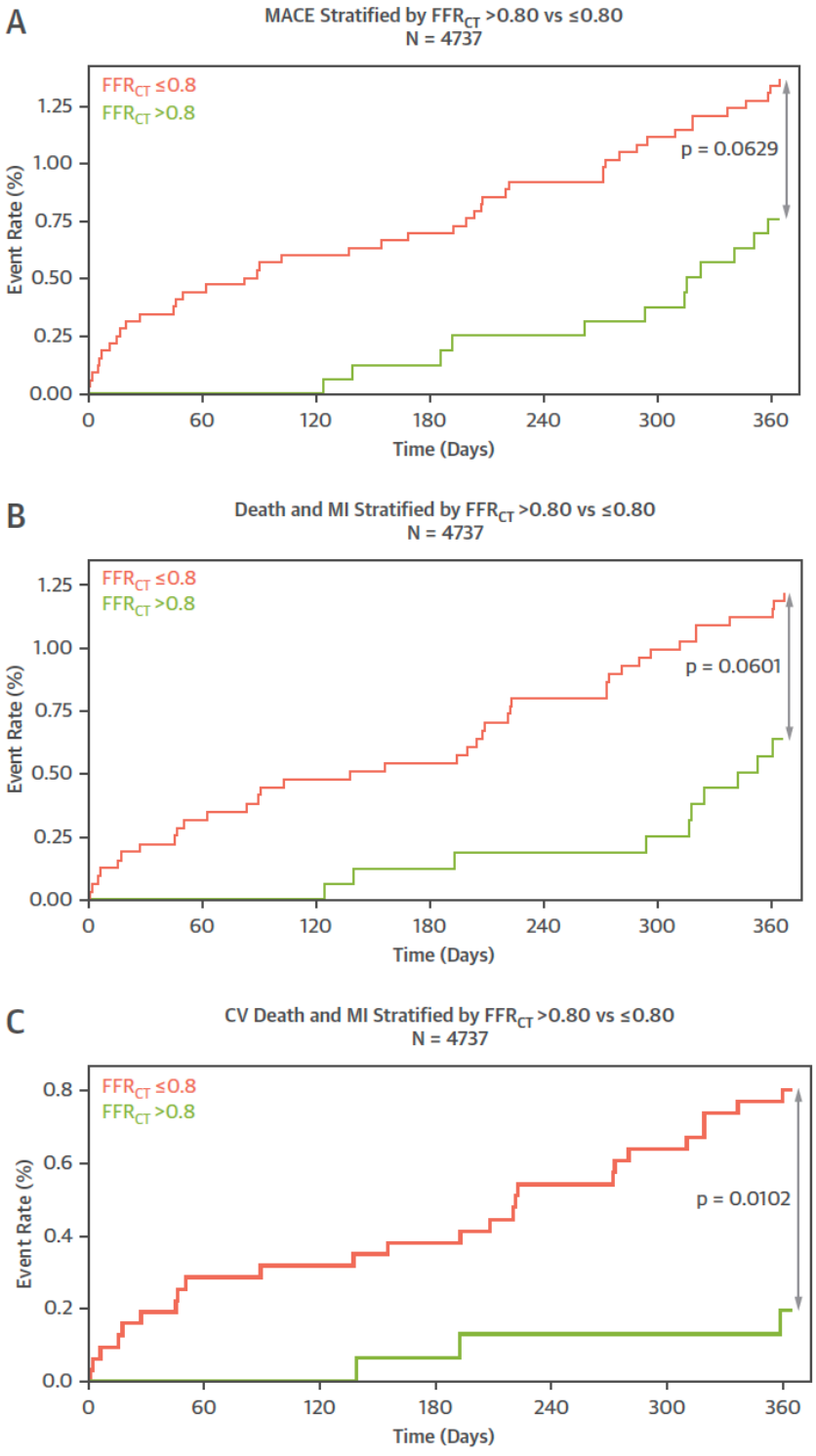

Patel, M.R. et al. J Am Coll Cardiol Img. 2020;13(1):97-105.

(A) All-cause mortality, myocardial infarction (MI), or acute coronary syndrome leading to unplanned hospitalization with urgent revascularization ($p = 0.06$); **(B)** MI and all-cause mortality alone ($p = 0.06$); and **(C)** cardiovascular (CV) death and MI ($p = 0.01$) at 1 year stratified by fractional flow reserve derived from coronary computed tomography angiography (FFR$_{CT}$) positive (≤0.80) and negative values (>0.80). Note that events are based on time to event analysis and there was 1 MI event that occurred in a patient after an acute coronary syndrome with unplanned hospitalization leading to revascularization. MACE = major adverse cardiac events.

Temporal Changes in FFR_{CT}-Guided Management of Coronary Artery Disease - Lessons from the ADVANCE Registry

The ADVANCE registry is a large prospective study of outcomes and resource utilization in patients undergoing coronary computed tomography angiography (CCTA) and CT-based fractional flow reserve (FFR_{CT})[62]. In the ADVANCE registry, intermediate coronary stenoses were frequently encountered. In real-life clinical situations, the potential significance of these lesions is assessed using additional functional testing. As such, CCTA consistently led to further downstream diagnostic and ambiguous therapeutic pathway selection. CT-derived fractional flow reserve (FFR_{CT}) is a novel non-invasive physiological analysis that can compute FFR values from standard CCTA images[38]. FFR_{CT} improves the diagnostic performance of CCTA alone and reduces the incidence of invasive coronary angiograms (ICA) without significant angiographic CAD[63,64]. Increasing experience with FFR_{CT} influences the clinical management strategies in a high proportion of patients with suspected CAD as shown in the ADVANCE registry[62]. In the current study, we investigated temporal changes in the use of FFR_{CT} within the ADVANCE registry.

5083 patients with coronary artery disease (CAD) on CCTA were prospectively enrolled in the ADVANCE registry and were divided into 3 equally sized cohorts based on the temporal order of enrollment per site. Demographics, CCTA and FFR_{CT} findings, and clinical outcomes through 1-year follow-up, were recorded and compared between tertiles.

The number of patients with a ≥70% stenosis on CCTA was similar over time (33.6%, 30.9%, and 33.8% for cohort 1-3). The rate of positive FFR_{CT} ≤0.80 was higher for cohorts 2 (67.3%) and 3 (74.6%) than for cohort 1 (57.1%, $p < 0.001$). Invasive FFR rates decreased from 25.8% to 22.4% between cohort 1 and 3 ($p = 0.023$). Moreover, patients with a FFR_{CT} ≤0.80 were less frequently referred for invasive coronary angiography (ICA) (from 62.9% to 52.9%, $p < 0.001$), and underwent fewer revascularizations between cohort 1 and 3 (from 41.9% to 32.0%, $p < 0.001$). The prevalence of major events was low (1.2%) and similar between cohorts.

Growing experience with FFR_{CT} improved the likelihood of identifying hemodynamically significant CAD and safely reduced the need for ICA and revascularization in patients with anatomically significant disease even in the instance of an abnormal FFR_{CT}.

Table 4
Overall changes in management at 90-days by FFR_{CT} within cohorts.

	Cohort 1			Cohort 2			Cohort 3			Trend all cohorts p-value	
	$FFR_{CT} \leq 0.80$ (n = 892)	FFR_{CT} > 0.80 (n = 671)	p-value	$FFR_{CT} \leq 0.80$ (n = 1056)	FFR_{CT} > 0.80 (n = 513)	p-value	$FFR_{CT} \leq 0.80$ (n = 1197)	FFR_{CT} > 0.80 (n = 408)	p-value	$FFR_{CT} \leq 0.80$	FFR_{CT} > 0.80
Functional testing	168 (18.8%)	74 (11.0%)	< 0.001	243 (23.0%)	61 (11.9%)	< 0.001	199 (16.6%)	38 (9.3%)	< 0.001	0.117	0.459
ICA	561 (62.9%)	156 (23.2%)	< 0.001	564 (53.4%)	93 (18.1%)	< 0.001	633 (52.9%)	80 (19.6%)	< 0.001	< 0.001	0.097
Invasive FFR	317 (35.5%)	97 (14.5%)	< 0.001	337 (31.9%)	50 (9.7%)	< 0.001	333 (27.8%)	33 (8.1%)	< 0.001	< 0.001	< 0.001
Medication	518 (58.1%)	638 (95.1%)	< 0.001	715 (67.7%)	493 (96.1%)	< 0.001	814 (68.0%)	391 (95.8%)	< 0.001	< 0.001	0.501
Revascularization	374 (41.9%)	33 (4.9%)	< 0.001	341 (32.3%)	20 (3.9%)	< 0.001	383 (32.0%)	17 (4.2%)	< 0.001	< 0.001	0.501

Categories are present as number of patients and % within FFR_{CT} finding of each cohort. Cochran-Armitage test for trend were used to test for trend over all cohorts.
FFR_{CT}: computed tomography-based fractional flow reserve; ICA: invasive coronary angiography.

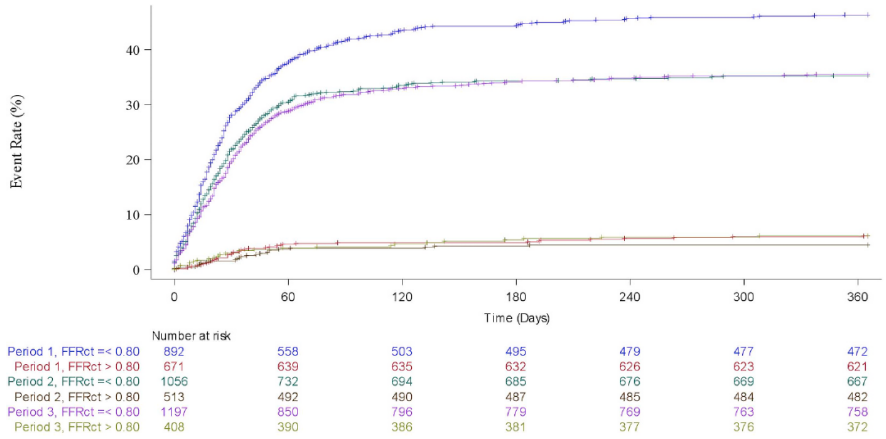

Fig. 2. Kaplan-Meier event curves for revascularization Kaplan-Meier event curves for revascularization stratified by $FFR_{CT} > 0.80$ versus ≤ 0.80 per cohort. Revascularization curves of all cohorts were compared by FFR_{CT} findings with the use of a log-rank test. FFR_{CT}: computed tomography-derived fractional flow reserve.

The Clinical Utility of FFR_{CT} Stratified by Age

Coronary computed tomography angiography (CTA) provides assessment of CAD in patients with symptomatic chest pain and has superior or similar prognostic benefit to other non-invasive imaging strategies[61]. However, CTA has limitations related to reduced specificity in the setting of coronary lesions with moderate to severe stenosis and high calcification[65]. This remains a significant concern given the increased use of CCTA in older, intermediate to high-risk groups and in some instances all ages regardless of cardiovascular disease risk. Non-invasive FFR determined from CTA (FFR_{CT}) correlates well with invasive FFR and improves the diagnostic accuracy of CTA for detection of flow-limiting coronary lesions[37,66]. CTA with FFR_{CT} is a safe alternative to invasive coronary angiography (ICA) as a negative FFR_{CT} has been shown to have low rates of revascularization and significantly lower cardiovascular death and MI compared to those with a positive FFR_{CT}[66–68]. FFR_{CT} accuracy appears to remain high in the instance of high coronary calcification, as in the elderly[36]. For instance, a recent study identified that the diagnostic accuracy, sensitivity and specificity of FFR_{CT} was similar across all calcium score categories, including for high Agatston scores (CAC≥400)[69]. However, there is limited data regarding the impact of FFR_{CT} on decision-making, downstream ICA, major adverse cardiovascular events (MACE) and revascularization according to age.

Patients in the ADVANCE (Assessing Diagnostic Value of Non-invasive FFR_{CT} in Coronary Care) registry were stratified into those ≥65 or <65 years of age. The impact of FFR_{CT} on clinical decision-making, as assessed by patient age, was determined by evaluating patient management using CTA results alone, followed by site investigators submitting a report on the treatment plan based upon the newly provided FFR_{CT} data. Outcomes at 1-year post CTA were assessed, including major adverse cardiovascular events (myocardial infarction, all-cause mortality or unplanned hospitalization for ACS leading to revascularization) and total revascularization. Positive FFR_{CT} was deemed to be ≤ 0.8.

FFR_{CT} was calculated in 1849 (40.6%) subjects aged <65 and 2704 (59.4%) ≥ 65 years of age. Subjects ≥65 years were more likely to have anatomic obstructive disease on CTA (≥50% stenosis), compared to those aged <65 (69.7% and 73.2% respectively, p = 0.008). There was a similar graded increase in recommended and actual revascularization with either CABG or PCI, with declining FFR_{CT} strata for subjects above and below the age of 65. MACE and revascularization rates were not significantly different for those ≥ or <65, regardless of FFR_{CT} positivity or stenosis severity <50% or ≥50%. With a negative FFR_{CT} result, and

anatomical stenosis ≥50%, those ≥ and <65 years of age, had similar rates of MACE (0.2% for both, p = 0.1) and revascularization (8.7% and 10.4% respectively p = 0.4). Logistic regression analysis, with age as a continuous variable, and adjustment for Diamond Forrester Risk, baseline FFR_{CT} and treatment (CABG, PCI, medical therapy), indicated a statistically significant, but small increase in the odds of a MACE event with increasing age (OR 1.04, 95% CI 1.006-1.08, p = 0.02). Amongst patients with a FFR_{CT} > 0.80, there was no effect of age on the odds of revascularization.

The findings of this study point to a low risk of MACE events or need for revascularization in those aged ≥ or <65 with a FFR_{CT}>0.80, despite the higher incidence of anatomic obstructive CAD in those ≥65 years. The findings show the clinical usefulness and outcomes of FFR_{CT} are largely constant regardless of age.

Table 4
Major Adverse Cardiovascular Events and Cardiovascular death or MI at 1 year.

	< 65 (n = 1849)	≥65 (n = 2704)	Total (n = 4553)	p-value
Maximum Stenosis ≥ 50% and FFR_{CT} > 0.80				
MACE	4 (0.2)	5 (0.2)	9 (0.2)	1.0
Myocardial infarction	3 (0.2)	5 (0.2)	8 (0.2)	1.0
All-Cause mortality	1 (0.1)	4 (0.1)	5 (0.1)	0.4
Unplanned hospitalization for ACS	1 (0.1)	0	1 (0.0)	0.4
Cardiovascular death or MI	2 (0.1)	1 (0.0)	3 (0.1)	0.6
Maximum Stenosis ≥ 50% and FFR_{CT} ≤ 0.80				
MACE	9 (0.5)	21 (0.8)	30 (0.7)	0.5
Myocardial infarction	7 (0.4)	19 (0.7)	26 (0.6)	0.3
All-Cause mortality	4 (0.2)	18 (0.7)	22 (0.5)	0.08
Unplanned hospitalization for ACS	3 (0.2)	3 (0.1)	4 (0.1)	0.4
Cardiovascular death or MI	5 (0.3)	11 (0.4)	16 (0.4)	0.6
Maximum Stenosis < 50% and FFR_{CT} > 0.80				
MACE	1 (0.1)	2 (0.1)	3 (0.1)	1.0
Myocardial infarction	0	2 (0.1)	2 (0.0)	0.5
All-Cause mortality	0	2 (0.1)	2 (0.0)	0.5
Unplanned hospitalization for ACS	1 (0.1)	0	1 (0.0)	0.4
Cardiovascular death or MI	0 (0.0)	0 (0.0)	0 (0.0)	–
Maximum Stenosis < 50% and FFR_{CT} ≤ 0.80				
MACE	1 (0.1)	4 (0.1)	5 (0.1)	0.4
Myocardial infarction	1 (0.1)	4 (0.1)	5 (0.1)	0.4
All-Cause mortality	1 (0.1)	3 (0.1)	4 (0.1)	0.6
Unplanned hospitalization for ACS	0	0	0	–
Cardiovascular death or MI	0	3 (0.1)	3 (0.1)	0.3

MACE: Major Adverse Cardiovascular Events (Myocardial Infarction, All-Cause mortality, unplanned hospitalization for ACS); MI: Myocardial infarction.

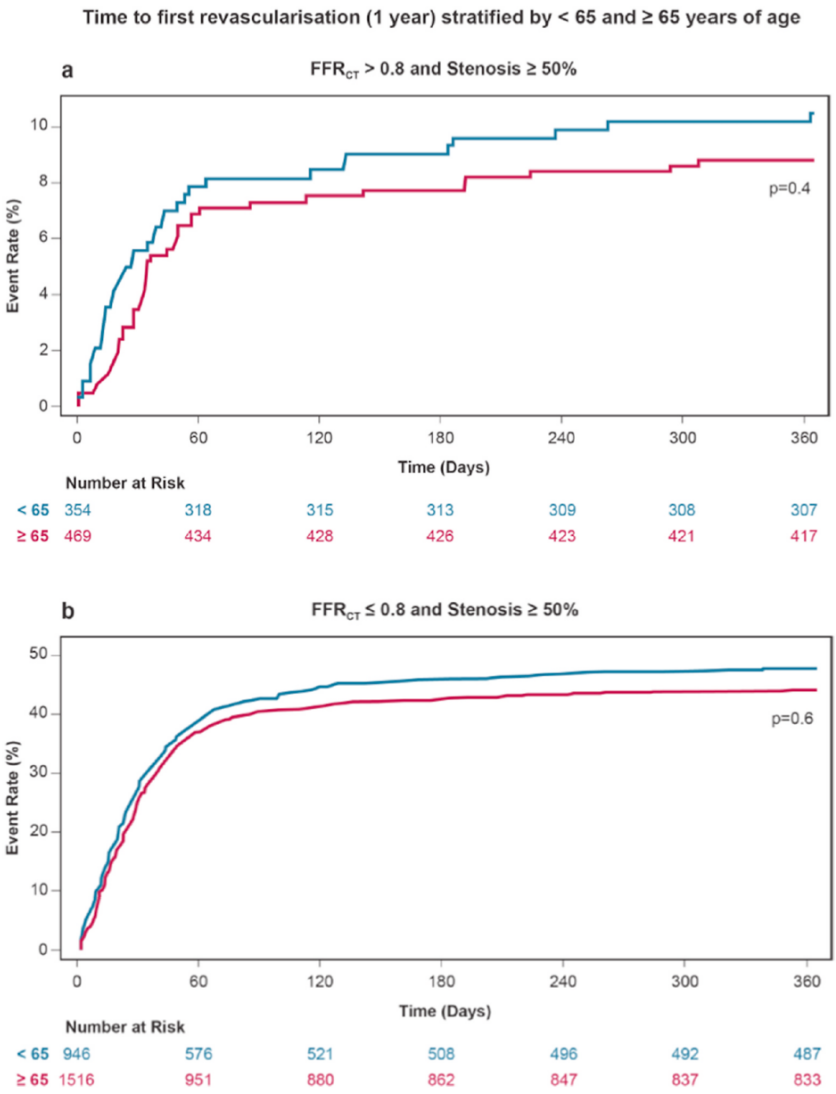

Fig. 4. First revascularisation rate event at 1 year stratified by patients above and below the age of 65 for those with (a) $FFR_{CT} > 0.80$ and stenosis > 50%, and (b) $FFR_{CT} \leq 0.80$ and stenosis ≥ 50%. Events are based upon time to event analysis.

Impact of Non-invasive Anatomical Testing on Optimal Medical Prescription in Patients with Suspected Coronary Artery Disease

Compared to functional testing, coronary computed tomography angiography (CTA) improves clinical outcomes in patients with suspected coronary artery disease (CAD). Indeed, in 2018 the randomized SCOT-HEART trial confirmed a difference in death or nonfatal myocardial infarction (MI) at 5 years between groups: 2.3% in the CTA group vs. 3.9% in the standard care group ($p = 0.004$). This is thought to be the result of an increased prescription of preventive medical therapy (statins and aspirin) when relying on a CTA imaging strategy[28]. Indeed, the presence of non-obstructive CAD assessed by coronary CT is associated with higher rate of major adverse cardiovascular events. Andreini et al. stratified 1,196 consecutive patients with suspected CAD undergoing coronary CTA according to the presence of atherosclerotic plaque and degree of obstruction. Patients without CAD experienced no events during a 52-month follow-up. Of note, the presence of non-obstructive coronary disease was associated with a similar rate of events compared to patients with obstructive CAD[31]. Further risk stratification assessing plaque characteristics and composition have identified the presence of positive remodeling, low-attenuation plaque, napkin-ring sign and spotty calcification as predictors of plaque rupture and acute coronary syndromes[70]. The identification of non-obstructive plaques, or adverse plaque characteristics should prompt the treating physician to initiate or intensify medical therapy[71].

In this study, we compared the rate of statins prescription in a patient cohort assessed either with coronary CTA or exercise testing and evaluated the agreement on medication prescriptions.

Consecutive patients who underwent coronary CTA and exercise test for suspected CAD were included. Four clinical cardiologists independently analyzed each case based on clinical information and the result of either coronary CTA or exercise test. For each case, treatment strategy and prescription were recorded while blinded to the results of the other cardiac test. Treatment strategy was reassessed using the alternative imaging modality three weeks after the first evaluation.

A total of 113 patients were included. Mean age was 56.7±11.5 years, 52% were males and diabetes were present in 6%. Coronary CTA showed an obstructive epicardial stenosis in 21.4% and any type of atherosclerotic plaque in 54.2%. Functional testing identified ischemia

in 9.1%. The use of coronary CTA resulted in higher number of statin (64.9% vs. 44.5%, P<0.001) and aspirin (21.4% vs. 4.3%, P<0.001) prescriptions. There was a substantial agreement on the prescription of statins (mean Cohen's κ coefficient of 0.79±0.07). Epicardial atherosclerotic disease was found in half of patients with suspected CAD as assessed by coronary CTA. Compared to functional testing, coronary CTA evaluation by coronary was associated with an increase in the rate of preventive therapy prescription.

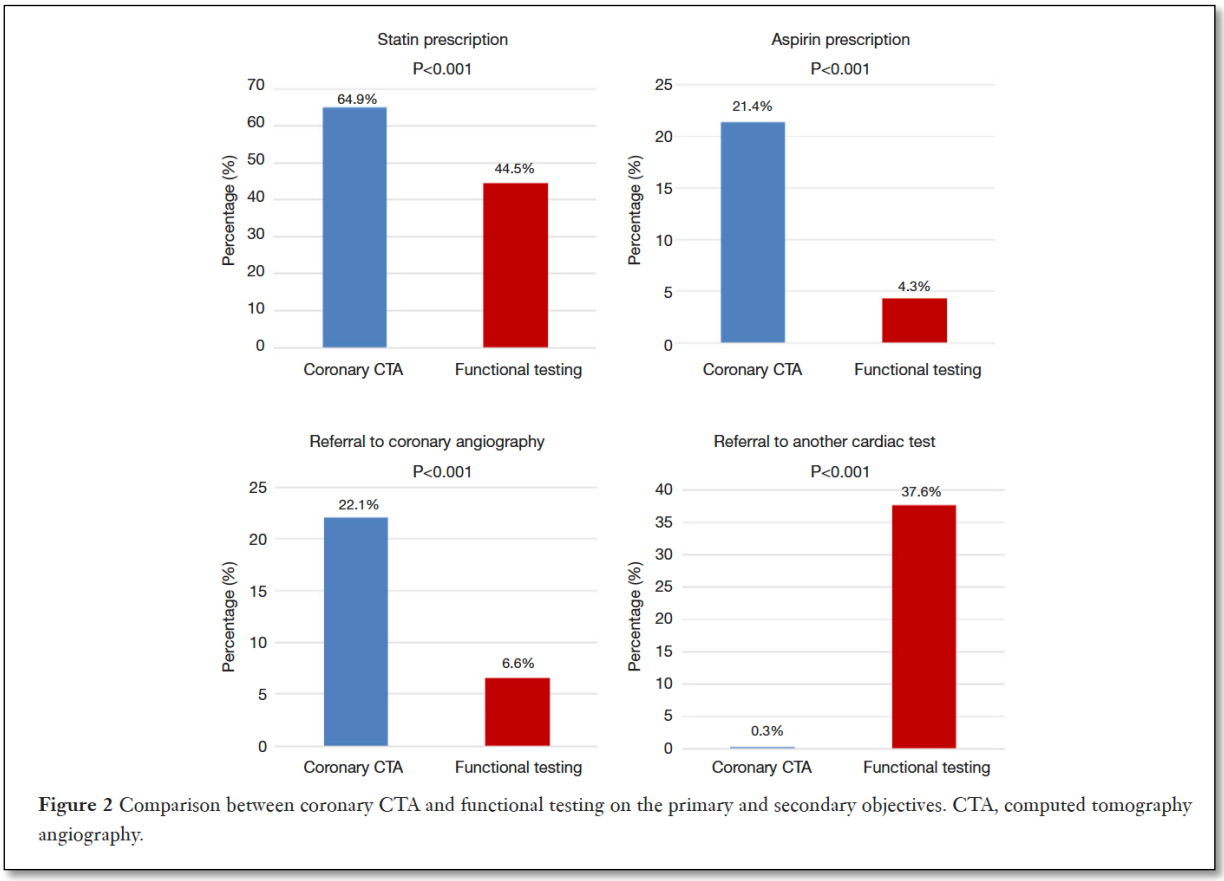

Figure 2 Comparison between coronary CTA and functional testing on the primary and secondary objectives. CTA, computed tomography angiography.

Chapter 2: Coronary CT angiography and non-invasive Fractional Flow Reserve derived from coronary CT angiography for heart team decision-making

Chapter introduction

In the second chapter, the research focus lies within the use of CT and FFR_{CT} for heart team decision-making. In 2011, the functional SYNTAX score (FSS) was introduced enhancing risk prediction as compared to the anatomical SYNTAX score. For this, the anatomical SYNTAX score was corrected by excluding lesions from non-significant vessels measured by iFR or FFR. In the first paper of this chapter, it was hypothesized that FFR_{CT} could provide identical functional information to calculate a non-invasive functional SYNTAX score derived from CCTA. The proportion of reclassification within the SYNTAX-tertiles was compared between the invasive and non-invasive approach and the performance of FFR_{CT} was evaluated compared to iFR. Calculation of the noninvasive FSS proved feasible and yielded similar results to those obtained with invasive pressure-wire assessment. The agreement on the SYNTAX score tertile classification improved with the inclusion of the functional component from slight to fair agreement. FFR_{CT} had good accuracy in detecting functionally significant lesions in patients with 3-vessel CAD as compared to iFR.

These results formed the foundation of the SYNTAX III Revolution trial. This study sought to determine the agreement between separate heart teams on treatment decision-making based on either coronary CTA or conventional angiography in patients with de novo left main or three-vessel coronary artery disease. Each heart team consisted of an invasive cardiologist, a cardiac surgeon and a radiologist. In contrary to most trials, not the patients but the heart teams were randomized to calculate the SYNTAX score II (anatomical SYNTAX score plus clinical data) treatment recommendation based on a mortality prediction at 4-years (recommending PCI, CABG or equipoise between CABG and PCI). The agreement concerning treatment decision between coronary CTA and conventional angiography was high (Cohen's kappa 0.82) and showed higher agreement than the anatomical SYNTAX score. The SYNTAX Score III (Anatomical SYNTAX score, clinical comorbidities and functional assessment using FFR_{CT}) enabled the heart team to refine the decision-making process regarding the optimal revascularization strategy and treatment planning of hemodynamically significant lesions.

In the SYNTAX III Revolution trial, addition of FFR_{CT} downgraded the proportion of three vessel disease and changed treatment recommendation in 7%. A detailed sub-analysis focused on the impact of FFR_{CT} on treatment decision-making and procedural planning.

In another ancillary paper, we investigated the agreement between SYNTAX scores and FSS as calculated by site and core laboratory and its potential impact on altered treatment

recommendation. In a last sub-analysis, we assessed the influence of coronary calcification on the evaluation of CCTA and the impact of severe calcification on heart team treatment decision-making and procedural planning.

Fractional Flow Reserve Derived from Computed Tomographic Angiography in Patients with Multivessel CAD

In the SYNTAX II study, 83% of the patients had anatomical (diameter stenosis>50%) 3-vessel coronary artery disease (CAD); the use of instantaneous wave-free ratio (iFR) reduced the number of patients with functionally significant 3-vessel disease to 37%[72].The functional SYNTAX score (FSS), a correction of the SYNTAX score (SS) using fractional flow reserve (FFR), reclassified 34% of patients from high- and moderate-risk SS tertiles to the low-risk tertile in the FAME trial[73]. The functional SYNTAX score (FSS) has been shown to improve the discrimination for major adverse cardiac events compared with the anatomic SYNTAX score (SS) while reducing interobserver variability[73]. Fractional flow reserve derived from computed tomography angiography (FFR_{CT}) can be used to calculate the noninvasive FSS. However, evidence supporting the noninvasive FSS in patients with multivessel coronary artery disease (CAD) is scarce. Also, the diagnostic accuracy of FFR_{CT} with iFR as a clinical reference was never explored before.

The purpose of this study was to assess the feasibility of and validate the noninvasive FSS derived from coronary computed tomography angiography (CTA) with fractional flow reserve (FFR_{CT}) in patients with 3-vessel CAD.

The CTA-SS was calculated in patients with 3-vessel CAD included in the SYNTAX II (SYNergy between percutaneous coronary intervention with TAXus and cardiac surgery II) study. The noninvasive FSS was determined by including only ischemia-producing lesions ($FFR_{CT} \leq 0.80$). SS derived from different imaging modalities were compared using the Bland-Altman and Passing-Bablok method, and the agreement on the SS tertiles was investigated with Cohen's Kappa. The risk reclassification was compared between the noninvasive and invasive physiological assessment, and the diagnostic accuracy of FFR_{CT} was assessed by the area under the receiver-operating characteristic curve using instantaneous wave-free ratio as a reference.

The CTA-SS was feasible in 86% of patients (66 of 77), whereas the noninvasive FSS was feasible in 80% (53 of 66). The anatomic SS was overestimated by CTA compared with conventional angiography (27.6 ± 6.4 vs. 25.3 ± 6.9; $p < 0.0001$) whereas the calculation of the FSS yielded similar results between the noninvasive and invasive imaging modalities (21.6 ± 7.8 vs. 21.2 ± 8.8; $p = 0.589$). The noninvasive FSS reclassified 30% of patients from

the high- and intermediate-SS tertiles to the low-risk tertile, whereas invasive FSS reclassified 23% of patients from the high- and intermediate-SS tertiles to the low-risk tertile. The agreement on the classic SS tertiles based on Kappa statistics was slight for the anatomic SS (Kappa = 0.19) and fair for the FSS (Kappa = 0.32). The diagnostic accuracy of FFR_{CT} to detect functional significant stenosis based on an instantaneous wave-free ratio ≤0.89 revealed an area under the receiver-operating characteristics curve of 0.85 (95% CI: 0.79 to 0.90) with a sensitivity of 95% (95% CI: 89% to 98%), specificity of 61% (95% CI: 48% to 73%), positive predictive value of 81% (95% CI: 76% to 86%), and negative predictive value of 87% (95% CI: 74% to 94%).

Calculation of the noninvasive FSS is feasible and yielded similar results to those obtained with invasive pressure-wire assessment. The agreement on the SYNTAX score tertile classification improved with the inclusion of the functional component from slight to fair agreement. FFR_{CT} has good accuracy in detecting functionally significant lesions in patients with 3-vessel CAD.

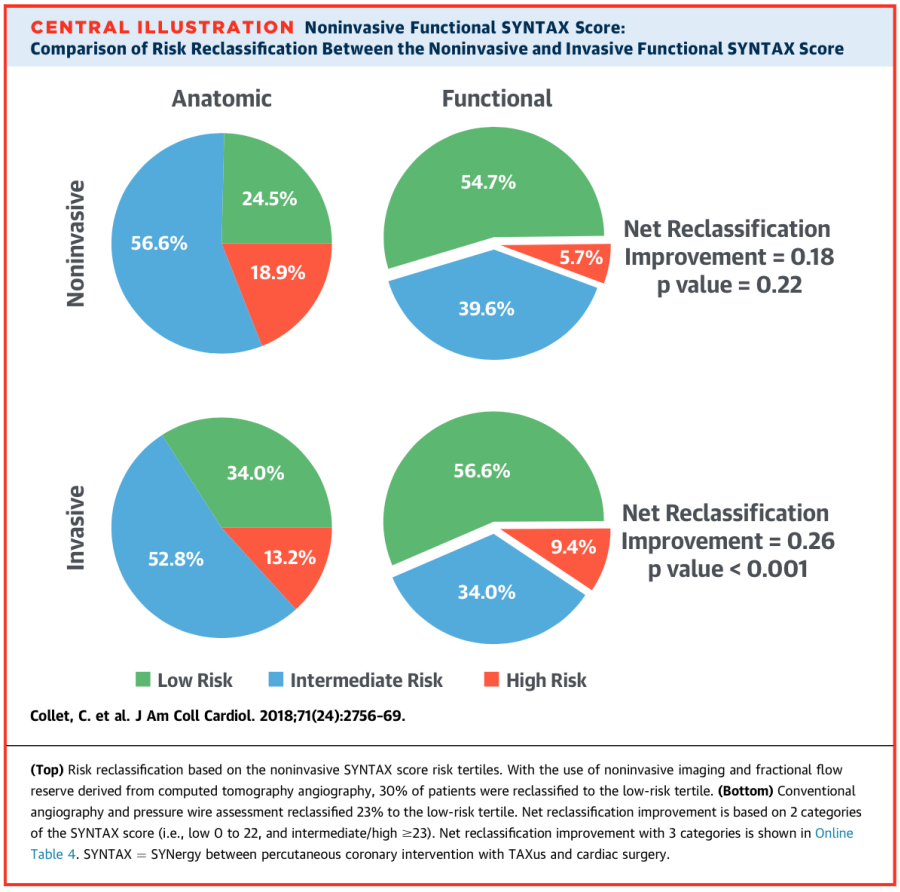

(Top) Risk reclassification based on the noninvasive SYNTAX score risk tertiles. With the use of noninvasive imaging and fractional flow reserve derived from computed tomography angiography, 30% of patients were reclassified to the low-risk tertile. **(Bottom)** Conventional angiography and pressure wire assessment reclassified 23% to the low-risk tertile. Net reclassification improvement is based on 2 categories of the SYNTAX score (i.e., low 0 to 22, and intermediate/high ≥23). Net reclassification improvement with 3 categories is shown in Online Table 4. SYNTAX = SYNergy between percutaneous coronary intervention with TAXus and cardiac surgery.

Coronary Computed Tomography Angiography for Heart Team Decision-making in Multivessel Coronary Artery Disease

Myocardial revascularization has proven to improve outcomes in patients with multi-vessel CAD[74]. The treatment decision and choice between PCI and coronary artery bypass grafting (CABG) is based mainly on anatomical complexity, clinical comorbidity and a heart team approach for final decision-making[75]. Invasive coronary angiography remained for years the mainstay modality to ascertain the anatomical CAD extent and severity. Recently, coronary CT angiography emerged as a novel non-invasive diagnostic tool providing the same anatomical information as invasive coronary angiography[76]. On top of the anatomical evaluation by CCTA, FFR_{CT} has the potential to assess the physiologic repercussion of coronary stenoses comparable to invasive fractional flow reserve (FFR)[36].

The SYNTAX score has been developed to aid in heart team treatment decision-making on a patient level. Calculation of the SYNTAX score derived from coronary CTA has been shown to be accurate with respect to the one derived from invasive angiographic assessment[77]. The SYNTAX score II combines the anatomical SYNTAX score I with clinical characteristics and comorbidities to provide a treatment recommendation based on the predicted 4-year mortality in patients undergoing coronary artery bypass grafting surgery (CABG) or percutaneous coronary intervention (PCI)[78,79]. The non-invasive functional SYNTAX score was additionally used in this study to calculate the SYNTAX Score III, which is conceptually a combination of coronary anatomical complexity with its physiological repercussion and patient's clinical characteristics and comorbidities.

Coronary computed tomography angiography (CTA) has emerged as a non-invasive diagnostic method for patients with suspected coronary artery disease, but its usefulness in patients with complex coronary artery disease remains to be investigated. The present study sought to determine the agreement between separate heart teams on treatment decision-making based on either coronary CTA or conventional angiography.

Separate heart teams composed of an interventional cardiologist, a cardiac surgeon, and a radiologist were randomized to assess the coronary artery disease with either coronary CTA or conventional angiography in patients with de novo left main or three-vessel coronary artery disease. Each heart team, blinded for the other imaging modality, quantified the anatomical complexity using the SYNTAX score and integrated clinical information using the SYNTAX

Score II to provide a treatment recommendation based on mortality prediction at 4 years: coronary artery bypass grafting (CABG), percutaneous coronary intervention (PCI), or equipoise between CABG and PCI. The primary endpoint was the agreement between heart teams on the revascularization strategy. The secondary endpoint was the impact of fractional flow reserve derived from coronary CTA (FFR_{CT}) on treatment decision and procedural planning. Overall, 223 patients were included. A treatment recommendation of CABG was made in 28% of the cases with coronary CTA and in 26% with conventional angiography. The agreement concerning treatment decision between coronary CTA and conventional angiography was high (Cohen's kappa 0.82, 95% confidence interval 0.74-0.91). The heart teams agreed on the coronary segments to be revascularized in 80% of the cases. FFR_{CT} was available for 869/1108 lesions (196/223 patients). Fractional flow reserve derived from coronary CTA changed the treatment decision in 7% of the patients.
In patients with left main or three-vessel coronary artery disease, a heart team treatment decision-making based on coronary CTA showed high agreement with the decision derived from conventional coronary angiography suggesting the potential feasibility of a treatment decision-making and planning based solely on this non-invasive imaging modality and clinical information.

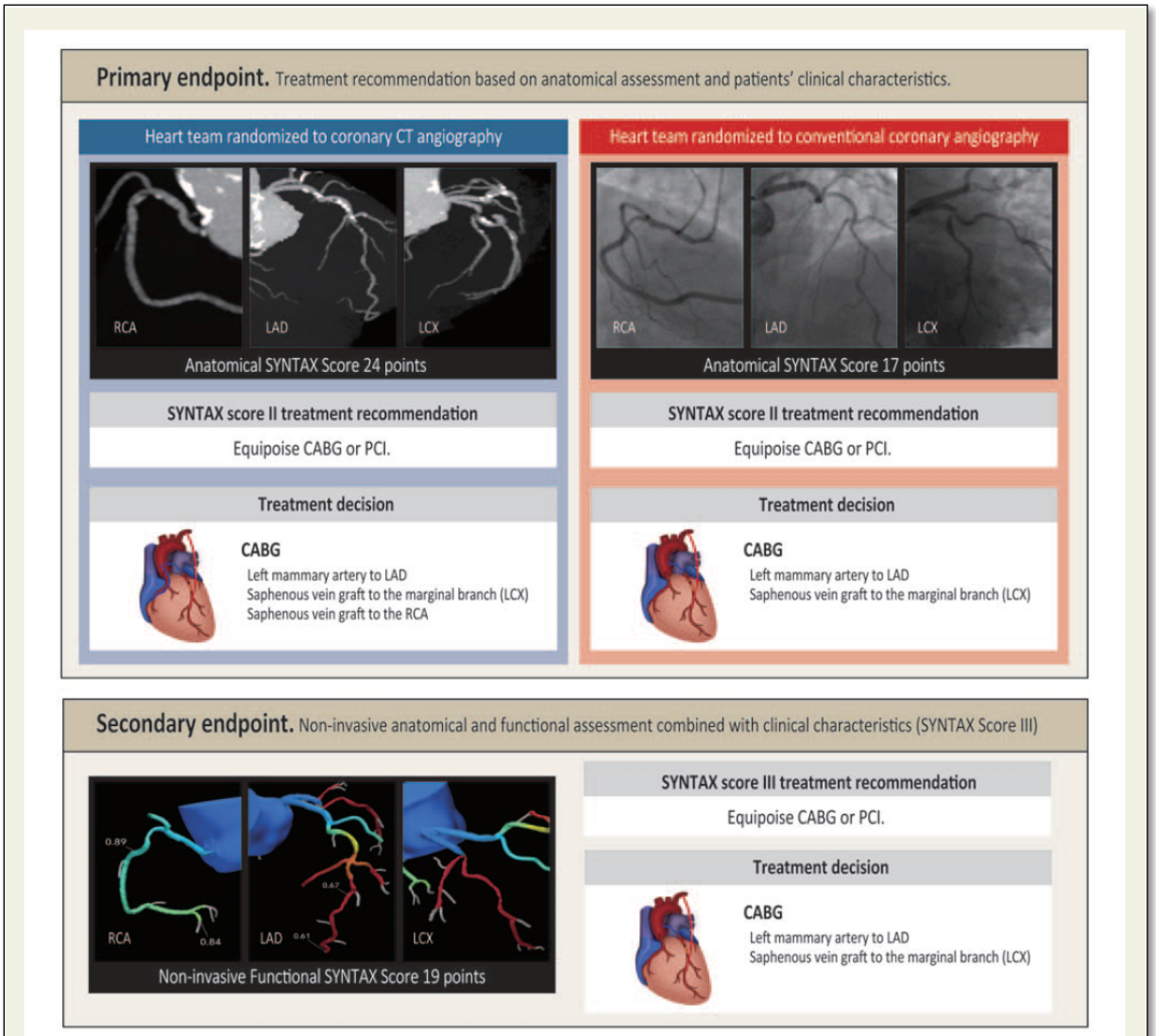

Take home figure Case example of the non-invasive and invasive assessment using the anatomical SYNTAX score and SYNTAX Score II. A 74-year-old man with a creatinine clearance 38 mL/min and left ventricular ejection fraction of 50% without history of chronic obstructive pulmonary disease or peripheral vascular disease. At the top, coronary computed tomography angiography shows three-vessel disease with a coronary narrowings located at the ostium and in the proximal segment of the right coronary artery; two narrowings located in the mid segment of the left anterior descending artery; and one additional narrowing in the proximal segment of the left circumflex artery involving the bifurcation with the first obtuse marginal coronary artery. Conventional angiography revealed also a three-vessel disease with one narrowing located at the proximal segment of the right coronary artery, one narrowing at the mid segment of the left anterior descending artery, and a bifurcation lesion involving the proximal segment of the left circumflex artery and the first obtuse marginal coronary artery. Each coronary narrowing was scored according to the anatomical SYNTAX score and the final anatomical SYNTAX score derived from each modality is shown. With both imaging modalities, the SYNTAX score II recommended either coronary artery bypass graft surgery or percutaneous coronary intervention based on a comparable predicted 4-year mortality. At the bottom, the non-invasive fractional flow reserve derived from coronary computed tomography angiography (FFR_{CT}) is presented. The FFR_{CT} showed that the lesions in the right coronary artery are not haemodynamically relevant, whereas the left anterior descending artery and left circumflex artery have haemodynamically relevant lesions. The treatment recommendation based on coronary computed tomography angiography with FFR_{CT} remained equipoise between coronary artery bypass graft surgery and percutaneous coronary intervention but the treatment planning changed based on the negative FFR_{CT} results in the right coronary artery. CABG, coronary artery bypass graft surgery; LAD, left anterior descending artery; LCX, left circumflex artery; PCI, percutaneous coronary intervention; RCA, right coronary artery.

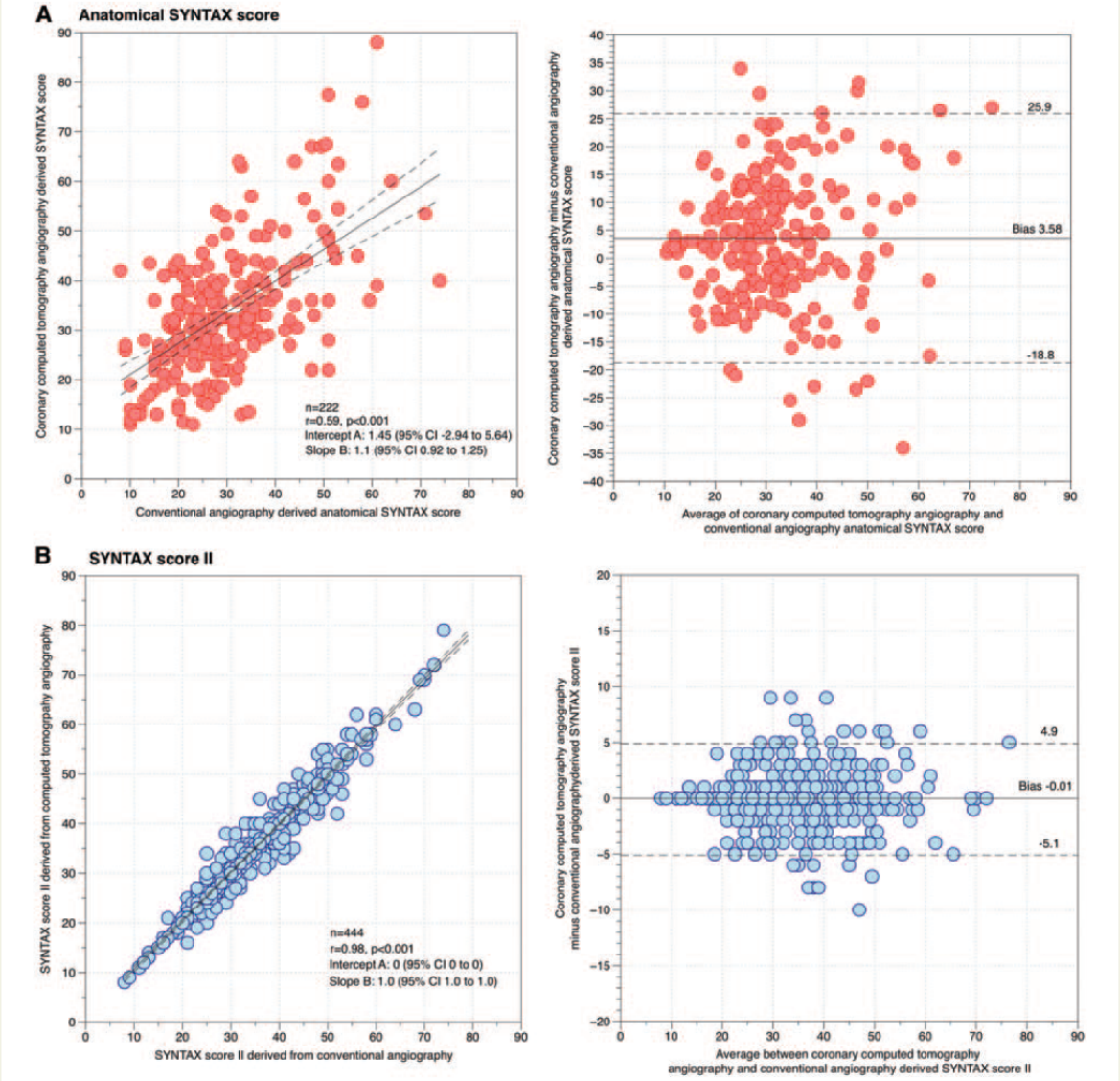

Figure 2 Correlation and agreement on the anatomical SYNTAX score (*A*) and SYNTAX score II (*B*) between coronary computed tomography angiography and conventional angiography.

Impact of Fractional Flow Reserve Derived from Coronary Computed Tomography Angiography on Heart Team Treatment Decision-Making in Patients with Multivessel Coronary Artery Disease: Insights from the SYNTAX III REVOLUTION Trial

Fractional flow reserve (FFR) is a reliable tool for the functional assessment of coronary stenoses. FFR-guided PCI has proven to prevent adverse events[7]. In patients with multivessel disease, FFR_{CT} has shown to have good diagnostic performance with invasive pressure-wire assessment as reference[80]. Moreover, the extent, severity, and functional component of CAD can be objectively quantified using the functional SYNTAX score[80]. The functional SYNTAX score has higher discrimination for clinical events compared with the anatomic SYNTAX score, while reducing inter-observer variability. The calculation of the SYNTAX score III, combining in a noninvasive setting anatomy, physiology and patient's clinical information provides the heart team with individualized risk stratification and treatment recommendation based on the predicted 4-year mortality in patients undergoing PCI or CABG[81].

The SYNTAX III REVOLUTION trial (Synergy Between Percutaneous Coronary Intervention with Taxus and Cardiac Surgery) showed that in patients with left main or 3-vessel CAD treatment decision-making based on coronary computed tomography angiography (CTA) is in high agreement with the decision derived from conventional angiography[82]. However, the influence of FFR_{CT} on treatment decision-making and selection of vessels for revascularization remains to be investigated. Thus, the present study sought to determine the impact of FFR_{CT} on heart team's treatment decision and procedural planning (selection of vessels for revascularization) in patients with left main or 3-vessel CAD.

The trial was an international, multicenter study randomizing 2 heart teams to make a treatment decision between percutaneous coronary interventions and coronary artery bypass grafting using either coronary computed tomography angiography or conventional angiography. The heart teams received the FFR_{CT} and had to make a treatment decision and planning integrating the functional component of the stenoses. Each heart team calculated the anatomic SYNTAX score, the noninvasive functional SYNTAX score and subsequently integrated the clinical information to compute the SYNTAX score III providing a treatment recommendation, that is, coronary artery bypass grafting, percutaneous coronary intervention, or equipoise coronary artery bypass grafting-percutaneous coronary intervention. The primary

objective was to determine the proportion of patients in whom FFR_{CT} changed the treatment decision and planning.

Overall, 223 patients were included. Coronary computed tomography angiography assessment was feasible in 99% of the patients and FFR_{CT} analysis in 88%. FFR_{CT} was available for 1030 lesions (mean FFR_{CT} value 0.64±13). A treatment recommendation of coronary artery bypass grafting was made in 24% of the patients with coronary computed tomography angiography with FFR_{CT}. The addition of FFR_{CT} changed the treatment decision in 7% of the patients and modified selection of vessels for revascularization in 12%. With conventional angiography as reference, FFR_{CT} assessment resulted in reclassification of 14% of patients from intermediate and high to low SYNTAX score tertile.

In patients with 3-vessel coronary artery disease, a noninvasive physiology assessment using FFR_{CT} changed heart team's treatment decision-making and procedural planning in one-fifth of the patients.

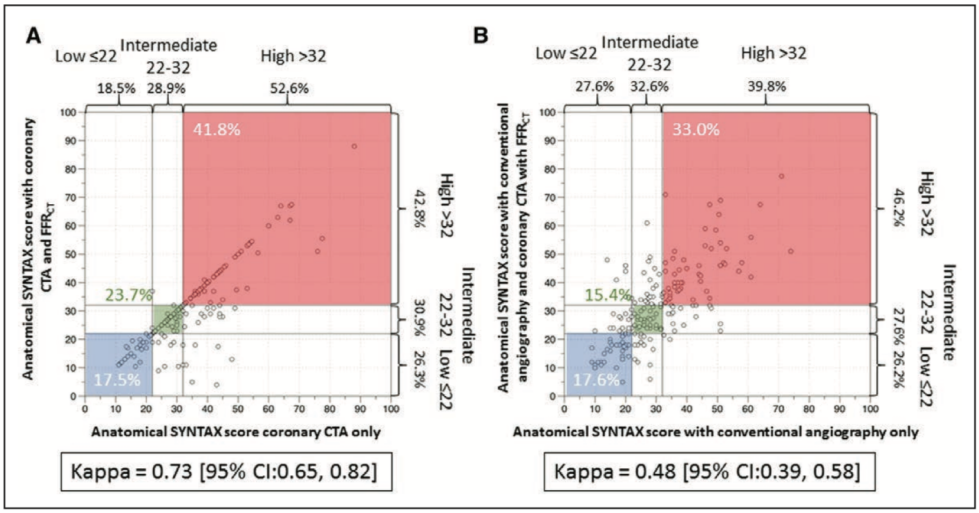

Figure 3. Fractional flow reserve derived from computed tomography (FFR_{CT}) and risk reclassification.
The figure shows the impact of the noninvasive functional SYNTAX score on risk reclassification of patients assessed by coronary computed tomography angiography (CTA; **A**) and invasive coronary angiography (**B**). The red, green, and blue squares show the proportion of patients in whom the 2 imaging techniques are concordant in SYNTAX risk classification, respectively.

Table 3. Level of Agreement Between Conventional Angiography Only Versus Coronary CTA and Conventional Angiography With Functional Assessment by FFR_{CT}

Recommendation Based on Angiography Only	Recommendation Based on Angiography and Coronary CTA With FFR_{CT}		
	CABG Only		PCI Only/Equipoise
CABG only	21.9% (43/196)		3.1% (6/196)
PCI only/equipoise	3.6% (7/196)		71.4% (140/196)
	Number	%, 95% CI	κ, 95% CI
Concordance	183	93.4 (88.9–96.4)	0.82 (0.73–0.92)

Recommendations are based on SYNTAX II Score. CABG indicates coronary artery bypass grafting; CTA, computed tomography angiography; FFR_{CT}, fractional flow reserve derived from computed tomography; and PCI, percutaneous coronary intervention.

Site vs. Core Laboratory Variability in Computed Tomographic Angiography-derived SYNTAX Scores in the SYNTAX III Trial

The SYNTAX score (SS) is recommended for the evaluation of the anatomical complexity and the decision-making process regarding the revascularization strategy[41]. The calculation of the SS derived from coronary CTA has been shown to be accurate with respect to the one derived from ICA assessment[77]. The SYNTAX score II combines the anatomical SS with clinical information providing a treatment recommendation based on mortality prediction at 4 years[83]. The primary report of the SYNTAX III Revolution study showed a high agreement between treatment decision-making based on coronary CTA and the decision derived from ICA with a kappa of 0.82 [95% confidence interval (CI) 0.74–0.91]. The results of the SYNTAX III study endorse an expansion of coronary CTA use in the decision-making process of the optimal revascularization strategy[82]. FFR can add the functional component of CAD to the anatomical SS to calculate the 'functional SYNTAX score' defined as a recalculated SS counting only ischemia producing lesions as assessed by FFR. The latter was reported to be a better predictor of clinical outcome in patients with multivessel coronary artery disease (CAD)[73]. Coronary CTA is capable to non-invasively assess the physiological repercussion of coronary narrowing by means of computational flow dynamics [FFR from CTA (FFR_{CT})[36,38]. In the SYNTAX III Revolution trial, the anatomical and functional SS were calculated by the participating sites, while these SS were also calculated by core laboratory (CL).

The present study investigates the variability between site and core laboratory (CL) calculation of the anatomical SYNTAX score (SS) based on coronary computed tomography angiography (CTA) alone and functional SS based on coronary CTA and fractional flow reserve derived from computed tomography (FFR_{CT}) in the SYNTAX III trial.

The SYNTAX III trial was a multicenter, international study that included 223 patients with three-vessel disease with or without left main involvement. Functional SS was computed by subtracting non-flow limiting stenoses ($FFR_{CT} > 0.80$) from anatomical SS. SS was combined with clinical information to generate the SYNTAX score II (SS II) that provides treatment recommendations. The mean anatomical SS based on coronary CTA alone was 33.4 ± 12.7 by sites and 37.1 ± 13.4 by CL ($P < 0.001$). The mean functional SS based on coronary CTA and FFR_{CT} was 30.5 ± 13.0 by sites and 33.3 ± 13.6 by CL ($P < 0.001$). The intraclass correlation

coefficient was 0.49 [95% confidence interval (CI) 0.37-0.59) in anatomical SS and 0.62 (95% CI 0.52-0.70) in functional SS. The Cohen's κ comparing treatment recommendation between sites and CL was 0.68 (95% CI 0.58-0.78) based on anatomical SS and 0.71 (95% CI 0.60-0.82) based on functional SS.

The mean anatomical SS derived from coronary CTA alone and functional SS based on coronary CTA and FFR_{CT} were higher when assessed by the CL than by the sites themselves. However, substantial agreement in treatment recommendation by SS II between sites and CL was demonstrated.

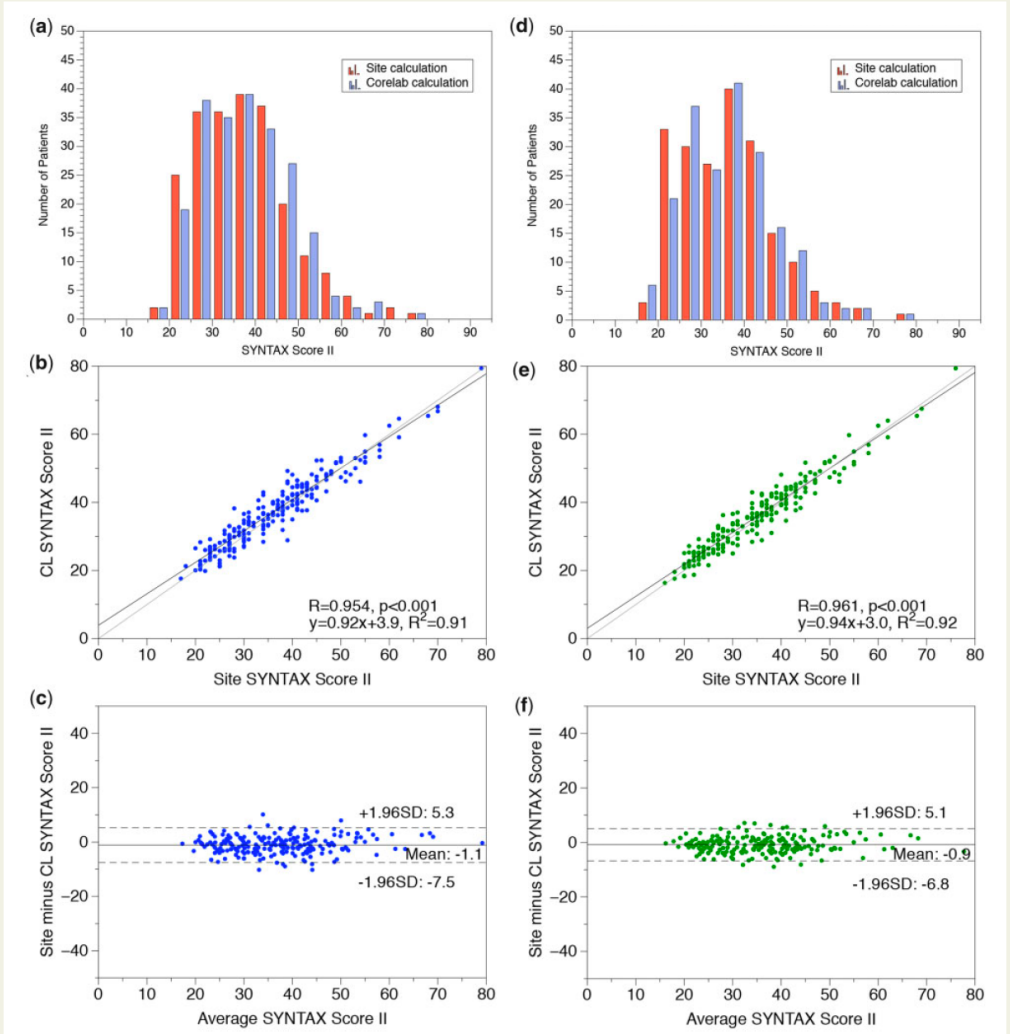

Figure 4 Histogram, correlation, and agreement between sites and CL SYNTAX score II based on either anatomical SS using coronary CTA alone or functional SS using coronary CTA and FFR_{CT}. (*A*) Histogram, (*B*) relationship between the site (*x* axis) and the CL (*y* axis) SYNTAX score II, and (*C*) Bland–Altman plots of the SYNTAX score II based on anatomical SS using coronary CTA alone. (*D*) Histogram, (*E*) relationship between the site (*x* axis) and the CL (*y* axis) SYNTAX score II, and (*F*) Bland–Altman plots of the SYNTAX score II based on functional SS using coronary CTA and FFR_{CT}. Despite initial difference in SYNTAX score (*Figures 2 and 3*), a high degree of agreement was demonstrated in SYNTAX score II in both diagnostic methods. CL, core laboratory; CTA, computed tomography angiography; FFR, fractional flow reserve; SD, standard deviation; SS, SYNTAX score.

Impact of Coronary Calcification Assessed by Coronary CT Angiography on Treatment Decision in Three Vessels CAD Patients: Insights from Syntax III trial

The aim of the current analysis was to determine Syntax Scores based on coronary computed tomography angiography (CCTA)and invasive coronary angiography (ICA) and to assess whether heavy coronary calcification significantly limits the CCTA evaluation and the impact of severe calcification on heart team's treatment decision and procedural planning in patients with three-vessel coronary artery disease (CAD) with or without left main disease.

The SYNTAX III was a multicenter, international study that included patients with three-vessel CAD with or without left main disease. The heart teams were randomized to either assess coronary arteries with coronary CCTA or ICA. We stratified the patients based on the presence of at least one lesion with heavy calcification defined as arc of calcium >180 within the lesion using CCTA. Agreement on the anatomical SYNTAX score and treatment decision was compared between patients with and without heavy calcifications.

Overall, 222 patients with available CCTA and ICA were included in this trial sub-analysis (104 with heavy calcification, 118 without heavy calcification). The mean difference in the anatomical SYNTAX score (CCTA-derived – ICA-derived) was lower in patients without heavy calcifications (mean [-1.96 SD; +1.96 SD] = 1.5 [-19.3; 22.4] versus 5.9 [-17.5; +29.3], p=0.004). The agreement on treatment decision did not differ between patients with (Cohen's Kappa 0.79) or without coronary calcifications (Cohen's Kappa 0.84). The agreement on the treatment planning did not differ between patients with (concordance 80.3%) or without coronary calcifications (concordance 82.8%).

An overall good correlation between CCTA- and ICA-derived Syntax score was found. The presence of heavy coronary calcification moderately influenced the agreement between CCTA and ICA on the anatomical SYNTAX score. However, agreement on the treatment decision and planning was high and irrespective of the presence of calcified lesions.

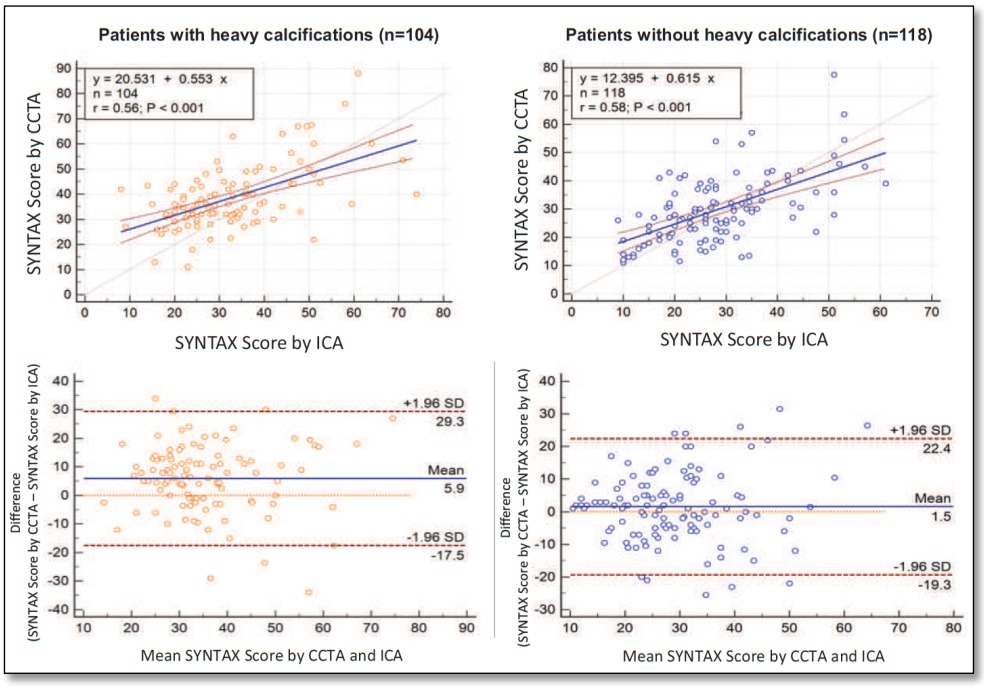

Correlations (upper panels) and differences (bottom panels) between anatomical Syntax Score derived from coronary computed tomography angiography (CCTA) and invasive coronary angiography (ICA) in patients with (left panels) and without (right panels) heavy coronary calcifications.

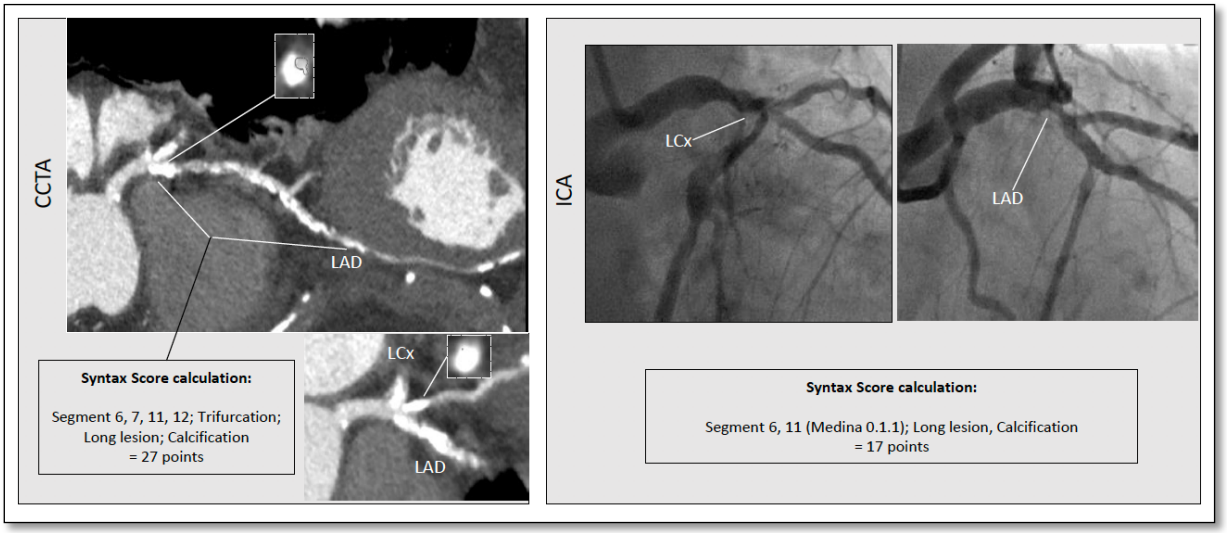

A case of a heavily calcified lesion leading to discrepancy between coronary computed tomography angiography (CCTA)-derived (panel A) and invasive coronary angiography (ICA)-derived (panel B) SYNTAX Scores.

Chapter 3: Coronary CT angiography as a non-invasive alternative to assess coronary plaque characteristics

Chapter introduction

Continuous technological advances in CCTA broadened its role from diagnosing CAD to a tool able to assess plaque characteristics. Indeed, CCTA can quantify the extent of the atherosclerotic process comparable to intra-vascular imaging (IVUS and OCT). This consists of volumetric plaque assessment but also plaque composition evaluation has proven feasible[34,44]. The latter can be important to risk stratify patients with CAD, e.g. adverse plaque characteristics[47–49]. In a first paper, we evaluated whether these last generation CT-scanner have improved coronary plaque volume assessment using IVUS as standard-of-reference.

When severely calcified atherosclerosis is identified, procedural and forethought plaque modification planning could improve PCI results[45]. The improved spatial resolution of whole-heart coverage CT scanner and calcium "removal" by dual-energy CT in latest state-of-the-art scanners has theoretically improved plaque level diagnostics. Calcified plaque volume (in mm^3) can accurately be assessed during catheterization by optical coherence tomography (OCT)[84]. The aim of the second study of this chapter was to investigate the accuracy of last-generation CTA-derived quantification of calcification volume as compared with OCT.

CCTA can accurately identify healthy coronary segments on top of plaque evaluation. As such, coronary CT may emerge as a tool for a comprehensive invasive procedural planning comparable to the use of intra-vascular imaging during PCI. The integration of plaque evaluation, luminal assessment and hemodynamic analysis is described in the last chapter on CT-guided PCI. The current chapter was instrumental to develop the plaque maps and IVUS-like algorithm used in the CT-guided PCI guidance.

Plaque Quantification by Coronary Computed Tomography Angiography using Intravascular Ultrasound as a Reference Standard: A Comparison between Standard and Last Generation Computed Tomography Scanners

The emerging role of coronary computed tomography angiography (CCTA) as a non-invasive tool for atherosclerosis evaluation is supported by data reporting a good correlation between CCTA and intravascular ultrasound (IVUS) for plaque volume quantification[34,35]. Aim of the present study was to evaluate whether a last generation CT-scanner may improve coronary plaque volume assessment using IVUS as standard-of-reference.

From a registry of 1915 consecutive, all-comers, patients who underwent a clinically indicated IVUS evaluation we enrolled 59 patients who underwent CCTA with a 64-slice CT (Group 1) and 59 patients who underwent CCTA with whole-heart coverage CT scanner (Group 2). Patients who underwent CCTA with unfavorable heart rhythm were not excluded from the analysis. Image quality (4-point Likert scale) focused on plaque analysis was evaluated. Plaque volume quantification by CCTA was compared to IVUS. No difference in clinical characteristics was found between Group 1 and Group 2. Plaque volume quantification by CCTA was considered not feasible in 11 plaques of Group 1 and in 4 plaques of Group 2 ($P = 0.09$). Higher correlation for plaque volume quantification by CCTA vs. IVUS was demonstrated in Group 2 when compared with Group 1 ($r = 0.9888$ vs. 0.9499; $P < 0.0001$). The Bland-Altman analysis showed plaque volume overestimation by CCTA of 11.9 mm3 in Group 1 and 4 mm2 in Group 2 ($P < 0.001$). Effective radiation dose of CCTA was significantly lower in Group 2 vs. Group 1 (2.7 ± 0.9 vs. 8.1 ± 3.6 mSv, respectively; $P < 0.001$).

CCTA using a new scanner generation showed to be an accurate non-invasive tool to assess and quantify coronary plaque volume.

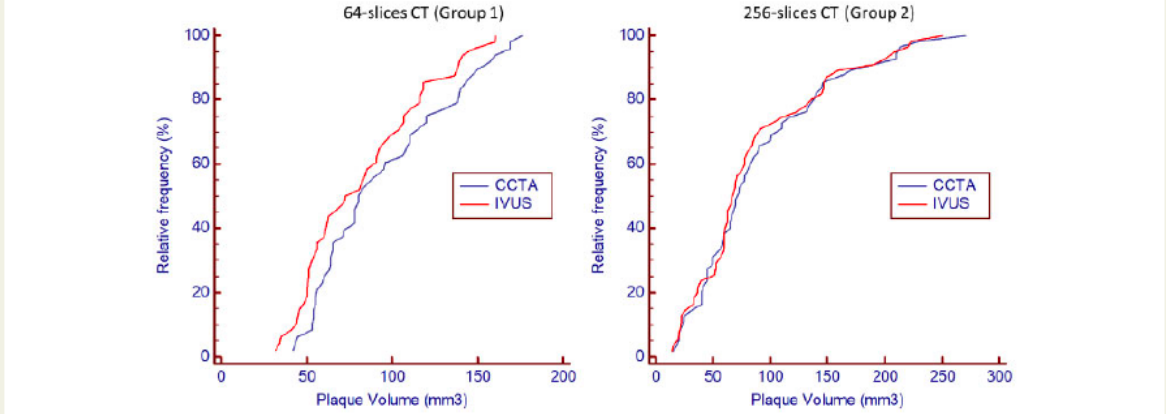

Figure 6 Plaque volume analysis compared by t-test for paired samples expressed as cumulative curves graph showing the overestimation of plaque volume quantification by 64-slices CT vs. IVUS (Group 1) that was significantly reduced by last generation 256-slice CT (Group 2).

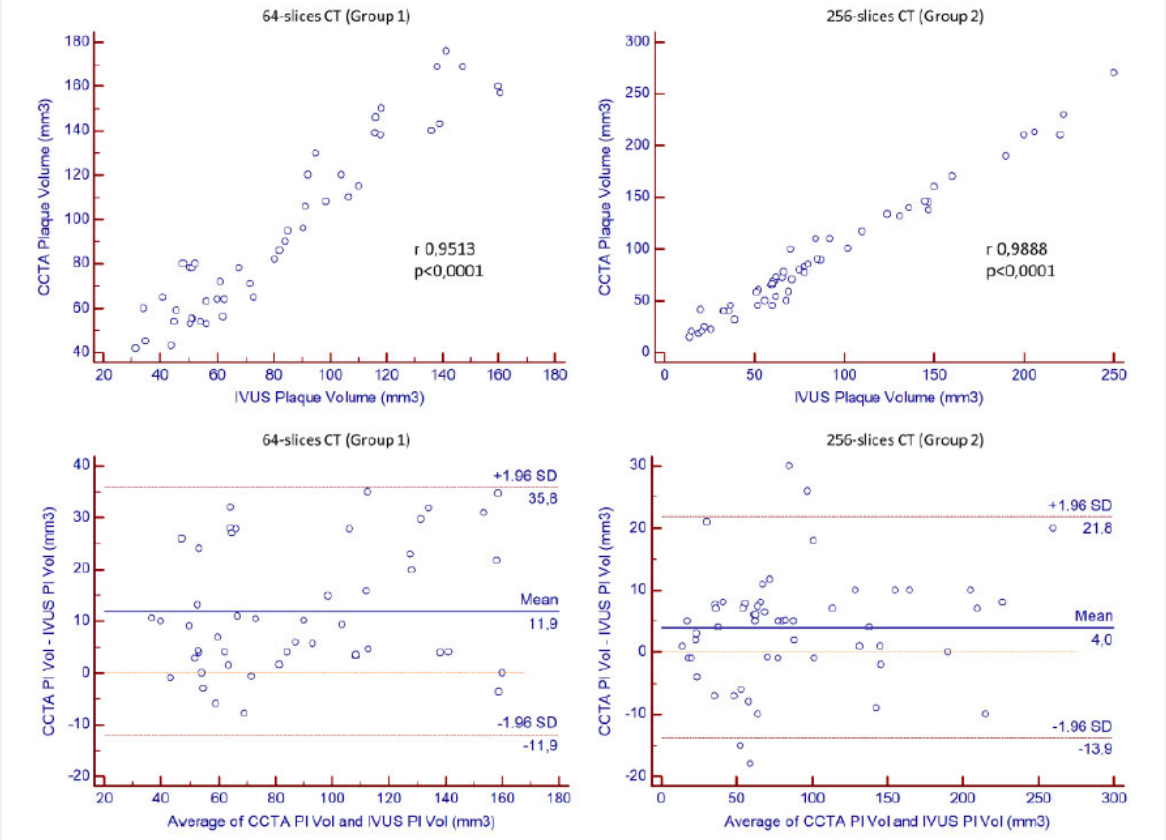

Figure 7 Pearson's correlation and Bland–Altman analysis for plaque volume quantification by CCTA vs. IVUS in 64-slice CT (Group 1) and 256-slice CT (Group 2).

Quantification of Calcium Burden by Coronary CT Angiography Compared to Optical Coherence Tomography

About one third of patients undergoing percutaneous coronary interventions (PCI) have moderate to severe coronary artery calcifications (CAC)[85]. Severe CAC often lead to stent under-expansions and have been linked with poor prognosis following PCI[86,87].

Coronary artery calcifications (CAC) are frequently observed in patients referred for coronary CT angiography (CTA)[44]. Calcification volume (in mm^3) can accurately be assessed during catheterization by optical coherence tomography (OCT)[84]. The aim of the present study was to investigate the accuracy of CTA-derived assessment of calcification volume as compared with OCT.

66 calcified plaques (32 vessels) from 31 patients undergoing OCT-guided PCI with coronary CT acquired as a standard of care were included. Coronary CT and OCT images were matched using fiduciary points. Calcified plaques were reconstructed in three dimensions to calculate calcium volume. A Passing-Bablok regression analysis and the Bland-Altman method were used to assess the agreement between imaging modalities. Twenty-seven left anterior descending arteries and 5 right coronary arteries were analyzed. Median calcium volume by CTA and OCT were 18.23 mm^3 [IQR 8.09, 36.48] and 10.03 mm^3 [IQR 3.6, 22.88] respectively; the Passing-Bablok analysis showed a proportional without a systematic difference (Coefficient A 0.08, 95% CI - 1.37 to 1.21, Coefficient B 1.61, 95% CI 1.45 to 1.84) and the mean difference was 9.69 mm3 (LOA - 10.2 to 29.6 mm^3). No differences were observed for minimal lumen area (Coefficient A 0.07, 95% CI - 0.46 to 0.15, Coefficient B 0.85, 95% CI 0.64 to 1.2).

CTA volumetric calcium evaluation overestimates calcium volume by 60% compared to OCT. This may allow for an appropriate interpretation of calcific burden in the non-invasive setting. Even in presence of calcific plaques, a good agreement in the MLA assessment was found. Coronary CT may emerge as a tool to quantify calcium burden for invasive procedural planning.

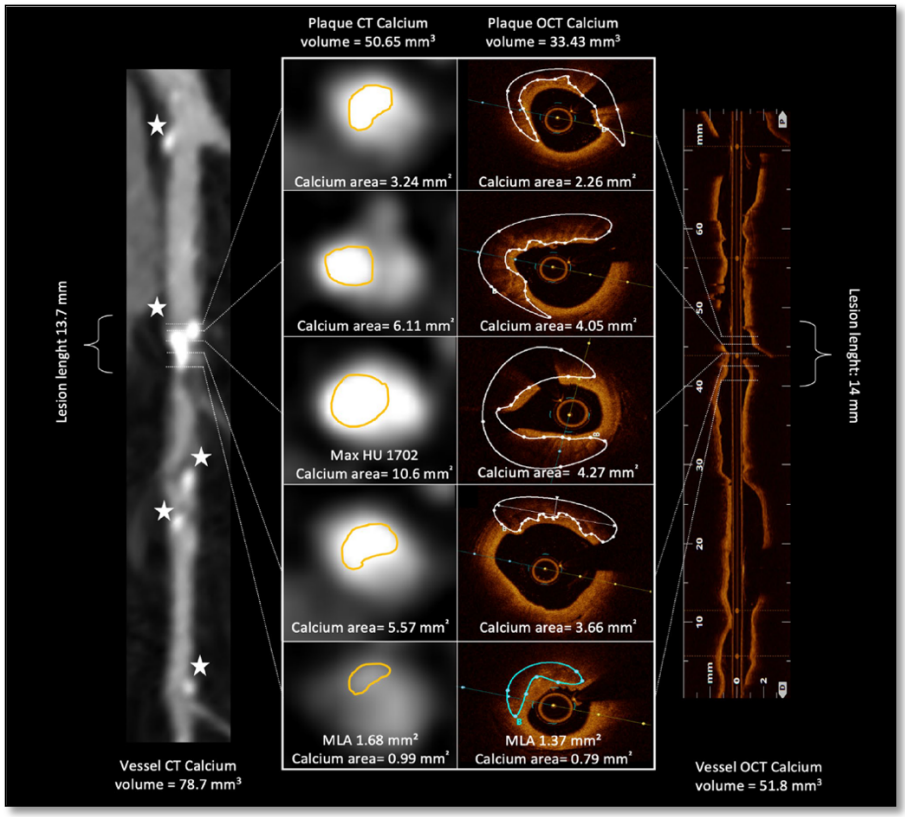

Fig. 1 The left side shows a straight multiplanar reconstruction derived from coronary CT angiography of a left anterior descending artery with five calcified plaques (white stars). Representative cross sections with the corresponding calcium areas are shown. On the right side, the same vessel is depicted with optical coherence tomography. Matched cross sections with CT show the calcium area. Calcium volume is presented at the plaque and vessel levels.

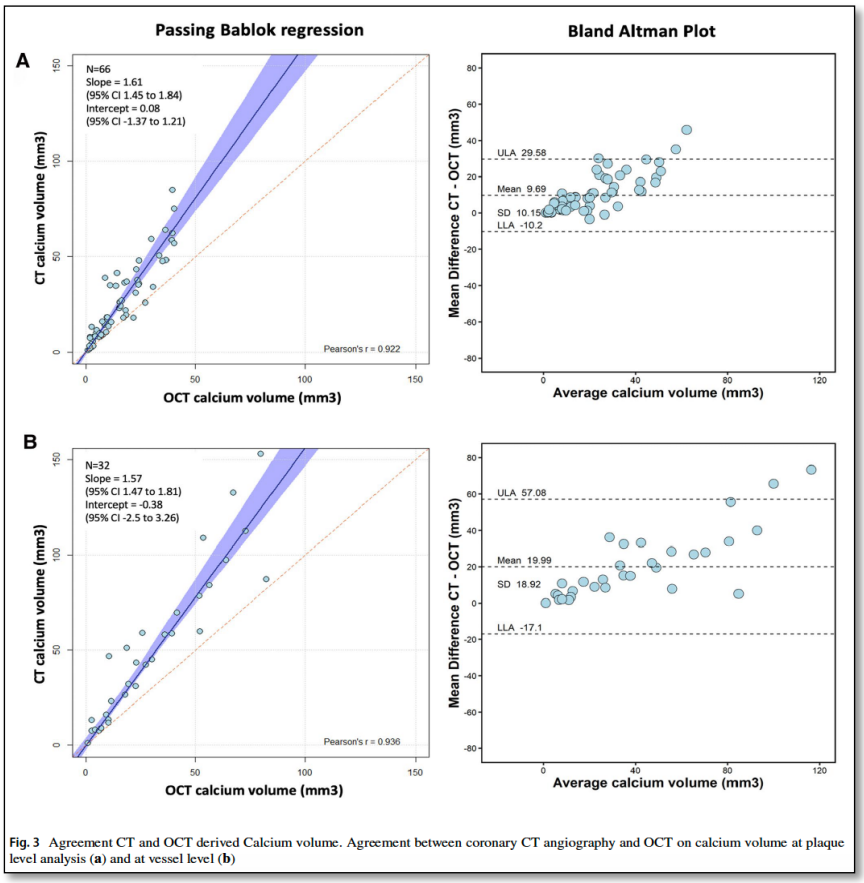

Fig. 3 Agreement CT and OCT derived Calcium volume. Agreement between coronary CT angiography and OCT on calcium volume at plaque level analysis (**a**) and at vessel level (**b**)

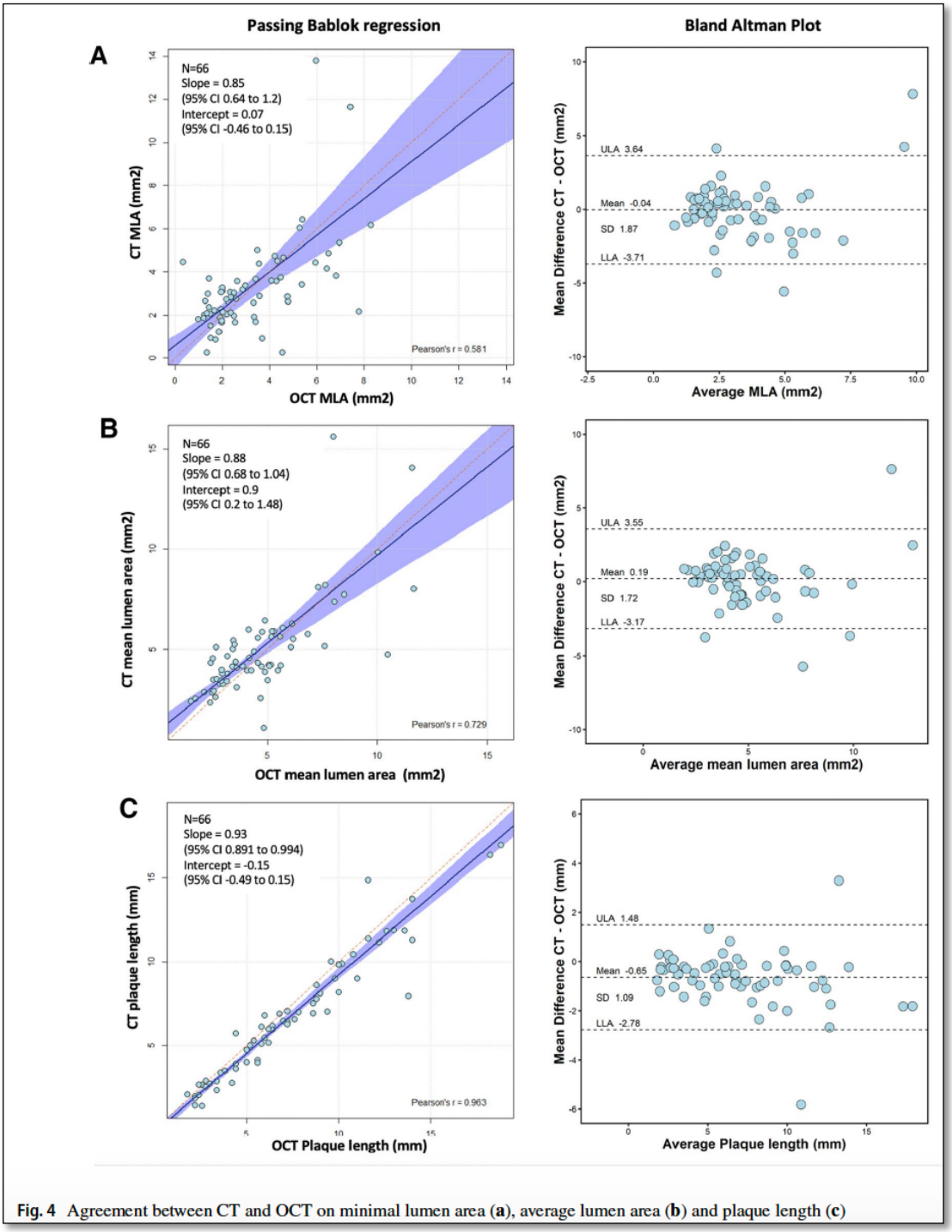

Fig. 4 Agreement between CT and OCT on minimal lumen area (**a**), average lumen area (**b**) and plaque length (**c**)

Chapter 4: Non-invasive assessment of the hemodynamic impact of CAD

Chapter introduction

In chapter four, we highlight the potential of the use of CT perfusion in the assessment of stented segments. CCTA and FFR_{CT} are technically hampered to assess in-stent restenosis by beam hardening artifacts caused by metallic stents[88,89]. CT perfusion has the potential to overcome these anatomical limitations. We investigated whether the combined anatomical and functional assessment with CCTA plus CTP may have higher diagnostic performance as compared to CCTA alone in identifying stented patients with significant ISR or CAD progression. In the attached review Sonck et Conte et al. reviewed the current evidence and position of FFR_{CT} and CT perfusion for the evaluation of the functional impact of coronary artery stenosis by cardiac CT.

Angiography-derived FFR has also the potential to improve the interpretation of the hemodynamic significance of a given coronary narrowing as compared to ICA. 3D-QCA enables to construct a patient-specific coronary geometry that can be further processed by computational fluid dynamics (CFD) to perform blood flow simulations that can derive pressure drops. The simulated FFR can be derived either from blood flow simulation using CFD or by a mathematical approach derived from the Lance Gould equation or by rapid pressure-flow simulations[90,91]. Angiography-derived FFR has been shown to provide similar risk stratification as with three-vessel invasive pressure wire interrogation[92]. As such, for patients with complex CAD, angiography-derived FFR could be instrumental to assess multi-vessel lesion significance. Pre-CABG, angiography-derived FFR could aid in demonstrating which vessel should be bypassed or not. Post-CABG, angiography-derived FFR provides insights in native coronary CAD progression. Moreover, accelerated progression of atherosclerosis in grafted native coronary arteries after CABG has been described before[93,94]. In our research paper, we aimed to characterize the functional progression of CAD in native vessels of patients treated with CABG in grafted and nongrafted vessels and to assess the relationship between preoperative angiography-derived FFR values and graft occlusion.

Likewise, post-heart transplant patients are systematically scheduled for ICA to detect cardiac allograft vasculopathy (CAV). Nowadays, a grading system based on coronary angiography is recommended by the international society of heart and lung transplantation (ISHLT) to evaluate the severity and extent of CAV[95]. However, coronary angiography lacks the resolution to diagnose early as well as diffuse stages of CAV. Also, intra-vascular imaging (IVUS) lacks the ability to assess the functional consequences of CAV. Fractional Flow Reserve (FFR) captures the hemodynamic consequences of vascular disease. In heart

transplant patients, an abnormal epicardial physiology on the basis of an FFR <0.90 predicts worse clinical outcome. Angiography-based FFR (vFFR) estimates have been shown to perform well against invasive FFR as shown in our presented review and meta-analysis on the diagnostic performance of angiography-derived FFR. Therefore, we aimed to evaluate CAV by comparing the standard ISHLT grading system with functional vFFR measurements. We also aimed at evaluating if the functional progression of CAV was captured by the angiography-derived FFR. If so, we could speculate that vFFR may be a helpful tool in the evaluation of CAV and risk stratification post heart transplantation. For this, vessel FFR has the advantage to abolish the need for invasive physiology or intra-vascular imaging.

In the Future Culprit study, we evaluated the interaction between wall shear stress (WSS), lesion severity and pressure gradients. Wall shear stress has been shown to be predictive for future plaque rupture and coronary events. In the EMERALD study, Koo et al. have depicted lower FFR_{CT} and higher ΔFFR_{CT}, WSS, and axial plaque stress in culprit lesions from patients with a CCTA available from before the acute coronary syndrome occurred[96]. In our angiographic analysis, the combination of luminal stenoses, pressure gradients derived from vFFR and WSS predicted the occurrence of ACS. Moreover, the topological shear variation index, representing the variation in contraction-expansion action of endothelial shear forces along the cardiac cycle, improved the discrimination of lesion prone for plaque rupture and ACS. Addition of accessible state-of-the-art computational fluid dynamics (CFD) on a standard computer to ICA and QCA-like software with vessel FFR (vFFR) could facilitate the adoption of WSS in a clinical setting. Also, the limited time necessary to calculate the WSS using the proposed algorithm could allow for the identification of coronary plaques at risk comparable to the approach based on CCTA and FFR_{CT}.

Rationale and Design of Advantage (Additional Diagnostic Value of CT Perfusion over Coronary CT Angiography in Stented Patients with Suspected In-stent Restenosis or Coronary Artery Disease Progression) Prospective Study

Recent studies demonstrated a significant improvement in the diagnostic performance of coronary CT angiography (CCTA)[97,98]. However, coronary stent assessment is still challenging, especially because of beam-hardening artifacts due to metallic stent struts and high atherosclerotic burden of non-stented segments[88,89]. Adenosine-stress myocardial perfusion assessed by CT (CTP) recently demonstrated to be a feasible and accurate tool for evaluating the functional significance of coronary stenoses in patients with suspected coronary artery disease (CAD)[99–101]. Yet, scarce data are available on the performance of CTP in patients with previous stent implantation[102].

We aim to assess the diagnostic performance of CCTA alone, CTP alone and CCTA plus CTP performed with a new scanner generation using quantitative invasive coronary angiography (ICA) and invasive fractional flow reserve (FFR) as standard of reference.

We will enroll 300 consecutive patients with previous stent implantation, referred for non-emergent and clinically indicated invasive coronary angiography (ICA) due to suspected ISR or progression of CAD in native coronary segments. All patients will be subjected to stress myocardial CTP and a rest CCTA. The first 150 subjects will undergo static CTP scan, while the following 150 patients will undergo dynamic CTP scan. Measurement of invasive FFR will be performed during ICA when clinically indicated.

The primary study end points will be: 1) assessment of the diagnostic performance (diagnostic rate, sensitivity, specificity, positive predictive value, negative predictive value and diagnostic accuracy) of CCTA, CTP, combined CCTA-CTP and concordant CCTA-CTP vs. ICA as standard of reference in a territory-based and patient-based analysis; 2) assessment of sensitivity, specificity, positive predictive value, negative predictive value and diagnostic accuracy of CCTA, CTP, combined CCTA-CTP and concordant CCTA-CTP vs. invasive FFR as standard of reference in a territory-based analysis.

The ADVANTAGE study aims to provide an answer to the intriguing question whether the combined anatomical and functional assessment with CCTA plus CTP may have higher

diagnostic performance as compared to CCTA alone in identifying stented patients with significant ISR or CAD progression.

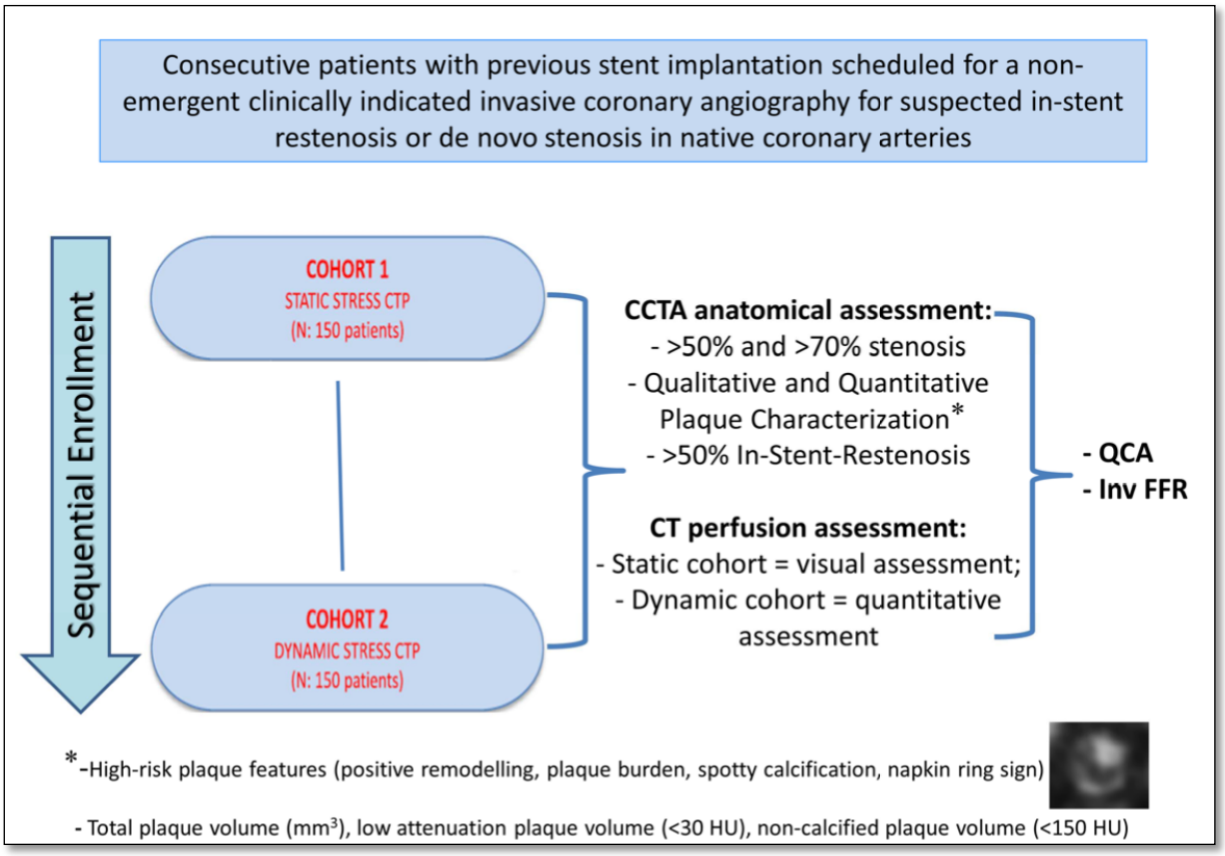

CT Perfusion vs Coronary CT Angiography in Patients with Suspected In-stent Restenosis or CAD Progression

The goal of this study was to assess the diagnostic performance of coronary computed tomography angiography (CTA) alone, adenosine-stress myocardial perfusion assessed by computed tomography (CTP) alone, and coronary CTA + CTP by using a 16-cm Z-axis coverage scanner versus invasive coronary angiography (ICA) and fractional flow reserve (FFR) as the clinical standard.

Diagnostic performance of coronary CTA for in-stent restenosis detection is still challenging. Coronary computed tomography angiography (CTA) is generally not recommended in patients with coronary stents due to artifacts resulting from metallic stent struts[103]. Recent evolutions in CT technology have dramatically improved image quality and broadened the potential applications including the improved combined CCTA and perfusion imaging[97,98]. Recently, CTP showed additional diagnostic power over coronary CTA in patients with suspected coronary artery disease[104]. However, few data are available on CTP performance in patients with previous stent implantation[102].

Consecutive stable patients with previous coronary stenting referred for ICA were enrolled. All patients underwent stress myocardial CTP and rest CTP + coronary CTA. Invasive FFR was performed during ICA when clinically indicated. The diagnostic rate and diagnostic accuracy of coronary CTA, CTP, and coronary CTA + CTP were evaluated in stent-, territory-, and patient-based analyses.

In the 150 enrolled patients (132 men; mean age 65.1 ± 9.1 years), the CTP diagnostic rate was significantly higher than that of coronary CTA in all analyses (territory based [96.7% vs. 91.1%; $p < 0.0001$] and patient based [96% vs. 68%; $p < 0.0001$]). When ICA was used as gold standard, CTP diagnostic accuracy was significantly higher than that of coronary CTA in all analyses (territory based [92.1% vs. 85.5%, $p < 0.03$] and patient based [86.7% vs. 76.7%, $p < 0.03$]). The concordant coronary CTA + CTP assessment exhibited the highest diagnostic accuracy values versus ICA (95.8% in the territory-based analysis). The diagnostic accuracy of CTP was significantly higher than that of coronary CTA (75% vs. 30.5%; $p < 0.001$). The radiation exposure of coronary CTA + CTP was 4.15 ± 1.5 mSv.

In patients with coronary stents, CTP significantly improved the diagnostic rate and accuracy of coronary CTA alone compared with both ICA and invasive FFR as gold standard.

CENTRAL ILLUSTRATION Diagnostic Accuracy of Coronary CTA, CTP, Combined and Concordant Coronary CTA + CTP Versus QCA and Invasive FFR

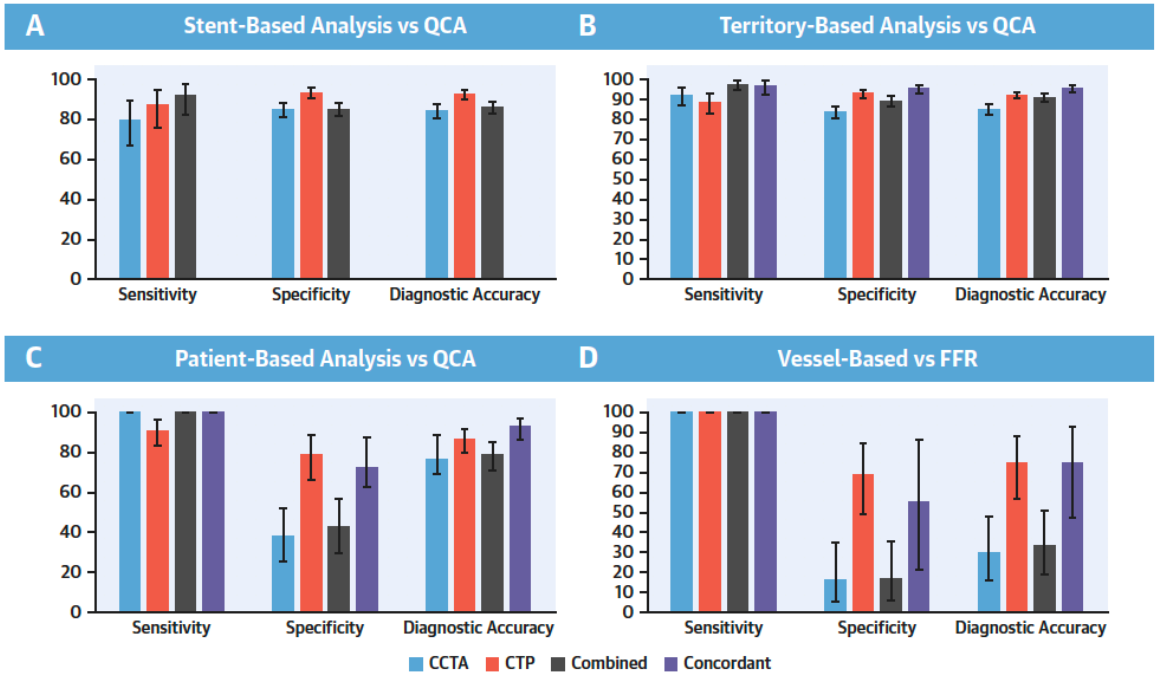

Andreini, D. et al. J Am Coll Cardiol Img. 2019;■(■):■–■.

Comparison of the sensitivity, specificity, and diagnostic accuracy between coronary computed tomography angiography (CTA), computed tomography perfusion (CTP), and combined and concordant coronary CTA + CTP versus quantitative coronary angiography (QCA) in **(A)** a vessel-based, **(B)** territory-based, and **(C)** patient-based analysis. **(D)** Comparison of the diagnostic accuracy of coronary CTA, CTP, and combined and concordant coronary CTA + CTP versus invasive fractional flow reserve (FFR) in a vessel-based analysis.

Contents lists available at ScienceDirect

International Journal of Cardiology

journal homepage: www.elsevier.com/locate/ijcard

FFR_{CT} and CT perfusion: A review on the evaluation of functional impact of coronary artery stenosis by cardiac CT

Edoardo Conte [a,1], Jeroen Sonck [b,c,1,2], Saima Mushtaq [a], Carlos Collet [b], Takuya Mizukami [b], Emanuele Barbato [b,c], Alessandra Tanzilli [d], Flavia Nicoli [a], Bernard De Bruyne [b,e], Daniele Andreini [a,f,*]

[a] Monzino Cardiology Center, IRCCS, Milan, Italy
[b] Cardiovascular Center Aalst, OLV Clinic, Aalst, Belgium
[c] Department of Advanced Biomedical Sciences, University of Naples, Federico II, Naples, Italy
[d] Sapienza University, Policlinico Umberto I, Rome, Italy
[e] Department of Cardiology, Lausanne University Center Hospital, Lausanne, Switzerland
[f] Department of Clinical Sciences and Community Health, Cardiovascular Section, University of Milan, Milan, Italy

ARTICLE INFO

Article history:
Received 28 March 2019
Received in revised form 14 June 2019
Accepted 5 August 2019
Available online xxxx

Keywords:
Myocardial CT perfusion
FFR_{CT}
Cardiac CT
Coronary artery disease

ABSTRACT

Coronary computed tomography angiography (CCTA) is at the frontline of the diagnostic strategies to detect coronary artery disease (CAD). Anatomical information have proven to be insufficient to detect hemodynamic significant epicardial stenosis. In the present invited review we discuss on FFR_{CT} and stress CTP, emerging technologies for an accurate and comprehensive evaluation of patients with suspected CAD, offering both anatomical (i.e. luminal and plaque) and functional assessment in one single technique.

1. Introduction

The Prospective trials PROMISE and SCOT-HEART have demonstrated the incremental value of coronary computed tomography angiography(CCTA) over conventional practice in investigating patients with suspected angina [1–2] Relying only of anatomical information with non-invasive or invasive coronary angiography(ICA) have proven to be insufficient to detect hemodynamic significant epicardial stenosis [3]. Basic principles, current evidence and future perspectives of FFR_{CT} and CTP, both static and dynamic, are the main topics of the present expert review, whose aim is to provide an updated overview on the functional evaluation of CAD by CCTA. Even if this is not a systematic review or a meta-analysis, in order to provide a comprehensive overview of literature on these fields, we systematically searched on PubMed using the following terms: "FFR_{CT}", "CT-derived fractional flow reserve", "myocardial CTP", "static CTP", and "dynamic CTP". Previous systematic reviews and meta-analysis were evaluated and reported, while animal studies and human studies enrolling <30 patients were excluded from the present review.

2. Fractional flow reserve derived from CT - FFR_{CT}

2.1. Technical principles

Fractional Flow Reserve (FFR) is the ratio of hyperemic flow in the presence of an epicardial stenosis to hyperemic flow in the absence of this epicardial stenosis. In clinical practice, FFR is derived from pressure i.e. the ratio of distal to proximal coronary pressures [4]. Current guidelines emphasize the role of invasive FFR to determine the functional significance of a coronary stenosis [5]. This recommendation is based on clinical benefit observed with FFR guidance in randomized clinical trials. Fractional flow reserve derived from CT (FFR_{CT}) is based on the application of computational flow dynamics to images extracted from CCTA [6–7] (Fig. 1). Three principles form the basis for the coronary blood flow simulation to calculate FFR_{CT}. First, baseline coronary flow depends on myocardial oxygen demand and resting flow can be computed accounting for myocardial territory-specific ventricular mass [8–9]. Second, the resistance of the microcirculatory bed at rest is inversely, not linearly, proportional to the size of the feeding vessel, meaning that vessels size follows to the amount of flow they carry [10]. Third, the coronary microcirculation has a predicable response to adenosine. Based

* Corresponding author at: Via C. Parea 4, 20138 Milan, Italy.
E-mail address: daniele.andreini@ccfm.it (D. Andreini).
[1] Equally contributed to the manuscript.
[2] Dr. Sonck has been supported by a research grant provided by the Cardiopath PhD program.

https://doi.org/10.1016/j.ijcard.2019.08.018
0167-5273/

Please cite this article as: E. Conte, J. Sonck, S. Mushtaq, et al., FFRCT and CT perfusion: A review on the evaluation of functional impact of coronary artery stenosis ..., International Journal of Cardiology, https://doi.org/10.1016/j.ijcard.2019.08.018

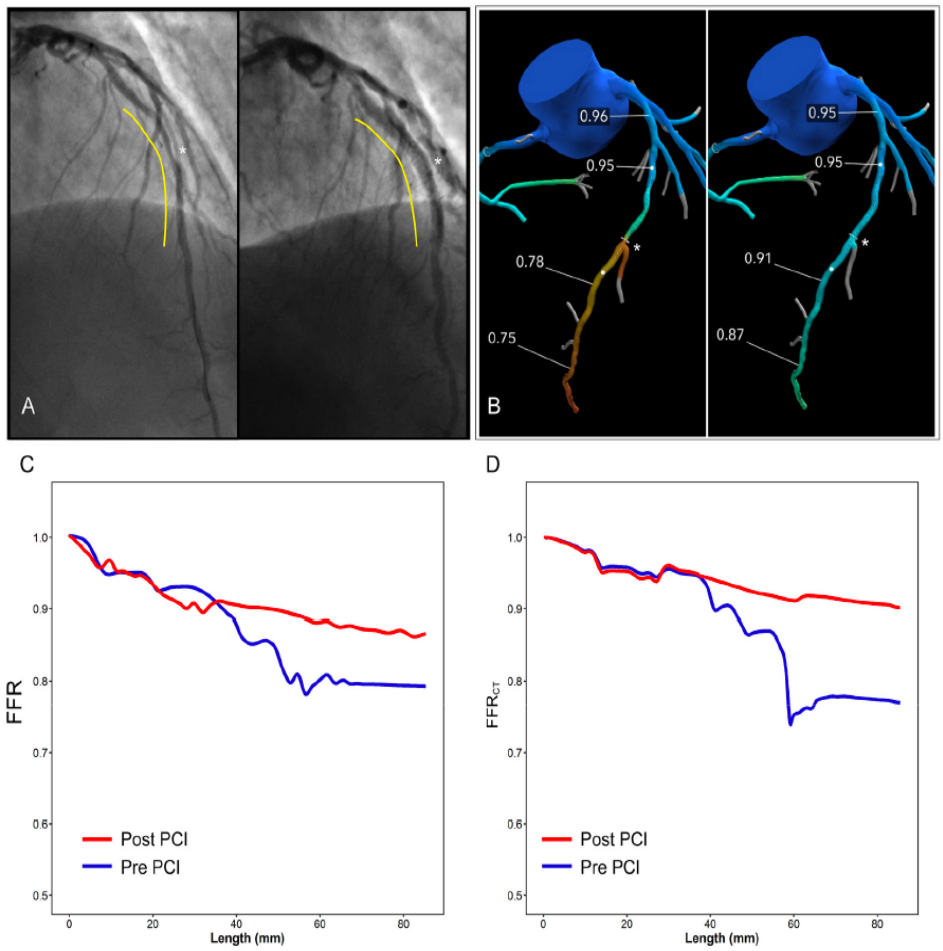

Fig. 1. Case example of invasive and non-invasive FFR pullbacks pre- and post-PCI and of the use of the HeartFlow Planner. Panel A left shows a lesion in the mid-LAD (DS 40% and lesion length 34 mm by QCA) (yellow line) and the result (A right panel) after PCI with a 3.0/38 mm stent. The HeartFlow analysis (panel B left and panel D blue line) suggested a hemodynamic significant disease with pressure drop in the mid LAD and distal FFR of 0.75. Invasive FFR confirmed a distal FFR of 0.75 (panel C blue line). Virtual PCI (panel B right) using the HeartFlow Planner enables remodellation of the luminal geometry of the diseased mid segment and recomputation of the post-PCI FFR_{CT} with a predicted, non-invasive post-PCI FFR of 0.87 (panel B right and panel D red line). Invasive FFR post-PCI reached 0.87 (panel C red line). The virtual pullback curves of FFR_{CT} pre and post-PCI with the resulting increase in vessel conductance post-PCI are depicted in panel D. In this particular case the gain in conductance was similar between non-invasive and invasive pullbacks. (For interpretation of the references to colour in this figure legend, the reader is referred to the web version of this article.)

on these principles and using 3D patient-specific luminal geometries, a volumetric finite element mesh is used to simulate blood flow incorporating the fluid properties of blood. FFR_{CT} is then defined as the computed mean coronary pressure distal to a lesion divided by the mean blood pressure in the aorta under conditions of simulated maximal hyperemia [6].

2.2. Overview of the current evidence

2.2.1. Clinical validation

The studies addressing the clinical validation of FFR_{CT} are shown in Table 1. FFR_{CT} improved stenosis evaluation in terms of prediction of functional significance compared to anatomical evaluation alone. These studies used invasive FFR as standard of reference and applied similar cut-off for lesion significance (<0.80 for both modalities) [11–13]. In a recent diagnostic performance meta-analysis, FFR_{CT} showed 82% diagnostic accuracy [14]. FFR_{CT} has been tested in the broad spectrum of CAD. In three vessels CAD, the SYNTAX-II FFR_{CT} confirmed high accuracy with an AUC of 0.85(95% CI:0.79–0.9) with instantaneous wave-free ratio as a reference [15]. These studies used the Heart Flow (Redwood City, California) technology.

Recently, other approaches like on-site computed CT-fractional flow reserve (CT_{FFR}) and non- invasive instantaneous wave-free ratio using CCTA (iFR_{CT}) have been developed. Initial retrospective studies have shown moderate correlation with invasive FFR.

2.2.2. FFR_{CT}: Real-world use and safety

The PLATFORM was a pragmatic trial including stable, symptomatic patients with planned invasive or non-invasive evaluation of suspected CAD. Patients were then subdivided to be evaluated either with usual care or CCTA with FFR_{CT} as diagnostic strategy. FFR_{CT} significantly reduced the rate of ICA without obstructive CAD (73.3% vs. 12.4%, risk difference 60.8% CI 53.0–68.7%, $p < 0.001$). As such, 61% of invasive coronary angiographies showing no obstructive epicardial disease were deferred. In addition, an increasing rate of patients were revascularized based on coronary physiology (95% CCTA/FFR_{CT} vs. 55% usual care) [16]. A CCTA/FFR_{CT} diagnostic work-up reduced costs. At one year patients who were in the planned invasive test group, FFR_{CT}–

Please cite this article as: E. Conte, J. Sonck, S. Mushtaq, et al., FFRCT and CT perfusion: A review on the evaluation of functional impact of coronary artery stenosis ..., International Journal of Cardiology, https://doi.org/10.1016/j.ijcard.2019.08.018

Table 1
Overview of FFR_{CT} studies.

		Sites	Regions	Study design	Population	Primary endpoint published	FFR_{CT} version used	Primary endpoint/ objective
DISCOVER-FLOW	103 pts. (159 vessels)	4	US, Korea, Latvia	Prospective	Pts with suspected or known CAD	Nov 2011 JACC	pre-1.x	To determine the diagnostic performance of noninvasively derived FFR_{CT} using invasive FFR as the gold standard
DEFACTO	252 pts. (407 vessels)	17	US, Canada, Korea, Europe	Prospective	Pts with suspected or known CAD	Aug 2012 JAMA	pre-1.x	To determine the diagnostic performance of noninvasively derived FFR_{CT} using invasive FFR as the gold standard
NXT	254 pts. (484 vessels)	10	Europe, Korea, Japan, Australia	Prospective	Pts with suspected stable CAD	Apr 2014 JACC	1.x	To determine the diagnostic performance of noninvasively derived FFR_{CT} using invasive FFR as the gold standard
PLATFORM	584 pts	11	Europe	Prospective consecutive cohort	Pts with stable chest pain, primary endpoint required planned ICA	Aug 2015 EHJ	1.x	To determine the impact of using a pathway of CTA ± FFR_{CT} instead of usual care on ICA showing no obstructive disease
RIPCORD FFR_{CT}	200 pts	11	Europe, Korea, Japan, Australia	Retrospective analysis of NXT study	Pts with suspected stable CAD	Oct 2016 JACC Imaging	1.x	To determine during a case review how management plan changes using cCTA alone compared to cCTA + FFR_{CT}
PROMISE FFR_{CT} sub study	181 analyzable cases	Analyzable cases came from 69 sites	US, Canada	Retrospective case review	Pts from the PROMISE study referred for ICA w/in 90 days of cCTA	Apr 2017 JACC Imaging	1.x	To determine if FFR_{CT} predicts revasc and outcomes and if its addition improves efficiency of referral to ICA
Syntax II sub study	77 pts	22	Europe	Subgroup analysis of a prospective study	Pts with 3 vessel disease by ICA	May 2018 JACC	1.x	To assess the feasibility of and validate the noninvasive functional SYNTAX score (FSS) derived from cCTA with FFR_{CT}
ADVANCE	5083 pts	38	US, Canada, Europe, Japan	Prospective registry	Pts with suspected stable CAD	Aug 2018 EHJ	1.x & 2.x	To determine if treatment plan changes using cCTA alone compared to cCTA + FFR_{CT}, as assessed by a core lab
Syntax III Revolution	223 pts	6	Europe	Prospective RCT	Pts with left main or 3 vessel disease by ICA	Sep 2018 EHJ	1.x & 2.x	To determine, in blinded fashion, the agreement of revascularization strategy based either on cCTA + FFR_{CT} or conventional angiography
PACIFIC FFR_{CT} sub study	208 pts	1	Europe	Retrospective analysis of a prospective study	Pts with suspected stable CAD	Jan 2019 JACC	2.x	To evaluate diagnostic performance of FFR_{CT} using invasive FFR as the gold standard, and compare to cCTA, SPECT, and $[^{15}O]H_2O$ PET.

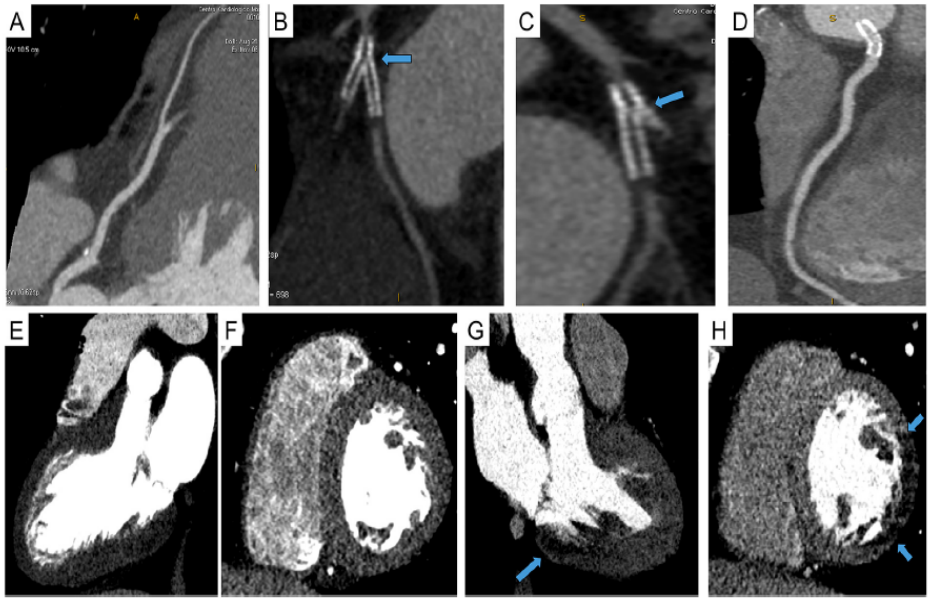

Fig. 2. A patients with previous stent on LCX and RCA underwent stress-rest CTP. LAD (panel A) was free from significative coronary disease and previous stent on ostial RCA was patent (panel D); on the contrary previous a significative intra-stent restenosis was evident on LCX-MO at CCTA (panel B–C). Rest CTP showed no myocardial perfusion deficit (panel E–F), while on stress CTP a transmural hypo-enhanced region appeared on posterolateral wall, suggesting inducible myocardial perfusion deficit (panel G–H).

Please cite this article as: E. Conte, J. Sonck, S. Mushtaq, et al., FFRCT and CT perfusion: A review on the evaluation of functional impact of coronary artery stenosis ..., International Journal of Cardiology, https://doi.org/10.1016/j.ijcard.2019.08.018

guided strategy cost was $8127 vs. $12,145 with a usual care strategy ($p < 0.0001$), not accounting for the cost of the FFR_{CT} test. The mean costs remained 26% lower among the FFR_{CT} patients than among usual care patients ($9036 vs. $12,145, $p < 0.0001$) when factoring in the cost of the FFR_{CT} analysis [16].

In the multicenter ADVANCE Registry, a large prospective examination of using FFR_{CT} diagnostic pathway in real-world settings(5083 patients), no death or MI occurred within 90 days in any subject whose FFR_{CT} was >0.80 [17]. Other real-world reports have also demonstrated the safety of deferral ICA based on the FFR_{CT} result [18]. These observational data should be interpreted in the context of a single arm design of the studies and lack of independent adjudication.

2.2.3. FFR_{CT}: As the preferred non-invasive test

The PACIFIC FFR_{CT} sub-study provided the first head-to-head comparison between CCTA, SPECT and PET for the diagnosis of ischemia using invasive FFR as a reference. FFR_{CT} outperformed CCTA, SPECT and PET in terms of sensitivity, was significantly more accurate than CCTA and SPECT and had higher specificity than SPECT. In an intention to diagnose analysis FFR_{CT} performance was equivalent to SPECT but inferior to PET for diagnosing myocardial ischemia [19]. These data suggest that FFR_{CT} may have advantage over other non-invasive test.

Today, clinical evidence alongside the current widespread availability of CCTA, the low radiation dose associated with the current technology of CT scanners, fast processing times of FFR_{CT} and emerging reimbursement by national health care systems challenge existing diagnostic pathways. The guideline in the United Kingdom has recommended use of CCTA with selective FFR_{CT} as first-line diagnostic test on the basis of cost and diagnostic certainty [20]. Further research will help identify the most cost-effective approach to identify patients with significant CAD.

2.2.4. FFR_{CT} for risk stratification

The evaluation of coronary resistance by FFR_{CT} may enhance risk stratification using hemodynamics metrics. In the EMERALD trial, seventy-two patients with documented ACS and available CCTA acquired between 1 month and 2 years before the development of ACS were analyzed. The culprit lesions showed higher prevalence of adverse plaque characteristics (80.3% vs. 42.0%; $p < 0.001$) than non-culprit lesions. Hemodynamic findings associated with plaque rupture were: low distal FFR_{CT}, higher ΔFFR_{CT} across the lesion, wall shear stress and axial plaque stress. Therefore, the integration of noninvasive hemodynamic assessments on top of high risk anatomical features may improve the identification of potential culprit lesions for future ACS [21].

2.2.5. FFR_{CT} for treatment decision and follow-up in complex CAD

In patients with multi-vessel disease, physiologic three-vessel assessment provides a complete functional evaluation of the ischemic burden. Nevertheless, despite the benefit observed in randomized trials, routine invasive three vessel interrogation by invasive pressure wire is seldom performed. Using FFR_{CT}, approximately 30% of patients with three-vessel disease can be re-classified to a lower risk category; therefore, modifying their treatment options. The SYNTAX III Revolution trial evaluated the agreement on treatment decision-making between either CCTA or ICA randomizing two heart teams to assess CAD in patients with left main or three-vessel disease. SYNTAX III showed an almost perfect agreement between the clinical decision (surgery or PCI) derived from CCTA and ICA (kappa coefficient 0.82;95%CI 0.74–0.91). The use of FFR_{CT} changed treatment recommendation in 6% and treatment planning in 16% [22]. These results suggest that clinical decision making between CABG and PCI based solely on non-invasive CCTA and FFR_{CT} is feasible. However, an outcomes trial testing this hypothesis is warranted to confirm the feasibility and safety of this approach.

2.2.6. Emerging tools based on FFR_{CT}; Planning your revascularization

CCTA with FFR_{CT} is able assess the anatomical and functional pattern of CAD (i.e. focal or diffuse) [23]. FFR_{CT} can provide an FFR value at any position of the coronary tree allowing for the assessment of the distribution of epicardial resistance non-invasively. Identifying the functional CAD pattern influences therapeutic options. PCI is likely to restore coronary physiology and relieve ischaemia in cases of focal CAD; whereas the clinical benefit of PCI in cases of diffuse CAD can be questioned. Diffuse CAD is readably assessed with CCTA by assessing the distribution of atherosclerotic plaque along the vessel. Similarly, FFR_{CT} can determine whether pressure drops are focal or gradually distributed in the coronary vessel [24,25].

A novel noninvasive FFR_{CT}-based planner tool (HeartFlow Planner) provides luminal remodeling using computer software enabling recalculation of the FFR after virtual removal of coronary artery stenoses and prediction post PCI FFR_{CT}. This technology is based on a geometric modeling technique to enable physicians to efficiently update the luminal geometry and employ a rapid blood flow solver to compute changes in FFR_{CT} in the updated geometry. This stenosis removal process virtually mimics stent implantation providing the virtual equivalent of the invasive FFR value measured after PCI [26]. This is the subject of ongoing validation in the Precise PCI Plan (ClinicalTrials.gov: NCT03782688).

2.3. Critical appraisal

The initial validation studies of the FFR_{CT} technology included patients with intermediate degree of stenosis at CCTA (50–70%) and have shown good accuracy and precision. The uncertainty around the FFR_{CT} value has shown a mean difference of 0.03 and SD of 0.07 with invasive FFR as a reference. This variability with FFR in absolute numbers should be accounted for in the clinical decision-making process. Cases with FFR_{CT} close to the cutoff of 0.80 might require confirmatory invasive FFR evaluation. Nevertheless, the observational data showing very low rate of adverse events in patients deferred from revascularization based on FFR_{CT} is reassuring. Moreover, higher degrees of calcification could influence the accuracy of FFR_{CT} results; however, in clinical studies FFR_{CT} proved to have an incremental value over CCTA alone for the identification of hemodynamic significant calcific CAD. The high accuracy of FFR_{CT} in heavily calcified lesion may be partially explained by the quality assessment process performed prior to the FFR_{CT} computation. Use of machine-learning algorithms may further overcome this issue. The benefit of FFR_{CT} on top of CCTA in severe CAD (stenosis >70%) might also be more limited in comparison with its role in the intermediate stenosis range. None of the trials to date have specifically assessed the diagnostic capabilities of FFR_{CT} in this high degree stenosis CAD.

In a PACIFIC sub-study, 25% of CCTA's was not evaluable by FFR_{CT}. In the recent SYNTAX III Revolution trial, using one specific and last generation CT scanner, FFR_{CT} analysis was feasible in 88% of a complex CAD population. Acceptance rates of CCTA images for FFR_{CT} analysis are prone to staff experience and depend on CT hardware and optimal patient preparation. Randomized trials are still needed to test the clinical benefit of FFR_{CT} on top of CCTA concerning clinical outcomes. Lastly, the cost-effectiveness outcomes of the inclusion of FFR_{CT} across the pathway of patient care require further evaluation.

2.4. Future perspectives

Two future randomized trials will examine the position of FFR_{CT} in the mainstream of stable CAD diagnosis and treatment. The PRECISE trial will evaluate whether an evaluation combining risk stratification using the PROMISE Risk Tool with CCTA and selective FFR_{CT} could improve outcomes over usual care while safely deferring further testing in low-risk patients. The DECISION trial will randomize patients between angiography and FFR- or non-hyperaemic pressure ratio-guided

Please cite this article as: E. Conte, J. Sonck, S. Mushtaq, et al., FFRCT and CT perfusion: A review on the evaluation of functional impact of coronary artery stenosis ..., International Journal of Cardiology, https://doi.org/10.1016/j.ijcard.2019.08.018

revascularization vs. a FFR_{CT}-guided strategy incorporating clinical decision making based on the HeartFlow Planner.

The aforementioned trials will provide data on the clinical benefit of a FFR_{CT} diagnostic strategy. Until now, non-invasive cardiac testing have been unable to identify which patients may benefit from revascularization. CCTA and FFR_{CT}, by providing a vessel level evaluation of epicardial resistance may prove to better identify patients that benefit from PCI or CABG.

3. CT perfusion

3.1. Static CT perfusion

3.1.1. Technical principles

Myocardial perfusion by cardiac computed tomography (CTP) enables evaluation of myocardial perfusion during both rest and stress (hyperemia) conditions, similarly to other noninvasive imaging techniques such as stress cardiac MR and nuclear imaging [27] (Fig. 2). Iodinated contrast attenuates X-rays proportionally to iodine content in tissue; thus, myocardial perfusion defects can be directly visualized as hypo-attenuated or non-enhancing regions. The static CTP imaging is based on acquisition of one single phase during the first-pass of the contrast agent; accordingly, one the major drawback of this technique is that the peak attenuation may be missed because only one sample of data is acquired [27].

There are two protocols mostly used, named according to the sequence of scan acquisitions: rest/stress or stress/rest. An interval of 10–15 min between the two sequences provides optimal contrast wash-out [27]. The rest/stress protocol uses the ability of CCTA to rule out obstructive CAD and the stress CTP is performed only in the presence of anatomically of intermediate CAD. This protocol is limited by the cross-contamination of contrast in the stress phase and beta-blocker administration before the rest acquisition, leading to a possible underestimation of myocardial ischemia. The stress/rest protocol is optimized for the detection of myocardial ischemia if a complete wash-out from anti-ischemic therapy (i.e. beta-blocker) can be obtained. However, performing stress CTP first may mask a fixed perfusion defect secondary to residual contrast media contamination in the rest phase, reducing sensitivity for infarction detection [27].

Visual assessment of CT perfusion images is the most common approach for qualitative assessment of myocardial perfusion. Areas of reduced perfusion appear hypo-enhanced compared with the normal myocardium, which implies either myocardial ischemia or myocardial infarction. Hypoperfusion in stress with normal perfusion in rest underlines ischemia, whereas hypoperfusion in stress that persists with same extension in rest is indicative of necrosis [28]. A narrow window width and level (200 to 350 W and 150–200 L) is recommended for perfusion defect evaluation.

In a static CTP protocol, review of multiple cardiac phase images can help to distinguish true perfusion defects from motion or beam-hardening artifacts [29–30]. In addition, true perfusion defects may persist on stress images throughout all cardiac phases, from systolic to diastolic. Unlike true perfusion defects, motion or beam hardening artifacts do not correspond to a coronary territory and might appear in only 1 or 2 cardiac phases [29].

The transmural perfusion ratio (TPR), defined as the ratio of segment-specific subendocardial attenuation to subepicardial attenuation, has been introduced as a quantitative index of static CTP. However, recent studies demonstrated that visual assessment of static CTP provides superior diagnostic performance over the TPR [29–33].

3.1.2. Overview of the current evidence

The diagnostic accuracy of CTP has been compared with that of other noninvasive imaging modalities, including SPECT, PET and MR [33–35] (Table 2). In a meta-analysis performed by Pelgrim et al. [36], CTP showed good diagnostic performance, with a sensitivity ranging from 75 to 89% and specificity from 78 to 95% compared with ICA, SPECT or MR.

The CORE320 study compared the diagnostic performance of static CTP acquired by a wide-detector scanner in 381 patients with SPECT and ICA [37]. In this study, the integrated CCTA-CTP diagnostic accuracy for detecting or excluding flow-limiting CAD showed an AUC of 0.87 [95% CI:0.84–0.91]. The PERFECTION study [38] evaluated the diagnostic accuracy of CTP, performed with a whole-heart coverage CT scanner by using ICA plus invasive FFR as the reference standard in 100 intermediate-to high-risk patients. CCTA alone demonstrated diagnostic accuracy of 83% and 76% in a per-vessel and per-patient analyses, respectively. Combining CCTA with stress CTP, per-vessel and per-patient accuracy were 93% and 91%, respectively.

The CATH2 was a randomized controlled trial aimed at evaluating the clinical efficacy of combined CCTA-CTP [39] in 300 patients hospitalized for acute-onset chest pain. A post-discharge diagnostic strategy of coronary CTA + CTP safely reduced the need for invasive examination and treatment in patients suspected of having ischemic heart disease.

3.1.3. Main clinical applications

Current evidence suggests that adding CTP imaging is a safe and good tool to improve the accuracy and the positive predictive value of CCTA alone. The combination of these two diagnostic methods provide anatomic information concerning luminal stenosis, plaque morphology, total plaque burden and also provides data on myocardial perfusion. Another setting in which CTP can improve the diagnostic accuracy of CCTA is patients with previous percutaneous interventions with metallic stents, as recently demonstrated by the ADVANTAGE study. Here, 150 patients previously treated with PCI underwent both stress CTP + CCTA and ICA, suggesting that CTP significantly improves the diagnostic accuracy of CCTA alone [40].

3.2. Dynamic CT perfusion

3.2.1. Technical principles

A dynamic CTP acquisition protocol is used to obtain a quantitative evaluation of myocardial perfusion and myocardial blood flow [41]. Patient preparation and pharmacological stress protocol are similar to static CTP; nonetheless, with dynamic CTP acquisitions repeated rapid CT scans during intravenous contrast medium injection are acquired to derive time-attenuation curves (TACs). From TACs a value of myocardial blood flow (MBF) is then obtained through different methods, all based on the dynamic change of attenuation values, that are proportional to concentration of contrast material in the myocardium and of consequence to MBF [42–43]. The post-processing phase is of utmost importance and regions of interest on myocardium, usually identifying 16-segments heart model, need to be correctly positioned.

After adequate post-processing, semi-automatic software provides a quantification of MBF, that is usually expressed as ml/100 ml/min for every segment of myocardium analyzed.

Clinical interpretation follows the common principles of myocardial perfusion physiology, similarly to static CTP.

3.2.2. Analysis of the current literature

In 2008, a first in human study with 16-slice CT scanner compared CTP to myocardial scintigraphy with promising results [44]. Similar findings were reported in 2012 by So et al. with 64-slice scanner at the expense of higher radiation dose (19.4 mSv) [45]. In 2014, Rossi et al. suggested that dynamic CTP had higher diagnostic accuracy than anatomical evaluation of coronary artery by CCTA when compared with invasive FFR, using a second-generation CT-scanner(AUC 0.95 vs. 0.89, respectively) [46].

In 2018, a meta-analysis was performed including 13 studies and 482 patients. Most of the studies used adenosine as hyperemic agent and dual-source CT was the most represented scanner type (69%). Dynamic CTP showed good diagnostic performance compared to different

Please cite this article as: E. Conte, J. Sonck, S. Mushtaq, et al., FFRCT and CT perfusion: A review on the evaluation of functional impact of coronary artery stenosis ..., International Journal of Cardiology, https://doi.org/10.1016/j.ijcard.2019.08.018

Table 2
Static and dynamic CTP previous studies.

Author	Year	N of patients	Clinical setting	Type of CT scanner	CT perfusion protocol	Gold standard	Level of analysis	Sn (95%CI)	Sp (95%CI)	Acc (95%CI)	Dose (mSV)*
Static CTP											
Blankstein et al.	2009	34	Suspected and stable CAD	64-slice dual source	Stress-rest	SPECT MPI	Vascular territory	84 (69–94)[ς]	78 (56–93)[ς]	n.p.	12.7 ± 4
Rocha-Filho et al.	2010	35	Suspected and stable CAD	64-slice dual source	Stress-Rest	QCA (stenosis>50%)	Vessel	91 (77.4–97.3)°	91 (80.4–96.4)°	n.p.	11.8 ± 4.5
Ko et al.	2011	50	Only suspected CAD	64-Dual source	Only Stress	MRI	Vessel	91	72	83	8.6 ± 1.6
Feuchtner et al.	2011	30	Suspected and stable CAD	128-slice dual source	Stress-rest	QCA (stenosis>70%)	Vessel	100 (94–100)°	74 (48–89)°	95	2.5 ± 2.1
Ko et al.	2012	40	Only suspected CAD	320-slice	Rest-stress	Invasive FFR	Vessel	87 (72–95)°	95 (87–98)°	92	9.2 ± 3.5
George et al.	2012	50	Suspected and stable CAD	320-slice	Rest-stress	SPECT MPT	Vessel	72 (46–89)[ς]	91 (74–98)[ς]	n.p.	13.8 ± 2.9
Bettencourt et al.	2013	101	Only suspected CAD	64-slice	Stress-rest	Invasive FFR	Vessel	71 (62–79)	90 (87–92)	85	5 ± 0.96
Wong et al.	2013	75	Suspected and stable CAD	320-slice	Rest-stress	Invasive FFR	Vessel	88°	83°	84	9.8
Rochitte et al.	2013	381	Suspected and stable CAD	320-slice	Only stress	SPECT MPI	Vessel	78 (73–82)[ς]	62 (58–67)[ς]	n.p.	5.3
Yang et al.	2015	75	Only suspected CAD	Dual source	Stress-rest	Invasive FFR	Vessel	86 (75–94)°	85 (57–98)°	87	n.p.
Cury et al.	2015	110	Suspected and stable CAD	Multivendor	Stress-rest	SPECT MPI	Patient	90 (71–100)[ς]	84 (77–91)[ς]	n.p.	17.7 ± 6.8
Pontone et al.	2018	147	Only suspected CAD	256-slice	Rest-stress	Invasive FFR	Vessel	92 (87–97)°	95 (92–97)°	94 (91–96)°	5.2
Andreini et al.	2019	100	Known CAD with prior PCI	256-slice	Stress-Rest	QCA (stenosis>50%)	Patient	100 (93.4–100)°	84.0 (63.9–95.5)°	94.9 (87.5–98.6)°	4.15 ± 1.5
Dynamic CTP											
Ho KT et al.	2010	35	Suspected and stable CAD	128-slice dual source	Stress-rest[§]	SPECT MPI	Segment	83[ς]	78 [ς]	n.p.	18.4
Wang et al.	2012	30	Only suspected CAD	128-slice dual source	Rest-stress[§]	SPECT MPI	Vessel	90°	81.4°	n.p.	12.8 ± 2.6
Huber et al.	2013	32	Only suspected CAD	256-slice dual source	Stress only	Invasive FFR	Patient	75.9 (56.5–89.7)[ς]	100 (94.6–100)[ς]	n.p.	9.5
Kim et al.	2013	33	Only suspected CAD	128-slice dual source	Stress-rest[§]	Stress MRI	Segment	81 (70–92)[ς]	94 (92–96)[ς]	93 (91–95)	10.3 ± 1.1
Rossi et al.	2014	80	Only suspected CAD	128-slice dual source	Rest-stress[§]	Invasive FFR	Vessel	88 (74–95)[ς]	90 (82–95)[ς]	n.p.	13.6
Kono et al.	2014	49	Suspected and stable CAD	128-slice dual source	Rest-stress[§]	Invasive FFR	Segment	89.9[ς]	47.8[ς]	68.1	12.9
Ebersberger et al.	2014	37	Only suspected CAD	128-slice dual source	Rest-stress[§]	SPECT MPI	Patient	86	96	95	9.6 ± 4.1
Bamberg et al.	2014	38	Suspected and stable CAD	128-slice dual source	Rest-stress[§]	Stress MRI	Segment	69.6 [ς]	70.5[ς]	70.3	16.9 ± 3.2
Tanabe Y et al.	2016	39	Only suspected CAD	256-slice dual source	Stress-rest[§]	Stress MRI	Segment	82 (76–88)[ς]	87 (80–92)[ς]	n.p.	n.p.
Coenen A et al.	2017	74	Suspected and stable CAD	128-slice dual source	Rest-stress[§]	Invasive FFR	Segment	73 (61–86)°	84 (75–93)°	79 (71–87)	13 ± 2.5
Pontone et al.	2019	85	Only suspected CAD	256-slice	Rest-stress[§]	QCA + iFFR	Vessel	73 (63–83)°	86 (81–91)°	82 (77–87)	8.1 ± 1.1

*Including both rest and stress CTP (complete CTP protocol) ° for integrated CTA + CTP [ς] for CTP alone; [§] Rest for CCTA only.
Sn: Sensitivity; Sp: Specificity; Acc: Accuracy; CAD: coronary artery disease; CTP: computed tomography perfusion.

reference standards, including invasive FFR. Sensitivity and specificity of 83% and 90% at the segment level, and of 93% and 82% at the patient level, respectively, were reported. However, mean radiation dose ranged from 5.3 to 10.5 mSv for the dynamic perfusion and from 9.5 to 18.4 mSv for the entire CT scan protocol, including coronary anatomy evaluation (Table 2) [47].

To the best of our knowledge, only few studies addressed the prognostic role of dynamic CTP. In 2017, Meinel FG et al. enrolled 144 patients who underwent both CCTA and dynamic CTP; here CTP had incremental predictive value over clinical risk factors and detection of CAD with CCTA [48]. More recently, CCTA, FFR_{CT} and dynamic CTP were evaluated in a multicenter trial that included 84 patients; authors demonstrated that myocardial blood flow evaluated by dynamic CTP has the highest prognostic value, over CCTA and FFR_{CT}, in terms of future MACE at an 18 months follow-up [49].

3.2.3. Main clinical applications

Dynamic CTP should be performed with new generations of CT scanners to reduce radiation dose. Dynamic CTP with last generation CT scanner can be used for accurate quantification of MBF and results obtained in recent studies demonstrated that dynamic CTP may have a prognostic role over anatomical evaluation and FFR_{CT} [49]. The main advantage over static CTP is the possibility to quantify MBF that is of fundamental importance to diagnose myocardial ischemia, in cases of multivessel disease where extensive but balanced ischemia may be underestimated and to detect microvascular angina. So far different blood flow cut-off values have been reported, ranging from 75 ml/100 g/min to >100 ml/100 g/min.

3.2.4. Future perspective

When coronary atherosclerosis is identified by CCTA, different pathways may be taken depending on the specific angiographic findings,

Please cite this article as: E. Conte, J. Sonck, S. Mushtaq, et al., FFRCT and CT perfusion: A review on the evaluation of functional impact of coronary artery stenosis ..., International Journal of Cardiology, https://doi.org/10.1016/j.ijcard.2019.08.018

patient risk profile, and individual preference. These paths may include direct referral for ICA, optimal medical therapy or additional noninvasive ischemia testing to evaluate the functional significance of the findings. Prognostic studies are needed to assess if a combined approach (CCTA+CTP) will have substantial impact on treatment costs, patient management, and outcome. The time to challenge this hypothesis with randomized prospective trials has come.

3.2.5. Critical appraisal

Radiation dose is one of the main concerns regarding CTP use in the clinical routine; in the most of studies available, it remains between 5 mSv and 10 mSv for static CTP and beyond 10 mSv for dynamic CTP. This would be of particular concern in patients with diffuse and progressive coronary atherosclerosis in whom serial scan evaluations would be needed to determine appropriateness and timing of myocardial revascularization. Of note, taking into consideration the elevated sensitivity but limited specificity of CCTA for the detection of significative coronary stenosis, patients with moderate and diffuse coronary lesions or patients already revascularized may particularly benefit from CTP on top of CCTA. A recent study performed in stented patients reports higher CCTA+CTP diagnostic accuracy vs. ICA when compared to CCTA alone, at the expense of low radiation dose (4.15 ± 1.5 mSv) [40]. However, it must be underlined that these results were obtained with a last generation CT scanner that is still not widely available.

A second potential limitation to the wide diffusion of stress CTP in the clinical setting is that both cardiological and radiological competences must be available in order to perform a safe and high-quality exam.

4. Conclusions

The most appropriate and comprehensive diagnostic flow-chart for patients with stable CAD is an evolving and still unresolved matter of debate. CCTA may provide an accurate and integrated evaluation of patients with suspected CAD offering both anatomical and functional assessment in one single technique. More specifically, adding stress CTP/FFR_{CT} on top of CCTA alone may help physician to better identify patient who may merit PCI or CABG, reducing the possible "over-indication" to myocardial revascularization after CCTA that has been previously described [1–2].

Declaration of Competing Interest

The authors report no relationships that could be construed as a conflict of interest.

References

[1] Douglas PS, Hoffmann U, Patel MR, Mark DB, Al-Khalidi HR, Cavanaugh B, et al. Outcomes of anatomical versus functional testing for coronary artery disease. N Engl J Med. 2015 Apr;372(14):1291–300. PubMed PMID: 25773919. eng.

[2] Investigators S-H. CT coronary angiography in patients with suspected angina due to coronary heart disease (SCOT-HEART): an open-label, parallel-group, multicentre trial. Lancet. 2015 Mar 13. PubMed PMID: 25788230.

[3] Meijboom WB1, Meijs MF, Schuijf JD, Cramer MJ, Mollet NR, van Mieghem CA, et al. Diagnostic accuracy of 64-slice computed tomography coronary angiography: a prospective, multicenter, multivendor study. J Am Coll Cardiol. 2008 Dec 16;52(25):2135–44. Pubmed PMID: 19095130.

[4] N.H. Pijls, J.A. van Son, R.L. Kirkeeide, B. De Bruyne, K.L. Gould, Experimental basis of determining maximum coronary, myocardial, and collateral blood flow by pressure measurements for assessing functional stenosis severity before and after percutaneous transluminal coronary angioplasty, Circulation. 87 (4) (1993 Apr) 1354–13678462157.

[5] Windecker S, Kolh P, Alfonso F, Collet JP, Cremer J, Falk V, et al. 2014 ESC/EACTS Guidelines on myocardial revascularization: The Task Force on Myocardial Revascularization of the European Society of Cardiology (ESC) and the European Association for Cardio-Thoracic Surgery (EACTS)Developed with the special contribution of the European Association of Percutaneous Cardiovascular Interventions (EAPCI). European heart journal. 2014 Oct;35(37):2541–619. PubMed PMID: 25173339. eng.

[6] Serruys PW, Girasis C, Papadopoulou SL, Onuma Y. Non-invasive fractional flow reserve: scientific basis, methods and perspectives. EuroIntervention. 2012 Aug;8(4):511–9. PubMed PMID: 22581414. (Epub 2012/05/15. eng).

[7] C.A. Taylor, T.A. Fonte, J.K. Min, Computational fluid dynamics applied to cardiac computed tomography for noninvasive quantification of fractional flow reserve: scientific basis, J. Am. Coll. Cardiol. 61 (22) (2013 Jun 4) 2233–224123562923.

[8] West GB, Brown JH, Enquist BJ. A general model for the origin of allometric scaling laws in biology. Science. 1997 Apr 4;276(5309):122–6. PubMed PMID: 9082983. (Epub 1997/04/04. eng).

[9] Steele BN, Olufsen MS, Taylor CA. Fractal network model for simulating abdominal and lower extremity blood flow during resting and exercise conditions. Comput. Methods Biomech. Biomed. Engin. 2007 Feb;10(1):39–51. PubMed PMID: 18651270. (Epub 2008/07/25. eng).

[10] Murray CD. The physiological principle of minimum work: I. the vascular system and the cost of blood volume. Proc. Natl. Acad. Sci. U. S. A. 1926 Mar;12(3):207–14. PubMed PMID: 16576980. (Epub 1926/03/01. eng).

[11] Min JK, Leipsic J, Pencina MJ, Berman DS, Koo BK, van Mieghem C, et al. Diagnostic accuracy of fractional flow reserve from anatomic CT angiography. Jama. 2012 Sep 26;308(12):1237–45. PubMed PMID: 22922562. Pubmed Central PMCID: PMC4281479. (Epub 2012/08/28. eng).

[12] Koo BK, Erglis A, Doh JH, Daniels DV, Jegere S, Kim HS, et al. Diagnosis of ischemia-causing coronary stenoses by noninvasive fractional flow reserve computed from coronary computed tomographic angiograms. Results from the prospective multicenter DISCOVER-FLOW (Diagnosis of Ischemia-Causing Stenoses Obtained Via Noninvasive Fractional Flow Reserve) study. J. Am. Coll. Cardiol. 2011 Nov 1;58(19):1989–97. PubMed PMID: 22032711. (Epub 2011/10/29. eng).

[13] Norgaard BL, Leipsic J, Gaur S, Seneviratne S, Ko BS, Ito H, et al. Diagnostic performance of noninvasive fractional flow reserve derived from coronary computed tomography angiography in suspected coronary artery disease: the NXT trial (analysis of coronary blood flow using CT angiography: next steps). J. Am. Coll. Cardiol. 2014 Apr 1;63(12):1145–55. PubMed PMID: 24486266.

[14] C.M. Cook, R. Petraco, M.J. Shun-Shin, Y. Ahmad, S. Nijjer, et al., Diagnostic accuracy of computed tomography-derived fractional flow reserve: a systematic review, JAMA Cardiol. 2 (7) (2017 Jul 1) 803–810, https://doi.org/10.1001/jamacardio.2017.131428538960.

[15] Collet C, Miyazaki Y, Ryan N, Asano T, Tenekecioglu E, Sonck J, et al. Fractional flow reserve derived from computed tomographic angiography in patients with multivessel CAD.J Am Coll Cardiol. 2018 Jun 19;71(24):2756–2769. doi:https://doi.org/10.1016/j.jacc.2018.02.053. PMID: 29802016.

[16] Douglas PS, Pontone G, Hlatky MA, Patel MR, Norgaard BL, Byrne RA, et al. Clinical outcomes of fractional flow reserve by computed tomographic angiography-guided diagnostic strategies vs. usual care in patients with suspected coronary artery disease: the prospective longitudinal trial of FFR (CT): outcome and resource impacts study. Eur Heart J. 2015 Dec 14;36(47):3359–67. doi:https://doi.org/10.1093/eurheartj/ehv444. Epub 2015 Sep 1.PMID: 26330417.

[17] T.A. Fairbairn, K. Nieman, T. Akasaka, B.L. Nørgaard, D.S. Berman, G. Raff, et al., Real-world clinical utility and impact on clinical decision-making of coronary computed tomography angiography-derived fractional flow reserve: lessons from the ADVANCE registry, Eur. Heart J. 39 (41) (2018 Nov 1) 3701–3711, https://doi.org/10.1093/eurheartj/ehy53030165613.

[18] Jensen JM, Bøtker HE, Mathiassen ON, Grove EL, Øvrehus KA, Pedersen KB, et al. Computed tomography derived fractional flow reserve testing in stable patients with typical angina pectoris: influence on downstream rate of invasive coronary angiography. Eur Heart J Cardiovasc Imaging. 2018 Apr 1;19(4):405–414. doi:https://doi.org/10.1093/ehjci/jex068. PMID: 28444153.

[19] R.S. Driessen, I. Danad, W.J. Stuijfzand, P.G. Raijmakers, S.P. Schumacher, P.A. van Diemen, et al., Comparison of coronary computed tomography angiography, fractional flow reserve, and perfusion imaging for ischemia diagnosis, J. Am. Coll. Cardiol. 73 (2) (2019 Jan 22) 161–17330654888.

[20] National Institute for Health and Clinical Excellence. Chest Pain of Recent Onset: Assessment and Diagnosis of Recent Onset Chest Pain or Discomfort of Suspected Cardiac Origin (update). CG95. London: National Institute for Health and Clinical Excellence; 2016.

[21] Lee JM, Choi G, Koo BK, Hwang D, Park J, Zhang J, et al. Identification of high-risk plaques destined to cause acute coronary syndrome using coronary computed tomographic angiography and computational fluid dynamics. JACC Cardiovasc Imaging. 2018 Mar 14. pii: S1936-878X(18)30134–7. doi:https://doi.org/10.1016/j.jcmg.2018.01.023. PMID: 29550316.

[22] C. Collet, Y. Onuma, D. Andreini, J. Sonck, G. Pompilio, S. Mushtaq, et al., Coronary computed tomography angiography for heart team decision-making in multivessel coronary artery disease, Eur. Heart J. 39 (41) (2018 Nov 1) 3689–3698, https://doi.org/10.1093/eurheartj/ehy58130312411.

[23] J. Butler, M. Shapiro, J. Reiber, T. Sheth, M. Ferencik, E.G. Kurtz, et al., Extent and distribution of coronary artery disease: a comparative study of invasive versus noninvasive angiography with computed angiography, Am. Heart J. 153 (2007) 378–384.

[24] Z. Piroth, G.G. Toth, P.A.L. Tonino, E. Barbato, S. Aghlmandi, N. Curzen, et al., Prognostic value of fractional flow reserve measured immediately after drug-eluting stent implantation, Circ. Cardiovasc. Interv. 10 (2017).

[25] C. Collet, Y. Katagiri, Y. Miyazaki, T. Asano, J. Sonck, et al., Impact of coronary remodeling on fractional flow reserve, Circulation. 137 (7) (2018 Feb 13) 747–749, https://doi.org/10.1161/CIRCULATIONAHA.117.03147829440200.

[26] B.N. Modi, S. Sankaran, H.J. Kim, H. Ellis, C. Rogers, C.A. Taylor, et al., Predicting the physiological effect of revascularization in serially diseased coronary arteries, Circ. Cardiovasc. Interv. 12 (2) (2019 Feb), e007577. https://doi.org/10.1161/CIRCINTERVENTIONS.118.00757730722688.

[27] A. Rossi, D. Merkus, E. Klotz, N. Mollet, P.J. de Feyter, G.P. Krestin, Stress myocardial perfusion: imaging with multidetector CT, Radiology. 270 (2014) 25–46.

Please cite this article as: E. Conte, J. Sonck, S. Mushtaq, et al., FFRCT and CT perfusion: A review on the evaluation of functional impact of coronary artery stenosis ..., International Journal of Cardiology, https://doi.org/10.1016/j.ijcard.2019.08.018

[28] V.C. Mehra, C. Valdiviezo, A. Arbab-Zadeh, et al., A stepwise approach to the visual interpretation of CT-based myocardial perfusion, J. Cardiovasc. Comput. Tomogr. 5 (2011) 357–369.
[29] D.H. Yang, Y.H. Kim, J.H. Roh, et al., Stress myocardial perfusion CT in patients suspected of having coronary artery disease: visual and quantitative analysis-validation by using fractional flow reserve, Radiology 276 (2015) 715–723.
[30] N. Bettencourt, A. Chiribiri, A. Schuster, et al., Direct comparison of cardiac magnetic resonance and multidetector computed tomography stress-rest perfusion imaging for detection of coronary artery disease, J. Am. Coll. Cardiol. 61 (2013) 1099–1107.
[31] R.T. George, A. Arbab-Zadeh, J.M. Miller, et al., Adenosine stress 64- and 256-row detector computed tomography angiography and perfusion imaging: a pilot study evaluating the transmural extent of perfusion abnormalities to predict atherosclerosis causing myocardial ischemia, Circ. Cardiovasc. Imaging 2 (2009) 174–182.
[32] B.S. Ko, J.D. Cameron, M. Leung, et al., Combined CT coronary angiography and stress myocardial perfusion imaging for hemodynamically significant stenoses in patients with suspected coronary artery disease: a comparison with fractional flow reserve, JACC Cardiovasc. Imaging 5 (2012) 1097–1111.
[33] R.T. George, A. Arbab-Zadeh, J.M. Miller, et al., Computed tomography myocardial perfusion imaging with 320-row detector computed tomography accurately detects myocardial ischemia in patients with obstructive coronary artery disease, Circ. Cardiovasc. Imaging 5 (3) (2012) 333–340.
[34] S.M. Ko, J.W. Choi, M.G. Song, et al., Myocardial perfusion imaging using adenosine induced stress dual-energy computed tomography of the heart: comparison with cardiac magnetic resonance imaging and conventional coronary angiography, Eur. Radiol. 21 (1) (2011) 26–35.
[35] Y. Kikuchi, N. Oyama-Manabe, M. Naya, et al., Quantification of myocardial blood flow using dynamic 320-row multidetector CT as compared with (1)(5)O-H(2)O PET, Eur. Radiol. 2014 (24) (2014) 1547–1556.
[36] G.J. Pelgrim, M. Dorrius, X. Xie, et al., The dream of a onestop-shop: meta-analysis on myocardial perfusion CT, Eur. J. Radiol. 84 (2015) 2411–2420.
[37] C.E. Rochitte, R.T. George, M.Y. Chen, et al., Computed tomography angiography and perfusion to assess coronary artery stenosis causing perfusion defects by single photon emission computed tomography: the CORE320 study, Eur. Heart J. 35 (17) (2014 May) 1120–1130.
[38] Pontone G, Andreini D, Guaricci AI, et al. Incremental diagnostic value of stress computed tomography myocardial perfusion with whole-heart coverage ct scanner in intermediate- to high-risk symptomatic patients suspected of coronary artery disease. JACC Cardiovasc Imaging. 2018 Feb 9. pii: S1936-878X(17)31149-X.
[39] M.H. Sørgaard, J.J. Linde, J.T. Kühl, et al., Value of myocardial perfusion assessment with coronary computed tomography angiography in patients with recent acute-onset chest pain, JACC Cardiovasc. Imaging 11 (2018) 1611–1621.
[40] Andreini D, Mushtaq S, Pontone G, et al. Additional diagnostic value of CT perfusion over coronary CT angiography in patients with suspected in-stent restenosis or coronary artery disease progression the ADVANTAGE prospective study. JACC Img 2019 In Press.
[41] I. Danad, J. Szymonifka, J. Schulman-Marcus, J.K. Min, Static and dynamic assessment of myocardial perfusion by computed tomography, Eur. Heart J. Cardiovasc. Imaging 8 (2016) 836–844.
[42] K.T. Ho, K.C. Chua, E. Klotz, C. Panknin, Stress and rest dynamic myocardial perfusion imaging by evaluation of complete time–attenuation curves withdual-source CT, JACC Cardiovasc. Imaging 3 (2010) 811–820.
[43] F. Bamberg, R.P. Marcus, A. Becker, K. Hildebrandt, K. Bauner, F. Schwarz, M. Greif, F. von Ziegler, B. Bischoff, H.C. Becker, T.R. Johnson, M.F. Reiser, K. Nikolaou, D. Theisen, Dynamic myocardial CT perfusion imaging for evaluation of myocardial ischemia as determined by MR imaging, JACC Cardiovasc. Imaging 7 (3) (2014 Mar) 267–277.
[44] T. Kido, A. Kurata, H. Higashino, Y. Inoue, R.E. Kanza, H. Okayama, J. Higaki, K. Murase, T. Mochizuki, Quantification of regional myocardial blood flow using first-pass multidetector-row computed tomography and adenosine triphosphate in coronary artery disease, Circ. J. 72 (7) (2008 Jul) 1086–1091.
[45] A. So, G. Wisenberg, A. Islam, et al., Noninvasive assessment of functionally relevant coronary artery stenoses with quantitative CT perfusion: preliminary clinical experiences, Eur. Radiol. 22 (1) (2012) 39–50.
[46] A. Rossi, A. Dharampal, A. Wragg, L.C. Davies, R.J. van Geuns, C. Anagnostopoulos, E. Klotz, P. Kitslaar, A. Broersen, A. Mathur, K. Nieman, M.G. Hunink, P.J. de Feyter, S.E. Petersen, F. Pugliese, Diagnostic performance of hyperaemic myocardial blood flow index obtained by dynamic computed tomography: does it predict functionally significant coronary lesions? Eur. Heart J. Cardiovasc. Imaging 15 (1) (2014 Jan) 85–94.
[47] M. Lu, S. Wang, A. Sirajuddin, A.E. Arai, S. Zhao, Dynamic stress computed tomography myocardial perfusion for detecting myocardial ischemia: a systematic review and meta-analysis, Int. J. Cardiol. 258 (2018 May 1) 325–331.
[48] F.G. Meinel, F. Pugliese, U.J. Schoepf, et al., Prognostic value of stress dynamic myocardial perfusion CT in a multicenter population with known or suspected coronary artery disease, AJR Am. J. Roentgenol. 208 (4) (2017 Apr) 761–769.
[49] M. van Assen, C.N. De Cecco, M. Eid et al. Prognostic value of CT myocardial perfusion imaging and CT-derived fractional flow reserve for major adverse cardiac events in patients with coronary artery disease. J Cardiovasc Comput Tomogr. 2019 Feb 12. pii: S1934–5925(18)30561–6.

Diagnostic Performance of Angiography-derived Fractional Flow Reserve: A Systematic Review and Bayesian Meta-analysis

Discrepancy between anatomy and physiology is found in approximately 20% of the lesions with QCA diameter stenosis >70% and in half of lesions with diameter stenosis between 50% and 70% with respect to fractional flow reserve (FFR)[105,106]. This fact has limited the usefulness of diameter stenosis and led to the recommendation to use pressure-wire derived metrics of functional stenosis significance to define the need for revascularization, particularly in intermediate coronary lesions[107]. Nowadays, 3D-QCA enables to construct a patient-specific coronary geometry that can be further processed by computational fluid dynamics (CFD) to perform blood flow simulations that can derive endothelial shear stress and pressure drop. The simulated FFR can be derived either from blood flow simulation using CFD or by a mathematical approach derived from the Lance Gould equation or by rapid pressure-flow simulations[90,91].

Pressure-wire assessment of coronary stenosis is considered the invasive reference standard for detection of ischemia-generating lesions. Recently, methods to estimate the fractional flow reserve (FFR) from conventional angiography without the use of a pressure wire have been developed and were shown to have an excellent diagnostic accuracy. The present systematic review and meta-analysis aimed at determining the diagnostic performance of angiography-derived FFR for the diagnosis of hemodynamically significant coronary artery disease.

A systematic review and meta-analysis of studies assessing the diagnostic performance of angiography-derived FFR systems were performed. The primary outcome of interest was pooled sensitivity and specificity. Thirteen studies comprising 1842 vessels were included in the final analysis. A Bayesian bivariate meta-analysis yielded a pooled sensitivity of 89% (95% credible interval 83-94%), specificity of 90% (95% credible interval 88-92%), positive likelihood ratio (+LR) of 9.3 (95% credible interval 7.3-11.7) and negative likelihood ratio (-LR) of 0.13 (95% credible interval 0.07-0.2). The summary area under the receiver-operating curve was 0.84 (95% credible interval 0.66-0.94). Meta-regression analysis did not find differences between the methods for pressure-drop calculation (computational fluid dynamics vs. mathematical formula), type of analysis (on-line vs. off-line) or software packages.

The accuracy of angiography-derived FFR was good to detect hemodynamically significant lesions with pressure-wire measured FFR as a reference. Computational approaches and software packages did not influence the diagnostic accuracy of angiography-derived FFR. A diagnostic strategy trial with angiography-derived FFR evaluating clinical endpoints is warranted.

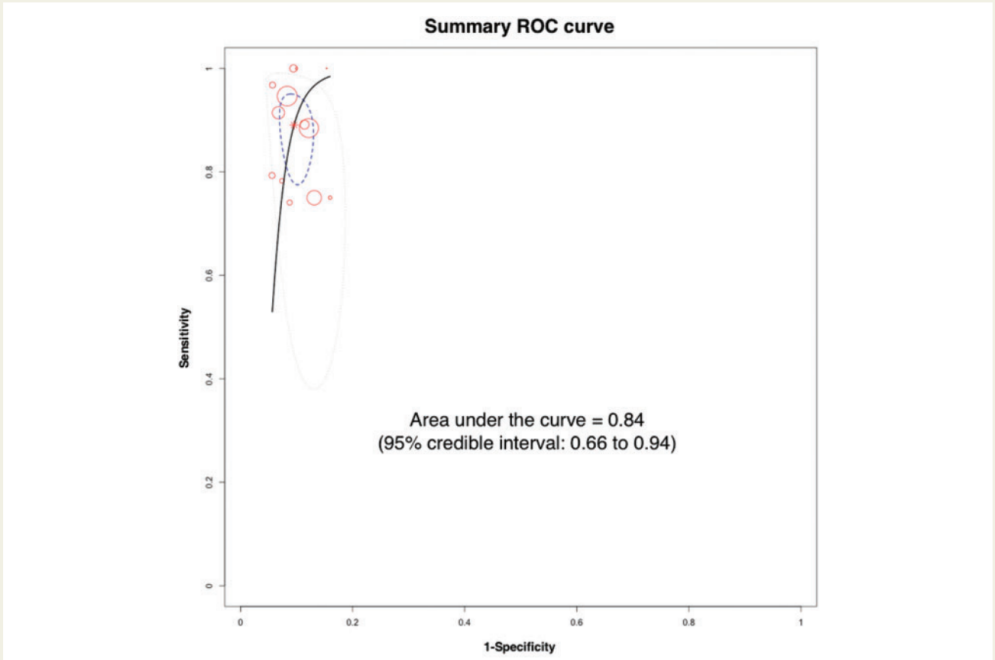

Figure 4 Summary of receiver operating curve. Each bubble represents one study and indicates its observed sensitivity and specificity. The size of the bubble is proportional to the number of individuals in this study. The solid black line is the summary of receiver operating curve line. The star point represents the summary point, the dashed blue line is the 95% credible region, and the dashed grey line is the 95% prediction region. The area under the summary receiver operating curve was 0.84 (95% credible interval 0.66–0.94).

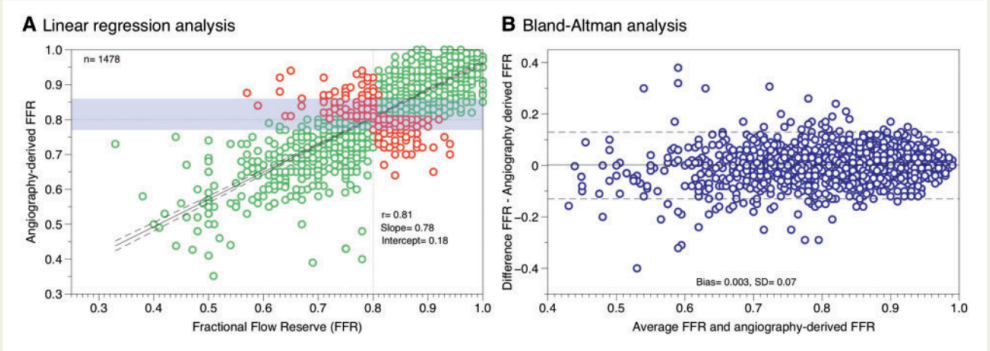

Figure 6 Lesion-level analysis. (*A*) The linear correlation between angiography-derived fractional flow reserve and invasive fractional flow reserve is shown. The green dots represent the lesion with agreement on lesion significance (n = 1296, 88%) whereas the red dots represent disagreement between methods (n = 182, 12%). The grey dashed lines represent the cut-off values for each method. The solid black line represents the line of best fit between angiography-derived fractional flow reserve and fractional flow reserve. The black dashed represents the 95% confidence interval for the line of best fit; the shade area represent the zone of uncertainty (i.e. 0.77–0.86). (*B*) The mean difference between angiography-derived fractional flow reserve and invasive fractional flow reserve is shown. The solid line represents the bias and the dashed line the limits of agreement.

Graft Patency and Progression of Coronary Artery Disease after CABG Assessed by Angiography-derived Fractional Flow Reserve.

Graft occlusion after coronary artery bypass graft surgery (CABG) has been associated with native coronary artery competitive flow. Saphenous graft occlusion occurs in approximately 25% of patients at 18 months of follow up whereas arterial grafts have been shown to have higher patency rates at long-term follow up[108,109]. Graft occlusion after CABG has been associated with patient-related factors, conduit type, surgical technique. Moreover, the presence of native coronary artery competitive flow has also been identified as a predictor of early graft occlusion[110–112]. Several studies have demonstrated an accelerated progression of atherosclerosis in grafted native coronary arteries after CABG.

Angiography-derived FFR software have been shown to be accurate with invasive FFR as reference[113]. This technology has also the potential to increase our understanding on the functional progression of CAD after CABG. Furthermore, angiography-derived FFR may aid to identify vessels that do not require bypass grafting.

The present study aims to characterize the functional progression of coronary artery disease (CAD) in native vessels after CABG, and to assess the relationship between preoperative FFR as derived from angiography and graft occlusion.

Multicenter study of consecutive patients undergoing CABG between 2013 and 2018, in whom a follow-up angiogram had been performed. Serial vessel-fractional flow reserve (vFFR) analyses were obtained in each major native coronary vessel before and after CABG, excluding post-anastomotic segments and graft conduits.

In 73 patients, serial angiograms were suitable for vFFR analysis, including 118 grafted (86 arterial and 32 saphenous grafts) and 64 non-grafted vessels. The median time between CABG and follow-up angiography was 2.4 years [IQR 1.5, 3.3]. Functional CAD progression, by means of decline in vFFR, was observed in grafted but not in non-grafted vessels (delta vFFR in grafted vessels 0.10 [IQR 0.05, 0.18] vs. 0.01 [IQR -0.01, 0.03], in non-grafted vessels, $p < 0.001$). Preoperative vFFR predicted graft occlusion (AUC: 0.66, 95% CI 0.52 to 0.80, $p = 0.031$).

In patients undergoing CABG, preoperative vFFR derived from conventional angiograms without use of pressure wire was able to predict graft occlusion. Graft occlusion was more frequent in vessels with high vFFR values. Grafted native coronary vessels exhibited

accelerated functional CAD progression, whereas in non-grafted native coronaries the functional status remained unchanged.

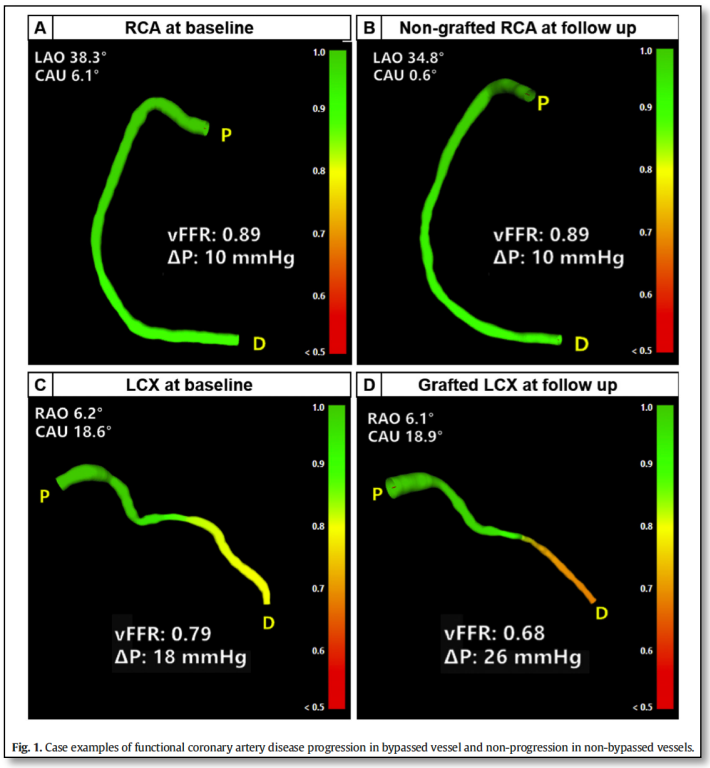

Fig. 1. Case examples of functional coronary artery disease progression in bypassed vessel and non-progression in non-bypassed vessels.

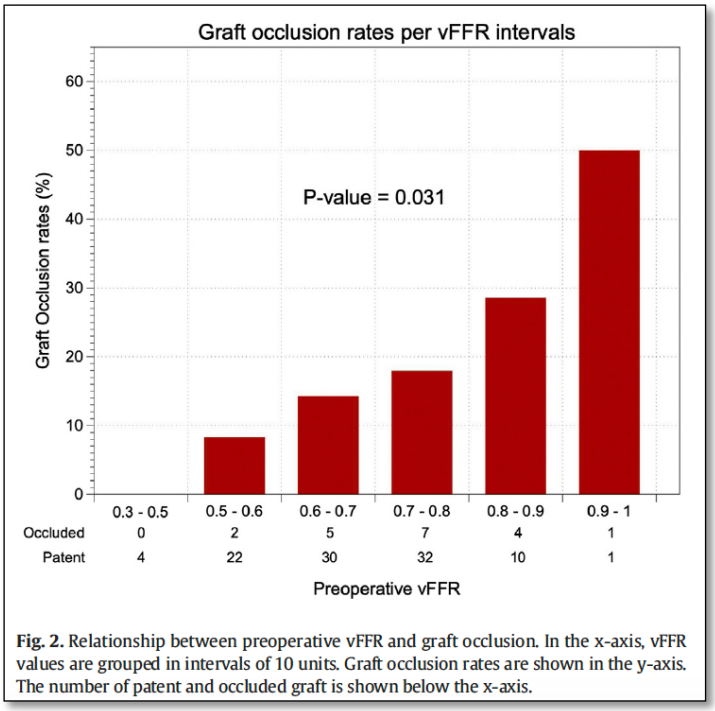

Fig. 2. Relationship between preoperative vFFR and graft occlusion. In the x-axis, vFFR values are grouped in intervals of 10 units. Graft occlusion rates are shown in the y-axis. The number of patent and occluded graft is shown below the x-axis.

Vessel Fractional Flow Reserve and Graft Vasculopathy in Heart Transplant Recipients

Cardiac allograft vasculopathy (CAV) remains the Achilles' heel of long-term survival after heart transplantation (HTx). The severity and extent of CAV is graded with conventional coronary angiography (COR) which has several limitations[95]. Coronary angiography lacks the resolution to diagnose early as well as diffuse stages of CAV. Also, intra-vascular imaging (IVUS) lacks the ability to assess the functional consequences of CAV. In contrary, fractional Flow Reserve (FFR) captures the hemodynamic consequences of vascular disease. Recently, vessel fractional flow reserve (vFFR) derived from COR has emerged as a diagnostic computational tool to quantify the functional severity of coronary artery disease. The present study assessed the usefulness of vFFR to detect CAV in HTx recipients.

In HTx patients referred for annual check-up, undergoing surveillance COR, the extent of CAV was graded according to the criteria proposed by the international society of heart and lung transplantation (ISHLT). In addition, three-dimensional coronary geometries were constructed from COR to calculate pressure losses using vFFR.

In 65 HTx patients with a mean age of 53.7 ± 10.1 years, 8.5 years (IQR 1.90, 15.2) years after HTx, a total number of 173 vessels (59 LAD, 61 LCX, and 53 RCA) were analyzed. The mean vFFR was 0.84 ± 0.15 and median was 0.88 (IQR 0.79, 0.94). A vFFR ≤ 0.80 was present in 24 patients (48 vessels). HTx patients with a history of ischemic cardiomyopathy (ICMP) had numerically lower vFFR as compared to those with non-ICMP (0.70 ± 0.22 vs. 0.79 ± 0.13, p = 0.06). The use of vFFR reclassified 31.9% of patients compared to the anatomical ISHLT criteria. Despite a CAV score of 0, a pathological vFFR ≤ 0.80 was detected in 8 patients (34.8%).

The impairment in epicardial conductance assessed by vFFR in a subgroup of patients without CAV according to standard ISHLT criteria suggests the presence of a diffuse vasculopathy undetectable by conventional angiography. Therefore, we speculate that vFFR may be useful in risk stratification after HTx.

Table 4: Agreement between the vFFR value and CAV score.

	vFFR > 0.80	vFFR ≤ 0.80	Total
CAV 0	15	8	23 (48.9)
CAV 1	6	6	12 (25.5)
CAV 2	1	3	4 (8.5)
CAV 3	0	8	8 (17.1)
Total	22 (46.8)	25 (53.2)	47

Values are *n* or *n* (%). vFFR, vessel fractional flow reserve derived from angiography; CAV, cardiac allograft vasculopathy.

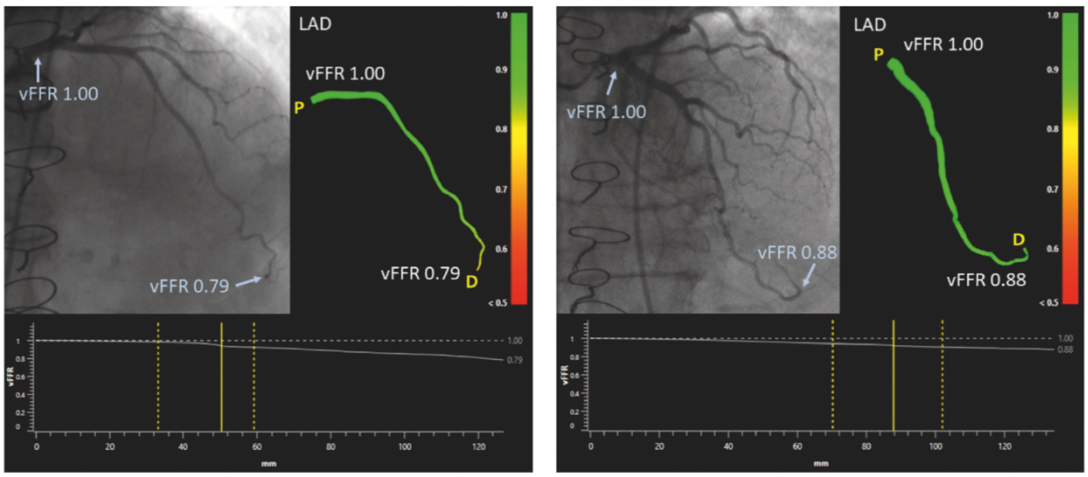

(a) (b)

Figure 2: (a) Normal coronary angiogram with functionally significant CAV according to the vFFR analysis. The LAD shows no stenosis on angiography; however, the vFFR shows diffuse pressure losses, and the distal vFFR value is 0.79. (b) Normal angiogram without functionally significant CAV according to the vFFR analysis. The LAD shows no stenosis on angiography, and the vFFR shows small pressure losses resulting in a distal FFR value of 0.88. CAV, cardiac allograft vasculopathy; LAD, left anterior descending coronary artery; and vFFR, vessel fractional flow reserve.

Risk of Myocardial Infarction based on Endothelial Shear Stress Analysis Using Coronary Angiography

To assess the capacity of shear stress analysis derived from conventional coronary angiography to detect lesions culprit for future myocardial infarction (MI).

Among 6885 patients with MI, 80 had previous invasive angiograms suitable for three-dimensional coronary reconstruction. Quantitative coronary angiography (QCA), fractional flow reserve derived from angiography (vFFR) and wall shear stress (WSS) were analyzed in 76 future culprit lesions and in 102 non-culprit lesions (controls). Endothelium-blood flow interaction was assessed by two quantities i.e., time-averaged wall shear stress (TAWSS) and topological shear variation index (TSVI). Mean age was 70.3±12.7 years, 29% of patients were female. Culprit lesions showed higher percent area stenosis (%AS), delta lesion vFFR, TAWSS and TSVI compared to non-culprit lesions ($p<0.05$ for all). TSVI was superior to TAWSS in predicting MI ($AUC_{TSVI} = 0.75$, 95% CI 0.69-0.81 vs. $AUC_{TAWSS} = 0.61$, 95% CI 0.55-0.67, $p<0.001$). The addition of TSVI increased the predictive and reclassification ability compared to a model based on %AS and delta lesion vFFR (net reclassification improvement = 1.04, $p<0.001$, relative integrated discrimination improvement = 0.21, $p<0.001$).

Lesions culprit for future MI can be identified using QCA-based WSS analysis. The combination of luminal stenosis, pressure gradients and WSS predicted the occurrence of MI. A WSS-based descriptor that accounts for the variation in the contraction and expansion action of shear forces on the endothelium along the cardiac cycle, i.e., TSVI, improved the discrimination of lesions prone to rupture.

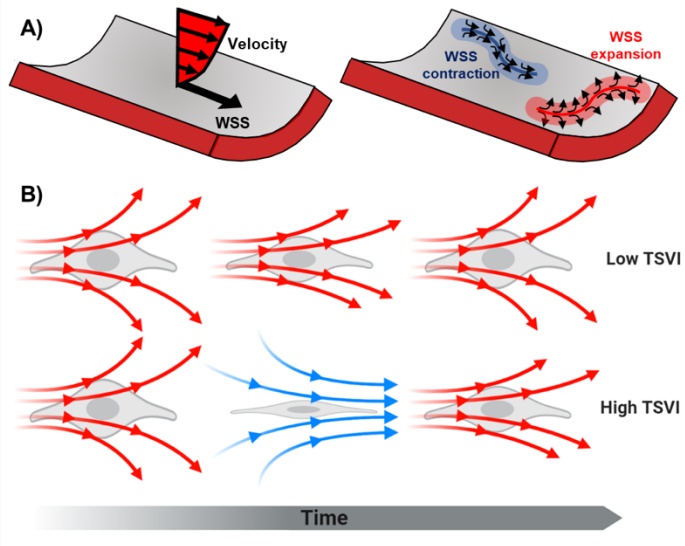

Left panel: schematic representation of shear stress at the luminal surface (i.e., the WSS) caused by blood flow. Right panel: schematic representation of WSS contraction/expansion regions, i.e., the regions where WSS exerts a push/pull action on endothelial cells, as identified by the divergence of the WSS unit vector field (DIVWSS). Positive DIVWSS values indicate an expansion region (red colour), while negative DIVWSS values indicate a contraction region (blue colour). B) Schematic representation of WSS contraction/expansion action on endothelial cells and its variability during the cardiac cycle. The variability of contraction/expansion action exerted by the WSS during the cardiac cycle can be quantified by the topological shear variation index (TSVI).

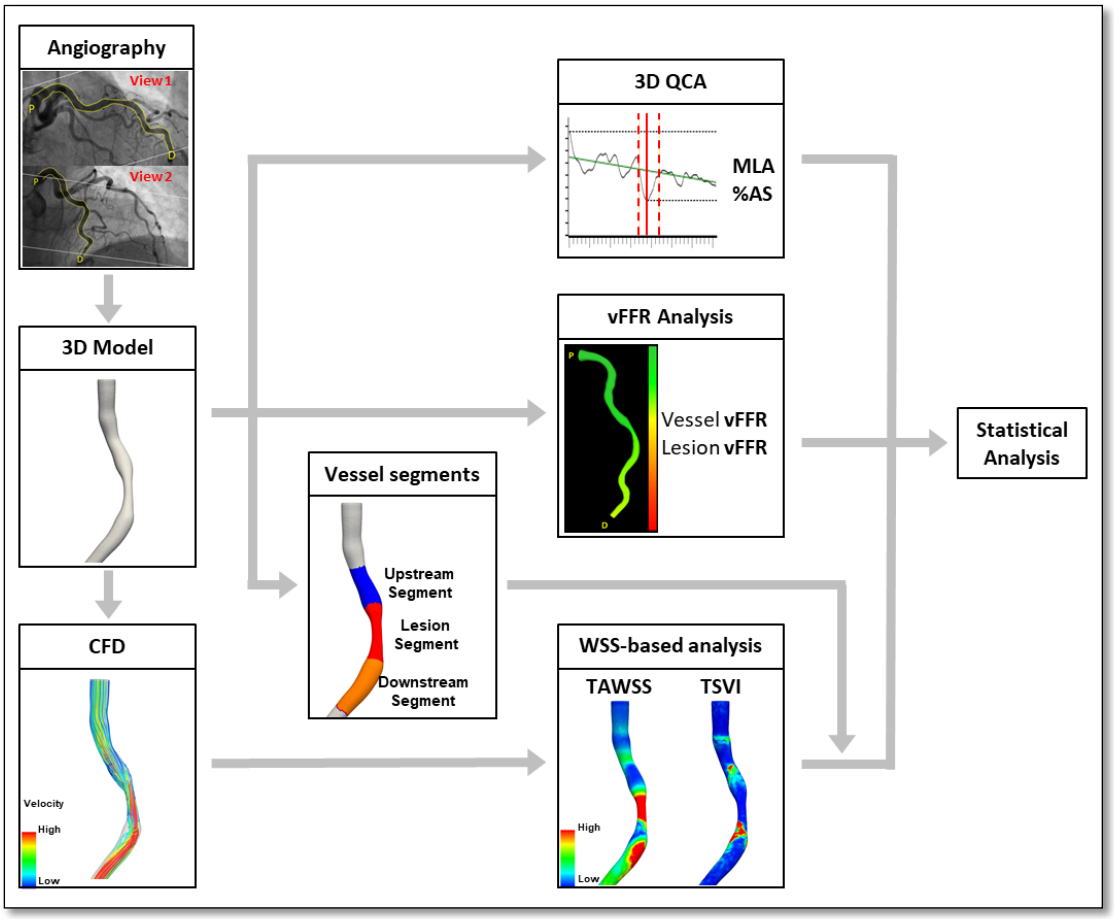

Workflow of the study: From routine two-dimensional coronary angiograms, a three-dimensional reconstruction of the vessel is obtained. Anatomical lesion characteristics, such as minimal lumen area (MLA) and percentage area stenosis (%AS), are obtained from quantitative coronary angiography (QCA). The geometrical information of the vessel reconstruction is exploited to compute the pressure drop along the vessel (virtual fractional flow reserve, vFFR) and to perform computational fluid dynamic (CFD) simulations to obtain wall shear stress (WSS)-based descriptors, such as the time-averaged wall shear stress (TAWSS) and the topological shear variation index (TSVI). WSS-based descriptors were surface-averaged according to a predefined lesion subdivision. Finally anatomical-based, pressure-based and WSS-based quantities were used to perform the statistical analysis comparing future culprit lesions vs non-future culprit lesions.

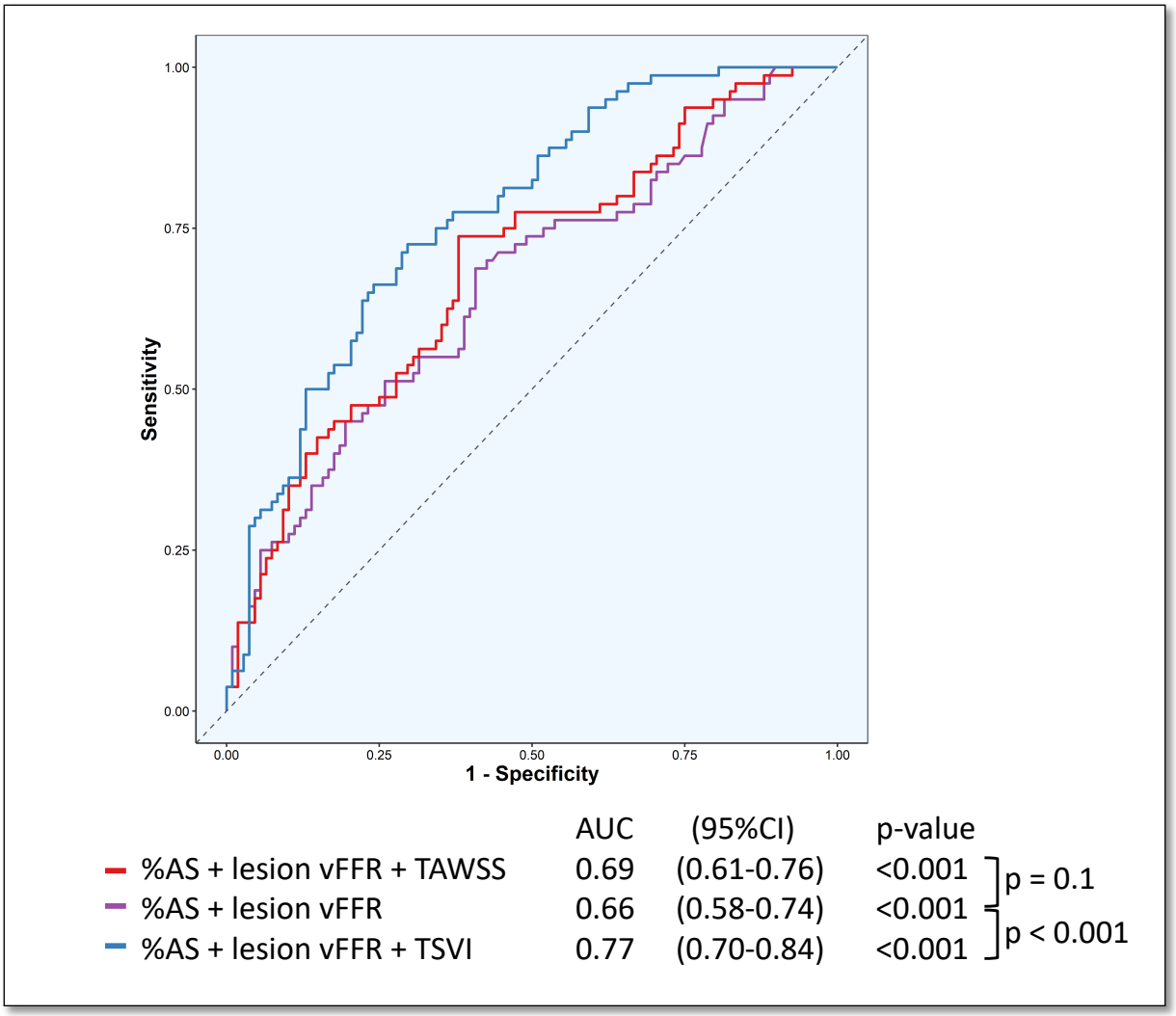

Receiver operating characteristic (ROC) curves of the multivariate models. A non-significant incremental predictive capacity was obtained by adding time-averaged wall shear stress (TAWSS) to a prediction model with lesion virtual fractional flow reserve (vFFR) and percentage area stenosis (%AS) (ΔAUC +0.03, De Long p = 0.1). On the contrary, adding topological shear variation index (TSVI) to the model with %AS and lesion vFFR added significant gain in predictive capacity (ΔAUC + 0.11, De Long p < 0.001).

Chapter 5: Redefining the patterns of coronary artery disease

Chapter introduction

Chapter five and six represent cardinal chapters for this thesis. Previously, it appeared feasible to measure even subtle hemodynamic changes in disease progression and coronary remodeling non-invasively using FFR_{CT}[114]. Comparably, invasive FFR has the potential to appraise functional changes in and patterns of coronary artery pressure and resistance. When performing an FFR measurement (Pressure wire X), Pd/Pa is measured with a sampling rate of 10 milliseconds. We introduced invasive motorized FFR pullbacks that were acquired using a dedicated pullback device at a speed of 1 mm/s generating thousands of pressure (Pd/Pa) points for pullback curve creation. The correlation between FFR_{CT} and FFR pullbacks proved strong (correlation coefficient 0.76 (95%CI 0.75 to 0.78; $p < 0.001$). Also, the mean difference in lesion gradient between FFR_{CT} and FFR was −0.07 (LOA -0.26 to 0.13) whereas in non-obstructive segments was −0.01 (LOA -0.06 to 0.05). As such, shown in a proof-of-concept paper, the evaluation of epicardial coronary resistance using coronary CT angiography with FFR_{CT} proved feasible and accurate for the evaluation of pressure gradients. On one hand this has enabled us to validate in depth the HeartFlow Planner (chapter 6). On the other hand, this facilitated the endeavors in further refining FFR.

For this purpose, we initially had to describe the accuracy and reproducibility of the motorized pullback technique. The mean difference between pullbacks was −0.002 (LOA −0.058 to 0.054) with a difference in AUPC between the two FFR pullbacks of 2.1 ± 1.6%. Also, at prespecified anatomical locations, the mean difference between the FFR derived from the pullback data and the measured FFR was neglectable: 0 (LOA −0.040 to 0.039) and the repeatability of the distal FFR measurement was high (bias −0.003, LOA −0.046 to 0.041). This work formed the basis for the paper on the "Measurement of Hyperemic Pullback Pressure Gradients to Characterize the Patterns of Coronary Atherosclerosis". In this paper, the objective was to characterize the pathophysiological patterns of CAD using motorized coronary pressure pullbacks during continuous hyperemia and to propose a quantitative assessment of the spatial distribution of the epicardial resistance in patients with stable CAD. The PPG index quantifies the spatial distribution of epicardial resistances and discriminates between focal and diffuse epicardial atherosclerosis:

$$PPG_{index} = \frac{\frac{\text{Maximal PPG over 20 mm}}{\text{Vessel FFR gradient}} + \left(1 - \frac{\text{Length with functional disease}}{\text{Vessel length}}\right)}{2}$$

Maximal PPGs over 20 mm of length quantified the magnitude of pressure drop, whereas length of functional deterioration measured the extent of disease. The higher the PPG index, the more focal the stenosis. The lower the PPG index, the more diffuse the CAD. Using the PPG, 36% of the vessel disease patterns were reclassified when compared with conventional angiography also increasing interobserver agreement concerning the identification of the CAD pattern.

To render the PPG a technique applicable in the daily clinical catheterization laboratory, we then wanted to facilitate the pullback measurement by bypassing the use of intravenous adenosine administration for hyperemia. Also, intra-coronary adenosine does not provide long enough hyperemia to perform an FFR pullback and PPG calculation. We re-introduced intra-coronary papaverine. In our study, using standardized papaverine doses, we found time to 90% of the hyperemic onset of 12.4 (IQR 8.8–19.2) seconds and a hyperemic plateau duration of 43.6 (IQR 36.1–60.7) seconds without adverse events related to the use of papaverine.

Then, the PPG derived from motorized pullbacks was adapted for manual pullbacks by making the original equation's parameters based on absolute values (i.e., mm) relative to the pullback duration. Therefore, the adapted equation resulted in:

$$\mathbf{PPG} = \frac{\frac{\text{Max Pressure Gradient over 20\% pullback length}}{\text{Vessel FFR gradient}} + (1 - \text{proportion of pullback length with FFR deterioration})}{2}$$

In a next analysis, we proved that PPG calculation for manual pullbacks resulted in similar values compared to motorized pullbacks, that both intra- and inter-operator reproducibility of manual PPG were excellent, and that the duration of the pullback did not affect the reproducibility of the PPG.

From the initial cohort of the JACC paper, the PPG performance was assessed in tandem disease. Serial stenoses often represent a physiological conundrum because the interaction (cross talk) between the different stenoses prevent merely summing up the trans-stenotic pressure gradients taken in isolation. As a consequence, isolating the functional contribution of each lesion in a serial circuit either in resting or hyperemic conditions remains challenging Intracoronary pressure pullbacks are essential to understand the physiological effect of serial lesions[40]. The ideal model is represented by a pressure curve depicting two focal pressure drops in a pullback curve. Nonetheless, vessels with angiographic serial lesions might also present diffuse pressure losses without evident drop. The Pullback Pressure Gradient (PPG)

index quantifies the functional pattern of CAD as either focal or diffuse. The presented study on “Hyperemic hemodynamic characteristics of serial coronary lesions assessed by Pullback Pressure Gradients” aimed at characterizing the functional pattern of CAD in vessels with serial lesions using mechanized FFR pullback and PPG.

Invasive functional assessment of epicardial CAD is recommended in myocardial revascularization guidelines.[42] Pressures ratios under hyperemic or in resting conditions can be used to assess the hemodynamic significance of an epicardial narrowing; this is particularly recommended in patients with intermediate epicardial stenosis (i.e. visual diameter stenosis between 30% and 70%)[115]. In 2002, results of an international registry showed that the higher was the post-PCI fractional flow reserve (FFR) value, the lower the probability of an adverse event at follow-up[116]. Subsequently, several studies have shown a relationship between post-PCI FFR and major adverse cardiac events, with various dichotomous predictive cutoff values[15,52,56,117]. Post-PCI FFR has been proposed as a clinical target to optimize PCI and as an endpoint of clinical outcomes in many trials.
After successful angiographic PCI, approximately one fourth of patients retains a sizable epicardial pressure gradient due to residual atherosclerotic disease or suboptimal stent deployment[55]. In the state-of-the-art paper “Invasive coronary physiology after stent implantation: Another step towards precision medicine”, the authors focus on the different tools available to improve and assess post-PCI physiology. Currently available invasive methods are described, i.e., Pd/Pa, FFR, iFR and QFR. For PPG, an extension of FFR, an exponential relationship has been observed between the PPG value and functional gain (i.e., FFR after PCI minus FFR before PCI), with a substantial improvement expected above PPG values of 0.50 to 0.60. PPG, therefore, shows strong potential to predict the physiologic response to PCI (Sonck J, EuroPCR 2020). Successful PCI re-establishes epicardial conductance and improves myocardial perfusion. Consequently, FFR measured after PCI can quantify the degree of functional revascularization.
Notwithstanding, we observed during our research a lower FFR post-PCI in LAD compared to non-LAD. in a pooled analysis we confirmed a difference in post-PCI FFR of 0.06 (standard error 0.002) units, lower in the LAD and higher in non-LAD vessels. Several factors contribute to this phenomenon: (1) the hydrostatic effect on the pressure wire, (2) the myocardial mass, absolute myocardial blood flow and volume to mass ratio, (3) post-PCI pressure pullback patterns and (4) pressure pullback endotypes e.g., focal vs. diffuse CAD patterns. The P3 study and PPG concept contributed to this understanding. Co-registration of

motorized FFR pullbacks and optical coherence tomography revealed characteristic patterns of post-PCI FFR pullback curves in LADs and non-LADs. In the LAD, gradual pressure decline was systematically present independent of the presence of disease. In other words, in LADs after optimal stent implantation, even in absence of residual atherosclerotic disease, the FFR pullback curve shows a downslope in the FFR pullback that is statistically different than non-LADs. In contrast, the pattern of the post-PCI FFR pullback curve in non-LAD vessels often exhibits a zero-slope profile leading to higher distal FFR values. Moreover, pressure deterioration can occur gradually along the coronary vessel with homogeneously distributed pressure gradients. Alongside, focal pressure gradients in the pullback curve arise from residual (or unmasked) stenosis or stent under-expansion (both potentially treatable). These two mechanisms can of course co-exist to produce a combination of focal and diffuse pressure loss. The former resembles the functional endotype observed in post-PCI LAD pullbacks due to greater viscous loss from larger distal mass even in a normal vessel but can also be appreciated in vessels with truly diffuse CAD.

Based on all observations, we defined recommendations for clinical interpretation of post-PCI FFR. Most importantly, post-PCI FFR can be considered a metric of functional revascularization, largely determined by the baseline phenotype of CAD (focal vs. diffuse) and PCI technique. Post-PCI FFR should be interpreted in a vessel specific manner. Due mainly to hydrostatic effects but also variable myocardial mass, the LAD is associated with lower post-PCI FFR values. Mechanisms leading to low post-PCI FFR should be elucidated by pullback and differentiated between focal jumps or diffuse residual pressure loss. Lastly, although a higher post-PCI FFR reduces the probability of adverse events, its predictive value remains modest.

Using FFR pullbacks, we hypothesized that we could quantify the mismatch in the extent of CAD compared with QCA or OCT with resulting potential impact on FFR after PCI. To calculate functional length, an automatic piece-wise linearization and classification of the FFR curve segments was developed. In detail, the functional length of disease for each coronary artery was obtained as the summation of the length of all linearized FFR curve segments classified as diseased by the algorithm. In summary, this novel approach confirmed that lesion length based on QCA and FFR pullbacks was not correlated. In contrast, CAD length derived from OCT correlated with functional CAD extent. The mismatch between the length of anatomical and functional CAD (i.e., Functional-Anatomical Mismatch (FAM), either derived from QCA or OCT) correlated with the improvement in epicardial conductance after percutaneous revascularization. Addition and fusion of FFR pullbacks with QCA or

intra-coronary imaging, as a second level of decision-making after the confirmation of hemodynamic lesion significance, has the potential to maximize functional gain and coronary conductance post-PCI.

Impact of Coronary Remodeling on Fractional Flow Reserve

In the early stage of coronary atherosclerosis, expansive remodeling compensates for plaque growth without affecting luminal dimensions or even results in a mild luminal enlargement.[118,119] However, the impact of subclinical coronary artery disease progression on physiological parameters remains elusive. Coronary computed tomography angiography has emerged as a noninvasive method to evaluate lumen and plaque dimensions.[120] In addition, vessel conductance can be assessed by the 3-dimensional reconstruction of the coronary lumen geometry and simulation of blood flow.[38,121]

This study aimed to evaluate the impact of coronary arterial remodeling and lumen dimensions on fractional flow reserve derived from coronary computed tomography angiography (FFR_{CT}).

Serial coronary computed tomography angiography was performed in 24 patients with known coronary artery disease at baseline and the 54-month follow-up. Coronary vessels ≥2.0 mm in diameter with at least 10 mm in length were analyzed by an independent core laboratory (Cardialysis BV) using a validated software package (Medis QAngioCT). For the serial analyses, vessels were matched in length between baseline and follow-up. The FFR_{CT} (HeartFlow, Inc) results are presented as the area under the virtual pullback curve (AUvPC), calculated by plotting the FFR_{CT} value at every 10 mm versus length of the vessel (Figure, A). The association between variables was investigated with the Spearman correlation coefficient. Mixed-effect models with random intercept were used to account for the within patient correlation of vessels. The definition of disease progression and regression was based on 2 times the SD of the mean difference of the repeated measurement.

The study was approved by the ethics committee of each institution, and all subjects signed informed consent.

Overall, 80 vessels from 24 patients were serially assessed and included in this study. All patients were treated with statins. Quantitative coronary computed tomography angiography analysis was feasible in 54 vessels, whereas FFR_{CT} was feasible in 45 of 54 (83%) of vessels. At baseline, the mean plaque burden was 53 ± 9% and mean luminal area was 9.41 ± 4.4 mm^2. Overall, plaque and lumen dimensions remained unchanged (Δplaque area, 0.19 mm2; 95% confidence interval, −0.91 to 0.53; P=0.60; and Δlumen area, 0.27 mm^2; 95% confidence

interval, −0.63 to 0.09; P=0.13). In addition, the FFR_{CT} remained stable (ΔFFR_{CT} AUvPC, 0.27; 95% confidence interval, −0.1 to 0.1; P=0.966). Nineteen vessels showed expansive remodeling; 16 exhibited negative remodeling; and 19 remained unchanged. The FFR_{CT} deteriorated in 15 vessels, improved in 23 vessels, and remained unchanged in 7 vessels.
The change in mean plaque area was strongly correlated with the change in mean vessel area (Figure, B), whereas changes in mean plaque area did not correlate with changes in mean lumen area (Figure, C). Expansive remodeling was associated with luminal enlargement; for every 1-mm^2 increase in vessel area, the lumen area increased by 0.24 mm^2 (Figure, D). The changes in mean vessel area and mean lumen area were positively correlated with changes in FFR_{CT} AUvPC, whereas plaque changes had no impact on FFR_{CT} (Figure, E through G).
The main findings of this study can be summarized as follows: (1) In patients with nonobstructive coronary artery disease, mean lumen area, plaque area, and vessel area remained unchanged during 4.5 years of observation; (2) the conductance of the vessel, as reflected in the FFR_{CT} AUvPC, did not significantly deteriorate or improve; and (3) vessel area changes were positively correlated with changes in mean lumen area and FFR_{CT} AUvPC.
Studies addressing the impact of statin treatment on coronary plaque have found that atherosclerosis progression can be associated with luminal enlargement. Transcending the anatomic findings, the present study incorporates the functional assessment of the conductance of the coronary vessels. Expansive remodeling was associated with an increase in mean lumen area and improvement in FFR_{CT}. The virtual physiological evaluation allowed us to calculate the FFR_{CT} AUvPC, which showed to be useful in reflecting the physiological changes in subclinical states of coronary artery disease, as an alternative to a topical FFR threshold used in clinical practice to detect ischemia (0.75–0.80).
In conclusion, this study shows that in patients with nonobstructive coronary artery disease, expansive remodeling has an impact on FFR_{CT}. Progression of coronary atherosclerosis leading to expansive remodeling can be associated with paradoxical luminal enlargement and improvement in FFR_{CT}.

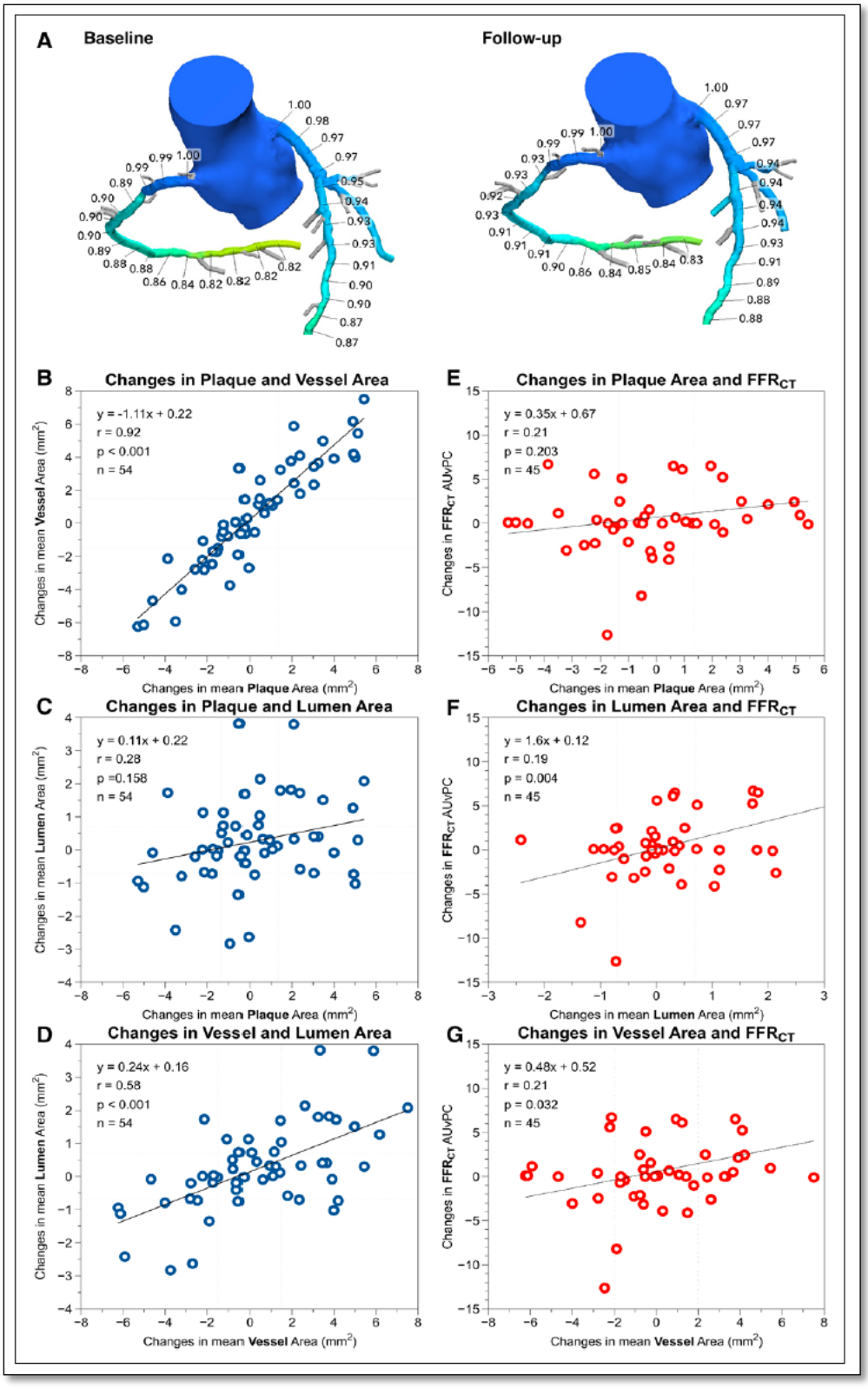

Correlation between changes in vessel, plaque, lumen area, and fractional flow reserve derived from computed tomography angiography (FFR_{CT}). A, An example of the serial measurement of FFR_{CT}. FFR_{CT} was assessed at every 10 mm to calculate the area under the virtual pullback curve (AUvPC). Morphometric relationships are shown on the left (blue circles) and the functional relationships on the right (red circles). B, Significant positive correlation between changes in mean plaque area and vessel area. C, Significant positive correlation between changes in mean vessel area and lumen area. D, Nonsignificant correlation between the changes in mean plaque area and mean lumen area. E, Significant positive correlation between the changes in mean vessel area and FFR_{CT} AUvPC. A nonsignificant correlation was found between plaque changes and FFR_{CT} changes (F), whereas a significant positive correlation was found between lumen changes and FFR_{CT} changes (G). The gray lines indicate the boundaries of the reproducibility of the measurements.

Evaluation of epicardial coronary resistance using computed tomography angiography: A proof of concept

Pressures ratios under hyperemic or in resting conditions can be used to assess the hemodynamic significance of an epicardial narrowing; this is particularly recommended in patients with intermediate epicardial stenosis (i.e. visual diameter stenosis between 30% and 70%).[115] The current approach relies on the assessment of pressure indexes using one measurement distal to the epicardial stenosis.[7] A single distal measurement accounts for the accumulation of pressure drops related to proximal stenoses and frictional pressure losses often observed in mild diffuse disease. An FFR pullback can depict the pattern and distribution of epicardial coronary artery resistance (e.g. focal vs diffuse).[9] Fractional flow reserve derived from coronary CT angiography (FFR_{CT}) is a non-invasive method that uses patient-specific coronary geometries to perform blood flow simulation providing an FFR_{CT} value at any position of the coronary tree.[36,58,59] An FFR_{CT} virtual pullback curve may provide additional information compared to one single distal FFR value.[122] However, the accuracy of the virtual FFR_{CT} pullback curve remains to be determined. The present study aims to investigate the accuracy of the virtual FFR_{CT} pullback curve using a motorized hyperemic FFR pullback as a clinical reference.

FFR values were extracted from coronary vessels at approximately 1 mm to generate pullback curves. Invasive motorized FFR pullbacks were acquired using a dedicated device at a speed of 1 mm/s. A total of 3172 matched FFR_{CT} and FFR values were obtained in 24 vessels. The correlation coefficient between FFR_{CT} and FFR was 0.76 (95%CI 0.75 to 0.78; $p < 0.001$). The area under the pullback curve was similar between FFR_{CT} and invasive FFR (79.0 ± 16.1 vs. 85.3 ± 16.4, p=0.097). The mean difference in lesion gradient between FFR_{CT} and FFR was −0.07 (LOA -0.26 to 0.13) whereas in non-obstructive segments was −0.01 (LOA -0.06 to 0.05).

The evaluation of epicardial coronary resistance using coronary CT angiography with FFR_{CT} was feasible. FFR_{CT} virtual pullback appears to be accurate for the evaluation of pressure gradients. FFR_{CT} has the potential to identify the pathophysiological pattern of coronary artery disease in the non-invasive setting.

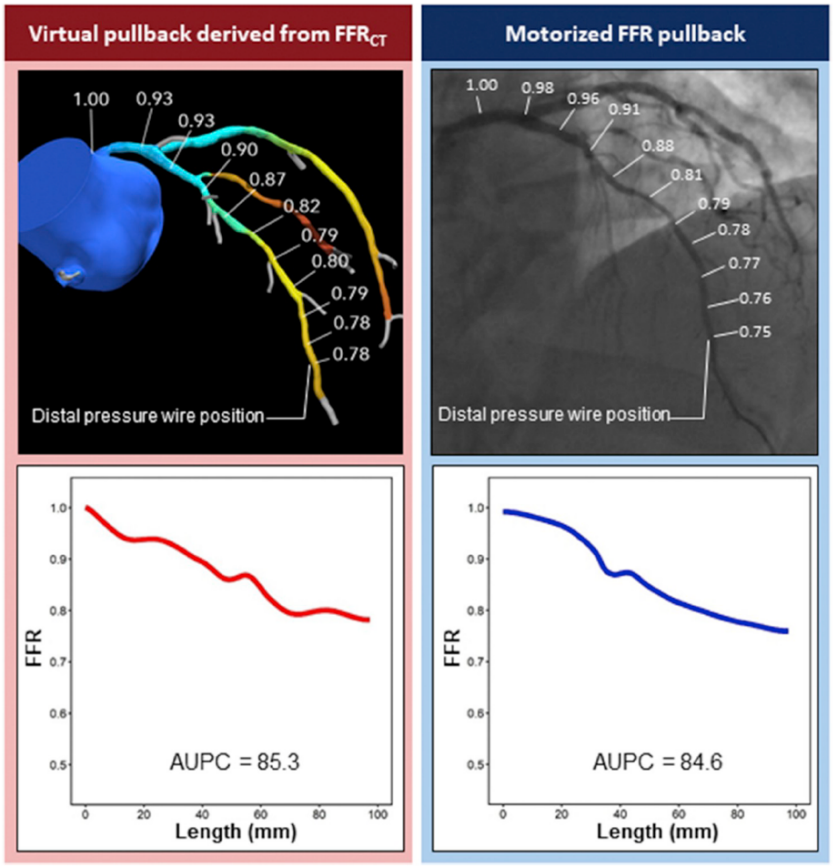

Fig. 2. Case example of FFR_{CT} (left) and invasive FFR (right) pullback analyses with colocalization of FFR values on the angiographic images. FFR_{CT}: fractional flow reserve derived from computed tomography, FFR: fractional flow reserve, AUPC: area under the pullback curve.

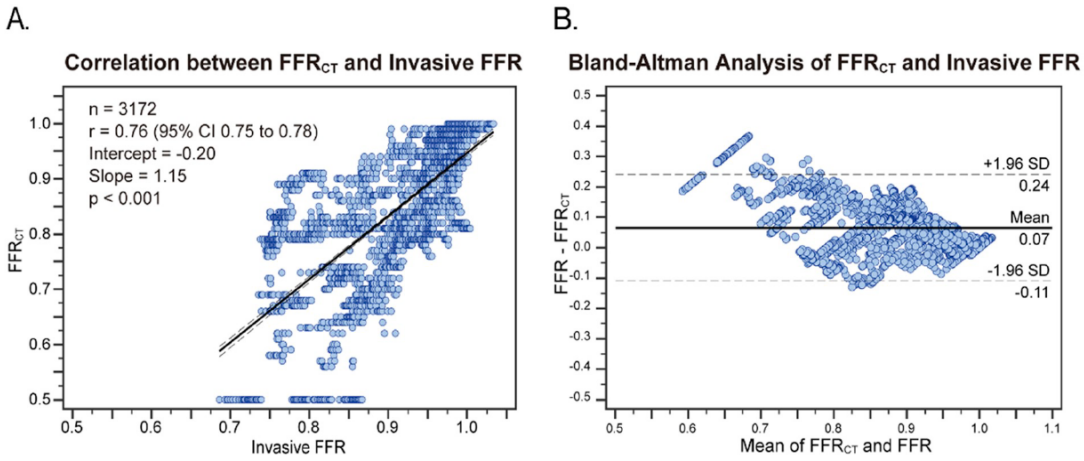

Fig. 4. Correlation and agreement of non-invasive and invasive FFR pullbacks. (A) Correlation between FFR_{CT} and FFR values extracted from the pullback curves. (B) Agreement on FFR values between FFR_{CT} and invasive FFR using the Bland Altman method. Abbreviation as previous figure.

Motorized fractional flow reserve pullback: Accuracy and reproducibility

The present study aimed at determining the accuracy and reproducibility of motorized FFR pullbacks in patients with stable coronary artery disease.

Fractional flow reserve (FFR) is recommended for decision making regarding myocardial revascularization. The distribution of epicardial resistance along coronary vessels can be assessed using FFR pullbacks.

Duplicated FFR pullbacks were acquired using a motorized device at a speed of 1 mm/s in intermediate coronary stenosis. In addition, a single FFR value was measured at an anatomical landmark. The agreement between FFR measurements was assessed using the Bland–Altman method, Pearson's correlation coefficient and area under the pullback curve (AUPC).

In 20 vessels, 37,326 FFR values were obtained. The mean FFR from the pullbacks was 0.91 ± 0.08 whereas the mean FFR at the distal location was 0.85 ± 0.09. The mean difference between pullbacks was −0.002 (LOA −0.058 to 0.054). The difference in AUPC between the two FFR pullbacks was 2.1 ± 1.6%. At prespecified anatomical locations, the mean difference between the FFR derived from the pullback data and the measured FFR was 0 (LOA −0.040 to 0.039). The repeatability of the distal FFR measurement was high (bias −0.003, LOA −0.046 to 0.041).

A motorized FFR pullback was accurate to assess the distribution of epicardial resistance in patients with intermediate coronary artery disease. The reproducibility of the FFR pullback was high. Further studies are required to determine the potential usefulness of a hyperemic FFR pullback strategy for decision making and treatment planning.

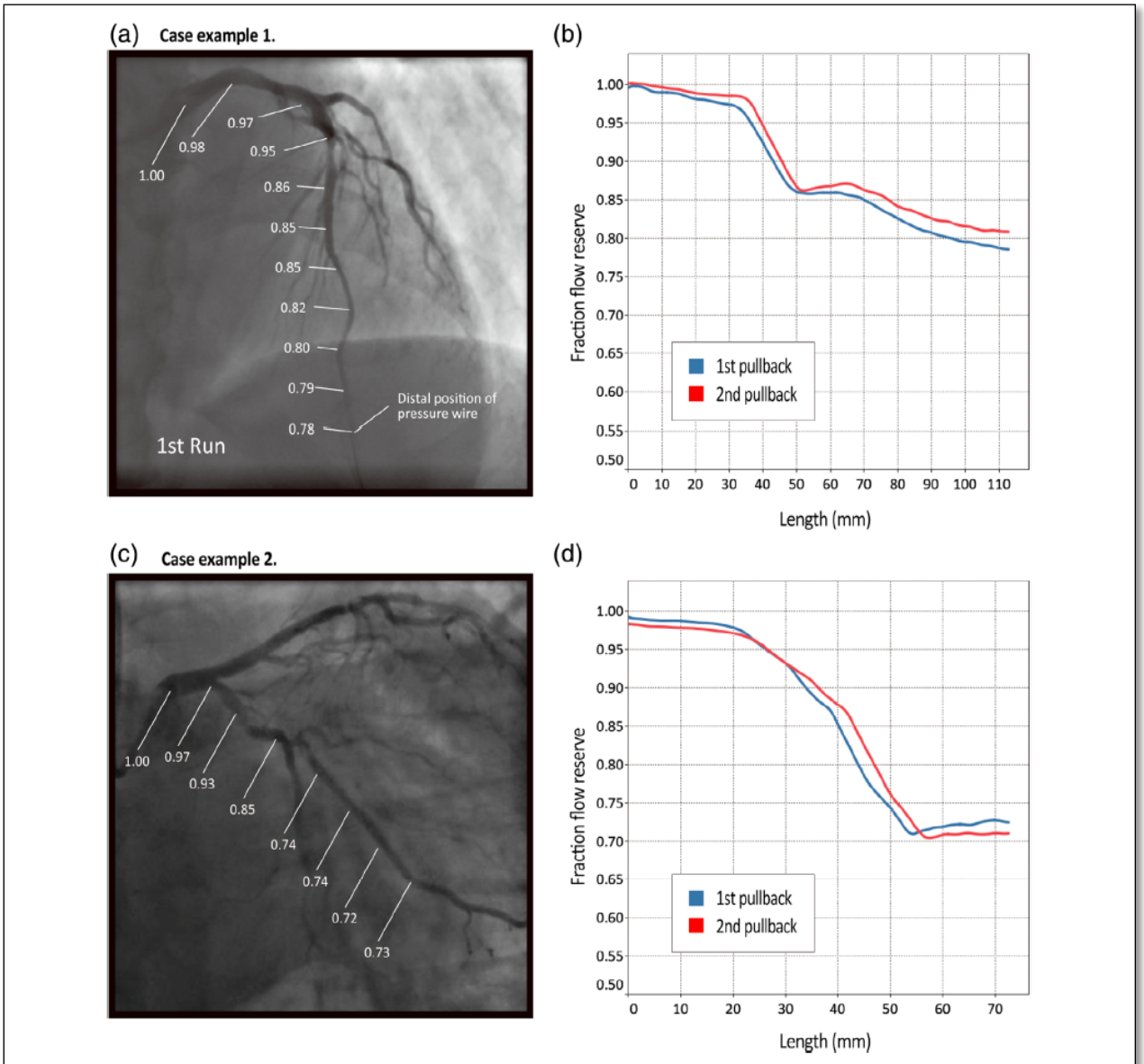

FIGURE 5 Case examples 1. Panel (a), left anterior descending artery with a moderate lesion in the mid segment and an FFR gradient of 0.09; FFR values were co-localized on the angiographic image with a distal FFR of 0.78 and 0.81 in the first and second pullback run, respectively. Panel (b) shows the pullback curves derived from the first and second FFR pullbacks. Case example 2. Panel (c), circumflex artery and first marginal branch with two obstructive lesions. The FFR gradients in the first and second lesions were 0.08 and 0.11, respectively. In panel D, duplicated pullback curves show a significant pressure drop produced by the summation of the pressure losses of the first and second lesion. FFR, fractional flow reserve [Color figure can be viewed at wileyonlinelibrary.com]

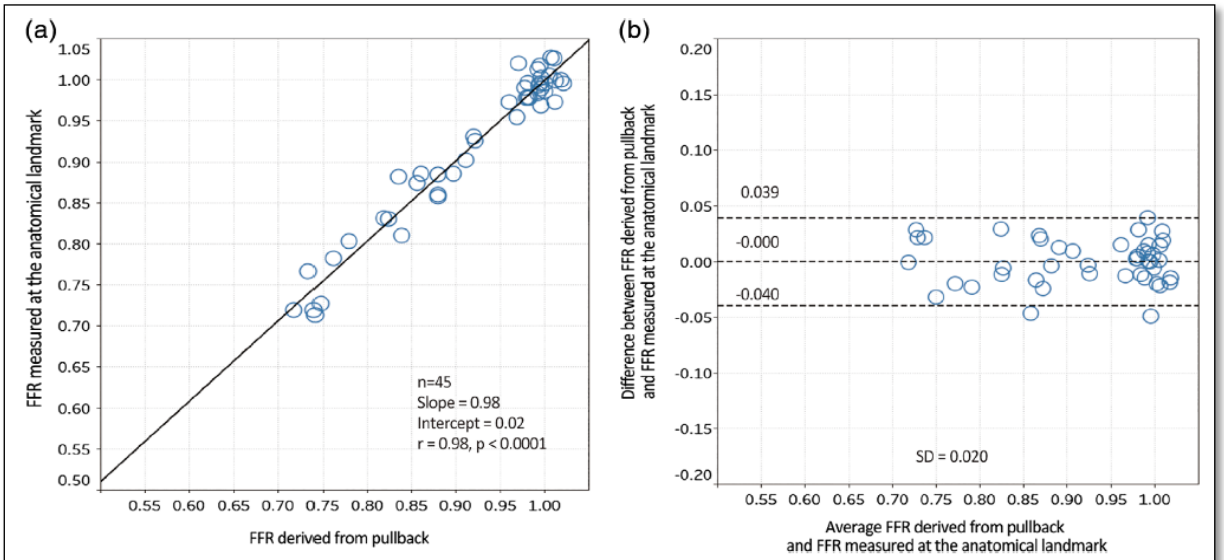

FIGURE 2 Panel (a) Correlation between the FFR values measured at an anatomical landmark and FFR-value derived from the pullback data. Panel (b) shown the mean difference between FFR values measured at an anatomical landmark and FFR-value derived from the pullback data. FFR, fractional flow reserve [Color figure can be viewed at wileyonlinelibrary.com]

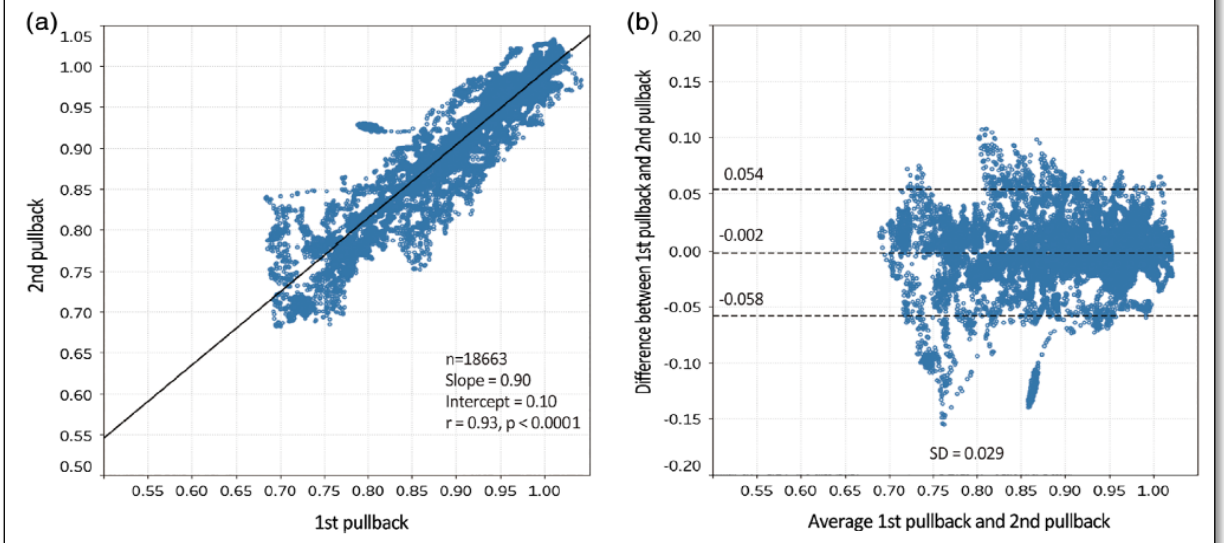

FIGURE 3 Pullback reproducibility analysis. Panel (a) shows the correlation between the first and second FFR pullback run and panel (b) shows the mean difference between the first and second pullback run. FFR, fractional flow reserve [Color figure can be viewed at wileyonlinelibrary.com]

Measurement of Hyperemic Pullback Pressure Gradients to Characterize Patterns of Coronary Atherosclerosis

Diffuse atherosclerosis is commonly observed in angiographically normal segments in patients with stable coronary artery disease (CAD). The distribution of epicardial resistance along the vessel can be evaluated using coronary physiology.

The purpose of this study was to characterize the pathophysiological patterns of CAD using invasive pressure pullbacks during continuous hyperemia.

In this prospective, multicenter study of patients undergoing clinically indicated coronary angiography due to stable angina, a pressure-wire pullback device was set at a speed of 1 mm/s. Based on coronary angiography and on the fractional flow reserve (FFR) pullback curve, the patterns of CAD were adjudicated as focal, diffuse, or a combination of both. The distribution of epicardial resistance was characterized using the hyperemic pullback pressure gradients (PPGs). The PPG index, a continuous metric based on the magnitude of pressure drop over 20 mm and on the extent of functional disease was computed to determine the pattern of CAD. Low PPG index indicates diffuse CAD.

A total of 158 vessels (117 patients) were included. Overall, 984.813 FFR values were used to generate 100 FFR pullback curves. Using coronary physiology, 36% of the vessel disease patterns were reclassified compared to angiography. The median of maximal PPG over 20 mm was 0.083 (interquartile range: 0.063 to 0.118) FFR units, and the mean extent of functional disease was 39.3 ± 21.3 mm. The mean PPG index was 0.58 ± 0.18 and differentiated pathophysiological focal and diffuse disease ($p < 0.001$).

Pathophysiological patterns of CAD can be characterized by motorized hyperemic PPGs. The evaluation of the FFR pullback curve reclassified one-third of the vessels' disease patterns compared with conventional angiography. The PPG index is a novel metric that quantifies the distribution of epicardial resistance and discriminates focal from diffuse CAD.

CENTRAL ILLUSTRATION Pathophysiological Coronary Artery Disease Patterns and PPG Index

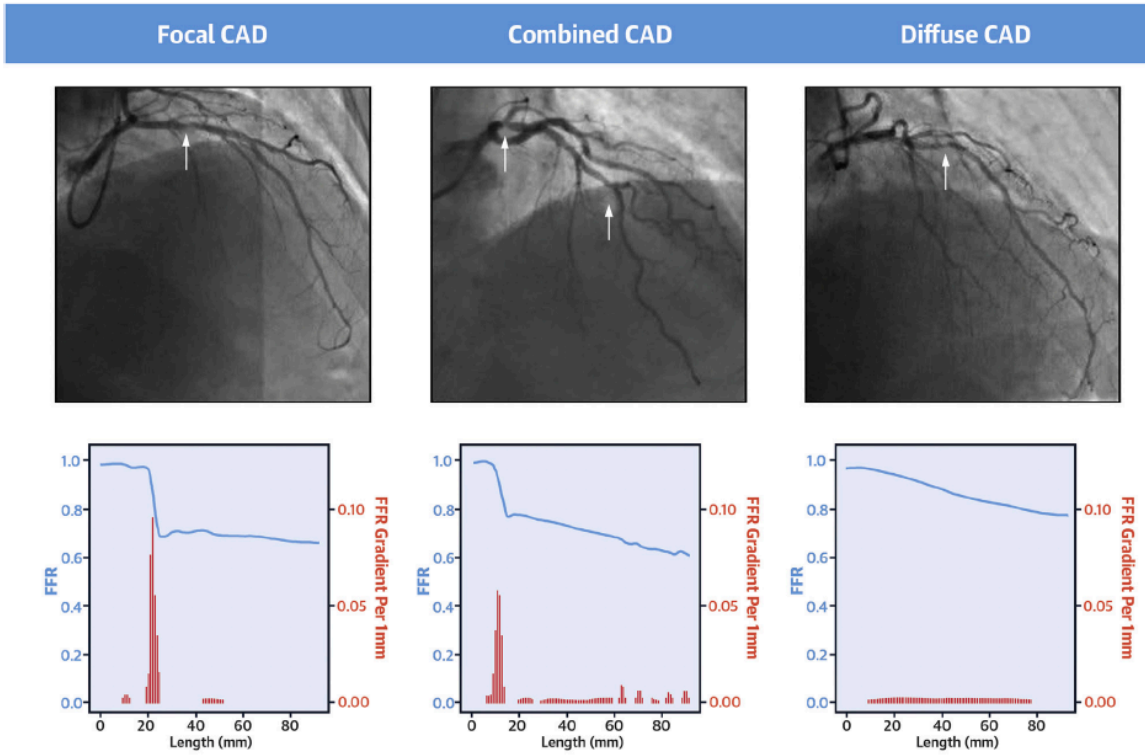

Pullback Pressure Gradients Index

$$\{MaxPPG_{20mm}/\Delta FFR_{vessel} + (1\text{-Length with Functional Disease (mm)/Total Vessel Length (mm)})\}/2$$

Focal CAD	Combined CAD	Diffuse CAD
$\frac{MaxPPG_{20mm}}{\Delta FFR_{vessel}} = \frac{0.300}{0.325} = 0.923$	$\frac{MaxPPG_{20mm}}{\Delta FFR_{vessel}} = \frac{0.236}{0.387} = 0.610$	$\frac{MaxPPG_{20mm}}{\Delta FFR_{vessel}} = \frac{0.056}{0.193} = 0.290$
Length CAD = $\frac{20}{100} = 0.200$	Length CAD = $\frac{65}{92} = 0.707$	Length CAD = $\frac{74}{101} = 0.733$
PPG Index = $\frac{0.923 + (1\text{-}0.20)}{2} = 0.86$	PPG Index = $\frac{0.610 + (1\text{-}0.707)}{2} = 0.45$	PPG Index = $\frac{0.290 + (1\text{-}0.733)}{2} = 0.28$

Collet, C. et al. J Am Coll Cardiol. 2019;74(14):1772-84.

Three case examples depicting the pathophysiological patterns of CAD. **(Top)** Conventional coronary angiography; **(middle)** the FFR pullback curves; and histograms depicting the magnitude and extension of FFR drop; and **(bottom)** details of the PPG calculation. The **red bars** indicate FFR drops ≥0.0015. On the **top left panel**, the angiography shows a severe lesion in the mid LAD **(white arrow)** with a distal FFR of 0.68. This lesion produced an FFR drop responsible for 86% of the distal FFR with a maximum pullback pressure gradient over 20 mm of 0.30 FFR units. Only 20% of the vessel showed functional disease. The PPG index was 0.86, indicating physiological focal CAD. The **top middle panel** shows a severe lesion at the proximal LAD and a moderate lesion at mid LAD **(white arrows)**. The maximum pullback pressure gradient over 20 mm was 0.236 FFR units, with 70.7% of the vessel length showing FFR deterioration, and the PPG index was 0.45. In the **top right panel**, an anatomical lesion at the mid LAD **(white arrow)** was observed with distal FFR of 0.78. The maximum pullback pressure gradient over 20 mm was 0.056, while 73.3% of the vessel length showed physiological disease. The PPG index was 0.28, indicating physiological diffuse CAD. CAD = coronary artery disease; FFR = fractional flow reserve; LAD = left anterior descending artery; PPG = pullback pressure gradient.

FIGURE 5 Distribution of the PPG Index

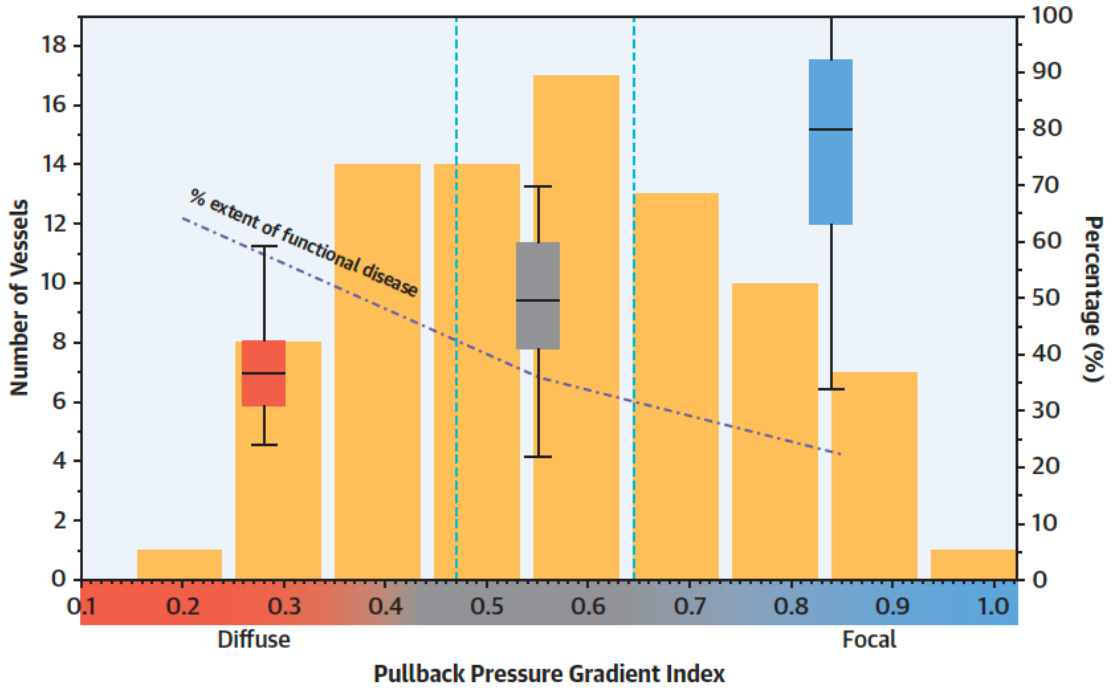

The **blue bars** show the distribution of the pullback pressure gradient (PPG) index; the number of vessels is shown in the left y-axis. PPG tertiles are shown by **dashed blue lines**, and the data cutoff were 0.47 and 0.65. The **box plots** represent the maximal pressure pullback gradients over 20 mm divided by vessel fractional flow reserve gradient in each of the PPG index tertiles. The extent of the vessel with functional deterioration normalized by total vessel length is shown with the **purple dashed line**. The mean value, in percentage, is plotted for each PPG index tertile linked with the right y-axis.

Duration of Hyperemia with Intracoronary Administration of Papaverine

Fractional flow reserve (FFR) and pressure pullback gradient (PPG) are 2 hyperemic indices used in clinical practice to determine the hemodynamic significance of coronary stenoses and distribution of epicardial resistance. The PPG is calculated using FFR values along the coronary vessels during a pullback maneuver for determination of the pattern (e.g., focal or diffuse) of coronary artery disease.[123] Insufficient hyperemia may minimize pressure drops and affecting pressure gradients quantification.

Papaverine has been validated for FFR measurements in several studies.[124,125] However, despite its relatively long duration of action, a detailed analysis of the vessel-specific dose–response and steady hyperemic state duration stratified by severity of coronary artery disease is still lacking.

The data that support the findings of this study are available from the corresponding author upon reasonable request. This was a prospective, single-center study of patients undergoing coronary angiography with an indication for FFR measurement. Approval was obtained from the local Ethics Committee (OLV-74690), and the study protocol was in accordance with the Declaration of Helsinki. Written informed consent was obtained from all patients before enrollment in this study. A 6F guiding catheter was inserted through the femoral or radial artery. A pressure guidewire (PressureWire X, Abbott Vascular, USA) was advanced in the distal part of the vessel to obtain (distal mean coronary pressure [Pd]) at least 30 mm beyond the epicardial lesion. Pd/mean aortic pressure (Pd/ Pa) values were recorded. The contrast was flushed from the guiding catheter and hyperemia was induced with intracoronary papaverine at a dose of 12 to 16 mg for the left coronary artery and 8 to 12 mg for the right coronary artery. The time to maximal hyperemia (time needed to reach 80% [T80] and 90% [T90] of the minimal value of Pd/Pa after the injection of papaverine) and plateau phase (time during which Pd/Pa remained at >90% of its minimal value) were computed (Figure A).3 Variability during the plateau phase was assessed extracting 1 FFR value per second. Groups were stratified according to the FFR value of ≤0.80.

Statistical comparisons between groups were performed using the Mann-Whitney U test. Overall, 46 patients (51 vessels) were included. Vessel types were 32 left anterior descending coronary arteries, 11 left circumflex coronary arteries, and 8 right coronary arteries. The mean diameter stenosis was 43.5 ± 13.0%. The mean pressure tracing recording time

after papaverine injection was 1.72 ± 0.65 minutes. The mean FFR was 0.82 ± 0.09 and 23 vessels had an FFR ≤0.80. There were no adverse effects or complications observed during the administration of papaverine. Median T80 and T90 were 9.2 (IQR 7.4–11.9) seconds and 11.4 (IQR 9.2–16.4) seconds, respectively. The plateau phase lasted for 40.5 (IQR 22.2–49.8) seconds. The changes of Pd/Pa value during the plateau phase were 0.001 (IQR −0.016 to 0.019; coefficient of variation of 11.4%). The median plateau phase was significantly longer in vessels with an FFR value ≤0.80 compared with vessels with FFR >0.80 (43.6 [IQR 36.1–60.7] seconds versus 32.6 [IQR 18.3–42.1] seconds, P value 0.027; Figure B). Distal FFR values were significantly correlated with the duration of the hyperemic plateau phase (ρ=−0.33 [95% CI −0.56 to −0.07]; Figure C).

Papaverine has been used as a hyperemic agent for the assessment of coronary flow reserve and FFR. Previous studies reported a mean time to onset of 17 to 23 seconds and the mean hyperemic duration of 22 to 51 seconds.[124,125] In the present study, using standardized papaverine doses, we found time to 90% of the hyperemic onset of 12.4 (IQR 8.8–19.2) seconds and a hyperemic plateau duration of 43.6 (IQR 36.1–60.7) seconds. We found an interaction between functional severity and time of microvascular dilation. The precise mechanisms behind this phenomenon remain to be elucidated. Concerns have been raised about the safety of intracoronary papaverine administration in terms of ventricular arrhythmias. Papaverine transitorily prolongs the QTc interval. Ventricular arrhythmias are observed in ≈1.4% of the cases.[126] In the present report there were no adverse events related to the use of papaverine.

The present analysis expands our knowledge by ascertaining that vessels with hemodynamically significant lesions, based on a contemporary criterion (i.e., FFR ≤0.80), have similar time to hyperemic onset and longer stable-state hyperemic duration compared with vessels with nonsignificant lesions. These findings portray clinical implications given the increased use of the FFR pullbacks to evaluate the functional pattern of coronary artery disease using PPG and refine percutaneous coronary intervention indication and strategy. Recently, PPG was described as potentially influencing percutaneous coronary intervention outcomes. In clinical practice, vessels with an FFR ≤0.80 will be considered for PPG measurement. Based on the results of the present study, papaverine provides sufficient time to perform a pullback maneuver for at least 30 seconds under maximal hyperemic conditions. Therefore, the current study provides the foundations for the recommendation of a pullback technique using intracoronary papaverine administration. Intracoronary administration of papaverine provides rapid onset hyperemia with a duration of steady-state sufficient for

pullback maneuvers with minimal variability. The duration of steady-state hyperemia is longer in vessels with hemodynamically significant lesions.

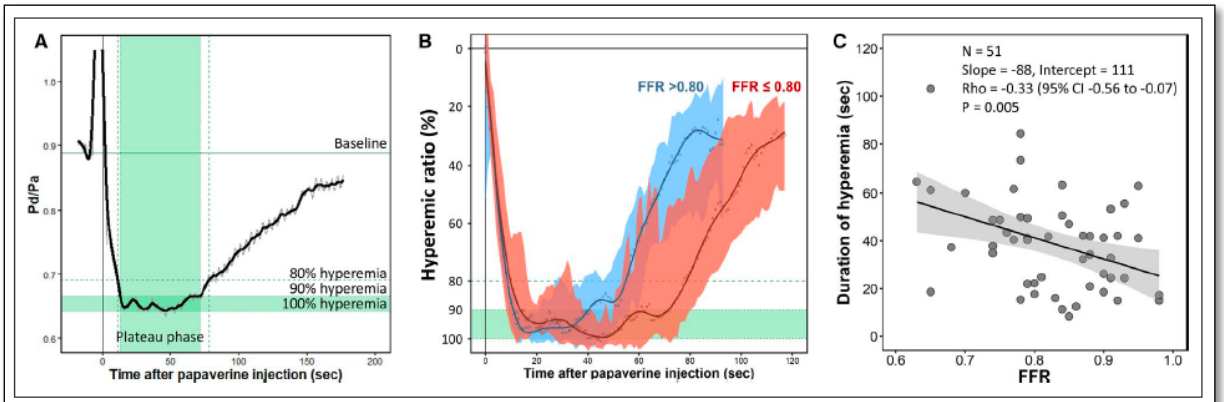

Figure. Case example of a pressure tracing after induction of hyperemia with papaverine and duration of hyperemic effect stratified by FFR.
A, An Pd/Pa tracing after the administration of intracoronary papaverine. The dashed green lines denote the plateau phase and 80%, 90%, and 100% of maximal hyperemia. The solid green areas represent the plateau phase. **B**, The duration of hyperemic plateau stratified by FFR 0.80. Pd/Pa values in the vessel with FFR ≤0.80 and FFR >0.80 are shown by red and blue curves, respectively; the shaded red and blue areas correspond to the 95% CIs. The solid green area represents the plateau phase. **C**, Correlation between distal FFR value and duration of maximal hyperemia. The gray area corresponds to the 95% CIs. FFR indicates fractional flow reserve; Pa, aortic pressure; and Pd, diastolic pressure.

Development, Validation, and Reproducibility of Pullback Pressure Gradient (PPG) derived from Manual Fractional Flow Reserve Pullbacks

FFR pullbacks allow to assess the location and magnitude of pressure drops along the coronary artery. The Pullback Pressure Gradient (PPG) quantifies the FFR pullback curve and provides a numeric expression of how focal or diffuse is the coronary artery disease. The aim of this study is (1) to validate the PPG using manual FFR pullbacks with motorized FFR pullbacks as a reference; and (2) to determine the intra- and inter-operator reproducibility of the PPG derived from manual FFR pullbacks.

Patients with stable coronary artery disease and an FFR ≤0.80 were included. All patients underwent FFR pullback evaluation either with a motorized device or manually dependent of the study cohort. The agreement on the PPG between repeated pullbacks was assessed using the Bland-Altman method.

Overall, 116 FFR pullbacks maneuvers (96 manual and 20 motorized) were analyzed. There was an excellent agreement between the PPG derived from manual and motorized pullbacks (mean difference -0.01 ± 0.07, limits of agreement [LOA] -0.14 to 0.12). The intra- and inter-operator reproducibility of PPG derived from manual pullbacks was excellent (mean difference 0, LOA -0.11 to 0.12 and mean difference 0, LOA -0.12 to 0.11, respectively). The duration of the pullback maneuver did not impact the reproducibility of the PPG (r=0.12, 95% CI -0.29 to 0.49, p=0.567).

Manual pullbacks allow for an accurate PPG calculation. The inter- and intra-operator reproducibility of PPG derived from manual pullback was excellent.

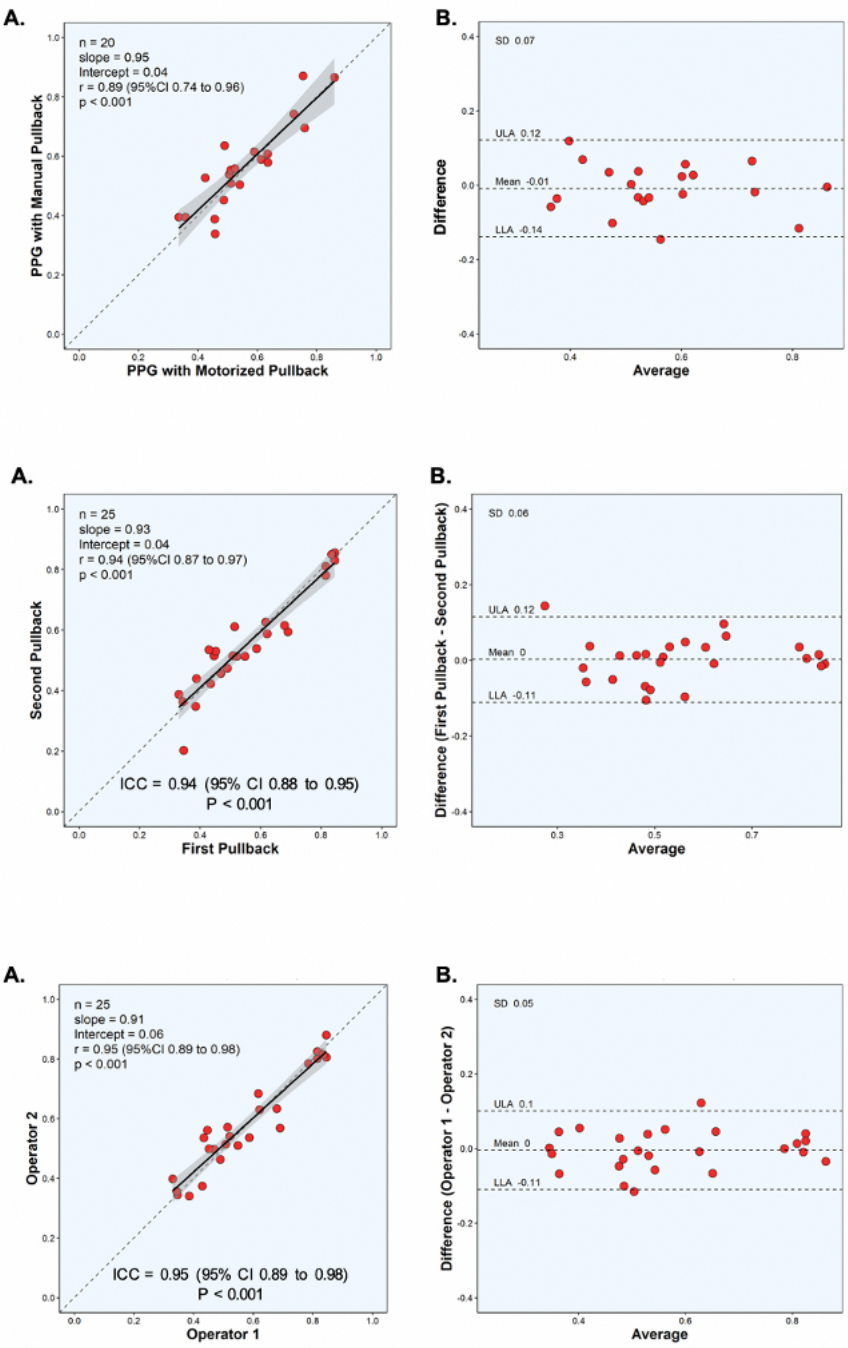

Agreement on the Pullback Pressure Gradient (PPG) between motorized and manual pullbacks (top A and B)), intra-operator agreement (middle A and B) and inter-operator agreement (bottom A and B) on PPG.

Intra- and inter-rater reproducibility of PPG and its components.

Variables	Mean difference ± SD	LLA to ULA	95% CI	COV	ICC (95% CI)
Intra reproducibility					
PPG	0.00 ± 0.06	-0.11 to 0.12	-0.02 to 0.02	0.0024	0.94 (0.88 to 0.98)
PPG20	0.01 ± 0.03	-0.05 to 0.06	-0.01 to 0.02	0.0015	0.99 (0.97 to 0.98)
%Disease	-0.76 ± 7.13	-14.74 to 13.22	-3.56 to 2.04	0.0002	0.83 (0.66 to 0.98)
Inter reproducibility					
PPG	0.00 ± 0.05	-0.11 to 0.1	-0.03 to 0.02	0.0062	0.95 (0.89 to 0.98)
PPG20	0.00 ± 0.02	-0.05 to 0.05	-0.01 to 0.01	0.0347	0.99 (0.97 to 0.98)
%Disease	-0.56 ± 5.99	-12.31 to 11.19	-2.91 to 1.79	0.3403	0.85 (0.69 to 0.98)

SD Standard deviation. LLA Lower limit of agreement. ULA Upper limit of agreement. CI Confidence interval. COV Coefficient of variance. ICC Intra-class correlation. PPG Pullback Pressure Gradient. PPG20 Maximum pressure gradient over 20% of pullback duration. %Disease Percent of pullback time with FFR deterioration

Hyperemic hemodynamic characteristics of serial coronary lesions assessed by Pullback Pressure Gradients

To characterize the hemodynamic of serial coronary stenoses using Fractional Flow Reserve (FFR) and the Pullback Pressure Gradients (PPG) index.

The cross-talk between stenoses within the same coronary artery makes the prediction of the functional contribution of each lesion challenging.

One-hundred seventeen patients undergoing coronary angiography for stable angina were prospectively recruited. Serial lesions were defined as presenting two or more narrowings with visual diameter stenosis >50% on conventional angiography. Motorized FFR pullback tracings were obtained at 1 mm/s. Pullback were visually adjudicated with two, one and no focal pressure drops. In addition, the PPG index was calculated. Twenty-five vessels presented serial lesions (mean PPG index 0.48±0.17). Two, one or no focal pressure drops were observed in 40% (n = 10; PPG index 0.59 ± 0.17), 52% (n = 13; PPG index 0.44 ± 0.12) and 8% of cases (n = 2; PPG index 0.27 ± 0.01; p-value = 0.01). Distal FFR was similar between vessels with two, one and no focal pressure drops in the pullback curve (p-value = 0.27). At the multivariate logistic regression analysis, the PPG index independently predicted the presence of two focal pressure drops (p = 0.04).

FFR-pullback tracings in serial coronary lesions exhibit three distinct functional patterns. PPG index was an independent predictor of the two-drop pattern. FFR pullback tracings with PPG provide a quantitative functional assessing of the pattern of CAD in cases with serial lesions, useful to assess the appropriateness of and to guide percutaneous revascularization strategy.

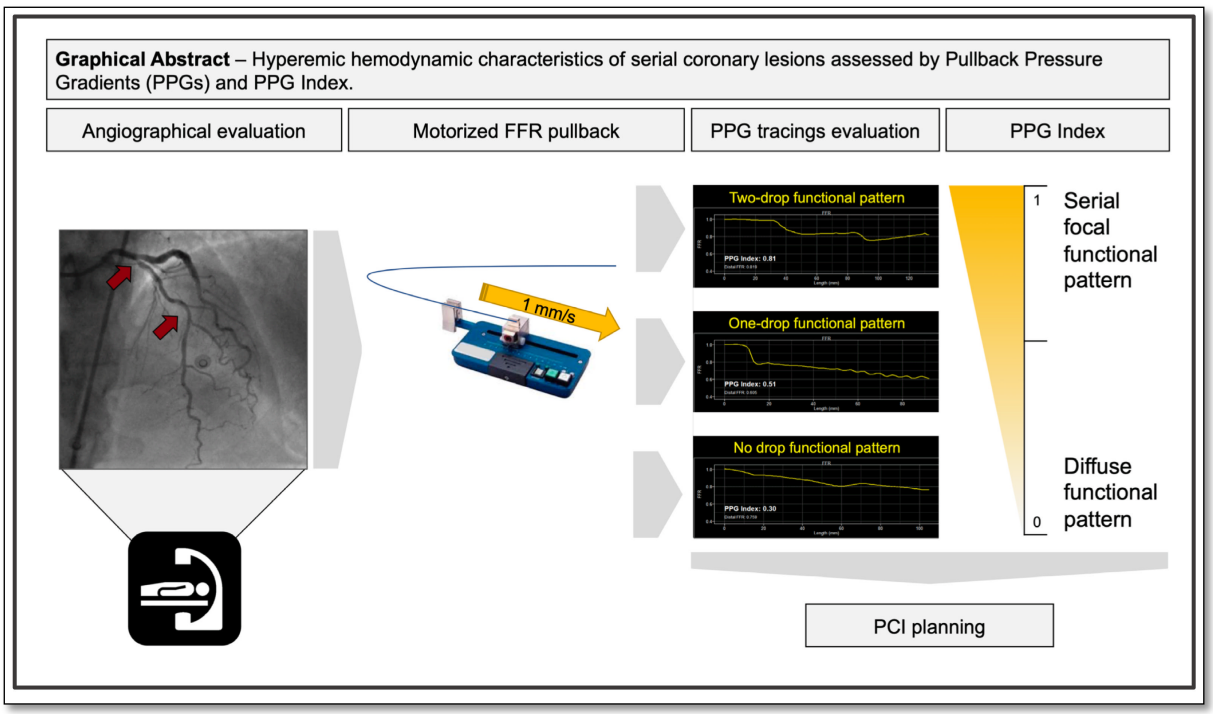

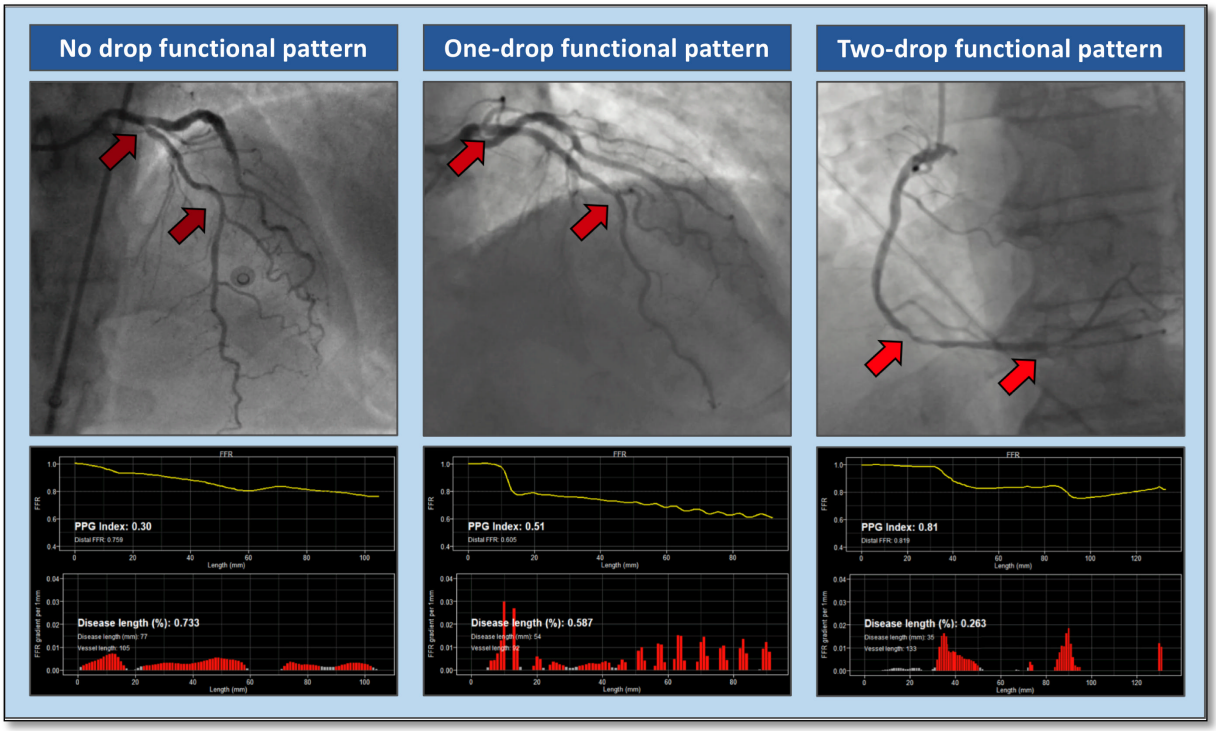

The hemodynamical cross-talk occurring between serial coronary lesions can be captured by motorized pressure pullback tracings during pharmacological hyperemia. These enable physicians to visually inspect pressure pullback curves for focal drops and intuitively locate in this way regions of low conductance, amenable of percutaneous coronary intervention (PCI). Complementary is in this setting the role of the Pullback Pressure Gradient (PPG) index, which was found in the present study predictive for the focal serial lesion pattern.

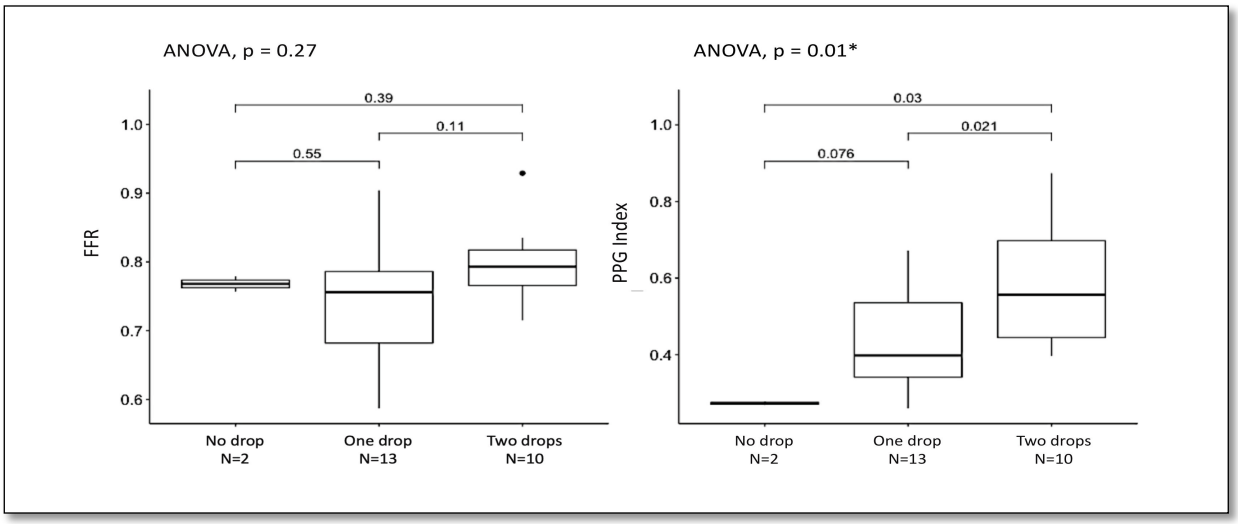

Distributions of the fractional flow reserve (left panel) and pullback pressure gradient index (right panel) according to the adjudicated functional pattern, underlining the inability for the distal FFR to capture difference among the three functional patterns. On the other hand, higher PPG index values were significantly associated with the focal serial lesion pattern, while no significance was found when comparing the distribution between mixed and diffuse functional patterns. FFR = functional flow reserve; PPG = pullback pressure gradient.

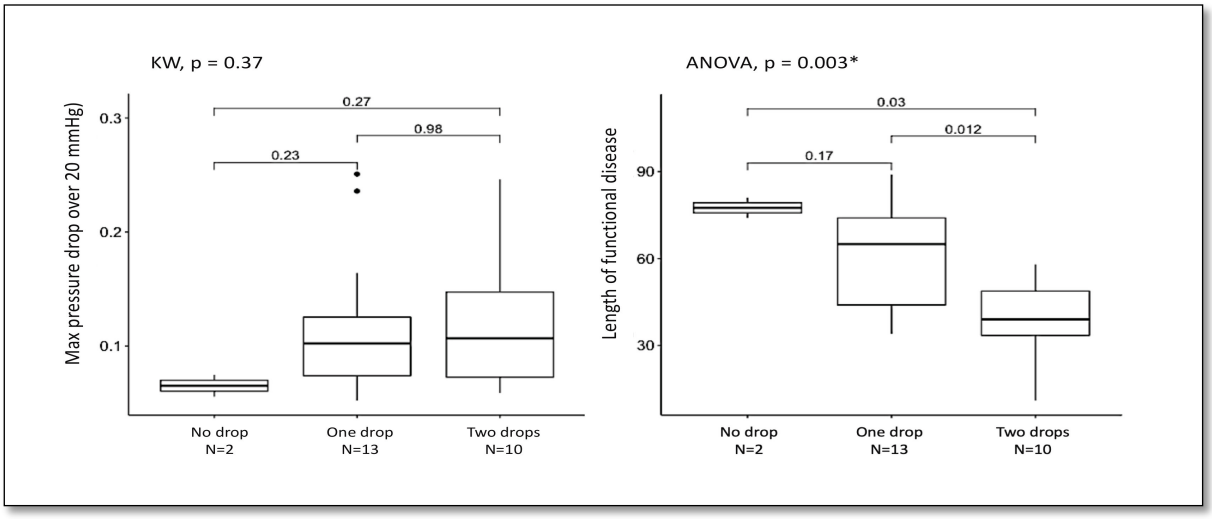

Distribution of two components of the pullback pressure gradient index equation, namely the maximal pressure gradients over 20 mm (left panel) and the length of functional disease (right panel), according to the three functional disease patterns. While the max PPG over 20 mm mean did not differ significantly between the groups, serial lesion presenting two pressure stenoses were significantly associated with shorter diseased vessel segments. KW = Kruskal-Wallis; ANOVA = (one way) analysis of variance.

Mismatch between the anatomical and functional extent of coronary artery disease

Morphological evaluation of coronary lesion length is a paramount step during invasive assessment of coronary artery disease. Likewise, the extent of epicardial pressure losses can be measured using longitudinal vessel interrogation with fractional flow reserve (FFR) pullbacks. We aimed to quantify the mismatch in lesion length between morphological (based on quantitative coronary angiography, QCA, and optical coherence tomography, OCT) and functional evaluations.

This is a prospective and multicenter study of patients evaluated by QCA, OCT and motorized fractional flow reserve pullbacks (mFFR). The difference in lesion length between the functional and anatomical evaluations was referred to as FAM.

117 patients (131 vessels) were included. Median lesion length derived from angiography was 16.05mm [11.40–22.05], from OCT was 28.00 mm [16.63–38.00] and from mFFR 67.12 mm [25.38–91.37]. There was no correlation between QCA and mFFR lesion length (r=0.124, 95% CI -0.168-0.396, p=0.390). OCT lesion length did correlate with mFFR (r=0.469, 95% CI 0.156–0.696, p =0.004). FAM was strongly associated with the improvement in vessel conductance with percutaneous coronary intervention (PCI), higher mismatch was associated with lower post-PCI FFR.

Lesion length assessment differs between morphological and functional evaluations. The morphological-functional mismatch in lesion length is frequent and influences the results of PCI in terms of post-PCI FFR. Integration of the extent of pressure losses provides clinically relevant information that may be useful for clinical decision-making concerning revascularization strategy.

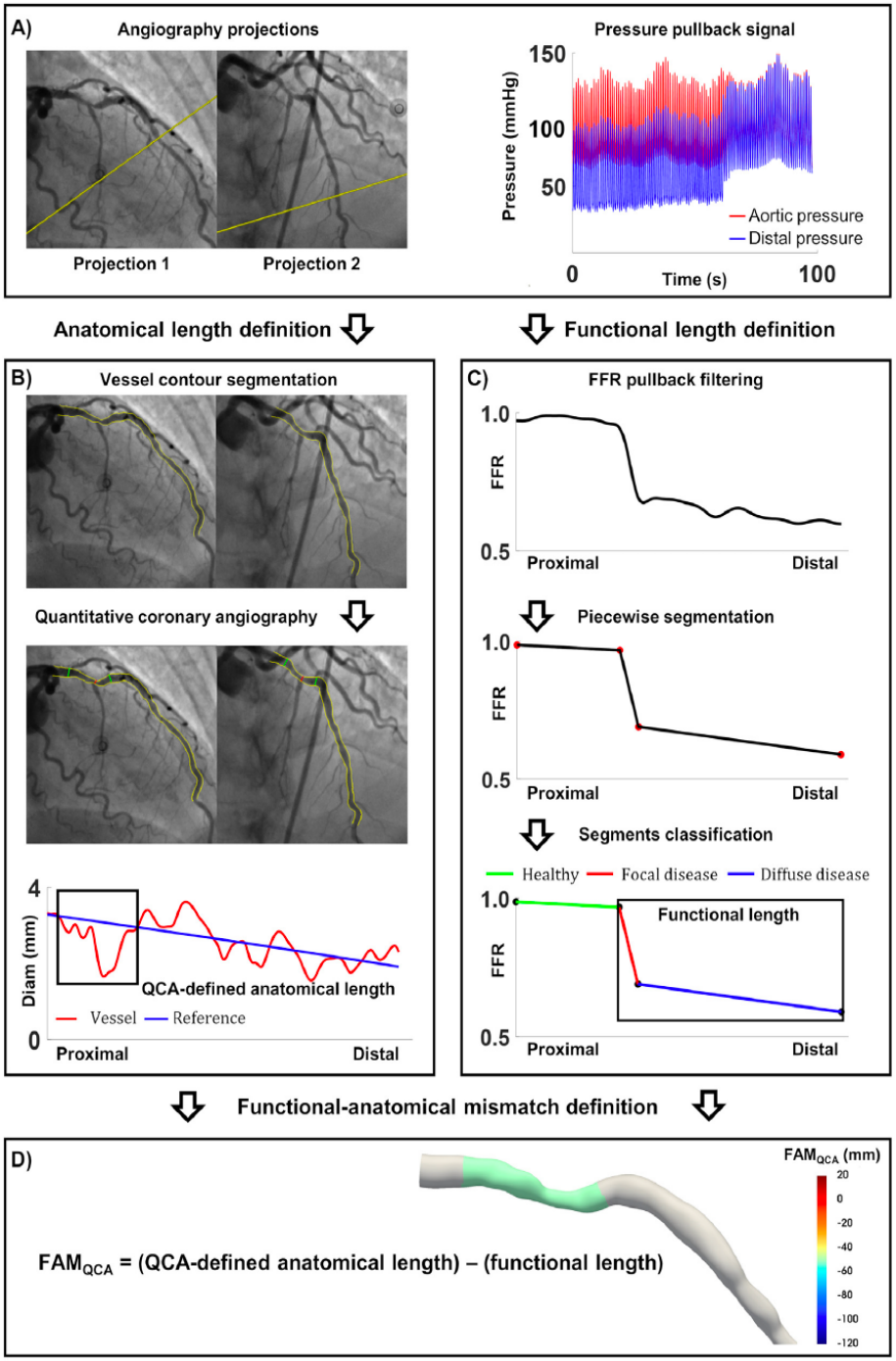

Fig. 1. Definition of QCA-derived anatomical lesion length, functional lesion length and functional-anatomical mismatch (FAM_{QCA}). A): The QCA-derived anatomical lesion length was obtained starting from two angiographic projections for each target lesion. B): 3D quantitative coronary angiography algorithm was used to obtain the QCA-derived anatomical lesion length as the distance where the reference diameter line intersects with the curve describing the local vessel diameter value. C): The functional lesion length was obtained from analysis of the FFR pullback curve after smoothing and piece-wise linearization as the sum of the segments characterized by FFR deterioration. D): The FAM_{QCA} is defined as the difference between the QCA-derived anatomical lesion length minus the functional lesion length.

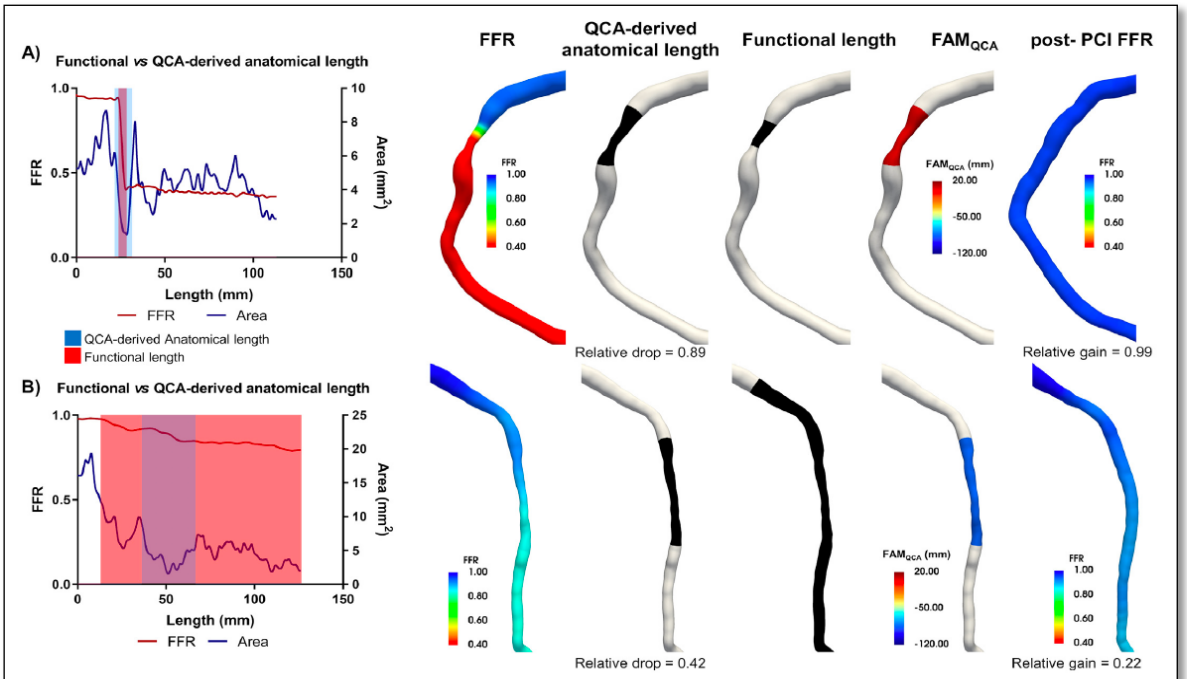

Fig. 2. Positive vs. negative FAM_{QCA}. A): example of vessel with positive FAM_{QCA}, where the QCA-derived anatomical lesion length is longer than the functional lesion length, respectively blue and red shade in the area and FFR curves (left panel). From left to right, FFR is displayed as a color-coded map on the 3-dimensional geometric reconstruction of the vessel. The extension of the anatomical and functional length is displayed in black, with indication of the relative FFR drop within the QCA-derived anatomical lesion. FAM_{QCA} is displayed as a color-coded map: the red color underlines that the functional disease was circumscribed within the anatomical lesion. Percutaneous coronary intervention (PCI) restored epicardial conductance and resulted in high post-PCI FFR (right panel), with a relative gain equal to 0.99. B) Example of vessel with negative FAM_{QCA}, where the anatomical lesion length is shorter than the functional lesion length, respectively blue and red shade in the area and FFR curves (left panel). From left to right, FFR is displayed as a color-coded map on the 3-dimensional geometric reconstruction of the vessel. The extension of the QCA-derived anatomical and functional length is displayed in black, with indication of the relative FFR drop within the anatomical lesion. FAM_{QCA} is displayed as a color-coded map: the blue color underlines that the functional disease extended beyond the anatomical lesion. Percutaneous coronary intervention (PCI) resulted in minor improvement of epicardial conductance and a low post-PCI FFR (right panel), with a relative gain equal to 0.22. (For interpretation of the references to color in this figure legend, the reader is referred to the web version of this article.)

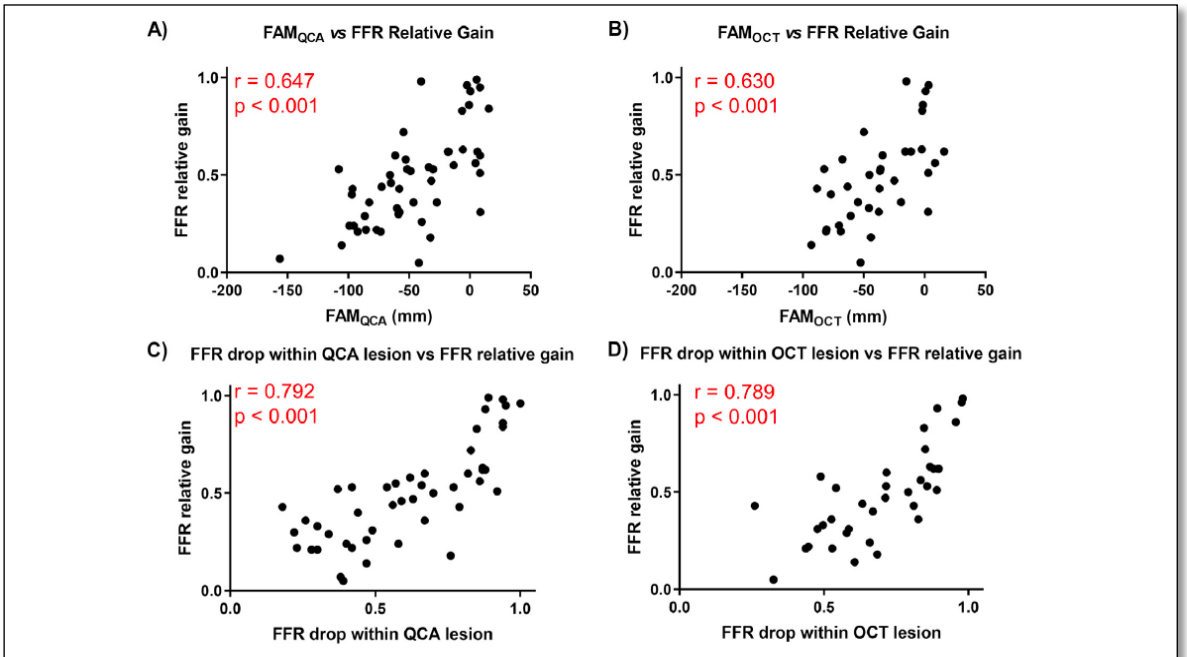

Fig. 6. Scatter plots illustrating the correlations among FAM, FFR relative gain and among the FFR drop within the anatomical lesion and FFR relative gain. A direct significant association was found between the FAM_{QCA} and the FFR relative gain after PCI, i.e. the larger the FAM the higher the functional relative gain after PCI (panel A). A direct significant association was also found between the FAM_{OCT} and the FFR relative gain after PCI (panel B). The FFR drop within the QCA-derived anatomical lesion was strongly correlated with the functional relative gain after PCI, i.e. the larger the drop is attributable to the anatomical lesion with respect to the functional lesion, the better the PCI outcome (panel C). The FFR drop within the OCT-derived anatomical lesion was strongly correlated with the functional relative gain after PCI (panel D).

Invasive Coronary Physiology After Stent Implantation: Another Step Toward Precision Medicine

JACC: CARDIOVASCULAR INTERVENTIONS
VOL. 14, NO. 3, 2021

PUBLISHED BY ELSEVIER

STATE-OF-THE-ART REVIEW

Invasive Coronary Physiology After Stent Implantation

Another Step Toward Precision Medicine

Simone Biscaglia, MD,[a] Barry Uretsky, MD,[b] Emanuele Barbato, MD, PhD,[c] Carlos Collet, MD, PhD,[d] Yoshinobu Onuma, MD, PhD,[e] Allen Jeremias, MD, MSc,[f] Matteo Tebaldi, MD,[c] Abdul Hakeem, MD,[g] Norihiro Kogame, MD,[h,i] Jeroen Sonck, MD,[c,d] Javier Escaned, MD,[j] Patrick W. Serruys, MD, PhD,[e,k] Gregg W. Stone, MD,[l] Gianluca Campo, MD[a,m]

ABSTRACT

Intracoronary physiology is routinely used in setting the indication for percutaneous coronary intervention (PCI) but seldom in assessing procedural results. This attitude is increasingly challenged by accumulated evidence demonstrating the value of post-PCI functional assessment in predicting long-term patient outcomes. Besides fractional flow reserve, a number of new indexes recently incorporated to clinical practice, including nonhyperemic pressure and functional angiographic indexes, provide new opportunities for the physiological assessment of PCI results. Largely, the benefit of these tools is derived from longitudinal analysis of the treated vessel, which allows precise identification of the vessel segment accounting for a suboptimal functional result and enabling operators to perform accurate PCI optimization. In this document the authors review available evidence supporting why physiological assessment should be extended to immediate post-PCI with the aim of improving patient outcomes. A step-by-step guide on how available physiological tools can be used for such purpose is provided. (J Am Coll Cardiol Intv 2021;14:237–46) © 2021 by the American College of Cardiology Foundation.

The impact of coronary physiology on clinical decision making according to its timing of use and the rationale and methodology of microcirculatory assessment have been elegantly addressed in recent state-of-the-art reviews (1,2). In the present paper we dissect the clinical implications of functional post-percutaneous coronary intervention (PCI) assessment. The main aim is to provide deeper insight and a step-by-step guide to identify suboptimal results of PCI, consider additional corrective measures, and ultimately improve patient outcomes through the application of new intracoronary indexes and functional coronary imaging tools.

From the [a]Cardiovascular Institute, Azienda Ospedaliero-Universitaria di Ferrara, Cona, Italy; [b]Central Arkansas VA Health System, Little Rock, Arkansas, USA; [c]Department of Advanced Biomedical Sciences, University of Naples, Federico II, Naples, Italy; [d]Cardiovascular Center Aalst, OLV Clinic, Aalst, Belgium; [e]Department of Cardiology, National University of Ireland Galway, Galway, Ireland; [f]St. Francis Hospital, Roslyn, New York, USA; [g]Rutgers Robert Wood Johnson Medical School, New Brunswick, New Jersey, USA; [h]Department of Cardiology, Amsterdam University Medical Center, Amsterdam, the Netherlands; [i]Department of Cardiology, Toho University Medical Center Ohashi Hospital, Tokyo, Japan; [j]Hospital Clínico San Carlos IDISCC, Complutense University of Madrid, Madrid, Spain; [k]Faculty of Medicine, National Heart and Lung Institute, Imperial College London, London, United Kingdom; [l]The Zena and Michael A. Wiener Cardiovascular Institute, Icahn School of Medicine at Mount Sinai and the Cardiovascular Research Foundation, New York, New York, USA; and the [m]Maria Cecilia Hospital, GVM Care & Research, Cotignola, Italy.
The authors attest they are in compliance with human studies committees and animal welfare regulations of the authors' institutions and Food and Drug Administration guidelines, including patient consent where appropriate. For more information, visit the Author Center.

Manuscript received June 30, 2020; revised manuscript received September 15, 2020, accepted October 13, 2020.

ISSN 1936-8798/$36.00
https://doi.org/10.1016/j.jcin.2020.10.055

JACC: CARDIOVASCULAR INTERVENTIONS VOL. 14, NO. 3, 2021
FEBRUARY 8, 2021:237–46

ABBREVIATIONS AND ACRONYMS

CAD = coronary artery disease

FFR = fractional flow reserve

FFR_{angio} = angiographic fractional flow reserve

IFR = instantaneous wave-free ratio

PCI = percutaneous coronary intervention

Pd/Pa = ratio of resting distal to aortic coronary pressure

PPG = pull back pressure gradient

QFR = quantitative flow ratio

vFFR = vessel fractional flow reserve

WHY SHOULD OPERATORS APPLY PHYSIOLOGY AFTER STENT IMPLANTATION?

Although in routine clinical practice acute procedural success is most frequently gauged only by visual angiographic assessment, use of intracoronary imaging techniques has demonstrated inadequate stent expansion with residual in-stent stenoses in a significant percentage of patients with angiographically successful interventions (3). Apart from stent-related issues, residual ischemia causing target vessel failure may also be a consequence of overlooked focal stenoses or diffuse disease outside the target PCI segment, vulnerable plaques left untreated, atheromatous disease progression, microvascular disease, and epicardial or microvascular spasm (2). All these mechanisms contribute to the high percentage of patients with recurrent angina at 1 year after PCI (20% to 30%) (4).

In 2002, results of an international registry showed that the higher was the post-PCI fractional flow reserve (FFR) value, the lower the probability of an adverse event at follow-up (5). Consequently, several studies with more contemporary technologies have shown a relationship between post-PCI FFR and major adverse cardiac events, with various dichotomous predictive cutoff values (3). Recently, post-PCI physiology value was integrated in a risk prediction model along with clinical and angiographic data and was determined to be the most important predictor of long-term outcome (6). In addition, 2 elegant studies demonstrated how physiology guarantees a greater ability to predict outcome, compared with angiography alone (7,8). The analysis of 607 patients from the FAME 2 (Fractional Flow Reserve Versus Angiography in Multivessel Evaluation 2) trial in whom revascularization was not performed demonstrated that the natural history of coronary stenoses is better predicted by physiology (FFR) compared with angiography (7). The same concept was demonstrated by the lack of predictive ability of the residual SYNTAX (Synergy Between PCI With Taxus and Cardiac Surgery) score after complete functional revascularization (8).

All this supports the suggestion that functional post-PCI assessment should be considered an important part of physiology-guided revascularization.

HIGHLIGHTS

- Physiology assessment post-PCI predicts outcome but is rarely used in clinical practice.
- Pullback can identify stent-related issues, overlooked lesions, and diffuse disease.
- Focal drops at pullback indicate the need of post-dilation or stent implantation.
- Diffuse disease demands aggressive medical therapy.
- Powered trials comparing physiology- and angio-guided PCI optimization are warranted.

WHY DO OPERATORS RARELY APPLY PHYSIOLOGY AFTER STENT IMPLANTATION?

Although post-stent FFR has been shown to correlate with long-term outcome, its penetration in clinical practice is low. In the recent ERIS (Evolving Routine Standards of FFR Use) study, post-PCI FFR was used in <10% of lesions investigated with physiology pre-PCI (9). Most interestingly, even when the FFR result after PCI was suboptimal, in 79% of the cases, no further action was performed (9). Reasons for the low use of functional assessment post-PCI and for subsequent intervention are multiple. First, physiology is used after PCI mostly in cases in which it was used pre-PCI. Second, randomized clinical trials addressing the use of FFR to assess PCI results have not been performed, so clear instructions and cutoffs for its use are lacking. Third, the need to administer adenosine several times during the same procedure results in increased procedure time, cost, and adverse side effects. Fourth, in case of a post-PCI suboptimal functional result, it may be difficult to ascertain the underlying cause. Fifth, reproducibility of physiological measurements can be challenging in the post-PCI setting, and operator's experience significantly affects the reliability of the assessment.

HOW SHOULD OPERATORS APPLY PHYSIOLOGY AFTER STENT IMPLANTATION?

Although the post-PCI FFR value has been linked to long-term outcome, how to "react" to a suboptimal FFR value, after an angiographically "perfect" stenting result, has been contentious, largely because of

CENTRAL ILLUSTRATION **Flowchart for Guide Physiology-Guided Percutaneous Coronary Intervention Optimization Considering Current Methods**

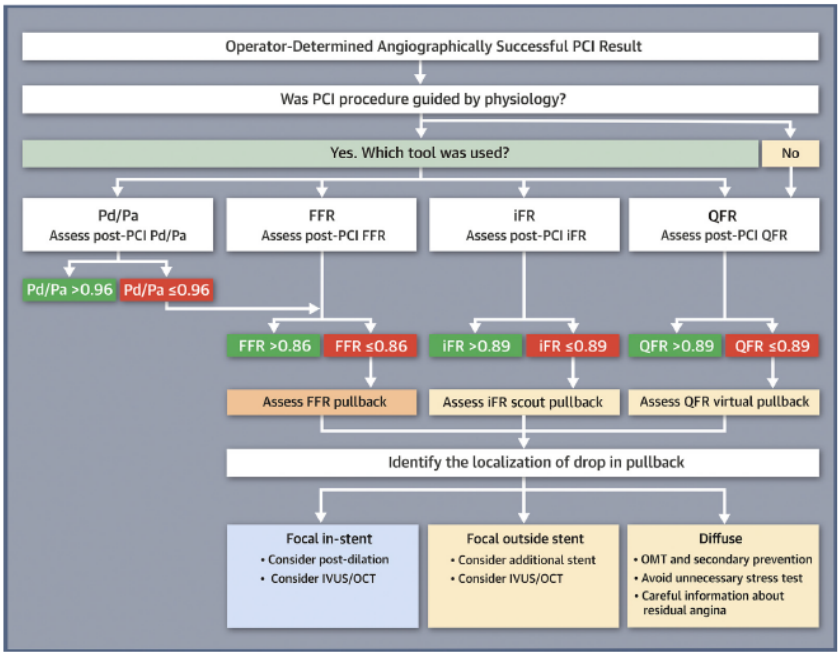

Biscaglia, S. et al. J Am Coll Cardiol Intv. 2021;14(3):237–46.

FFR = fractional flow reserve; iFR = instantaneous wave-free ratio; IVUS = intravascular ultrasound; OCT = optical coherence tomography; OMT = optimal medical therapy; PCI = percutaneous coronary intervention; Pd/Pa = ratio of resting distal to aortic coronary pressure; QFR = quantitative flow ratio.

the lack of dedicated studies and the existence of multiple mechanisms influencing post-PCI values, each requiring different actions from the operator. Ongoing trials such as FFR-REACT (FFR-Guided PCI Optimization Directed by High-Definition IVUS Versus Standard of Care and TARGET-FFR (An Evaluation of a Physiology-Guided PCI Optimisation Strategy) may fill this gap (10,11). Understanding the mechanisms of abnormal physiological values is key in making the right choice on which actions should be performed to improve PCI outcomes.

There are at least 5 main causes of abnormal FFR values documented after PCI (1–3). First, stent-related issues, including stent underexpansion and stent edge dissection, may compromise intrastent or intraluminal dimensions and cause intrasegment pressure loss. Second, additional stenoses to the target PCI site may be present, whose hemodynamic significance had been overlooked or escaped identification by FFR. For example, the functional severity of stenoses located proximally to the target PCI site may be concealed by hemodynamic crosstalk during FFR interrogation (12). Third, the presence of diffuse vessel disease, which in many cases remains unnoticed from an angiographic standpoint, can produce a suboptimal functional result. Fourth, coronary spasm or simply increased vasomotor tone may be present, despite or in the absence of intracoronary nitrates. And fifth, pseudostenoses may develop, caused by straightening of vessel bends by the pressure guidewire, typically occurring in tortuous coronary arteries.

Untreated lesions and stent-related issues are likely treatable in most cases. With diffuse disease, however, it is unlikely that further stenting will significantly improve the outcome in view of the propensity for long stent lengths to increase risk for restenosis. In

TABLE 1 Recent Clinical Studies Evaluating the Role of Post-PCI Physiology

First Author, Year	N	Primary EP	Follow-Up (Months)	Threshold	Results	Note
Hakeem et al., 2019 (14)	574	MACE	30	Pd/Pa ≤0.96, FFR ≤0.86	Pd/Pa ≤0.96 and FFR ≤0.86 in 25% vs. Pd/Pa >0.96 and FFR >0.86 in 15%	In a fully adjusted Cox regression analysis, Pd/Pa was an independent predictor of MACE (HR: 2.07; 95% CI: 1.3-3.3; p = 0.002)
Jeremias et al., 2019 (16)	500	iFR <0.90	NA	iFR <0.90	iFR <0.90 in 24%	Causes of iFR <0.90 • Diffuse disease: 18.4% • In-stent drop: 31.3% • Untreated lesion: 50.3%
Biscaglia et al., 2019 (18)	602	VOCE	21	QFR <0.90	QFR <0.90 in 25% vs. QFR ≥0.90 in 3.5%	Causes of QFR<0.90 • Diffuse disease: 34% • In-stent drop: 13% • Untreated lesion: 32% • Combination: 21%
Kogame et al., 2019 (19)	393	VOCE	24	QFR <0.91	QFR <0.91 in 12% vs. QFR ≥0.91 in 3.7%	The impact of low post-PCI QFR on 2-yr VOCE was greater in vessels treated without IVUS guidance compared with vessels treated with IVUS guidance (p for interaction = 0.063)

CI = confidence interval; EP = endpoint; FFR = fractional flow reserve; HR = hazard ratio; iFR = instantaneous wave-free ratio; IVUS = intravascular ultrasonography; MACE = major adverse cardiac events; NA = not available; PCI = percutaneous coronary intervention; Pd/Pa = ratio of resting distal to aortic coronary pressure; QFR = quantitative flow ratio; VOCE = vessel-oriented composite endpoint.

conclusion, physiological indexes can be used to detect and discriminate among different underlying mechanisms of suboptimal PCI results associated with long-term adverse events (Central Illustration).

Pressure guidewires may theoretically obtain a longitudinal FFR map of the whole vessel. Pressure pull back is a key tool in understanding which coronary segment accounts for residual intracoronary pressure gradients. However, FFR pull back never became supported by prospective studies, and its adoption was hampered by the need to perform intravenous administration of adenosine. Yet some evidence was obtained on this topic. Agarwal et al. (13) showed that post-PCI FFR was in the ischemic range in 21% of lesions after angiographic successful PCI. The investigators performed an FFR pull back characterizing the underlying issue leading to subsequent intervention in 95.8% of lesions in the ischemic subgroup. Further intervention improved FFR from 0.78 ± 0.07 to 0.87 ± 0.05 ($p < 0.0001$). One of the main advantages of an FFR pull back is that hyperemia amplifies gradients and improves the signal-to-noise ratio. There are specific challenges in the interpretation of FFR pull back, such as the evaluation of serial lesions (3) and the need for at least 5 beats at each pull back position to ensure measurement reliability. These limitations are among the main causes of its underuse in clinical practice (9).

The strategy of "functional optimized coronary intervention," namely, defining procedural success using a physiological measure throughout the entire spectrum of coronary stenoses (50% to 99%), has been tested and was successfully performed in 92% of cases, thus demonstrating its feasibility (14).

HOW MIGHT NEW TECHNOLOGIES HELP IN APPLYING POST-PCI PHYSIOLOGY?

New indexes and tools have been developed in an effort to overcome barriers to the widespread adoption of functional assessment. Nonhyperemic pressure indexes, including instantaneous wave-free ratio (iFR), ratio of resting distal to aortic coronary pressure (Pd/Pa), and other resting indexes, have enabled functional evaluation without pharmacological arteriolar vasodilation, while angiography-based functional assessment (quantitative flow ratio [QFR], angiographic FFR [FFR_{angio}], and vessel FFR [vFFR]) have eliminated the need for a dedicated pressure wire.

Importantly, these newer tools may allow operators to understand the mechanism underlying an abnormal physiologic value after angiographically successful intervention. In fact, the real novelty related to their development is the shift from a binary interpretation of physiology (positive or negative) to a quantitative, site-specific one. For these reasons, they are extremely appealing post-PCI, and several studies have been recently conducted to validate them in this setting (Table 1).

PD/PA. Pd/Pa (the baseline ratio of pressure distal to the lesion and aortic pressure) is a simple measure that may allow selection of those cases needing FFR. Hakeem et al. (15) investigated whether a combined strategy of Pd/Pa with or without FFR post-PCI could predict long-term clinical outcomes better than either marker alone in 664 lesions who had documented FFR and Pd/Pa pre- and post-PCI (Table 1). The analysis demonstrated the complementary role of Pd/Pa

FIGURE 1 Examples of Different Post-Percutaneous Coronary Intervention iFR Traces According to Underlying Coronary Artery Disease Mechanisms (In-Stent Drop, Proximal Gradient, Distal Gradient)

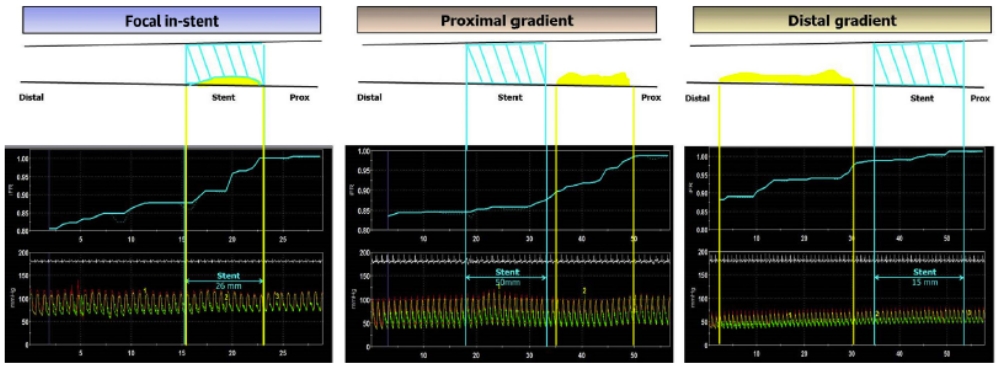

Blue lines delimit the proximal and distal ends of the stent. **Yellow lines** delimit the diseased portion of the vessel. iFR = instantaneous wave-free ratio; Prox = proximal.

to FFR post-PCI. The investigators suggested a post-PCI assessment with Pd/Pa; if >0.96, the procedure can be confidently concluded. Otherwise, FFR should be performed and if ≤0.86, pull back should be performed to elucidate the mechanism of the suboptimal result. The limit of Pd/Pa, however, is the inability to discriminate among different patterns of coronary artery disease (CAD) causing the suboptimal result, which is possible only through an FFR pull back.

iFR. iFR is a resting physiological index without need for drug-induced hyperemia. Beyond the avoidance of adenosine, iFR has distinct advantages in performing hemodynamic mapping of the entire vessel using pressure guidewire pull back (iFR Scout pull back system, Philips Medical Systems, Best, the Netherlands). Its main downside is the necessity for proprietary software from a single vendor. In contradistinction to FFR, iFR pull back curves are obtained on the basis of a beat-by-beat analysis and displayed by specific software that avoids fluctuations of the pull back curve associated with the Venturi effect. In theory, under resting conditions, flow is more constant, consistent, and predictable across in-series stenoses; as such, iFR pull back has a theoretical advantage and requires empirical testing (Figure 1). iFR pull back may identify lesions, estimate length, and integrate with coronary angiography (16). The same approach has been taken in the post-PCI

FIGURE 2 Examples of Different Post-Percutaneous Coronary Intervention QFR Traces According to Underlying Coronary Artery Disease Mechanisms (In-Stent Drop, Physiological Miss, Diffuse Disease)

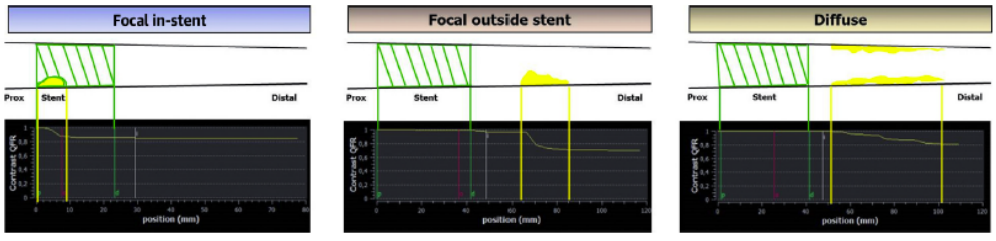

Green lines delimit the proximal and distal ends of the stent. **Yellow lines** delimit the diseased portion of the vessel. Prox = proximal; QFR = quantitative flow ratio.

TABLE 2 How to Perform and Interpret Physiology Post-PCI

	FFR	iFR	QFR
How to perform post-PCI physiology			
Step 1	Angiographically satisfactory PCI		
Step 2	Inject nitroglycerin (100–200 μg) and flush with saline (in case of FFR, intravenous administration of adenosine is required)		
Step 3	Disengage catheter and perform manual or motorized pull back		Take 2 angiographic projections at least 25° apart avoiding foreshortening and overlap
Step 4	Check for drift		Perform post-PCI QFR analysis
Step 5	Assess the value and the presence of in-stent drop, physiological miss, and/or diffuse disease		
How to interpret post-PCI physiology			
Focal drop	Change in the angle of the FFR pull back curve between pull back sites	Abrupt drop-down in the iFR curve with ΔiFR ≥0.03 in <15 mm	Abrupt pressure drop-down with ΔQFR >0.05 in <10 mm
Diffuse disease	Progressive and constant FFR decrease without significant drop-down	Progressive and constant iFR decrease without significant drop-down	Progressive and constant QFR decrease without significant drop-down

Abbreviations as in Table 1.

setting in the DEFINE PCI (Physiologic Assessment of Coronary Stenosis Following PCI) study, although the pull back was performed manually. A blinded iFR pull back was performed after angiographically successful PCI in 562 vessels in 500 patients in whom iFR had been used also pre-PCI to guide revascularization. Residual low iFR (expressed as an iFR value post-PCI <0.90) was present in 24% of patients. Among patients with ischemic post-PCI iFR, 81.6% had untreated focal stenoses that were angiographically inapparent, and 18.4% had diffuse disease. Among iFR detected focal lesions, 38.4% were located within the stented segment, while 61.6% were amenable to treatment with additional PCI (Table 1, Figure 1) (17). Limitations of the study included a large percentage of serial or tandem lesions that may have increased the proportion of abnormal iFR after PCI than previously reported. Importantly, the results of iFR were not shared with the operator at the time of the index procedure, so it is unclear what proportion of these persistently abnormal iFR values could have been "corrected" by undertaking further interventions during the index procedure.

QFR. QFR is an angiographically derived estimate of FFR developed as an alternative to wire-based intracoronary physiology. There are several third-generation quantitative coronary angiographic systems able to simulate FFR from conventional angiography (e.g., QFR, vFFR, FFR_{angio}). There appears to be no major differences in their diagnostic performance (18). One advantage of QFR is that, being an angiography-based reconstruction without the need for a wire, its application in the post-PCI setting is not related to its use before PCI. In addition, it allows generation of a pull back curve and discrimination of the physiological contribution of each single lesion as well as diagnosis of diffuse disease. The value of QFR to assess the functional results of PCI was tested in the prospective HAWKEYE (Angio-Based Fractional Flow Reserve to Predict Adverse Events After Stent Implantation) study. Seven hundred fifty-one vessels in 602 patients undergoing angiographically satisfactory second-generation DES implantation were analyzed (19). At the end of the procedure, the operator acquired projections for QFR computation performed offline by an independent core laboratory. Receiver-operating characteristic curve analysis identified a post-PCI QFR best cutoff of ≤0.89 (area under the curve 0.77; 95% confidence interval: 0.74 to 0.80; $p < 0.001$). After correction for potential confounding factors, post-PCI QFR ≤0.89 was associated with a 3-fold increase in risk for the vessel-oriented composite endpoint at 2 years (hazard ratio: 2.91; 95% confidence interval 1.63 to 5.19; $p < 0.001$). In a retrospective evaluation of the SYNTAX II trial, the post-PCI QFR threshold for prediction of a vessel-oriented composite endpoint at 2 years was similar, at <0.91 even in patients with anatomic complexity such as 3-vessel disease (20).

Furthermore, a very important finding of the HAWKEYE study was the demonstration that QFR could discriminate among different CAD patterns. In vessels with suboptimal functional results, the site of the QFR drop was in-stent in 13% of the cases, while a focal drop outside the stent was identifiable in 32% of the cases. Thirty-four percent of vessels showed diffuse disease, while in 21% a combination of the aforementioned possibilities was present (Table 1, Figure 2).

Currently QFR requires off-line analysis. If it can be performed in real time, it may become an important

FIGURE 3 Illustrative Case of Virtual PCI QFR

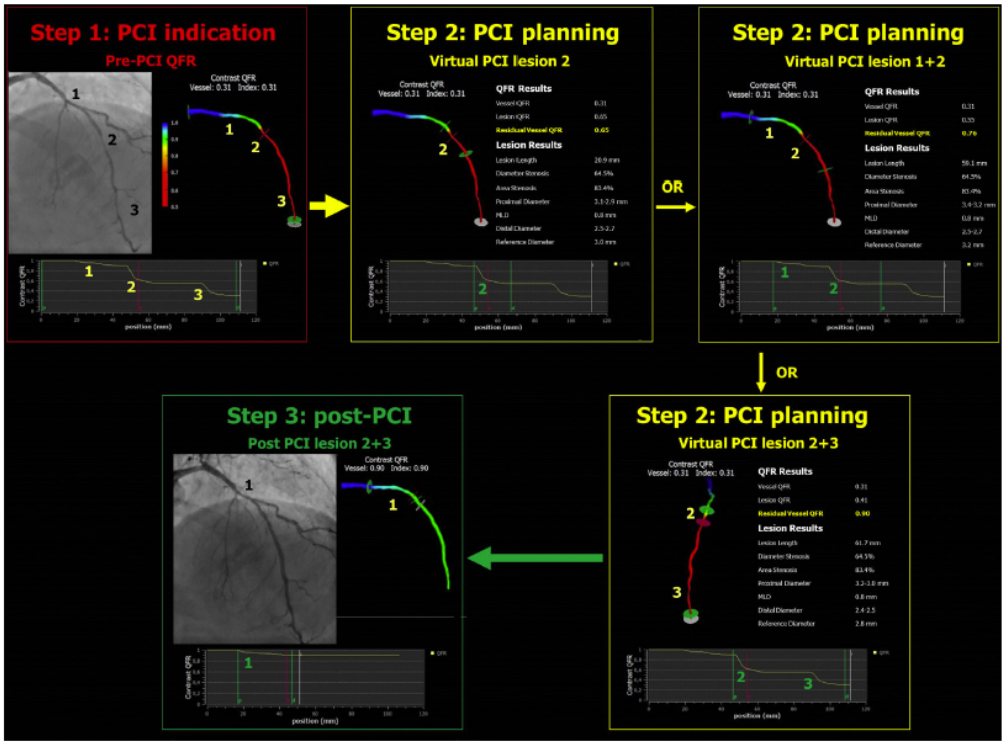

Step 1: quantitative flow ratio (QFR) is used as a gatekeeper for percutaneous coronary intervention (PCI). The QFR analysis shows 3 pressure step-downs (see 1, 2, and 3 both in angiogram and in QFR trace). Step 2: once PCI is deemed indicated, it is possible to plan different treatment strategies ("virtual PCI") obtaining the "residual vessel QFR," which is the QFR value once the segment between p and d (in **green** in the QFR traces) is treated. P and d can be decided and moved by the operator to obtain different post-PCI scenarios (see examples in step 2). Step 3: the operator decided to treat lesions 2 and 3 according to pre-PCI QFR assessment and to perform post-PCI QFR that confirmed the previous estimation.

tool to optimize interventions. In addition, QFR analyzability depends on the quality of angiography, and it is feasible in about 80% of cases (19,20). Moreover, QFR is not applicable in specific lesion subsets, such as left main, bifurcation, and ostial lesions.

WHEN SHOULD OPERATORS APPLY PHYSIOLOGY AFTER STENT IMPLANTATION?

The development of multiple and complementary strategies enables operators to apply physiology-guided PCI in almost all cases. The only exception is the "culprit" lesion in ST-segment elevation myocardial infarction and possible high-risk "culprit" lesions in non-ST-segment elevation myocardial infarction, in which the microcirculation subtended by the infarct-related coronary artery might be impaired. Table 2 summarizes how to perform and interpret post-PCI physiologic assessment. In the Central Illustration we provide a flowchart to optimize all PCIs combining the use of the different physiology tools, while in Figures 1 to 3 we provide examples of the different mechanisms of CAD for each technology.

WHAT SHOULD OPERATORS EXPECT IN THE COMING YEARS? VIRTUAL PCI IS COMING

Angiography-guided PCI optimization is still the most used approach in clinical practice. For this reason, the next step in terms of physiology-guided PCI

JACC: CARDIOVASCULAR INTERVENTIONS VOL. 14, NO. 3, 2021
FEBRUARY 8, 2021:237–46

FIGURE 4 Examples of Different Pre-Percutaneous Coronary Intervention FFR Traces With PPG Index According to Underlying Coronary Artery Disease Mechanisms (High PPG/Focal Disease, Low PPG/Diffuse Disease)

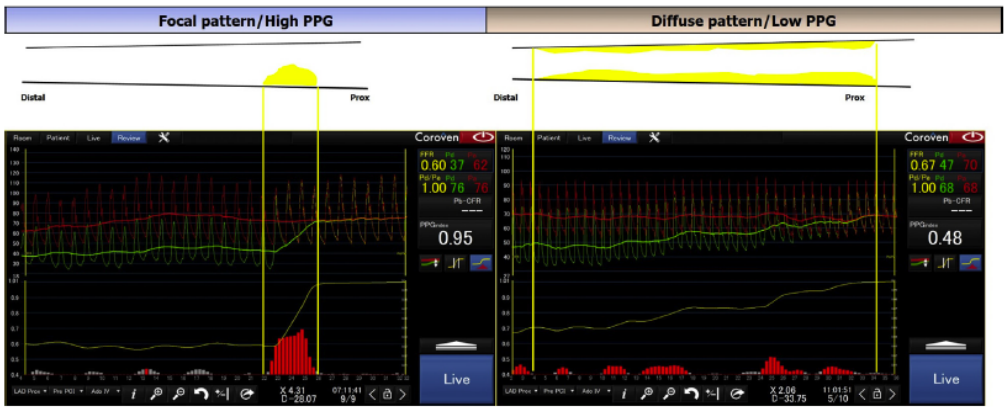

Yellow lines delimit the diseased portion of the vessel. PPG = pull back pressure gradient; Prox = proximal.

optimization should be conducting a randomized controlled trial comparing physiology-guided versus conventional angiography-guided PCI optimization, adequately powered for hard clinical endpoints.

A full physiology-guided procedure is theoretically possible thanks to the virtual PCI tools that are already available for iFR, QFR, and computed tomographic FFR (Figure 3). Recently, the ability of FFR to discriminate pathophysiological patterns of CAD using coronary pressure pull back has been prospectively evaluated (21). The investigators proposed a quantitative assessment, namely, the pull back pressure gradient (PPG) index, to discriminate between focal and diffuse disease. The PPG index is a continuous metric with values close to 0 indicating diffuse disease, whereas those close to 1 suggest focal disease and are useful in the pre-PCI setting to predict post-PCI vFFR (Figure 4). However, a limitation of this technique is the necessity for a motorized system for FFR pull back and prolonged adenosine infusions (21). A new online automatic evaluation of the PPG index with manual pull back will be soon available to overcome this limitation.

These tools make it possible to obtain not only a single physiological value to determine the need for PCI but also a full physiological map of the vessel with point-by-point detailed information of the functional impact of a given stenosis. In addition, it is possible to simulate the treatment of 1 or more lesions (virtual PCI) to estimate the final functional value post-PCI (Figure 5). Functional assessment can be easily checked also after PCI and eventually guide further optimization. The final goal is to achieve optimal physiological results in all procedures. Seminal experiences of virtual PCI have been recently published (22). A validation of virtual intervention with pre-PCI iFR pull back was performed in serial lesions and diffuse CAD in 32 coronary arteries by Nijjer et al. (16). Obviously, the results of these proof-of-concept studies are only hypothesis generating, but they pave the way for future studies comparing physiology-guided virtual PCI with conventional angiography-guided PCI. To this end, coregistration of angiographic, imaging, and physiological information could have an additional value for PCI optimization (23). The DEFINE GPS (Distal Evaluation of Functional Performance With Intravascular Sensors to Assess the Narrowing Effect: Guided Physiologic Stenting) trial will randomize more than 3,000 patients to evaluate patient outcomes of PCI guided by an integrated coregistration platform, which aggregates data from an instant iFR measurement and angiography compared against the current standard-of-care treatment guided by angiography alone (NCT04451044).

CONCLUSIONS

Current evidence supports the concept that angiography has major limitations in depicting the

FIGURE 5 **Illustrative Case of Virtual PCI With FFR and PPG Index**

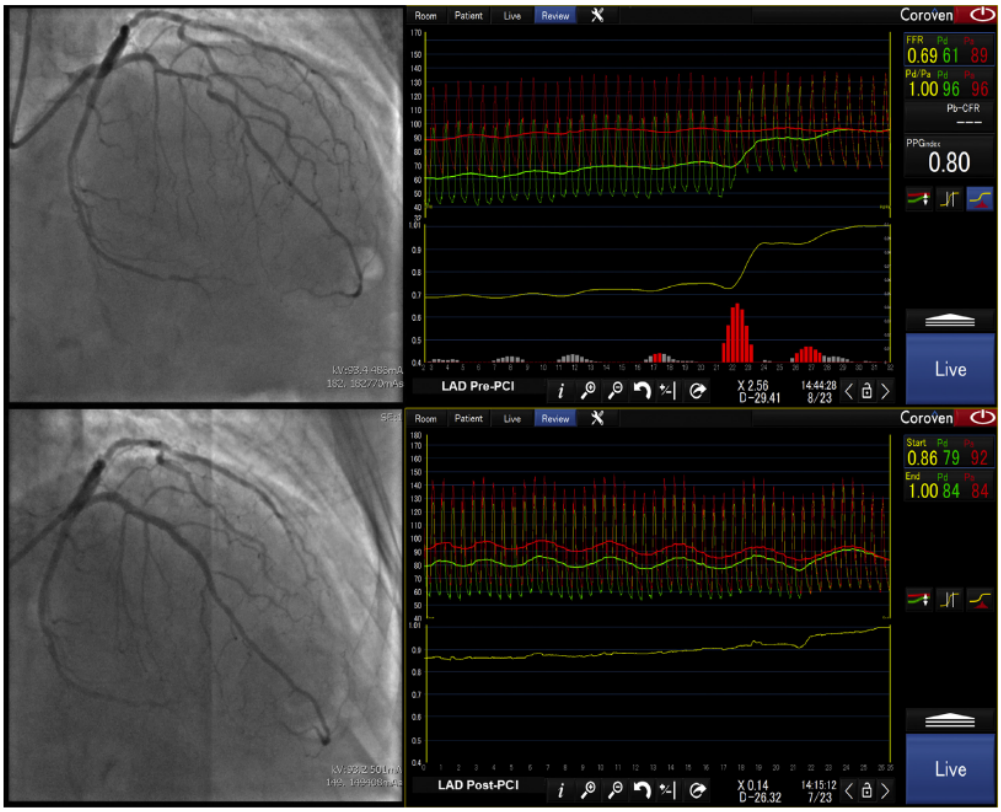

The **top panel** shows a severe angiographic lesion in the mid segment of the left anterior descending coronary artery with an fractional flow reserve (FFR) value in the distal vessel of 0.69. In the **right top panel**, a manual FFR pull back tracing is shown (Coroventis Research, Uppsala, Sweden). The **red bars** depict pressure drops by millimeter. An important drop was identified in the mid segment of the vessel. The functional pattern of coronary artery disease (CAD) was quantified by the pull back pressure gradient (PPG) index of 0.80 (i.e., predominant focal functional CAD). In the **bottom panel**, the results after percutaneous coronary intervention (PCI) are shown. FFR post-PCI was 0.86, and the pull back identified a small pressure step up followed by diffuse pressure losses in the distal segment.

functional results of PCI and that the performance of physiological interrogation at the end of the procedure can identify suboptimal PCI results associated with poorer patient outcomes. Nonhyperemic pressure indexes (iFR, resting full-cycle ratio, diastolic pressure ratio, Pd/Pa) and angiography-based FFR (QFR, FFR_{angio}, and vFFR) provide additional opportunities to those offered by FFR for post-PCI functional assessment. Overall, these new technologies provide much more than binary information about the presence or absence of flow-limiting stenoses, allowing identification of the mechanism of suboptimal result and the exact location of the problem in the investigated vessel, both key aspects in choosing corrective interventional measures or, in specific patients, coadjuvant medical therapy as the best complementary treatment for PCI. The next evolution of physiology-guided PCI is to use the possibility of mapping physiologically the vessel before PCI and simulating the result of PCI in advance. Virtual PCI is

JACC: CARDIOVASCULAR INTERVENTIONS VOL. 14, NO. 3, 2021
FEBRUARY 8, 2021:237–46

the natural step forward for physiology in the precision medicine era. Randomized studies are warranted to demonstrate the benefit of this approach on outcome.

FUNDING SUPPORT AND AUTHOR DISCLOSURES

Dr. Biscaglia has received research grants from Medis, SMT, and Siemens. Dr. Campo has received research grants from Boston Scientific, Medis, SMT, and Siemens. Dr. Tebaldi has received a research grant from Boston Scientific. Dr. Barbato has received speaker fees from Abbott Vascular, Boston Scientific, and GE. Dr. Uretsky has received a research grant from Opsens. Dr. Serruys has received personal fees from Sino Medical Sciences Technology, Philips/Volcano, and Xeltis. Dr. Sonck has received a research grant from the CardioPath PhD program. Dr. Collet has received consultancy fees from HeartFlow, Opsens, Biosensors, Boston Scientific, Philips/Volcano, and Abbott Vascular; and has received research grants from HeartFlow, Abbott Vascular, and ShockWave Medical. Dr. Stone has received speaker or other honoraria from Cook, Terumo, Qool Therapeutics, and Orchestra Biomed; has served as a consultant to Valfix, TherOx, Vascular Dynamics, Robocath, HeartFlow, Gore, Ablative Solutions, Miracor, Neovasc, V-Wave, Abiomed, Ancora, MAIA Pharmaceuticals, Vectorious, Reva, and Matrizyme; and has equity or options from Ancora, Qool Therapeutics, Cagent, Applied Therapeutics, the Biostar family of funds, SpectraWave, Orchestra Biomed, Aria, Cardiac Success, the MedFocus family of funds, and Valfix. Dr. Jeremias has received institutional grants and consulting fees from Abbott Vascular and Philips/Volcano; and is a consultant for ACIST and Boston Scientific. Dr. Escaned has received consulting and/or speaker fees from Abbott, Boston Scientific, Opsens, and Philips Healthcare. All other authors have reported that they have no relationships relevant to the contents of this paper to disclose.

ADDRESS FOR CORRESPONDENCE: Dr. Simone Biscaglia, Cardiovascular Institute, Azienda Ospedaliera Universitaria S. Anna, Via Aldo Moro 8, 44124 Cona (FE), Italy. E-mail: bscsmn@unife.it.

REFERENCES

1. Kogame N, Ono M, Kawashima H, et al. The impact of coronary physiology on contemporary clinical decision making. J Am Coll Cardiol Intv 2020;13:1617–38.

2. Ford TJ, Ong P, Sechtem U, et al. Assessment of vascular dysfunction in patients without obstructive coronary artery disease: why, how, and when. J Am Coll Cardiol Intv 2020;13:1847–64.

3. Hakeem A, Uretsky BF. Role of postintervention fractional flow reserve to improve procedural and clinical outcomes. Circulation 2019;139:694–706.

4. Abdallah MS, Wang K, Magnuson EA, et al. Quality of life after PCI vs CABG among patients with diabetes and multivessel coronary artery disease: a randomized clinical trial. JAMA 2013;310:1581–90.

5. Pijls NH, Klauss V, Siebert U, et al. Coronary pressure measurement after stenting predicts adverse events at follow-up: a multicenter registry. Circulation 2002;105:2950–4.

6. Hwang D, Lee JM, Yang S, et al. Role of post-stent physiological assessment in a risk prediction model after coronary stent implantation. J Am Coll Cardiol Intv 2020;13:1639–50.

7. Ciccarelli G, Barbato E, Toth GG, et al. Angiography versus hemodynamics to predict the natural history of coronary stenoses: Fractional Flow Reserve Versus Angiography in Multivessel Evaluation 2 substudy. Circulation 2018;137:1475–85.

8. Kobayashi Y, Lonborg J, Jong A, et al. Prognostic value of the residual SYNTAX score after functionally complete revascularization in ACS. J Am Coll Cardiol 2018;72:1321–9.

9. Tebaldi M, Biscaglia S, Fineschi M, et al. Evolving routine standards in invasive hemodynamic assessment of coronary stenosis: the nationwide Italian SICI-GISE Cross-Sectional ERIS Study. J Am Coll Cardiol Intv 2018;11:1482–91.

10. van Zandvoort LJC, Masdjedi K, Tovar Forero MN, et al. Fractional flow reserve guided percutaneous coronary intervention optimization directed by high-definition intravascular ultrasound versus standard of care: rationale and study design of the prospective randomized FFR-REACT trial. Am Heart J 2019;213:66–72.

11. Collison D, McClure JD, Berry C, Oldroyd KG. A randomized controlled trial of a physiology-guided percutaneous coronary intervention optimization strategy: rationale and design of the TARGET FFR study. Clin Cardiol 2020;43:414–22.

12. Modi BN, Rahman H, Ryan M, et al. Comparison of fractional flow reserve, instantaneous wave free ratio and a novel technique for assessing coronary arteries with serial lesions. EuroIntervention 2020;16:577–83.

13. Agarwal SK, Kasula S, Hacioglu Y, Ahmed Z, Uretsky BF, Hakeem A. Utilizing post-intervention fractional flow reserve to optimize acute results and the relationship to long-term outcomes. J Am Coll Cardiol Intv 2016;9:1022–31.

14. Uretsky BF, Agarwal SK, Vallurupalli S, et al. Prospective evaluation of the strategy of functionally optimized coronary intervention. J Am Heart Assoc 2020;9:e015073.

15. Hakeem A, Ghosh B, Shah K, et al. Incremental prognostic value of post-intervention Pd/Pa in patients undergoing ischemia-driven percutaneous coronary intervention. J Am Coll Cardiol Intv 2019;12:2002–14.

16. Nijjer SS, Sen S, Petraco R, et al. Pre-angioplasty instantaneous wave-free ratio pullback provides virtual intervention and predicts hemodynamic outcome for serial lesions and diffuse coronary artery disease. J Am Coll Cardiol Intv 2014;7:1386–96.

17. Jeremias A, Davies JE, Maehara A, et al. Blinded physiological assessment of residual ischemia after successful angiographic percutaneous coronary intervention: the DEFINE PCI study. J Am Coll Cardiol Intv 2019;12:1991–2001.

18. Collet C, Onuma Y, Sonck J, et al. Diagnostic performance of angiography-derived fractional flow reserve: a systematic review and Bayesian meta-analysis. Eur Heart J 2018;39:3314–21.

19. Biscaglia S, Tebaldi M, Brugaletta S, et al. Prognostic value of QFR measured immediately after successful stent implantation: the international multicenter prospective HAWKEYE study. J Am Coll Cardiol Intv 2019;12:2079–88.

20. Kogame N, Takahashi K, Tomaniak M, et al. Clinical implication of quantitative flow ratio after percutaneous coronary intervention for 3-vessel disease. J Am Coll Cardiol Intv 2019;12:2064–75.

21. Collet C, Sonck J, Vandeloo B, et al. Measurement of hyperemic pullback pressure gradients to characterize patterns of coronary atherosclerosis. J Am Coll Cardiol 2019;74:1772–84.

22. Rubimbura V, Guillon B, Foumier S, et al. Quantitative flow ratio virtual stenting and post stenting correlations to post stenting fractional flow reserve measurements from the DOCTORS (Does Optical Coherence Tomography Optimize Results of Stenting) study population. Catheter Cardiovasc Interv 2020;96:1145–53.

23. Frimerman A, Abu-Fane R, Levi Y, et al. Novel method for real-time coregistration of coronary physiology and angiography by iFR. J Am Coll Cardiol Intv 2019;12:692–4.

KEY WORDS coronary physiology, fractional flow reserve, instantaneous wave-free ratio, outcome, percutaneous coronary intervention, precision medicine, quantitative flow ratio

Go to http://www.acc.org/jacc-journals-cme to take the CME/MOC/ECME quiz for this article.

Chapter 6: FFR_{CT}: Non-invasive Fractional Flow Reserve derived from coronary CT angiography for treatment planning

Chapter introduction

In the sixth chapter, we focus on treatment planning. In the SYNTAX III trial, it became clear that the agreement concerning treatment decision between coronary CTA and conventional angiography was high (Cohen's kappa 0.82) and showed higher agreement than the anatomical SYNTAX score. The SYNTAX Score III (Anatomical SYNTAX score, clinical comorbidities and functional assessment) enabled the heart team to refine the decision-making process regarding the optimal revascularization strategy and treatment planning of hemodynamically significant lesions. FFR_{CT} downgraded the proportion of three vessel disease and changed treatment recommendation in 7%. The integration of coronary lumen assessment, atherosclerotic plaque evaluation including the calcium burden and the assessment of lesion-specific ischemia by FFR_{CT} prompted the hypothesis that CCTA coupled with FFR_{CT} might provide sufficient information to plan CABG. As such, we designed a pilot study to determine the theoretical feasibility of surgical treatment planning only based on CCTA with FFR_{CT}. Based on our presented analysis, the FAST-TRACK CABG study is currently recruiting patients investigating if CABG based on sole CCTA and FFR_{CT} is feasible and safe[43].

Comparably, FFR_{CT} provides insight in vessel and lesion significance including the phenotype of CAD. Theoretically, by virtual remodeling the lumen PCI could be mimicked enhancing treatment planning. For this, the lumen is opened to an "idealized" lumen or a lumen without regions of narrowing. This idealized lumen is automatically generated by seeking a radius profile that is monotonically non-increasing from the ostium to the end of each vessel based on the pre-PCI anatomy. This gives only one possible configuration for an expanded lumen and is not dependent on the user (Sankaran S. et al., Physics driven real-time blood flow simulations, Computer Methods in Applied Mechanics and Engineering 364 (2020): 112963.) Also, the boundary conditions on the Planner are intended to be nearly identical to the pre-PCI FFR_{CT} simulation boundary conditions. On the Planner, a small difference due to the opened lumen is taken into account in the re-calculation of the boundary conditions providing a recalculated FFR_{CT} value and coronary pressure profile post-virtual PCI.

In the Precise PCI trial, a multicenter, investigator-initiated, prospective study, we evaluated the capability of the FFR_{CT} Planner to predict the result of PCI in terms of post-PCI FFR. Patients with chronic coronary syndromes and significant lesions based on invasive FFR≤0.80 were selected. The FFR_{CT} Planner was applied to the FFR_{CT} model, simulating PCI. This was compared with invasive FFR following an OCT-guided PCI. In total, 123 patients with

chronic coronary syndromes with invasive FFR≤0.80 were included. Invasive FFR post-PCI was 0.88±0.06, and FFR_{CT} Planner FFR 0.86±0.06 (mean difference 0.02±0.07 FFR units, limits of agreement -0.12 to 0.15). The P^3 study met its pre-specified primary endpoint and the FFR_{CT}-based technology proved accurate and precise for predicting FFR after PCI. The FFR_{CT} Planner may improve the strategy for percutaneous revascularization and as such may facilitate complete functional revascularization.

The performance of the Planner in diffuse CAD and calcific atherosclerosis was assessed in a pre-specified sub-analysis. In the Precise PCI Plan trial, patients with predominant focal or diffuse disease were divided using a threshold of median PPG value 0.66. As expected, patients with low PPG (diffuse CAD) at baseline had lower post-PCI FFR compared to patients with high PPG (0.86±0.05 vs. 0.91±0.07, p<0.001). The FFR_{CT} Planner also predicted significantly lower FFR in patients with low PPG (0.85±0.06 vs. 0.87±0.05, p-value=0.048). The functional gain was significantly greater in patients with high PPG (focal CAD) compared to patients with low PPG (p<0.001 for both FFR_{CT} and invasive FFR). The FFR_{CT} Planner's accuracy was similar in cases of diffuse or focal CAD (mean difference between FFR_{CT} Planner and invasive post-PCI FFR in diffuse CAD 0.01±0.05 vs. 0.03±0.08 in focal CAD, p=0.057. Post-PCI FFR_{CT} Planner FFR was similar between high and low calcium burden (0.86±0.06 vs. 0.87±0.06, p=0.537). The FFR_{CT} Planner's accuracy was comparable in cases with high and low calcium burden (mean difference between FFR_{CT} Planner and invasive post-PCI FFR in high calcium burden 0.01±0.07 vs. low calcium burden 0.01±0.07, p=0.192.

In summary, there is increasing awareness of the potential of CCTA and FFR_{CT} to help plan and guide coronary interventions. CCTA allows optimization of visualization angles in the catheterization laboratory, provides information on plaque morphology and through FFR_{CT} provides lesion specific functional evaluation of CAD. This information allows for a pre-procedural tailored planning of PCI in a fashion not previously possible. The FFR_{CT} Planner expands the use of CCTA from a diagnostic method to a planning tool for revascularization. Hence, the FFR_{CT} Planner may help clinicians better select patients to be referred to an invasive procedure, avoiding futile PCI and anticipating the benefit of an intervention. Another niche for this technology is inside the catheterization laboratory. The FFR_{CT} Planner can be beneficial in tandem stenosis cases to quantify the added value of stenting each of the lesions, and in cases of diffuse disease to maximize the benefit of the intervention while minimizing procedural risks and total stent length[40]. The impact of a PCI strategy guided by the FFR_{CT} Planner on clinical outcomes requires further investigation.

Feasibility of planning coronary artery bypass grafting based only on coronary computed tomography angiography and CT-derived fractional flow reserve: a pilot survey of the surgeons involved in the randomized SYNTAX III Revolution trial

Invasive coronary angiography has been the preferred diagnostic method to guide the decision-making process between coronary artery bypass grafting (CABG) and percutaneous coronary intervention and plan a surgical revascularization procedure. Guidelines recommend a heart team approach and assessment of coronary artery disease (CAD) complexity, objectively quantified by the anatomical SYNTAX score[41]. Coronary computed tomography angiography (CCTA) and CT-derived fractional flow reserve (FFR_{CT}) are emerging technologies in the diagnosis of stable CAD[36]. In this study, data from patients with left main or 3-vessel CAD who underwent CABG were evaluated to assess the feasibility of developing a surgical plan based on CCTA integrated with FFR_{CT}. The primary objective was to assess the theoretical feasibility of surgical decision-making and treatment planning based only on non-invasive imaging.

This study represents a survey of surgeons involved in the SYNTAX III Revolution trial[82]. In this trial, heart teams were randomized to make treatment decisions using CTA. CCTAs and FFR_{CT} results of 20 patients were presented to 5 cardiac surgeons.

Surgical treatment decision-making based on CCTA with FFR_{CT} was considered feasible by a panel of surgeons in 84% of the cases with an excellent agreement on the number of anastomoses to be made in each patient (intraclass correlation coefficient 0.77, 95% confidence interval 0.35–0.96).

Using non-invasive imaging only in patients with left main or 3-vessel CAD, an excellent agreement on treatment planning and the number of anastomoses was found among cardiac surgeons. Thus, CABG planning based on non-invasive imaging appears feasible. Further investigation is warranted to determine the safety and feasibility in clinical practice.

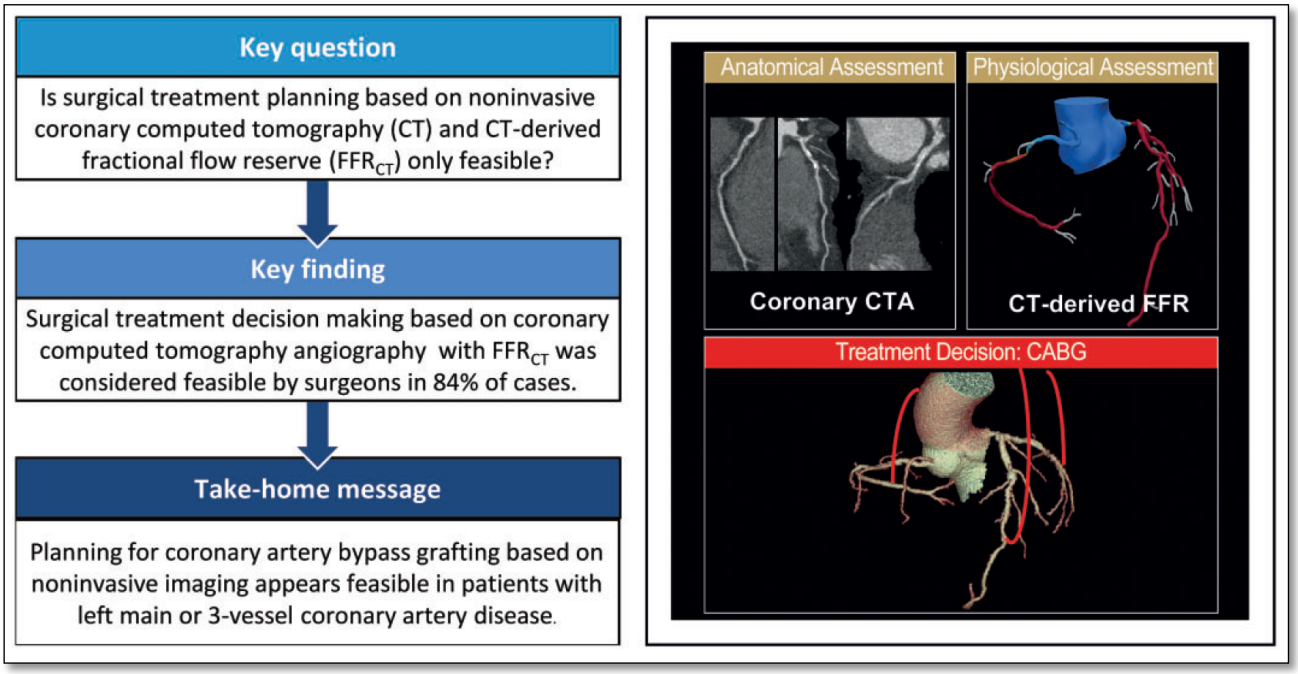

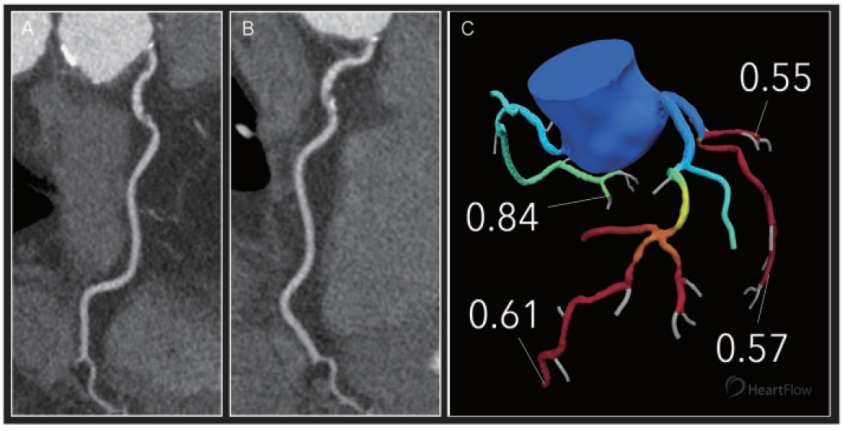

Figure 3: Ostial and proximal RCA stenoses (**A** and **B**) with negative computed tomography-derived fractional flow reserve (0.84) (**C**). All surgeons planned coronary artery bypass grafting (CABG) based on coronary computed tomography angiography but 4 surgeons changed their treatment strategy based on the computed tomography-derived fractional flow reserve result in the RCA resulting in a planned revascularization of only LAD and circumflex artery. During CABG, the patient received a left internal mammary artery on the distal LAD and a venous graft on segment 12a. LAD: left anterior descending artery; RCA: right coronary artery.

Rationale and Design of the Precise PCI Plan (P3) Study: Prospective evaluation of a virtual CT-based percutaneous intervention planner

Fractional flow reserve (FFR) measured after percutaneous coronary intervention (PCI) has been identified as a surrogate marker for vessel related adverse events[15,50]. FFR can be derived from standard coronary computed tomography angiography (CTA)[36]. Moreover, the FFR derived from coronary CTA (FFR_{CT}) Planner is a tool that simulates PCI providing modeled FFR_{CT} values after stenosis opening[39].

The aim of the study is to validate the accuracy of the FFR_{CT} Planner in predicting FFR after PCI with invasive FFR as a reference standard.

Prospective, international and multicenter study of patients with chronic coronary syndromes undergoing PCI. Patients will undergo coronary CTA with FFR_{CT} prior to PCI. Combined morphological and functional evaluations with motorized FFR hyperemic pullbacks, and optical coherence tomography (OCT) will be performed before and after PCI. The FFR_{CT} Planner will be applied by an independent core laboratory blinded to invasive data, replicating the invasive procedure. The primary objective is to assess the agreement between the predicted FFR_{CT} post-PCI derived from the Planner and invasive FFR. A total of 127 patients will be included in the study.

Patient enrollment started in February 2019. Until December 2020, 100 patients have been included. Mean age was 64.1 ± 9.03, 76% were males and 24% diabetics. The target vessels for PCI were LAD 83%, LCX 6%, and RCA 11%. The final results are expected in 2021.

This study will determine the accuracy and precision of the FFR_{CT} Planner to predict post-PCI FFR in patients with chronic coronary syndromes undergoing percutaneous revascularization.

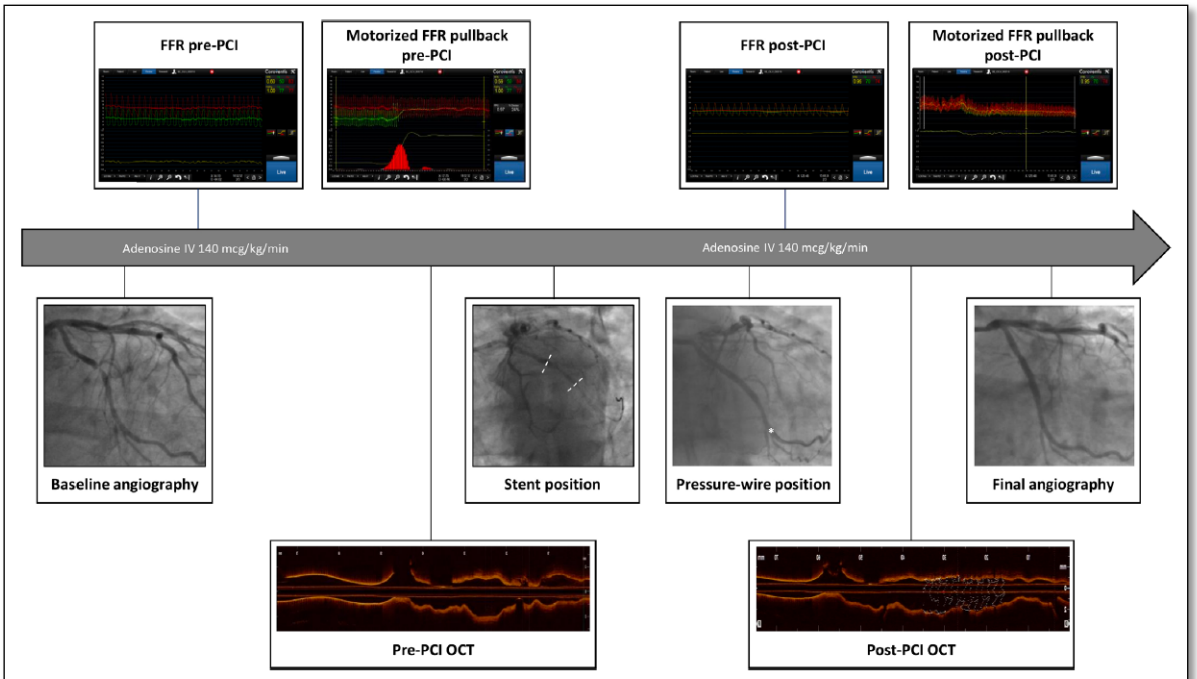

FIGURE 2 Invasive procedure steps. After acquisition of the baseline angiography, pre-PCI FFR is measured followed by a motorized pullback evaluation. The wire position for the distal FFR measurement is recorded with a contrast injection for off-line co-registration with the FFR_{CT} model. Subsequently, OCT is performed to assess lesion characteristics, define stent size and PCI strategy. The position of the stent, before deployment, is recorded with a contrast injection to co-localize the stent position in the FFR_{CT} model for application of the Planner (dashed white line). Following PCI, OCT is performed to assess final stent expansion and apposition. FFR and motorized pullback evaluation are then repeated. The position of the pressure sensor is recorded with a contrast injection (white star). The procedure is completed with final coronary angiography of the target vessel. FFR_{CT}, fractional flow reserve derived from CT. FFR Fractional flow reserve; OCT, optical coherence tomography

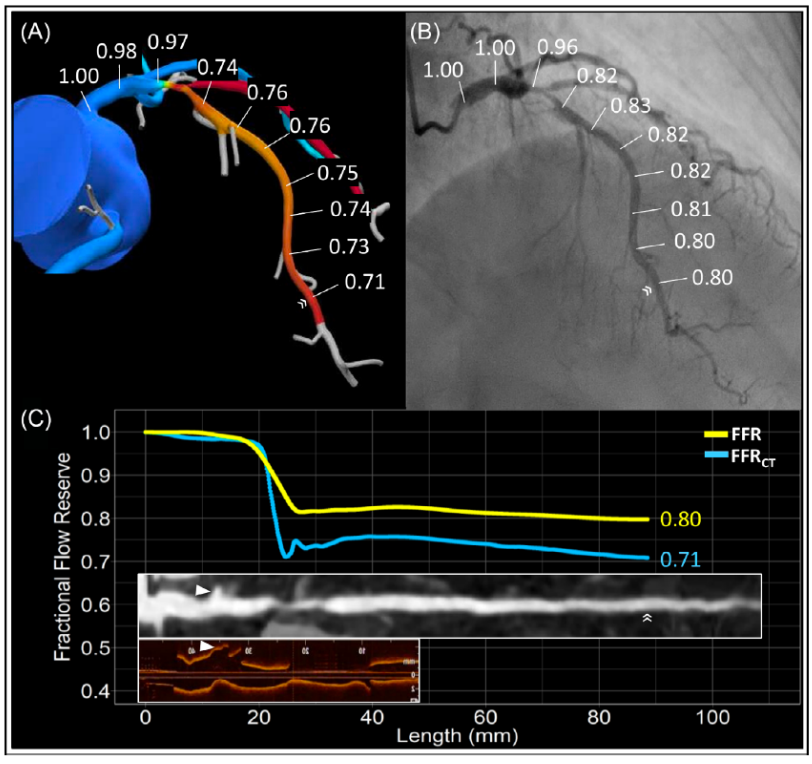

FIGURE 3 Co-registration of FFR_{CT}, FFR, Coronary CTA and OCT. Panels A and B show a left anterior descending artery with the corresponding FFR_{CT} and FFR. The FFR_{CT} and FFR values along the vessel are used to generate pullback curves shown in panel C in blue and yellow, respectively. The white double arrows point the location of the pressure wire sensor used to co-register invasive and non-invasive functional data. On the bottom of panel C, a CT straight multiplanar reconstruction and OCT longitudinal view are co-registered with the physiologic data. The white arrow heads show the position of side branches used to co-register OCT and coronary CTA. Coronary CTA coronary computed tomography angiography. FFR_{CT}, fractional flow reserve derived from CT. FFR Fractional flow reserve; OCT, optical coherence tomography

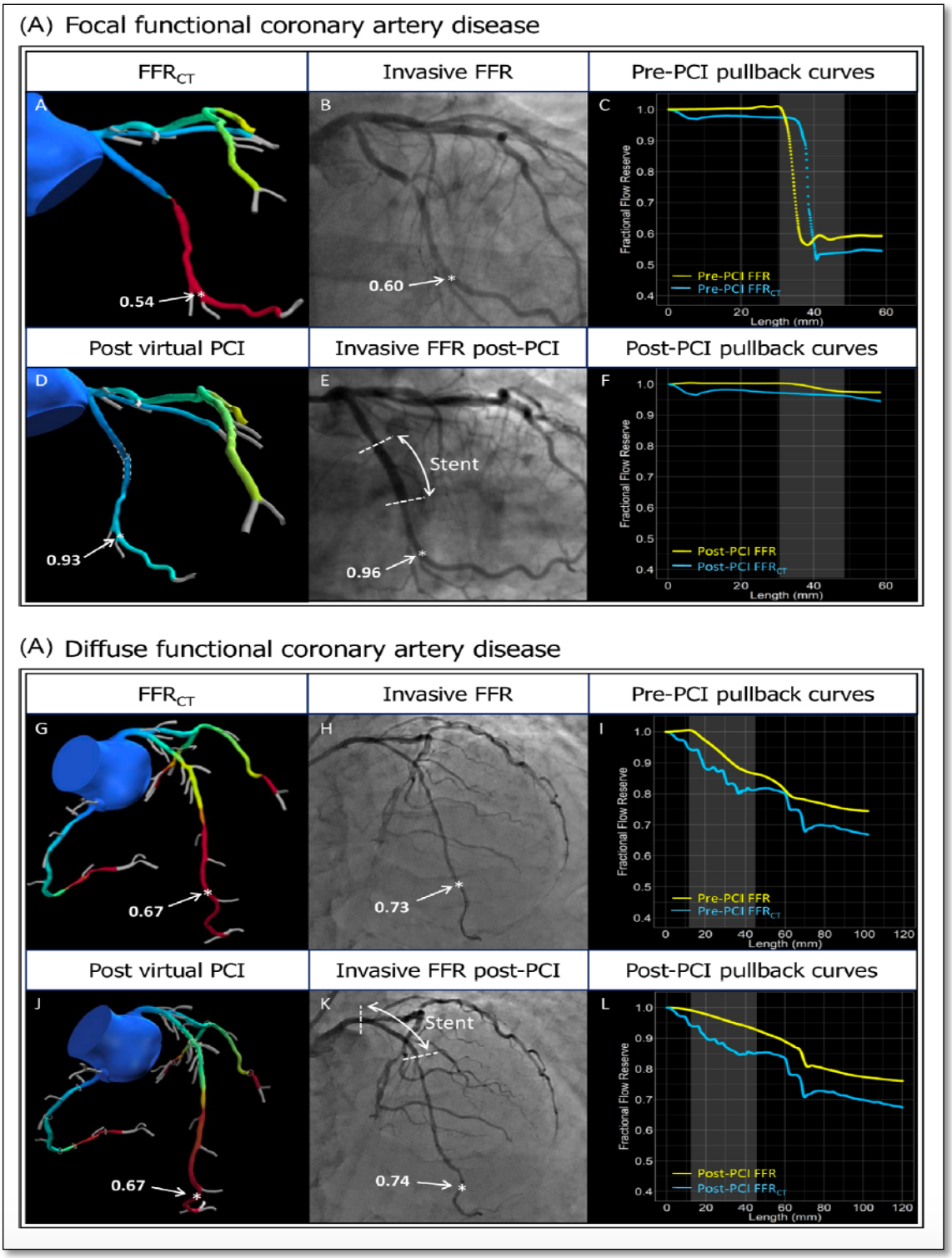

Case example of the application of FFRCT Planner in cases with focal and diffuse functional coronary artery disease. (A) Focal functional coronary artery disease. Panel A shows the FFRCT model showing a focal, hemodynamic significant lesion in the Circumflex coronary artery. Panel B shows invasive angiography confirming an angiographic focal lesion. The position of the pressure wire sensor is denoted by a white star. Panel C shows the FFRCT and invasive FFR pullback curves. Panel D shows the remodeled geometry (white dashed lines) and presents the results of the blinded luminal remodeling using the FFRCT Planner. Panel E shows the location of distal invasive FFR assessment post-PCI (white star) matched with the FFRCT model. The FFRCT Planner predicted a FFRCT value of 0.93 at the same position (white star) where the invasive FFR post-PCI recorded 0.96. Panel F shows the corresponding post-PCI pullback curves derived from FFRCT and invasive FFR (blue and yellow lines, respectively). (B) Diffuse functional coronary artery disease. Panel G shows a patient specific FFRCT model with diffuse pressure loss along the LAD and distal FFRCT value of 0.67. Panel H shows invasive coronary angiography with distal invasive FFR value of 0.73 (white stars). Panel I shows the FFRCT and FFR pullback curves pre-PCI. Panel J shows the remodeled segment in the FFRCT model (white dashed lines) predicting a FFR of 0.67. Panel K shows the location of the invasive FFR measurement of 0.74 (white star). Panel L shows the post-PCI pullback curves derived from FFRCT and invasive FFR (blue and yellow lines, respectively).

Clinical Validation of a Virtual Planner for Coronary Interventions Based on Coronary CT Angiography and Blood Flow Simulations

Low fractional flow reserve (FFR) values after percutaneous coronary intervention (PCI) carry a worse prognosis than high post-PCI FFR values[15,50]. Therefore, the ability to predict post-PCI FFR might play an important role in procedural planning. Post-PCI FFR values can now be computed from pre-PCI coronary CT angiography (CCTA) using the FFR_{CT} Planner.

This study aims at validating the accuracy of the FFR_{CT} Planner.

In this multicenter, investigator-initiated, prospective study, we recruited patients with chronic coronary syndromes and significant lesions based on invasive FFR≤0.80. The FFR_{CT} Planner was applied to the FFR_{CT} model, simulating PCI. The primary objective was the agreement between the predicted post-PCI FFR by the FFR_{CT} Planner and measured post-PCI FFR. Accuracy of the FFR_{CT} Planner's luminal dimensions was assessed using post-PCI optical coherence tomography (OCT) as the reference.

Overall, 259 patients were screened, with 123 included in the final analysis. The mean patient age was 64±9 years and 24% were diabetic. Measured FFR post-PCI was 0.88±0.06, and FFR_{CT} Planner FFR 0.86±0.06, mean difference 0.02±0.07 FFR units, limits of agreement -0.12 to 0.15. OCT minimal stent area (MSA) was 5.60±2.01 $mm^{2,}$ and FFR_{CT} Planner MSA 5.0±2.2 mm^2 (mean difference 0.66±1.21 mm^2, limits of agreement -1.7 to 3.0). The accuracy and precision of the FFR_{CT} Planner remained high in cases with focal and diffuse disease and with low and high calcium burden. Pre-PCI FFR_{CT} was associated with the occurrence of major adverse events (OR 1.69, 95% CI 1.06 to 2.80, p=0.032).

The FFR_{CT}-based technology was accurate and precise for predicting FFR after PCI.

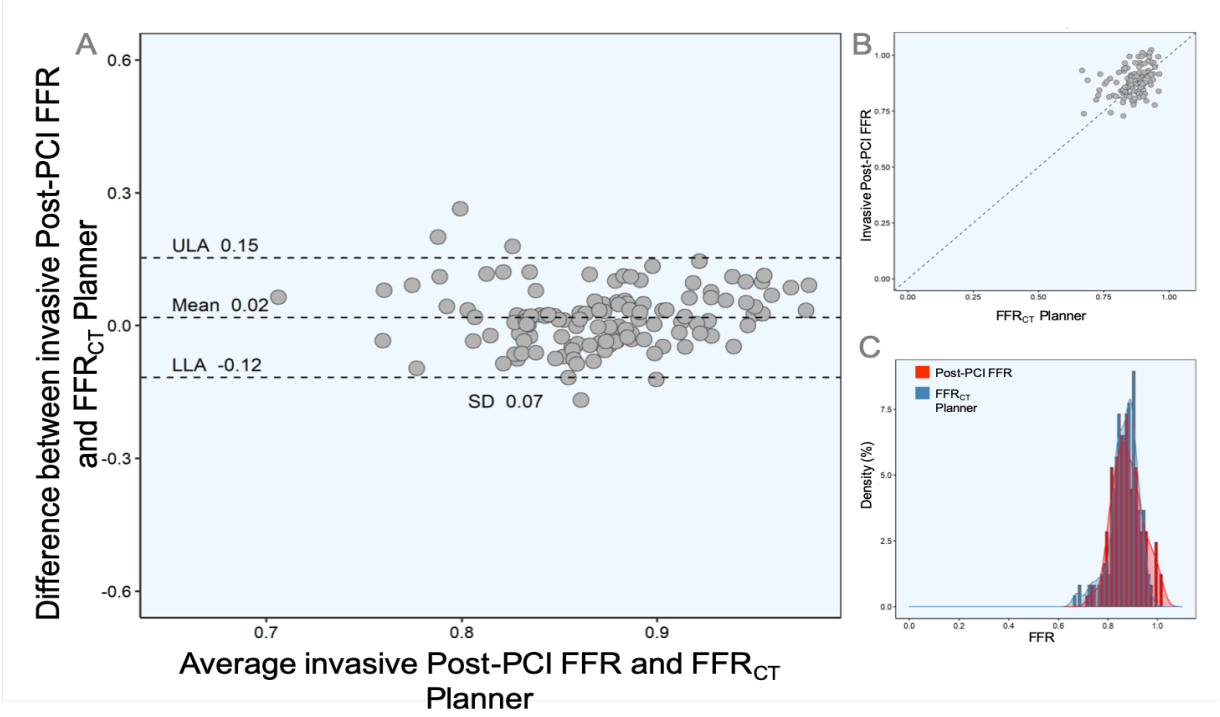

Agreement between FFR_{CT} Planner and invasive post-PCI FFR (primary endpoint). Panel A shows the mean difference on post-PCI FFR between the FFR_{CT} Planner and invasive post-PCI FFR. Panel B displays a moderate correlation (r=0.35, 95% CI 0.18 to 0.49) between the FFR_{CT} Planner and invasive post-PCI FFR. Panel C shows the distribution of post-PCI FFR and FFR_{CT} Planner values.

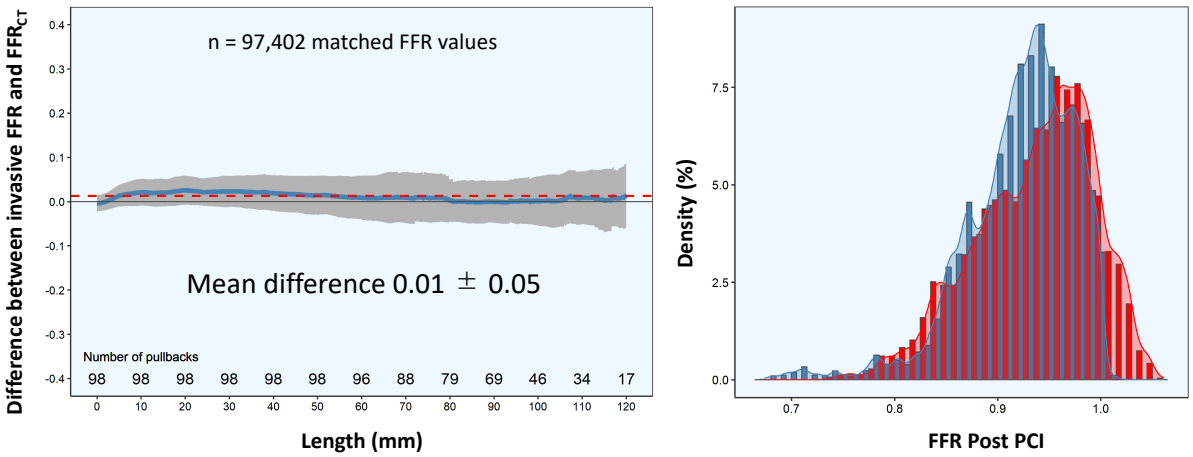

Agreement between FFR_{CT} Planner and invasive post PCI FFR pullback curves. The left panel shows in the x-axis the length of the vessels and the number of pullbacks reaching the given length. The y-axis represents the difference between invasive FFR and FFR_{CT} post-PCI. The red dashed bar represents the mean difference in the whole pullback. The blue line shows the position-dependent mean difference between invasive FFR and FFR_{CT}. The shaded gray area depicts the standard deviation of the difference. The right panel shows the distribution of post-PCI FFR invasive (red) and FFR_{CT} (blue).

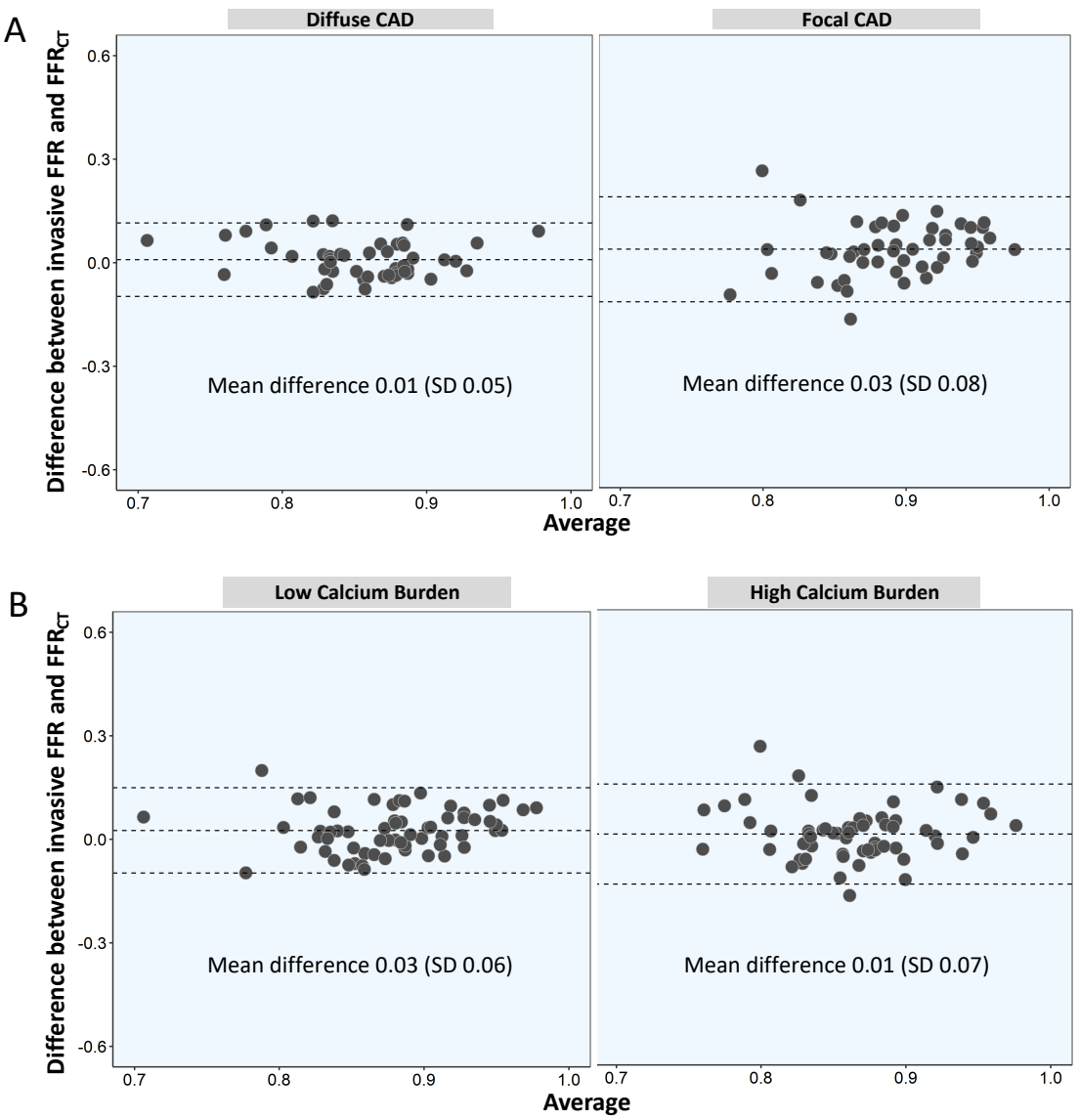

Accuracy of the FFR_{CT} Planner stratified by focal or diffuse coronary artery disease and by calcium burden. The top panel shows Bland Altman plots with the mean difference between the FFR_{CT} Planner and post-PCI FFR stratified by focal or diffuse CAD using the pullback pressure gradient (PPG) index. The bottom panel shows Bland Altman plots with the mean difference between the FFR_{CT} Planner and post-PCI FFR stratified by lesion calcium burden. (ratio between calcium volume and plaque volume in the lesion). The median values of the PPG and calcium burden were used to divide the groups.

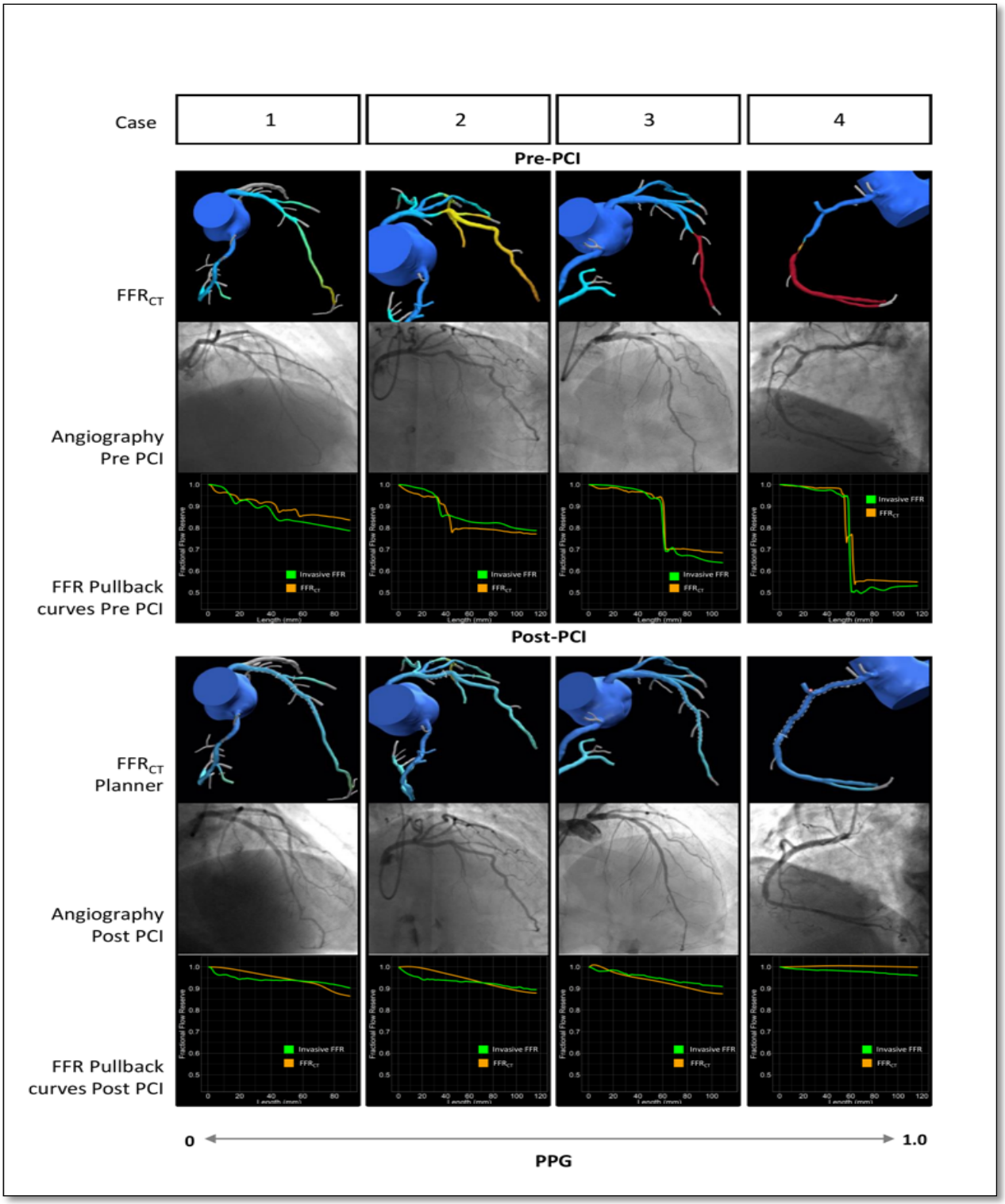

Four case examples with (from top to bottom) FFR$_{CT}$, baseline invasive angiography, pre-PCI fractional flow reserve (FFR) pullback curves (orange FFR$_{CT}$ pullback curve and green invasive motorized pullback curve), FFR$_{CT}$ Planner model, post-PCI angiogram and post-PCI invasive FFR and FFR$_{CT}$ pullback curves. Ranked, from left to right, diffuse to focal coronary artery disease.

Expert Recommendations for Assessing Fractional Flow Reserve After Percutaneous Coronary Intervention

Fractional flow reserve (FFR) measured immediately after percutaneous coronary intervention (PCI) has been proposed as a marker of prognosis. Accordingly, post-PCI FFR has recently been used both as a clinical target to optimize PCI and as an endpoint in clinical trials. In the present document we pooled individual patient-level post-PCI FFR data from 9 studies encompassing 2,760 patients to investigate the predictive power of post-PCI FFR for adverse cardiac events stratified by coronary artery and describe the mechanisms that account for inter-vessel differences. Finally, we provide recommendations for clinicians and trialists on the use of post-PCI FFR measurements.

Extracts from the paper:

Post-PCI FFR stratified by coronary artery:

The mean post-PCI FFR of 0.89±0.07 differed significantly among coronary vessels (post-PCI FFR LAD 0.86±0.06, LCX 0.93±0.06 and RCA 0.91±0.06, p<0.0001. The were no differences in pre-PCI FFR between coronary arteries. The difference in post-PCI FFR between LAD and non-LAD was consistent between randomized and observational trials (-0.057 [95% CI -0.104 to -0.011] FFR units in randomized vs. -0.070 [-0.095 to -0.045] FFR units in observational studies, p=0.473. The LAD vessel, pre-PCI FFR, diabetes mellitus, and stent number and length were independent predictors of low post-PCI FFR.

Predictive power of post-PCI FFR adverse events:

Overall, post-PCI FFR had a moderate predictive capacity for TVF with an AUC of 0.56 (95% CI 0.45 to 0.69). The risk of TVF increased by 44% per every reduction of 0.10 FFR units (Supplemental Figure S4). In a multivariable analysis adjusting for clinical and procedural variables, post-PCI FFR emerged as the only independent predictor of adverse events (Supplemental Table S7 and S8). When stratified by vessel, the predictive capacity of post-PCI FFR for TVF showed an AUC 0.54 (95% CI 0.48-0.59) for the LAD and AUC 0.61 (95% CI 0.56 to 0.67) for non-LAD (p-value=0.052). The optimal binary FFR to predict TVF differed

between territories at 0.80 for the LAD and 0.91 for non-LAD vessels. The predictive capacity of post-PCI FFR was mainly driven by the occurrence of TVR and target-vessel MI. Patients with high post-PCI FFR (i.e., FFR >0.80 in the LAD and >0.90 in non-LAD) also had a lower incidence of cardiac death or MI.

Mechanisms differentially affecting FFR by coronary artery.

Hydrostatic effects:

Because FFR systems rely on an aortic pressure recorded by a fluid-filled catheter, and on a coronary pressure recorded by a microtip sensor, a small hydrostatic gradient arises when the artery courses above or below the plane of the guide catheter. On average for a patient in the supine position, the mid segment of the LAD runs approximately 5 cm above the ostium of the left main stem. Conversely, the distal LCX and right posterolateral branches course approximately 3-4 cm below the ostium.

These differences may explain circa 0.04 FFR units in a single vessel (assuming a mean aortic pressure of 100 mmHg and noting 5 cm H2O * 10 mm/cm / 13.6 H_2O/Hg = 3.7 mmHg due to differences in specific gravity between water and mercury). This means that, theoretically, the highest possible FFR in the LAD would be 0.96 when measured with a standard pressure wire. In the RCA and the LCX this hydrostatic phenomenon goes in the opposite direction.

Myocardial mass and vascular volume:

Overall, total myocardial mass and total epicardial coronary volume display a proportional relationship that becomes distorted by atherosclerosis: in general, higher V/M ratios are associated with higher FFR values and vice versa. It has been reported that the vessel volume of the RCA is significantly bigger that of the LAD. The main reason for this may lie in the LAD progressive tapering, which in turn could be the consequence of the higher number of branching stemming from this vessel. As a consequence, the V/M ratio of the LAD is smaller than that of the non-LAD arteries. Stated another way, to perfuse a larger tissue mass, the LAD needs a higher flow to go through a smaller vascular volume.

Post-PCI Pressure Pullback Patterns:

In the Precise PCI Plan study, co-registration of motorized FFR pullbacks and optical coherence tomography revealed characteristic patterns of post-PCI FFR pullback curves in LADs and non-

LAD. In the LAD, gradual pressure decline along the course of the vessel was systematically observed. In other words, in the LAD after optimal stent implantation, even in absence of residual atherosclerotic disease, the FFR pullback curve shows a downslope that is statistically different than non-LAD. In contrast, the pattern of the post-PCI FFR pullback curve in non-LAD vessels often exhibits a flat slope profile leading to higher distal FFR values.

Pressure pullback patterns leading to low post-PCI FFR:

Low post-PCI FFR is a consequence of two predominant mechanisms identifiable in the pullback curve. First, pressure deterioration can occur gradually along the coronary vessel with homogeneously distributed pressure gradients (i.e., diffuse disease). This is a predominant phenotype in post-PCI LAD pullbacks and may be due to either greater viscous loss from the larger distal mass (even in a normal vessel), could be the manifestation of diffuse CAD or the cumulative hydrostatic pressure effect. Second, focal pressure gradients in the pullback curve may arise from residual (or unmasked) stenosis or stent under-expansion. Focal trans-lesion pressure gradients arise from focal vessel narrowing. These two mechanisms can of course co-exist to produce a combination of focal and diffuse pressure loss. Both post-PCI pullback curve patterns lead to lower post-PCI FFR values but carry different clinical implications. The presence of focal pressure gradients has been associated with a higher risk of adverse events, and high trans-lesion pressure gradients have been linked with plaque rupture and myocardial infarction. Furthermore, from a therapeutic perspective, focal pressure drops can be addressed by additional post-dilatation (for in-stent pressure drops) or by the implantation of an additional stent (for residual or unmasked lesions). In contrast, viscous loss along a normal vessel is physiologic and only medical therapy can address residual diffuse disease.

Achieving functionally complete revascularization (a high post-PCI FFR) likely depends upon the baseline distribution of CAD in the vessel (i.e., focal or diffuse disease) and PCI technique. PCI in patients with focal CAD results in higher post-PCI FFR compared to patients with diffuse disease. Therefore, the distribution of pressure losses represented on the pre-PCI pullback curve is likely to be the major determinant of post-PCI FFR.

Recommendations

We believe that the current data on post-PCI FFR support the following recommendations:

1. Post-PCI FFR should be interpreted in a vessel-specific manner. Due mainly to hydrostatic effects but also variable myocardial mass to vessel ratio, the LAD

coronary artery is associated with lower post-PCI FFR threshold than non-LAD arteries.

2. Post-PCI FFR can be considered a metric of functional revascularization. While influenced by the procedural technique, post-PCI FFR is largely determined by the coronary artery LAD vs. non-LAD and baseline phenotype of CAD (focal vs. diffuse).
3. Mirroring pre-PCI physiology, the mechanisms leading to low post-PCI FFR should be elucidated by pressure pullback and differentiation between focal jumps or diffuse residual pressure loss.
4. Although a higher post-PCI FFR reduces the probability of adverse events, its predictive value remains modest. There is insufficient evidence to support the use of post-PCI FFR as a surrogate of outcomes in clinical trials. Further investigation is necessary to understand if additional PCI in response to post-PCI FFR translates into better clinical outcomes.

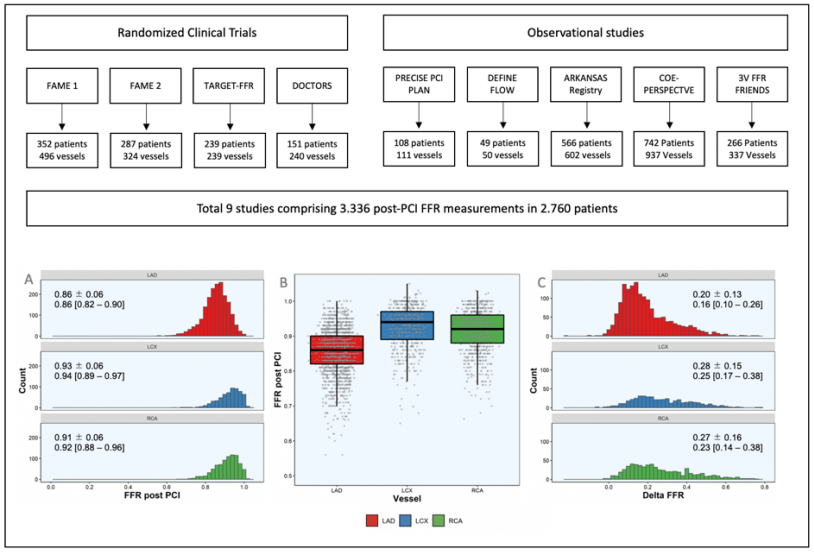

Overview of included studies with post-PCI FFR and functional gain stratified by vessel. In the top panel, the type of study (randomized vs. observational), study name and number of patients and vessels included in the present analysis. In the lowest panels, A) shows the distribution of post-PCI FFR stratified by coronary artery, B) box plot of post-PCI FFR stratified by coronary artery and C) functional gain (post-PCI FFR minus pre-PCI FFR) stratified per coronary artery.

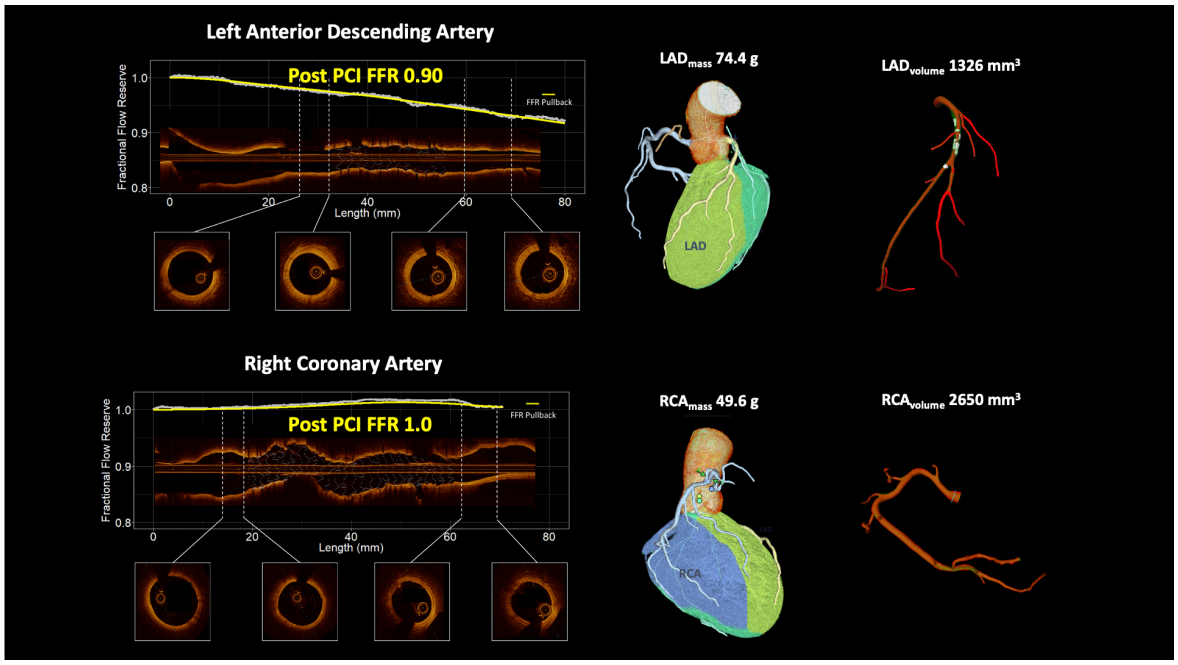

Case example of a motorized FFR pullback co-registered with optical coherence tomography in a LAD and non-LAD. The top panel shows a left anterior descending artery (LAD) post-PCI assessed by motorized FFR pullback (yellow line) and optical coherence tomography (OCT). The OCT showed optimal stent expansion and absence of residual disease outside the treated region (cross-sections proximal and distal to the stent). Despite adequate stent expansion and absence of disease, the post-PCI FFR was 0.90 the pullback curve shows a gradual deterioration of the pressure with a constant slope along the coronary vessel. Using coronary CT angiography, the estimated myocardial mass subtended by the LAD is 74.4 grams and the total volume of the vessel is 1326 mm3, leading to a V/M of 17.8. The lower panel shows a right coronary artery (RCA) from the same subject. OCT also showed adequate stent expansion and absence of residual disease outside the treated region (cross-sections proximal and distal to the stent). The post-PCI FFR was 1.0. The pullback demonstrated a flat slope along the coronary vessel. Using coronary CT angiography, the estimated myocardial mass subtended by the RCA is 49.6 grams and the total volume of the vessel is 2650 mm3, leading to a V/M of 53.4.

Chapter 7: CT-guided percutaneous coronary interventions

State of the art paper: Implementing coronary computed tomography angiography in the catheterization laboratory

In this last chapter we describe the "summary" and clinical extrapolation of most research topics described in previous chapters. Coronary CT evolved from a tool to exclude CAD to a comprehensive method detecting atherosclerosis in its early phase, assessing for the presence of obstructive disease, and risk stratifying patients based on plaque characteristics[30–33]. Current guidelines emphasize the role of CCTA as a first-line test for patients with symptoms suggestive of obstructive CAD[42]. Subsequently, CCTA remains a diagnostic tool. Its usefulness beyond this diagnostic phase has not been yet fully explored. There is increasing awareness of the potential of CCTA to help plan and guide coronary interventions in the catheterization laboratory. For this purpose, our research group developed a novel hardware and software solution to integrate the comprehensive CAD assessment by CCTA in the diagnostic and therapeutic workflow of the invasive coronary angiography and percutaneous coronary interventions.

The diagnostic part of the state-of-the-art paper focusses on diagnostic novelties and the CT-based evaluation of revascularization procedures with respect to luminal assessment, plaque characterization and the evaluation of lesion significance.

First, several improvements in luminal assessment were described when integrating CCTA in the invasive workflow. Using CT in the planning phase of a coronary intervention aids in providing the best angiographic projection in the catheterization lab, thereby minimizing foreshortening and overlapping of the segment of interest. Angiographic foreshortening observed in 2-dimensional (2D) projection images impairs accurate evaluation of lesion length, a frequent cause of incomplete plaque coverage and geographic miss. Also, CT-derived lesion length evaluation incorporates the atherosclerotic extension that is not visible with conventional angiography and comparable to intra-vascular imaging. Moreover, even stent sizing can be performed based on non-invasive CCTA luminal assessment results. In the clinical setting, minimal lumen diameter is used to define lesion severity, whereas, for percutaneous revascularization planning, reference vessel diameter distal to the lesion is used to select stent diameter. CT-based quantitative coronary analysis has been shown to have a very high agreement concerning luminal dimensions compared to conventional angiography,

and measurements based on CCTA have shown to be smaller compared with those derived from IVUS[127,128].

Second, we describe the advantages of pre-angiography CCTA for plaque characterization integrating also the results of this PhD thesis chapter 3. Beyond the identification of high-risk plaque characteristics, CCTA is very sensitive for calcium detection and assessment as described in the paper comparing CCTA calcium burden with OCT as a reference. Also, plaque characteristics could prompt the invasive cardiologist to interrogate the hemodynamic consequences of the stenosis by FFR or NHPR or to select lesion preparation devices to facilitate stent expansion and deployment[45,129]. Meanwhile, CCTA has the potential to identify the normal coronary segments delineating the atherosclerotic plaque in a way comparable to IVUS or OCT[130]. This facilitates PCI from "normal to normal" coronary segments important to select the optimal landing zone for stent deployment.

Third, the performance of FFR_{CT} is similar to positron-emission tomography and cardiac magnetic resonance stress and perfusion imaging and is significantly superior to single-photon emission computed tomography[37]. Moreover, the adoption of FFR_{CT} has allowed to assess lesion-specific ischemia comparable to invasive fractional flow reserve or non-hyperemic pressure ratios (NHPR)[36,38,131]. As such, FFR_{CT} is instrumental for diagnosis and heart-team decision making as described in the first two chapters of this thesis.

The novelty of this state-of-the-art paper is described in the central topic of CCTA-derived 3D reconstructions to guide catheterization laboratory procedures. The Precise PCI and Procedural Planning algorithm is shown in the Central Illustration. Based on 3 mainstays, namely diagnostic evaluation, catheterization laboratory preparation and online guidance, the algorithm proposes the incorporation of CT into all phases of the management of patients with obstructive CAD.

During the diagnostic evaluation, the operator should focus on the determination of the pattern of CAD (i.e., focal or diffuse); and 2) the prediction of PCI results. Functional evaluation with FFR_{CT} characterizes the pathophysiological pattern (e.g., focal or diffuse) of CAD noninvasively. This can be visualized either on the color-coded geometry or by a virtual FFR_{CT} pull back curve[132]. The pattern of CAD is important to distinguish pressure losses that are circumscribed to anatomic stenoses (i.e., lesion-specific ischemia). This vessel phenotype is favorable for PCI in terms of post-intervention vessel physiology. In contrast, cases of diffuse functional CAD show no focal pressure drop. These vessels often exhibit diffuse atherosclerosis on CCTA, and despite the presence of one or several vessels narrowing, PCI

results are suboptimal in terms of post-PCI FFR. Therefore, the evaluation of the anatomic and physiological pattern of CAD aids in predicting the likelihood of functional complete revascularization and potentially relief from angina. These concepts were developed in the papers in the chapter 5 “Redefining the patterns of coronary artery disease”. In terms of PCI result prediction, we refer to the main “Precise PCI plan” paper introducing the FFR_{CT} Planner to predict functional revascularization results. The FFR_{CT} planner simulates luminal changes produced by PCI and recalculates coronary pressures using the modified “stented” geometry. This may assist to predict the potential benefit of a given PCI strategy. With the FFR_{CT} planner, the normal-to-normal can be demarcated based on coronary physiology next to the anatomical “normal to normal” concept derived from CCTA.

Specifically, for catheterization laboratory preparation purposes, CCTA can aid in the pre-intervention assessment and prediction of more complex interventions or procedures. CCTA visualizes the coronary ostia, coronary anomalies and coronary grafts potentially leading to less contrast and radiation use when this information is readily available pre-intervention. CCTA has a proven role in the evaluation of chronic coronary occlusions and in other challenging lesion subsets such as left main disease, ostial lesions, bifurcations, or severely calcified coronary vessels[127,133–135]. As such, CCTA can inform upfront on the best strategy and the need for dedicated devices.

For the online procedural and PCI guidance, visualization of the coronary circulation derived from CCTA provides a 3D view of the coronary tree and the plaque components during conventional angiography procedures. Both lumen and atherosclerotic plaques are reconstructed using dedicated software. To facilitate online interpretation, plaque components are color-coded based on their HU. The movement of the C-arm is tracked in real time to synchronize the orientation of the 3D coronary tree with the projection of the fluoroscopic C-arm. A manufacturer-independent approach was accomplished by attaching an external sensor, called an inertial measurement unit to the C-arm. The inertial measurement unit is connected to a Raspberry Pi, which continuously communicates the sensor’s—and therefore, also the C-arm’s—orientation with the 3D visualization software. During the procedure, the coronary anatomy derived from CCTA is continuously projected during changes in angiographic projections. At each projection, it is possible to assess the degree of overlapping and foreshortening without additional radiation or contrast. Tailored angulations optimize lesion evaluation and prevent unnecessary angiographic acquisitions. Furthermore, the 3D CCTA model can be used as a 3D roadmap to assist during vessel wiring, further reducing the need for additional contrast injection while the wire is advanced. Guidance of

PCI with CCTA follows the same principles as with intravascular imaging (e.g., IVUS or OCT)[57]. Pre-procedural assessment starts with the evaluation of plaque characteristics, composition, and extension. Lesion length is determined based on healthy landing zones proximal and distal to the lesion. The continuous display of CCTA and invasive angiography allows also the use of anatomic landmarks to visually co-register both modalities.

The clinical implications of this novel approach are diverse. CCTA has the potential to improve patient selection for both invasive diagnostic procedures and therapeutic interventions. The presumed reduction in contrast usage and radiation burden implies a potential advantage in terms of patient safety. Also, the integration of non-invasive information comparable to per-procedural assessments by intra-vascular imaging could enhance PCI techniques with complete plaque coverage entailing improve clinical outcomes after PCI. Dedicated software has been developed that aims to simplify procedural workflow. This novel software solution simulates intravascular imaging tools that may facilitate adoption and image interpretation by interventionists.

JACC: CARDIOVASCULAR IMAGING VOL. ■, NO. ■, 2020

PUBLISHED BY ELSEVIER

REVIEW

STATE-OF-THE-ART PAPER

Implementing Coronary Computed Tomography Angiography in the Catheterization Laboratory

Carlos Collet, MD, PhD,[a] Jeroen Sonck, MD,[a,b] Jonathon Leipsic, MD,[c] Giovanni Monizzi, MD,[a] Dimitri Buytaert, MSc,[a] Pieter Kitslaar, MSc,[d,e] Daniele Andreini, MD, PhD,[f] Bernard De Bruyne, MD, PhD[a,g]

ABSTRACT

Coronary computed tomography angiography (CCTA) is now an established tool in the diagnostic work-up of patients suspected to have coronary artery disease. Yet, its usefulness beyond this phase has not been fully explored. The current review focuses on the implementation of CCTA as a tool to plan and guide coronary interventions in the catheterization laboratory. Specifically, we explore the potential of CCTA to improve patient selection for percutaneous revascularization, provide the rationale for better resource use, and present a novel approach to incorporate 3-dimensional CT guidance for percutaneous coronary interventions. (J Am Coll Cardiol Img 2020;■:■–■) © 2020 by the American College of Cardiology Foundation.

Over the last 2 decades, computed tomography (CT) has become an established tool in the diagnostic work-up of patients with suspected coronary artery disease (CAD). Noninvasive imaging of coronary arteries by computed tomography coronary angiography (CCTA) allows detecting atherosclerosis in its early phase, assessing for the presence of obstructive disease, and risk-stratifying patients based on plaque characteristics (1,2).

In addition, fractional flow reserve can be derived from computed tomography coronary angiography (FFR_{CT}), providing a surrogate of coronary flow and myocardial ischemia (3,4). Also, FFR_{CT} defines the severity and the functional pattern (e.g., focal or diffuse) of CAD (5). The combination of CCTA and FFR_{CT} has increased our understanding of the interactions among luminal obstruction, plaque characteristics, and physiology at different stages of the atherosclerotic process (6).

Current guidelines emphasize the role of CCTA as a first-line test for patients with symptoms suggestive of obstructive CAD (7). Nevertheless, CCTA remains a diagnostic tool, its usefulness beyond this phase has not been yet fully explored. There is increasing awareness of the potential of CCTA to help plan and guide coronary interventions in a fashion similar to how cardiac CCTA has transformed transcatheter heart valve interventions. This state-of-the-art review summarizes the emerging role of CT in decision making about revascularization and focuses on the

From the [a]Cardiovascular Center Aalst, Onze Lieve Vrouw Ziekenhuis, Aalst, Belgium; [b]Department of Advanced Biomedical Sciences, University of Naples, Federico II, Naples, Italy; [c]St. Paul's Hospital, University of British Columbia, Vancouver, British Columbia Vancouver, Canada; [d]Department of Radiology, Leiden University Medical Center, Leiden, the Netherlands; [e]Medis Medical Imaging Systems, Leiden, the Netherlands; [f]Centro Cardiologico Monzino, Milano, Italy; and the [g]Department of Cardiology, Lausanne University Hospital, Lausanne, Switzerland.
The authors attest they are in compliance with human studies committees and animal welfare regulations of the authors' institutions and Food and Drug Administration guidelines, including patient consent where appropriate. For more information, visit the Author Center.

Manuscript received February 4, 2020; revised manuscript received July 10, 2020, accepted July 14, 2020.

ISSN 1936-878X/$36.00 https://doi.org/10.1016/j.jcmg.2020.07.048

ABBREVIATIONS AND ACRONYMS

2D = 2-dimensional

CAD = coronary artery disease

CCTA = coronary computed tomography angiography

CT = computed tomography

CTO = chronic total occlusion

FFR = fractional flow reserve

FFR_{CT} = fractional flow reserve derived from computed tomography

HU = Hounsfield units

IVUS = intravascular ultrasound

OCT = optical coherence tomography

PCI = percutaneous coronary intervention

implementation of CCTA in the catheterization laboratory to guide coronary interventions.

CT-BASED EVALUATION FOR REVASCULARIZATION PROCEDURES

LUMINAL ASSESSMENT. CCTA overcomes a frequent problem of invasive angiography—that of vessel foreshortening (8). CT in the planning phase of a coronary intervention aids in providing the best angiographic projection in the cath lab, thereby minimizing foreshortening and overlapping of the segment of interest. This becomes even more relevant in the evaluation of bifurcation lesions where the visualization of the side-branch ostium is often suboptimal with conventional angiography (9). Furthermore, angiographic foreshortening observed in 2-dimensional (2D) projection images impairs accurate evaluation of lesion length (8). This is a frequent cause of incomplete plaque coverage and geographic miss, and these latter issues are associated with adverse events after stent implantation (10). Besides, CT-derived lesion length evaluation incorporates the atherosclerotic extension that is not visible with conventional angiography; this approach mimics the evaluation obtained by intravascular imaging techniques (e.g., intravascular ultrasound [IVUS] and optical coherence tomography [OCT]).

The 2 most relevant metrics derived from CCTA analysis are minimal lumen diameter and reference vessel diameter. CT-derived quantitative coronary analysis has been shown to have a high degree of agreement with the true luminal dimensions (11). In the clinical setting, minimal lumen diameter is used to define lesion severity, whereas, for percutaneous revascularization planning, reference vessel diameter distal to the lesion is used to select stent diameter. CT-based quantitative coronary analysis has been shown to have a very high agreement concerning luminal dimensions compared to conventional angiography, and measurements based on CCTA have shown to be smaller compared with those derived from IVUS (12). The systematic differences in vessel dimensions between these methods are partially explained by the differences in spatial resolution and the physical properties of the techniques. For percutaneous coronary intervention (PCI) planning, CT-derived reference vessel diameter, obtained at healthy coronary segments, can be incorporated in the decision process concerning stent diameter selection.

PLAQUE ASSESSMENT. In addition to the lumen, CCTA allows us to visualize the atherosclerotic plaque and determine its burden. Plaques can be qualitative and quantitatively characterized (13,14). It has been shown that CCTA helps identify high-risk plaques using measures of remodeling (e.g., remodeling index) and also allows the characterization of lesions through their Hounsfield units (HU) and appearances. Calcified plaques can be visualized as white structures with high HU, and their burden and circumference can be evaluated (15). High calcium burden is associated with lower stent expansion and higher rates of adverse events after PCI (16,17). Hence, visualization of high calcium burden in the planning phase of coronary intervention may prompt use of calcium modification techniques (e.g., rotational atherectomy, orbital atherectomy, excimer laser, or intravascular lithoplasty) to facilitate stent expansion (18–20). Stent expansion, which depends partially on the underlying plaque, is an independent predictor of major adverse events after PCI. On the other side of the plaque spectrum, plaques with low HU, the so-called soft plaques (i.e., HU <50) have been identified as independent predictors of acute coronary syndromes, periprocedural myocardial infarction, and no-reflow phenomenon (1,21,22). Also, identification of high-risk plaques before conventional angiography assists in the diagnostic strategy. Low-attenuation noncalcified plaques have been identified as independent predictors of low FFR (23). Therefore, the presence of high-risk plaques, even in mild to moderate stenosis, should prompt the operator to complement the invasive evaluation of the coronary lesion with invasive pressure measurements such as FFR. The assessment of plaque extension with CCTA allows extrapolating the normal-to-normal concept described with intravascular imaging (24). By "landing" the stents on healthy coronary segments, the atherosclerotic plaque is covered, mimicking the approach used with IVUS or OCT and potentially reducing the risk associated with a geographic miss.

Quantitative plaque assessment forms the basis of the 3D plaque reconstructions used during online CT guidance (as discussed later). Atherosclerotic plaque components are color-coded based on HU (e.g., white for calcified structures with >320 HU, green for plaque components between 50 and 320 HU, and red for low-attenuation plaques). This results in a 3D plaque portray or plaque map that facilitates imaging interpretation and the evaluation of disease extension, volume, and composition. Simultaneous plaque visualization during conventional angiography optimizes the interpretation of the images given that apparently normal segments may be diffusely

CENTRAL ILLUSTRATION CT-Guided PCI Algorithm

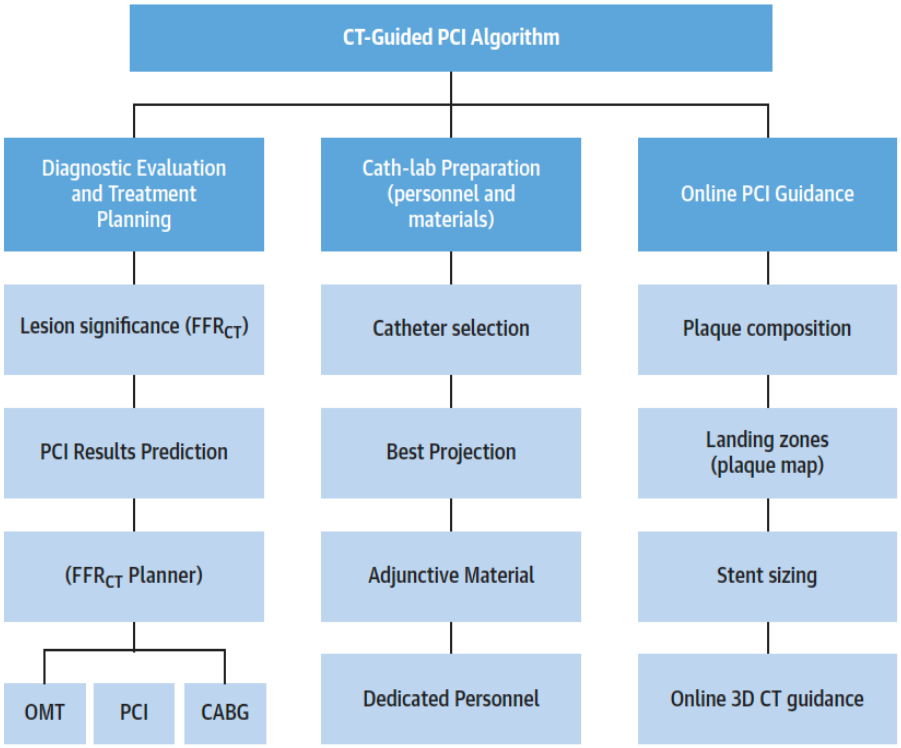

Collet, C. et al. J Am Coll Cardiol Img. 2020;■(■):■-■.

The percutaneous coronary intervention (PCI) algorithm starts with the diagnostic evaluation to ascertain hemodynamic lesion significance based on fractional flow reserve derived from computed tomography (FFR_{CT}). In this pre-cath lab phase, the results in terms of post-PCI FFR_{CT} can be predicted using the HeartFlow Planner. Based on the degree of functional revascularization assessed by virtual PCI, the clinician may opt for a given PCI strategy, coronary artery bypass graft (CABG), or medical therapy. The next step in the algorithm addresses the preparation of the cath lab based on the patient-specific characteristics. The selection of the coronary catheters is performed accounting for the position of the ostia, size of the aorta, and required support for the coronary intervention. Also, the best angulation for the visualization of the lesion can be determined. Adjunctive material and personnel corresponding to the case complexity can be prepared before starting the procedure. During the procedure, the availability of the online PCI guidance further aids in the visualization of the coronary tree. Furthermore, vessel size, extent, and composition of the atherosclerotic plaque are visualized side by side with the invasive coronary angiography helping in the selection of the diameter and length of the stent. 3D = 3-dimensional; OMT = optimal medical therapy.

diseased. It should be highlighted that the interpretation of calcified plaques demands a special consideration given the overestimation of calcium volume due to blooming artifacts. Further research is required to determine the clinical implications of plaque features assessed by CCTA on PCI results.

FUNCTIONAL ASSESSMENT. Using CCTA, 3D coronary geometries can be extracted and used to perform fluid dynamic simulations. Assuming a normal response of the coronary microcirculation to hyperemic stimulus, and adjusting microvascular resistance to vessel-specific myocardial mass, blood flow simulations can estimate coronary pressures, enabling us to compute FFR, the ratio of distal coronary pressure and aortic pressure during hyperemia. Clinical trials have demonstrated improved diagnostic performance of FFR_{CT} compared with a visual assessment for the detection of hemodynamically significant lesions (4). Moreover, the diagnostic performance of FFR_{CT} to detect hemodynamically significant lesions is similar to positron-emission tomography and cardiac magnetic resonance stress

FIGURE 1 Case Examples of Focal and Diffuse CAD

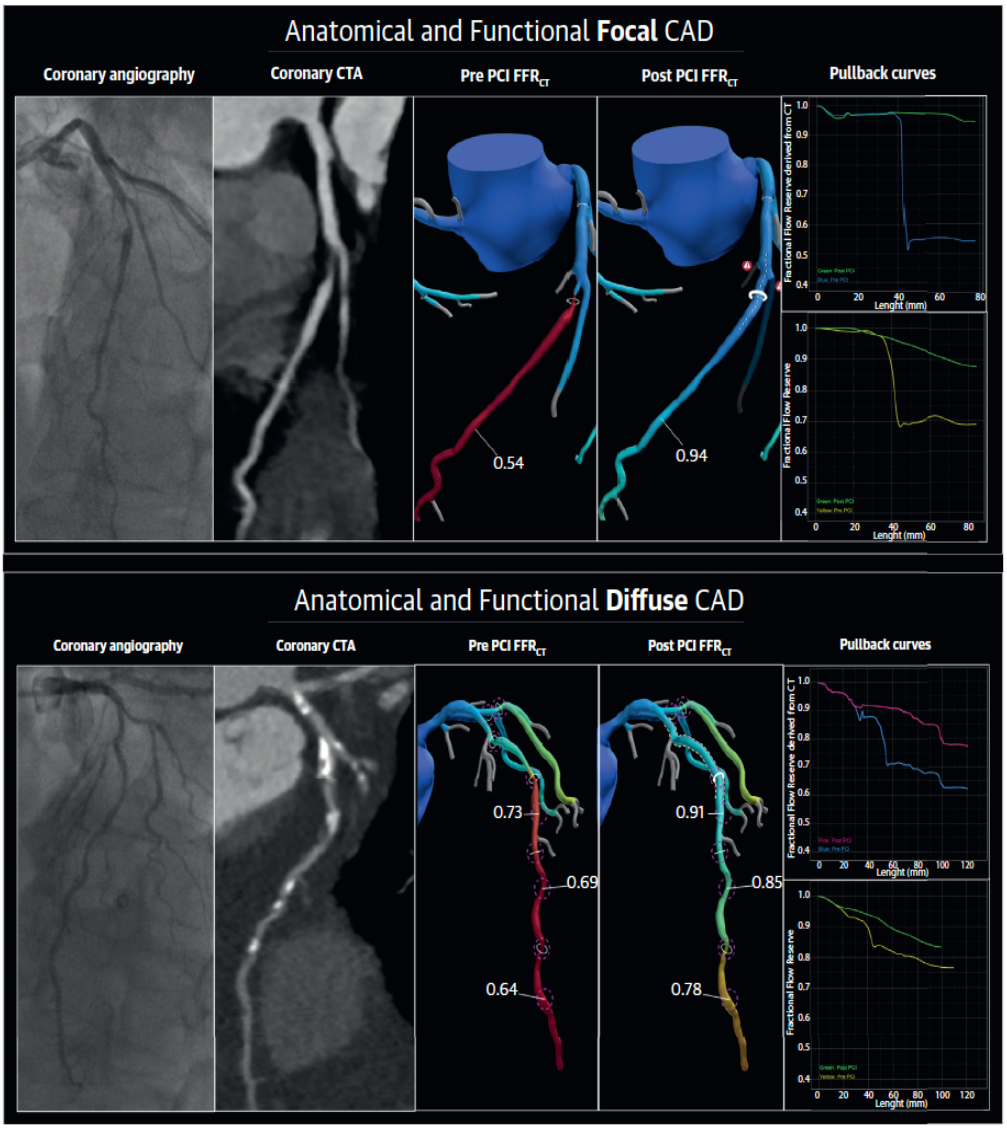

(Top) This case shows an anatomical and functional focal lesion located in the mid-left anterior descending artery. The virtual pull back curve derived from fraction flow reserve derived from computed tomography (FFR_{CT}) shows a focal pressure drop of approximately 40 FFR_{CT} units related to the lesion **(top right)**. No pressure losses are observed either proximal or distal to the lesion. After virtual percutaneous coronary intervention (PCI), the predicted FFR was 0.94 and invasively measured FFR was 0.90. **(Bottom)** This case shows anatomical and functional diffuse coronary artery disease (CAD) in a left anterior descending artery. The virtual pull back curve derived from FFR_{CT} shows diffuse pressure losses along the vessel length **(bottom right)**. After virtual PCI, the predicted FFR was 0.78 and invasively measured FFR was 0.82. CTA = computed tomography angiography.

perfusion imaging and is significantly superior to single-photon emission computed tomography (25,26). In the cath lab, the interpretation of the FFR_{CT} should also incorporate the agreement between the CT-derived coronary 3D anatomic model and invasive coronary angiography. By discordant anatomic information, invasive FFR should be considered to confirm lesion significance. A detailed

FIGURE 2 Process of 3D Lumen and Plaque Reconstruction

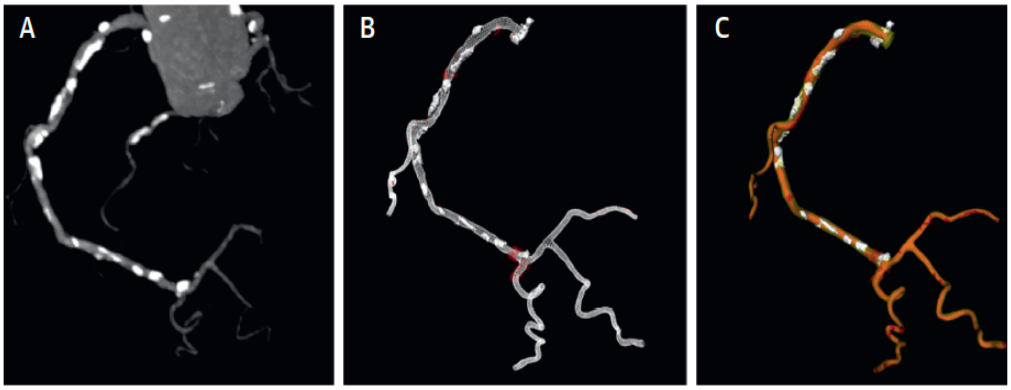

Computed tomography reconstruction made by QAngioCT/3D Workbench. **(A)** A 3-dimensional (3D) maximum intensity projection image is shown of a right coronary artery with diffuse calcifications. **(B)** 3D geometry reconstruction of lumen mesh and plaques. **(C)** Colored-coded lumen and plaques.

description of the principles, the different options for the calculation of FFR_{CT}, and outcome data are beyond the scope of this review. In the next section, we describe the usefulness of FFR_{CT} for patient selection for PCI.

CCTA-DERIVED 3D RECONSTRUCTION AS A GUIDE IN THE CATH LAB

PRECISE PCI AND PROCEDURAL PLANNING ALGORITHM. The precise PCI and procedural planning algorithm is shown in the Central Illustration. Based on 3 mainstays,—namely diagnostic evaluation, cath lab preparation and online guidance—the algorithm proposes the incorporation of CT into several phases of the management of patients with obstructive CAD.

DIAGNOSTIC EVALUATION. The initial part of the algorithm extends the evaluation of the hemodynamic significance of CAD in 2 domains: 1) determination of the pattern of CAD (i.e., focal or diffuse); and 2) the prediction of PCI results. Functional evaluation with FFR_{CT} characterizes the pathophysiological pattern (e.g., focal or diffuse) of CAD noninvasively (5). This can be visualized either on the color-coded geometry or by a virtual FFR_{CT} pull back curve (27). In cases of focal functional disease, pressure losses are circumscribed to anatomic stenoses (i.e., lesion-specific ischemia), this vessel phenotype is favorable for PCI in terms of post-intervention vessel physiology. In contrast, cases of diffuse functional CAD show no focal pressure drops, these vessels often exhibit diffuse atherosclerosis on CCTA, and despite the presence of one or several vessels narrowing, PCI results are suboptimal in terms of post-PCI FFR. Therefore, the evaluation of the anatomic and physiological pattern of CAD aids predicting the likelihood of functional complete revascularization and relief from angina (27,28).

The FFR_{CT} planner (HeartFlow Planner; HeartFlow Inc., Redwood City, California) tool is a new approach to predict the results of PCI in terms of post-PCI FFR.

FIGURE 3 Cath Lab Setup for Online CT Guidance

The cath lab setup comprises the addition of synchronization hardware between the C-arm and CT software **(black arrow)** with the projection of the 3D CT-derived geometry projected side by side to the angiographic image **(white arrow)**. Abbreviations as in Figures 1 and 2.

FIGURE 4 Impact of Optimal Projection for the Evaluation of Lesion Length

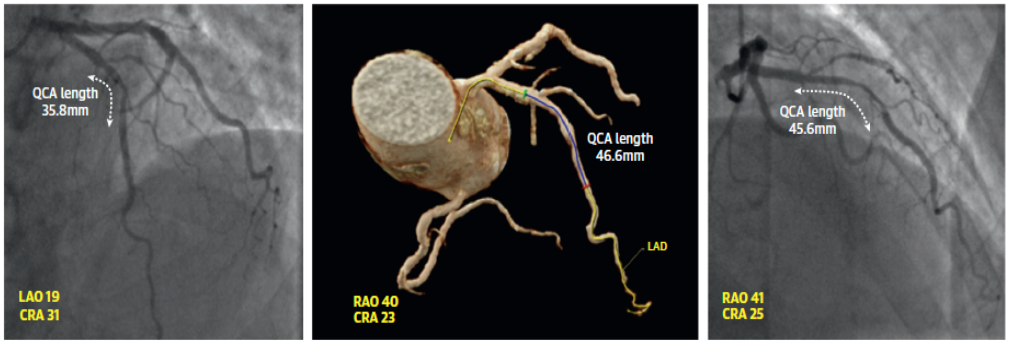

(Left) A left cranial 2-dimensional projection is shown with a lesion in the mid segment of the left anterior descending artery, and the quantitative coronary analysis (QCA) lesion length was 35.8 mm. **(Center)** Nevertheless, computed tomography showed that lesion length was longer and suggested a steep right cranial (CRA) projection to depict the true lesion length. **(Right)** The conventional angiography projection was adapted based on computed tomography-confirmed lesion length of 45.6 mm. LAO = left anterior oblique; RAO = right anterior oblique.

The FFR_{CT} planner simulates luminal changes produced by PCI and recalculates coronary pressures using the modified "stented" geometry. This may assist to predict the benefit of a given PCI strategy. With the FFR_{CT} planner, the normal-to-normal can be demarcated based on coronary physiology. Two case examples of the application of the planner in cases of focal and diffuse CAD are shown in Figure 1. As shown in the case example, PCI restored vessel physiology in focal functional CAD and this is likely to be translated in clinical benefit, that is, relief from angina. In contrast, in cases of diffuse functional CAD, suboptimal post-PCI results are plausibly responsible for persistent angina after PCI. Therefore, patient selection for PCI is individualized based on the potential benefit from percutaneous revascularization (29). The prospective multicenter validation of the FFR_{CT} planner is ongoing, and the results are expected by early 2021 (P3 [Precise Percutaneous Coronary Intervention Plan]; NCT03782688).

CATH LAB PREPARATION. From the evaluation of the position of the coronary ostia to the planning of complex PCI, a noninvasive stratification of the complexity of CAD aids on the organization of the cath lab. Although relatively uncommon, identification of coronary anomalies informs about the more adequate type of coronary catheters and cannulation technique (30). Moreover, CAD in the coronary ostia may change the cannulation strategy avoiding deep vessel catheterization that may conceal an obstructive lesion and could potentially affect an FFR measurement. Furthermore, in patients with graft anastomosis in the aorta, CCTA aids in localizing conduits and expediting cannulation. In these scenarios, a CT-guided approach saves time, contrast, and reduces unnecessary radiation exposure.

Based on CCTA, complex interventions can be better planned in the cath lab. In the case of chronic coronary occlusions, CCTA helps to better identify the distal vessel and route for PCI than invasive angiography and predicts guidewire crossing and procedural success (31). The CT RECTOR (Computed Tomography Registry of Chronic Total Occlusion Revascularization) and J-CTO (Multicenter CTO Registry of Japan) score is helpful to predict the likelihood of success of chronic total occlusion (CTO) intervention integrating several CT variables allowing the planning of intervention in advance of angiography (32,33). CTO characteristics such as occlusion length, stump morphology, angulation, cross-sectional area of calcification, and the outlet morphology can all be routinely obtained from CCTA and help inform the likelihood of CTO recanalization (33). In addition to the diagnosis and characterization (e.g., calcification, tortuosity, length and stump morphology) of the CTO lesion, the 3D visualization in the cath lab allows for determining the exact vessel trajectory with accurate measurement of the occlusion (or occlusions) length. The real-time integration of 3D CCTA data and fluoroscopic images in the cath lab guides coronary wire progression in the occluded segment, reassuring the operator on the vessel-specific trajectory. Furthermore, based on the anatomic features of the CTO, for example, severe calcium in the proximal cap and good collateral circulation, an alternative CTO

FIGURE 5 The Prototype Software Package for Cath Lab Integration

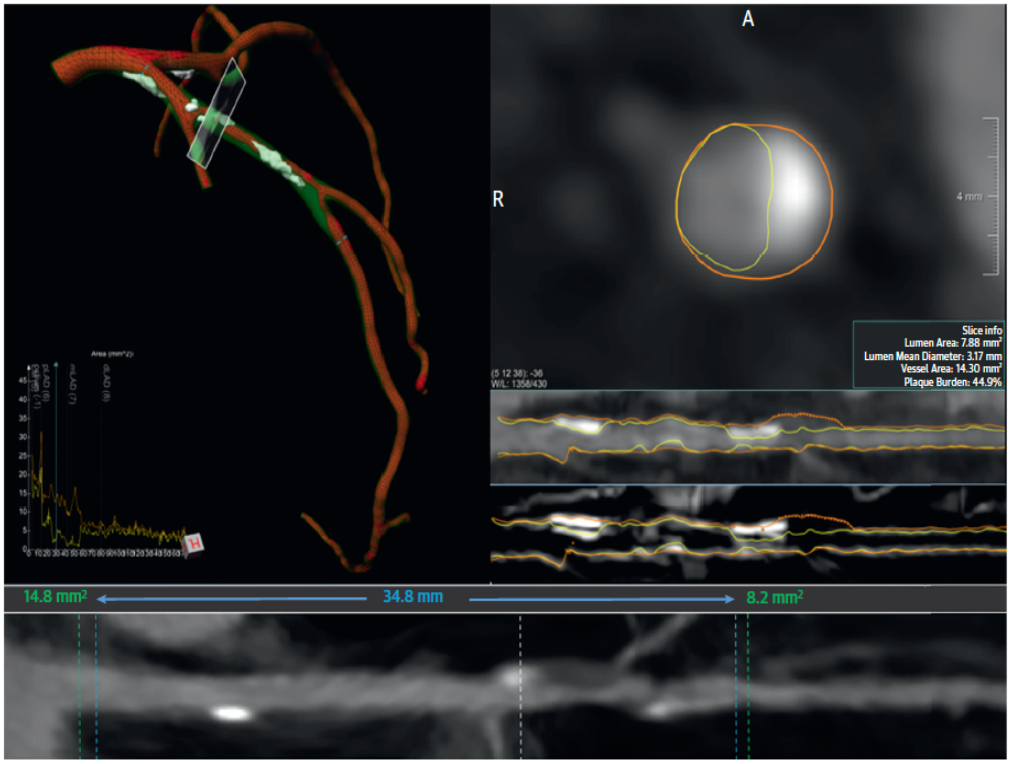

(Top left) A 3D reconstruction of a coronary lesion located in the proximal segment of the left anterior descending artery is shown. **(Top right)** A tomographic cross-section at the level of the marker **(dashed white line)** is shown. **(Bottom)** A straight multiplanar reconstruction is shown including the measurement tool and selection of the landing zones and lesion length. Images were created using Prototype CT Workbench for Cath Lab (3D Workbench, Medis Medical Imaging Systems).

technique using a retrograde approach can be selected (34). Beyond CTOs, in other challenging lesion subsets such as left main disease, ostial lesions, bifurcations, or severely calcified coronary vessels, CCTA can inform upfront on the best strategy and the need for dedicated devices to increase the likelihood of success.

ONLINE PROCEDURAL AND PCI GUIDANCE. The visualization of the coronary circulation derived from CCTA provides a 3D view of the coronary tree and the plaque component during conventional angiography procedures. Both lumen and atherosclerotic plaques are reconstructed using dedicated software (QAngioCT RE/3D Workbench, Medis Medical Imaging Systems, Leiden, the Netherlands) and projected side by side with the 2D invasive angiography. To facilitate online interpretation, plaques components are color-coded based on their HU. The process of coronary vessel reconstruction is shown in Figure 2. During the diagnostic procedure, the right and left coronary arteries are displayed sequentially in coordination with the invasive catheterization (Video 1). The movement of the C-arm is tracked in real time to synchronize the orientation of the 3D coronary tree with the projection of the fluoroscopic C-arm. A manufacturer-independent approach was accomplished by attaching an external sensor, called an inertial measurement unit to the C-arm. The inertial measurement unit is connected to a Raspberry Pi, which continuously communicates the sensor's—and therefore also the C-arm's—orientation with the 3D visualization software (Figure 3) (35).

During the procedure, the coronary anatomy derived from CCTA is continuously projected during changes in angiographic projections. At each projection, it is possible to assess the degree of overlapping and foreshortening without additional radiation or contrast. Figure 4 shows a case example on the impact

FIGURE 6 Atherosclerotic Disease in Apparently Normal Angiographic Vessel

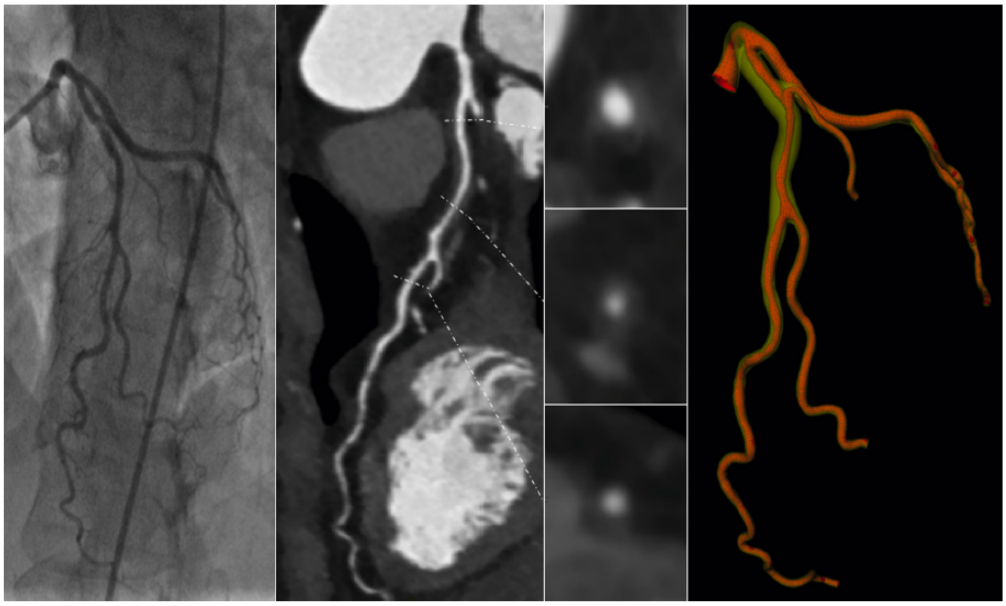

(Far left) Conventional angiography shows mild disease in the proximal and mid LAD. **(Center left)** Multiplanar reconstruction image is shown of a left anterior descending artery (LAD) with a long noncalcified plaque from the ostial LAD until the takeoff the second diagonal branch. **(Center right)** The cross-sections show positive remodeling and plaque burden of 80%. **(Far right)** colored-coded 3D reconstruction of lumen and plaque depicting the burden and extension of the plaque. The online co-registrationf coronary computed tomography angiography and angiography triggered a further invasive functional evaluation of the vessel resulting in an invasive fractional flow reserve of 0.76 (not shown).

of patient-specific projection on lesion length assessment. Tailored angulations optimize lesion evaluation and prevent unnecessary angiographic acquisitions. Furthermore, the 3D CCTA model can be used as a 3D roadmap to assist during vessel wiring, further reducing the need for additional contrast injection while the wire is advanced.

Guidance of PCI with CCTA follows the same principles as with intravascular imaging (e.g., IVUS or OCT) (24). Pre-procedural assessment starts with the evaluation of plaque characteristics, composition, and extension. Lesion length is determined based on healthy landing zones proximal and distal to the lesion (Figure 5). The continuous display of CCTA and invasive angiography allows also the use of anatomic landmarks to visually co-register both modalities.

CLINICAL IMPLICATIONS. CCTA is emerging as the preferred method for noninvasive assessment of CAD. Consequently, the number of patients referred for an invasive angiography with a CCTA is expected to increase (36). Clinical decision based on the morphological and functional component may translate to better selection of patients for percutaneous revascularization in a fashion similar to the way CTA has been used to better inform and plan structural heart disease interventions. Likewise, a pre-procedural stratification of case complexity may help to better organize time slots and personnel and, in this way, improve the cath lab workflow, efficiency, and resource use.

The integration of CCTA images in the cath lab is also likely to improve the safety of the procedure in terms of radiation dose and contrast volume. Moreover, the visualization of atherosclerotic disease in apparently normal or mild disease angiographic segments might increase the use of invasive functional and imaging assessment (Figure 6). Altogether, the integration of CCTA in the cath lab has the potential to improve the diagnostic performance of conventional angiography and patient management.

During PCI, CCTA provides a "live" IVUS-like imaging of the atherosclerotic plaque. The optimization of the angiographic information with plaque visualization is likely to be translated into improved PCI technique with complete plaque coverage and might improve clinical outcomes after PCI. Nonetheless, it

should be highlighted that after stent implantation, IVUS or OCT are the preferred methods to assess stent expansion and apposition.

FUTURE PERSPECTIVES

The integration of CCTA inside the cath lab represents a novel approach for the evaluation of CAD. Dedicated software has been developed that aims to simplify procedural workflow (Figure 5). This novel software solution simulates intravascular imaging tools that may facilitate adoption and image interpretation by interventionists. The Precise Procedure and PCI Planning and Guidance (P4) study will compare CT- versus IVUS-guided PCI, and the results of this study will set the foundation for the integration of CCTA in the routine of coronary interventions.

In the future, software that enables online coregistration and simulates cardiac cycle movement can further expand the synergism between these 2 techniques. Procedural planning of coronary procedures is likely to become an integral part of the percutaneous treatment of patients with CAD because most of the patients referred for invasive catheterization are evaluated with CCTA in the diagnostic phase. In the next decade, the interpretation of CCTA should become a core competency of interventional cardiologists. This would require a new training pathway focused on the guidance of coronary interventions.

CONCLUSIONS

CCTA has become the method of choice for the evaluation of CAD. Beyond the diagnostic phase, CCTA can be used to improve patient selection for PCI and to plan and guide therapeutic interventions in a fashion similar to structural heart interventions. CCTA adds 3Ds to conventional angiography and incorporates the visualization of atherosclerotic plaque in the entire coronary tree. This novel approach has the potential to enhance invasive procedures and improve clinical outcomes.

HIGHLIGHTS

- The role of CCTA for the diagnosis and stratification of CAD is well established; however, its usefulness beyond the diagnostic phase remains to be determined.
- For patients referred to the cath lab, CCTA aids evaluating the likelihood of functional revascularization, adapting the cath lab resources to the case complexity, complementing conventional angiography based on the information of 3-dimensional model and by online real-time integration of CCTA data in the cath lab.
- Online CT-guidance for coronary procedures has the potential to improve diagnostic and therapeutic intervention.
- The clinical benefit of this CT-guided PCI warrants demonstration is a randomized trial.

ACKNOWLEDGMENT The authors would like to thank Dr. Sakura Naguno for her assistance in the preparation of this manuscript.

AUTHOR DISCLOSURES

Dr. Collet has received research grants from Biosensors, Heart Flow Inc., and Abbott Vascular; and consultancy fees from Opsens, Boston Scientific, HeartFlow Inc., and Philips Volcano. Dr. Sonck has received research grants provided by the Cardiopath PhD program. Dr. Kitslaar is an employee of Medis Medical Imaging Systems. Dr. De Bruyne has received institutional consultancy fees and/or research grants from Abbott, Boston Scientific, and Biotronic. All other authors have reported that they have no relationships relevant to the contents of this paper to disclose.

ADDRESS FOR CORRESPONDENCE: Dr. Carlos Collet, Cardiovascular Center Aalst, Onze Lieve Vrouw Hospital, Moorselbaan 164, Aalst 9300, Belgium. E-mail: Carloscollett@gmail.com.

REFERENCES

1. Motoyama S, Sarai M, Harigaya H, et al. Computed tomographic angiography characteristics of atherosclerotic plaques subsequently resulting in acute coronary syndrome. J Am Coll Cardiol 2009;54:49-57.

2. Newby DE, Adamson PD, Berry C, et al., for the SCOT-HEART Investigators. Coronary CT angiography and 5-year risk of myocardial infarction. N Engl J Med 2018;379:924-33.

3. Taylor CA, Fonte TA, Min JK. Computational fluid dynamics applied to cardiac computed tomography for noninvasive quantification of fractional flow reserve: scientific basis. J Am Coll Cardiol 2013;61:2233-41.

4. Norgaard BL, Leipsic J, Gaur S, et al., for the NXT Trial Study Group. Diagnostic performance of noninvasive fractional flow reserve derived from coronary computed tomography angiography in suspected coronary artery disease: the NXT trial (Analysis of Coronary Blood Flow Using CT Angiography: Next Steps). J Am Coll Cardiol 2014;63:1145-55.

5. Mizukami T, Tanaka K, Sonck J, et al. Evaluation of epicardial coronary resistance using computed tomography angiography: a proof concept. J Cardiovasc Comput Tomogr 2020;14:177–84.

6. Collet C, Katagiri Y, Miyazaki Y, et al. Impact of coronary remodeling on fractional flow reserve. Circulation 2018;137:747–9.

7. Knuuti J, Wijns W, Saraste A, et al. 2019 ESC guidelines for the diagnosis and management of chronic coronary syndromes. Eur Heart J 2020;41:407–77.

8. Collet C, Grundeken MJ, Asano T, Onuma Y, Wijns W, Serruys PW. State of the art: coronary angiography. EuroIntervention 2017;13:634–43.

9. Collet C, Onuma Y, Cavalcante R, et al. Quantitative angiography methods for bifurcation lesions: a consensus statement update from the European Bifurcation Club. EuroIntervention 2017;13:115–23.

10. Campbell PT, Mahmud E, Marshall JJ. Interoperator and intraoperator (in)accuracy of stent selection based on visual estimation. Catheter Cardiovasc Interv 2015;86:1177–83.

11. Collet C, Onuma Y, Grundeken MJ, et al. In vitro validation of coronary CT angiography for the evaluation of complex lesions. EuroIntervention 2018;13:e1823–30.

12. Collet C, Chevalier B, Cequier A, et al. Diagnostic accuracy of coronary CT angiography for the evaluation of bioresorbable vascular scaffolds. J Am Coll Cardiol Img 2018;11:722–32.

13. Conte E, Mushtaq S, Pontone G, et al. Plaque quantification by coronary computed tomography angiography using intravascular ultrasound as a reference standard: a comparison between standard and last generation computed tomography scanners. Eur Heart J Cardiovasc Imaging 2020;21:191–201.

14. van Rosendael AR, Al'Aref SJ, Dwivedi A, et al. Quantitative evaluation of high-risk coronary plaque by coronary CTA and subsequent acute coronary events. J Am Coll Cardiol Img 2019;12:1568–71.

15. Dettmer M, Glaser-Gallion N, Stolzmann P, et al. Quantification of coronary artery stenosis with high-resolution CT in comparison with histopathology in an ex vivo study. Eur J Radiol 2013;82:264–9.

16. Genereux P, Madhavan MV, Mintz GS, et al. Ischemic outcomes after coronary intervention of calcified vessels in acute coronary syndromes: pooled analysis from the HORIZONS-AMI (Harmonizing Outcomes With Revascularization and Stents in Acute Myocardial Infarction) and ACUITY (Acute Catheterization and Urgent Intervention Triage Strategy) trials. J Am Coll Cardiol 2014;63:1845–54.

17. Fujino A, Mintz GS, Matsumura M, et al. A new optical coherence tomography-based calcium scoring system to predict stent underexpansion. EuroIntervention 2018;13:e2182–9.

18. Ali ZA, Brinton TJ, Hill JM, et al. Optical coherence tomography characterization of coronary lithoplasty for treatment of calcified lesions: first description. J Am Coll Cardiol Img 2017;10:897–906.

19. Fujino A, Mintz GS, Lee T, et al. Predictors of calcium fracture derived from balloon angioplasty and its effect on stent expansion assessed by optical coherence tomography. J Am Coll Cardiol Intv 2018;11:1015–7.

20. Kobayashi N, Ito Y, Yamawaki M, et al. Optical frequency-domain imaging findings to predict good stent expansion after rotational atherectomy for severely calcified coronary lesions. Int J Cardiovasc Imaging 2018;34:867–74.

21. Uetani T, Amano T, Kunimura A, et al. The association between plaque characterization by CT angiography and post-procedural myocardial infarction in patients with elective stent implantation. J Am Coll Cardiol Imaging 2010;3:19–28.

22. Williams MC, Kwiecinski J, Doris M, et al. Low-attenuation noncalcified plaque on coronary computed tomography angiography predicts myocardial infarction: results from the multicenter SCOT-HEART trial (Scottish Computed Tomography of the HEART). Circulation 2020;141:1452–62.

23. Gaur S, Øvrehus KA, Dey D, et al. Coronary plaque quantification and fractional flow reserve by coronary computed tomography angiography identify ischaemia-causing lesions. Eur Heart J 2016;37:1220–7.

24. Maehara A, Matsumura M, Ali ZA, Mintz GS, Stone GW. IVUS-guided versus OCT-guided coronary stent implantation: a critical appraisal. J Am Coll Cardiol Img 2017;10:1487–503.

25. Sand NPR, Veien KT, Nielsen SS, et al. Prospective comparison of FFR derived from coronary CT angiography with SPECT perfusion imaging in stable coronary artery disease: the ReASSESS study. J Am Coll Cardiol Img 2018;11:1640–50.

26. Driessen RS, Danad I, Stuijfzand WJ, et al. Comparison of coronary computed tomography angiography, fractional flow reserve, and perfusion imaging for ischemia diagnosis. J Am Coll Cardiol 2019;73:161–73.

27. Collet C, Sonck J, Vandeloo B, et al. Measurement of hyperemic pullback pressure gradients to characterize patterns of coronary atherosclerosis. J Am Coll Cardiol 2019;74:1772–84.

28. Fournier S, Ciccarelli G, Toth GG, et al. Association of improvement in fractional flow reserve with outcomes, including symptomatic relief, after percutaneous coronary intervention. JAMA Cardiol 2019;4:370–4.

29. Modi BN, Sankaran S, Kim HJ, et al. Predicting the physiological effect of revascularization in serially diseased coronary arteries. Circ Cardiovasc Interv 2019;12:e007577.

30. Grani C, Buechel RR, Kaufmann PA, Kwong RY. Multimodality imaging in individuals with anomalous coronary arteries. J Am Coll Cardiol Img 2017;10:471–81.

31. Mollet NR, Hoye A, Lemos PA, et al. Value of preprocedure multislice computed tomographic coronary angiography to predict the outcome of percutaneous recanalization of chronic total occlusions. Am J Cardiol 2005;95:240–3.

32. Fujino A, Otsuji S, Hasegawa K, et al. Accuracy of J-CTO score derived from computed tomography versus angiography to predict successful percutaneous coronary intervention. J Am Coll Cardiol Img 2018;11:209–17.

33. Opolski MP, Achenbach S, Schuhback A, et al. Coronary computed tomographic prediction rule for time-efficient guidewire crossing through chronic total occlusion: insights from the CT-RECTOR multicenter registry (Computed Tomography Registry of Chronic Total Occlusion Revascularization). J Am Coll Cardiol Intv 2015;8:257–67.

34. Opolski MP, Achenbach S. CT angiography for revascularization of CTO: crossing the borders of diagnosis and treatment. J Am Coll Cardiol Img 2015;8:846–58.

35. Wink O, Hecht HS, Ruijters D. Coronary computed tomographic angiography in the cardiac catheterization laboratory: current applications and future developments. Cardiol Clin 2009;27:513–29.

36. Moss AJ, Williams MC, Newby DE, Nicol ED. The updated NICE guidelines: cardiac CT as the first-line test for coronary artery disease. Curr Cardiovasc Imaging Rep 2017;10:15.

KEY WORDS cath lab, conventional angiography, coronary artery disease, CT-guided PCI

APPENDIX For a supplemental video, please see the online version of this paper.

Pre-procedural Planning of Coronary Revascularization by Cardiac-CT: An Expert Consensus Document of the SCCT

Extract of the expert consensus document on "Pre-procedural surgical planning of Coronary Revascularization by Cardiac-CT"

Although ICA is the preferred diagnostic method to guide the treatment decision between CABG and PCI, SYNTAX III Revolution trial has demonstrated the potential usefulness of CCTA in this clinical setting whereas the addition of a functional assessment by FFR_{CT} further refines treatment decision and planning prior to revascularization[82].

The identification of hemodynamic significance of a lesion and visualization of landing zone for the distal surgical anastomosis emerged as the two most important factor supporting the feasibility of this approach. CCTA identifies non-diseased target segments for grafting; in addition, it provides insights in the vessel course including an intra-myocardial coronary path, presence of coronary anomalies and target vessel size. In case of chronic coronary occlusions (CTO), assessment of the vessel distal to the occlusion proves usually feasible providing also information not always readily available with ICA, where only in case of well-developed collateral flow the course and size of the distal coronary bed is as evaluable. Moreover, the amount of subtended myocardium and identification of potential myocardial scar by CTTA and optional CTP can help omit futile grafting or optimize CABG strategies when limited grafting material is available.

CCTA 3D-volume rendering also facilitates the assessment of coronary anatomy. The course of and distance between the LAD and diagonal branches is relevant for planning of minimal invasive sequential MIDCAB LIMA-LAD or sequential bypass grafting. Furthermore, CCTA can also assess the anatomy, caliber and length of the left and right internal mammary artery grafts. The presence of disease in the ascending aorta may prompt alternative surgical techniques such as no-touch aorta technique with the potential to minimize cerebral embolization during surgery. Maximal Intensity Projection (MIP) are particularly useful for the evaluation of the aortic atherosclerosis patterns and calcification eventually changing cannulation or impacting the selection of a good location to sew the origin of the bypass graft.[136]

In patients referred to redo-CABG, CCTA informs about the distance between sternum and heart and warns about a potential pre-aortic graft path for sternotomy.
The role of CCTA to assess graft patency is well recognized. Future research should confirm if FFR_{CT}, providing not only a distal FFR_{CT} value but also insights in the endotype of CAD e.g. focal or diffuse CAD, could predict long-term graft patency comparable to invasive FFR or angiography-derived functional assessment.[137–139]

Bullet Points:
- Volume rendering and MIP reconstructions derived from CCTA may help cardiac surgeons in the planning of CABG procedure.
- The on-going multicenter FAST TRACK CABG study is aimed at assessing whether CCTA alone is able to support the cardiac surgeon in the procedural planning of CABG without information from invasive coronary angiography. [140,141]

Conclusion and future perspectives

Recently, the International Study of Comparative Health Effectiveness with Medical and Invasive Approaches – ISCHEMIA trial failed to show that routine invasive therapy was associated with a reduction in major adverse ischemic events compared with optimal medical therapy[142]. During the course of the trial, a quarter of initially conservatively managed patients crossed over to an invasive strategy. Moreover, notwithstanding fractional flow reserve is the gold standard for the assessment of lesion-specific ischemia, only one fifth of coronary lesions was interrogated by a pressure wire. As such, today the conundrum of an optimal treatment for ischemic heart disease remains intricate. In this thesis, we have aimed at improving current non-invasive and invasive strategies for ischemia-driven coronary treatment.

Beyond the confirmation of the presence of ischemia by pressure wire interrogation pre-PCI, assessing the longitudinal functional pattern of CAD is of utmost importance. Only focal CAD can be adequately addressed by PCI with the degree of improvement in coronary resistance reflected by the value of post-PCI FFR. Post-PCI FFR can be considered a metric of functional revascularization and represents a surrogate marker for vessel related adverse events. As shown in this thesis, post-PCI FFR, bearing a modest predictive value for adverse events, should be interpreted in a vessel-specific manner. Nevertheless, a higher post-PCI FFR reduces the probability of adverse events. As such, the mechanisms leading to low post-PCI FFR should be elucidated by pressure pullback pre-PCI to differentiate between focal jumps or diffuse residual pressure loss. The distribution of pressure losses represented on the pre-PCI pullback curve is likely to be the major determinant of post-PCI FFR. The here presented pullback pressure gradient (PPG) quantifies the FFR pullback curve and objectively and reproducibly provides a numeric expression of the endotype of coronary artery disease. Moreover, PPG has been shown to predict the degree of functional revascularization, bearing the potential to enhance patient selection for PCI and improve clinical outcomes. Indeed, higher PPG at baseline results in high post-PCI FFR. Patients with a high PPG are often free from angina after PCI, whereas PCI in patients with a low PPG results in lower post-PCI FFR and a higher rate of recurrent angina. It can be hypothesized that patients with a high PPG have a better clinical prognosis than patients with a low PPG. This hypothesis is being tested in the ongoing prospective evaluation of the impact of the PPG index on clinical decision-making and outcomes in the "PPG Global Registry" (NCT04789317). For this trial, the recently published adapted PPG formula for

manual pullbacks is being used. This manual pull back represents a drastic simplification of the method as compared to its initial description and validation and allows for an expanded use in routine daily catheterization laboratories FFR measurements.
Derived from the initial FFR pullbacks for PPG development, we have introduced another novel metric that quantifies the functional-anatomical mismatch (FAM) based on FFR pullbacks and quantitative coronary angiography (QCA) or optical coherence tomography (OCT). The discrimination between functional disease circumscribed within the anatomical defined lesion (i.e., FAM> 0), and (2) functional disease extending beyond the anatomical defined lesion (FAM < 0) also has the potential to enhance patient selection for PCI and to subsequently improve patient outcomes. This will warrant a dedicated trial.

Concurrently, the author of this thesis was involved in trials investigating the role of CCTA and additional FFR_{CT} for the diagnosis of CAD and for heart team decision-making in multivessel disease. Recent developments in the field of CCTA scans have enabled to accurately assess CAD on a plaque level. For a long time, patients with presumed calcific CAD were excluded for evaluation of atherosclerosis by CCTA. As shown in chapter 3 of this thesis, even in severely calcified CAD, CCTA remains precise to assess both lumen and coronary plaque composition and volume. Patients with coronary stents remain just about the only reason to move away from a CCTA as a first-line choice for the diagnosis of CAD. In these cases, CT perfusion proved an alternative approach significantly improving the diagnostic rate and accuracy of coronary CTA. Nowadays, FFR can be computed from CCTA images (FFR_{CT}) by performing blood flow simulations using computational fluid dynamics. Since the NXT trial in 2014, FFR_{CT} built a vast body of evidence with invasive FFR as a reference. In this thesis, we investigated the potential role of CT-derived FFR to evaluate the pattern of epicardial coronary resistance. It appeared feasible to derive accurate FFR_{CT} pullbacks for the evaluation of epicardial coronary resistance comparable to invasive FFR pullbacks. These FFR_{CT} pullbacks unmask physiological focal and diffuse CAD patterns. In addition, by virtual remodeling the lumen of the patient specific FFR_{CT} model, PCI could be mimicked enhancing treatment planning. In the presented Precise PCI Plan trial, the HeartFlow Planner has shown to accurately and precisely predict post-PCI FFR. The Planner appeared even to be most accurate in predicting the repercussions of PCI in diffuse CAD. Hence, the FFR_{CT} Planner may help clinicians better select patients to be referred to an invasive procedure, avoiding futile PCI and anticipating the benefit of an intervention. Randomized trials elucidating the role of PPG and FFR_{CT} Planner to improve outcomes are warranted.

Simultaneously, we developed a novel hardware and software solution to integrate the comprehensive CAD assessment by CCTA and FFR_{CT} in the diagnostic and therapeutic workflow of the invasive coronary angiography and percutaneous coronary interventions. We developed a three-dimensional, patient specific coronary tree reconstruction visualizing both lumen and color-coded atherosclerotic plaques maps. This coronary reconstruction is then synchronized with the C-arm of the catheterization lab using an inertial measurement unit connected to a Raspberry Pi. This enables the physician to identify normal coronary segments and guides a PCI procedure comparable to intra-vascular imaging guided PCI. Integrating the information on plaque components, FFR_{CT} and the HeartFlow Planner, a comprehensive PCI guidance is offered. The CT-guided PCI concept is going to be evaluated against a conventional IVUS-guided PCI in a non-inferiority outcomes trial: The Precise Procedural PCI Planning trial (P^4 trial). This approach could tailor the revascularization plan combining the best of both worlds: ischemia- and imaging-guided revascularization derived from non-invasive CCTA and FFR_{CT} available from the diagnostic work-up preceding the invasive coronary angiography and PCI.

In summary, this thesis provides insights into the patterns of epicardial atherosclerosis and introduces novel metrics and tools to identify which coronary lesion could benefit from percutaneous revascularization. This has broadened the current role of CCTA and FFR_{CT} from sole diagnosis of significant CAD to a tool for heart team decision making, detailed plaque characterization and treatment planning, including the non-invasive prediction of the outcome of invasive coronary revascularization. Simultaneously, in the catheterization laboratory, FFR pullbacks extended with pullback pressure gradient (PPG) or functional-anatomical mismatch (FAM) have expanded a single-point FFR measurement to a comprehensive functional evaluation of the pattern of CAD to tailor percutaneous revascularization procedures. These developments in ischemia-driven revascularization and its hybrid applications with intra-vascular imaging or CT-guided PCI have the potential to further improve clinical outcomes of patients suffering from coronary artery disease.

References:

1. Danad I, Szymonifka J, Twisk JWR, et al. Diagnostic performance of cardiac imaging methods to diagnose ischaemia-causing coronary artery disease when directly compared with fractional flow reserve as a reference standard: a meta-analysis. *Eur Heart J*. 2017;38(13):991-998. doi:10.1093/eurheartj/ehw095
2. Pijls NH, van Son JA, Kirkeeide RL, De Bruyne B, Gould KL. Experimental basis of determining maximum coronary, myocardial, and collateral blood flow by pressure measurements for assessing functional stenosis severity before and after percutaneous transluminal coronary angioplasty. *Circulation*. 1993;87(4):1354-1367. http://www.ncbi.nlm.nih.gov/pubmed/8462157. Accessed July 13, 2018.
3. Pijls NH, De Bruyne B, Peels K, et al. Measurement of fractional flow reserve to assess the functional severity of coronary-artery stenoses. *N Engl J Med*. 1996;334(26):1703-1708. doi:10.1056/NEJM199606273342604
4. De Bruyne B, Baudhuin T, Melin JA, et al. Coronary flow reserve calculated from pressure measurements in humans. Validation with positron emission tomography. *Circulation*. 1994;89(3):1013-1022. doi:10.1161/01.cir.89.3.1013
5. Bech GJ, De Bruyne B, Pijls NH, et al. Fractional flow reserve to determine the appropriateness of angioplasty in moderate coronary stenosis: a randomized trial. *Circulation*. 2001;103(24):2928-2934. doi:10.1161/01.cir.103.24.2928
6. De Bruyne B, Pijls NHJ, Kalesan B, et al. Fractional flow reserve-guided PCI versus medical therapy in stable coronary disease. *N Engl J Med*. 2012;367(11):991-1001. doi:10.1056/NEJMoa1205361
7. Xaplanteris P, Fournier S, Pijls NHJ, et al. Five-Year Outcomes with PCI Guided by Fractional Flow Reserve. *N Engl J Med*. 2018;379(3):250-259. doi:10.1056/NEJMoa1803538
8. Neumann FJ, Sechtem U, Banning AP, et al. 2019 ESC Guidelines for the diagnosis and management of chronic coronary syndromes. *Eur Heart J*. 2020;41(3):407-477. doi:10.1093/eurheartj/ehz425
9. Toth GG, Johnson NP, Jeremias A, et al. Standardization of Fractional Flow Reserve Measurements. *J Am Coll Cardiol*. 2016;68:742-753. doi:10.1016/j.jacc.2016.05.067
10. Gould KL. Pressure-flow characteristics of coronary stenoses in unsedated dogs at rest and during coronary vasodilation. *Circ Res*. 1978;43(2):242-253. doi:10.1161/01.res.43.2.242

11. De Bruyne B, Hersbach F, Pijls NH, et al. Abnormal epicardial coronary resistance in patients with diffuse atherosclerosis but "Normal" coronary angiography. *Circulation*. 2001;104(20):2401-2406. doi:10.1161/hc4501.099316
12. Ando H, Takashima H, Suzuki A, et al. Impact of lesion characteristics on the prediction of optimal poststent fractional flow reserve. *Am Heart J*. 2016;182:119-124. doi:10.1016/j.ahj.2016.09.015
13. Gould KL, Nakagawa Y, Nakagawa K, et al. Frequency and clinical implications of fluid dynamically significant diffuse coronary artery disease manifest as graded, longitudinal, base-to-apex myocardial perfusion abnormalities by noninvasive positron emission tomography. *Circulation*. 2000;101(16):1931-1939. doi:10.1161/01.cir.101.16.1931
14. Lee JM, Choi G, Koo B-K, et al. Identification of High-Risk Plaques Destined to Cause Acute Coronary Syndrome Using Coronary Computed Tomographic Angiography and Computational Fluid Dynamics. *JACC Cardiovasc Imaging*. 2019;12(6):1032-1043. doi:10.1016/j.jcmg.2018.01.023
15. Piroth Z, Toth GG, Tonino PAL, et al. Prognostic Value of Fractional Flow Reserve Measured Immediately After Drug-Eluting Stent Implantation. *Circ Cardiovasc Interv*. 2017;10(8):e005233. doi:10.1161/CIRCINTERVENTIONS.116.005233
16. Baranauskas A, Peace A, Kibarskis A, et al. FFR result post PCI is suboptimal in long diffuse coronary artery disease. *EuroIntervention*. 2016;12(12):1473-1480. doi:10.4244/EIJ-D-15-00514
17. Sianos G, Morel M-A, Kappetein AP, et al. The SYNTAX Score: an angiographic tool grading the complexity of coronary artery disease. *EuroIntervention*. 2005;1(2):219-227. http://www.ncbi.nlm.nih.gov/pubmed/19758907. Accessed August 21, 2021.
18. Shiono Y, Kubo T, Honda K, et al. Impact of functional focal versus diffuse coronary artery disease on bypass graft patency. *Int J Cardiol*. 2016;222:16-21. doi:10.1016/j.ijcard.2016.07.052
19. Zir LM, Miller SW, Dinsmore RE, Gilbert JP, Harthorne JW. Interobserver variability in coronary angiography. *Circulation*. 1976;53(4):627-632. doi:10.1161/01.cir.53.4.627
20. Mintz GS, Painter JA, Pichard AD, et al. Atherosclerosis in angiographically “normal” coronary artery reference segments: An intravascular ultrasound study with clinical correlations. *J Am Coll Cardiol*. 1995;25(7):1479-1485. doi:10.1016/0735-1097(95)00088-L

21. Layland J, Carrick D, Lee M, Oldroyd K, Berry C. Adenosine: physiology, pharmacology, and clinical applications. *JACC Cardiovasc Interv*. 2014;7(6):581-591. doi:10.1016/j.jcin.2014.02.009
22. Johnson NP, Johnson DT, Kirkeeide RL, et al. Repeatability of Fractional Flow Reserve Despite Variations in Systemic and Coronary Hemodynamics. *JACC Cardiovasc Interv*. 2015;8(8):1018-1027. doi:10.1016/j.jcin.2015.01.039
23. van der Voort PH, van Hagen E, Hendrix G, van Gelder B, Bech JW, Pijls NH. Comparison of intravenous adenosine to intracoronary papaverine for calculation of pressure-derived fractional flow reserve. *Cathet Cardiovasc Diagn*. 1996;39(2):120-125. doi:10.1002/(SICI)1097-0304(199610)39:2<120::AID-CCD3>3.0.CO;2-H
24. De Bruyne B, Pijls NHJ, Barbato E, et al. Intracoronary and intravenous adenosine 5'-triphosphate, adenosine, papaverine, and contrast medium to assess fractional flow reserve in humans. *Circulation*. 2003;107(14):1877-1883. doi:10.1161/01.CIR.0000061950.24940.88
25. Tonino PAL, De Bruyne B, Pijls NHJ, et al. Fractional Flow Reserve versus Angiography for Guiding Percutaneous Coronary Intervention. *N Engl J Med*. 2009;360(3):213-224. doi:10.1056/NEJMoa0807611
26. Toth G, Hamilos M, Pyxaras S, et al. Evolving concepts of angiogram: fractional flow reserve discordances in 4000 coronary stenoses. *Eur Heart J*. 2014;35(40):2831-2838. doi:10.1093/eurheartj/ehu094
27. Fournier S, Ciccarelli G, Toth GG, et al. Association of Improvement in Fractional Flow Reserve With Outcomes, Including Symptomatic Relief, After Percutaneous Coronary Intervention. *JAMA Cardiol*. 2019;4(4):370-374. doi:10.1001/jamacardio.2019.0175
28. Coronary CT Angiography and 5-Year Risk of Myocardial Infarction. *N Engl J Med*. 2018;379(10):924-933. doi:10.1056/nejmoa1805971
29. Scot-heart T. CT coronary angiography in patients with suspected angina due to coronary heart disease (SCOT-HEART): an open-label, parallel-group, multicentre trial. *Lancet*. 2015;385(9985):2383-2391. doi:10.1016/S0140-6736(15)60291-4
30. Min JK, Dunning A, Lin FY, et al. Age- and sex-related differences in all-cause mortality risk based on coronary computed tomography angiography findings results from the International Multicenter CONFIRM (Coronary CT Angiography Evaluation for Clinical Outcomes: An International Multicenter Registry) of 23,854 patients without known coronary artery disease. *J Am Coll Cardiol*. 2011;58(8):849-860.

doi:10.1016/j.jacc.2011.02.074

31. Andreini D, Pontone G, Mushtaq S, et al. A long-term prognostic value of coronary CT angiography in suspected coronary artery disease. *JACC Cardiovasc Imaging*. 2012;5(7):690-701. doi:10.1016/j.jcmg.2012.03.009
32. Conte E, Annoni A, Pontone G, et al. Evaluation of coronary plaque characteristics with coronary computed tomography angiography in patients with non-obstructive coronary artery disease: a long-term follow-up study. *Eur Hear journal Cardiovasc Imaging*. 2017;18(10):1170-1178. doi:10.1093/ehjci/jew200
33. Thomsen C, Abdulla J. Characteristics of high-risk coronary plaques identified by computed tomographic angiography and associated prognosis: a systematic review and meta-analysis. *Eur Hear journal Cardiovasc Imaging*. 2016;17(2):120-129. doi:10.1093/ehjci/jev325
34. Voros S, Rinehart S, Qian Z, et al. Coronary atherosclerosis imaging by coronary CT angiography: Current status, correlation with intravascular interrogation and meta-analysis. *JACC Cardiovasc Imaging*. 2011;4(5):537-548. doi:10.1016/j.jcmg.2011.03.006
35. Fischer C, Hulten E, Belur P, Smith R, Voros S, Villines TC. Coronary CT angiography versus intravascular ultrasound for estimation of coronary stenosis and atherosclerotic plaque burden: A meta-analysis. *J Cardiovasc Comput Tomogr*. 2013;7(4):256-266. doi:10.1016/j.jcct.2013.08.006
36. Norgaard BL, Leipsic J, Gaur S, et al. Diagnostic Performance of Noninvasive Fractional Flow Reserve Derived From Coronary Computed Tomography Angiography in Suspected Coronary Artery Disease The NXT Trial (Analysis of Coronary Blood Flow Using CT Angiography: Next Steps). *J Am Coll Cardiol*. 2014;63(12):1145-1155. doi:Doi 10.1016/J.Jacc.2013.11.043
37. Driessen RS, Danad I, Stuijfzand WJ, et al. Comparison of Coronary Computed Tomography Angiography, Fractional Flow Reserve, and Perfusion Imaging for Ischemia Diagnosis. *J Am Coll Cardiol*. 2019;73(2):161-173. doi:10.1016/j.jacc.2018.10.056
38. Taylor CA, Fonte TA, Min JK. Computational fluid dynamics applied to cardiac computed tomography for noninvasive quantification of fractional flow reserve: Scientific basis. *J Am Coll Cardiol*. 2013;61(22):2233-2241. doi:10.1016/j.jacc.2012.11.083

39. Sonck J, Miyazaki Y, Mandry D, Andreini D. Non-invasive planning of complex coronary artery disease using a novel Interactive Planner for PCI. *EuroIntervention*. October 2017. doi:10.4244/EIJ-D-17-00815
40. Modi BN, Sankaran S, Kim HJ, et al. Predicting the Physiological Effect of Revascularization in Serially Diseased Coronary Arteries. *Circ Cardiovasc Interv*. 2019;12(2):e007577. doi:10.1161/CIRCINTERVENTIONS.118.007577
41. Neumann FJ, Sousa-Uva M, Ahlsson A, et al. 2018 ESC/EACTS Guidelines on myocardial revascularization. *Eur Heart J*. 2019;40(2):87-165. doi:10.1093/eurheartj/ehy394
42. Knuuti J, Wijns W, Saraste A, et al. 2019 ESC Guidelines for the diagnosis and management of chronic coronary syndromes. *Eur Heart J*. 2020;41(3):407-477. doi:10.1093/eurheartj/ehz425
43. Kawashima H, Pompilio G, Andreini D, et al. Safety and feasibility evaluation of planning and execution of surgical revascularisation solely based on coronary CTA and FFRCT in patients with complex coronary artery disease: study protocol of the FASTTRACK CABG study. *BMJ Open*. 2020;10(12):e038152. doi:10.1136/bmjopen-2020-038152
44. Conte E, Annoni A, Pontone G, et al. Evaluation of coronary plaque characteristics with coronary computed tomography angiography in patients with non-obstructive coronary artery disease: A long-term follow-up study. *Eur Heart J Cardiovasc Imaging*. 2017;18(10):1170-1178. doi:10.1093/ehjci/jew200
45. Fujino A, Mintz GS, Matsumura M, et al. A new optical coherence tomography-based calcium scoring system to predict stent underexpansion. *EuroIntervention*. 2018;13(18):e2182-e2189. doi:10.4244/EIJ-D-17-00962
46. Driessen RS, Stuijfzand WJ, Raijmakers PG, et al. Effect of Plaque Burden and Morphology on Myocardial Blood Flow and Fractional Flow Reserve. *J Am Coll Cardiol*. 2018;71(5):499-509. doi:10.1016/j.jacc.2017.11.054
47. Motoyama S, Sarai M, Harigaya H, et al. Computed tomographic angiography characteristics of atherosclerotic plaques subsequently resulting in acute coronary syndrome. *J Am Coll Cardiol*. 2009;54(1):49-57. doi:10.1016/j.jacc.2009.02.068
48. Motoyama S, Ito H, Sarai M, et al. Plaque Characterization by Coronary Computed Tomography Angiography and the Likelihood of Acute Coronary Events in Mid-Term Follow-Up. *J Am Coll Cardiol*. 2015;66(4):337-346. doi:10.1016/j.jacc.2015.05.069

49. Otsuka K, Fukuda S, Tanaka A, et al. Napkin-ring sign on coronary CT angiography for the prediction of acute coronary syndrome. *JACC Cardiovasc Imaging*. 2013;6(4):448-457. doi:10.1016/j.jcmg.2012.09.016
50. Choi KH, Lee JM, Koo B-K, et al. Prognostic Implication of Functional Incomplete Revascularization and Residual Functional SYNTAX Score in Patients With Coronary Artery Disease. *JACC Cardiovasc Interv*. 2018;11(3):237-245. doi:10.1016/j.jcin.2017.09.009
51. Lee JM, Hwang D, Choi KH, et al. Prognostic Impact of Residual Anatomic Disease Burden After Functionally Complete Revascularization. *Circ Cardiovasc Interv*. 2020;13(9):e009232. doi:10.1161/CIRCINTERVENTIONS.120.009232
52. Lee JM, Hwang D, Choi KH, et al. Prognostic Implications of Relative Increase and Final Fractional Flow Reserve in Patients With Stent Implantation. *JACC Cardiovasc Interv*. 2018;11(20):2099-2109. doi:10.1016/j.jcin.2018.07.031
53. Kobayashi Y, Lønborg J, Jong A, et al. Prognostic Value of the Residual SYNTAX Score After Functionally Complete Revascularization in ACS. *J Am Coll Cardiol*. 2018;72(12):1321-1329. doi:10.1016/j.jacc.2018.06.069
54. Li S-J, Ge Z, Kan J, et al. Cutoff Value and Long-Term Prediction of Clinical Events by FFR Measured Immediately After Implantation of a Drug-Eluting Stent in Patients With Coronary Artery Disease: 1- to 3-Year Results From the DKCRUSH VII Registry Study. *JACC Cardiovasc Interv*. 2017;10(10):986-995. doi:10.1016/j.jcin.2017.02.012
55. Agarwal SK, Kasula S, Hacioglu Y, Ahmed Z, Uretsky BF, Hakeem A. Utilizing Post-Intervention Fractional Flow Reserve to Optimize Acute Results and the Relationship to Long-Term Outcomes. *JACC Cardiovasc Interv*. 2016;9(10):1022-1031. doi:10.1016/j.jcin.2016.01.046
56. Hwang D, Lee JM, Lee H-J, et al. Influence of target vessel on prognostic relevance of fractional flow reserve after coronary stenting. *EuroIntervention*. 2019;15(5):457-464. doi:10.4244/EIJ-D-18-00913
57. Maehara A, Matsumura M, Ali ZA, Mintz GS, Stone GW. IVUS-Guided Versus OCT-Guided Coronary Stent Implantation: A Critical Appraisal. *JACC Cardiovasc Imaging*. 2017;10(12):1487-1503. doi:10.1016/j.jcmg.2017.09.008
58. Min JK, Leipsic J, Pencina MJ, et al. Diagnostic Accuracy of Fractional Flow Reserve From Anatomic CT Angiography. *Jama*. 2012;308(12):1237. doi:10.1001/2012.jama.11274
59. Koo B, Erglis A, Doh J, et al. Diagnosis of Ischemia-Causing Coronary Stenoses by

Non-invasive Fractional Flow Reserve Computed From Coronary CT Angiograms: A Prospective Multicenter Study. *J Am Coll Cardiol*. 2011;58(19):1-23. doi:10.1016/j.jacc.2011.06.066

60. Meijboom WB, Van Mieghem CAG, van Pelt N, et al. Comprehensive assessment of coronary artery stenoses: computed tomography coronary angiography versus conventional coronary angiography and correlation with fractional flow reserve in patients with stable angina. *J Am Coll Cardiol*. 2008;52(8):636-643. doi:10.1016/j.jacc.2008.05.024
61. Hoffmann U, Ferencik M, Udelson JE, et al. Prognostic Value of Noninvasive Cardiovascular Testing in Patients with Stable Chest Pain: Insights from the PROMISE Trial (Prospective Multicenter Imaging Study for Evaluation of Chest Pain). *Circulation*. 2017;135(24):2320-2332. doi:10.1161/CIRCULATIONAHA.116.024360
62. Fairbairn TA, Nieman K, Akasaka T, et al. Real-world clinical utility and impact on clinical decision-making of coronary computed tomography angiography-derived fractional flow reserve: Lessons from the ADVANCE Registry. *Eur Heart J*. 2018;39(41):3701-3711. doi:10.1093/eurheartj/ehy530
63. Douglas PS, Pontone G, Hlatky MA, et al. Clinical outcomes of fractional flow reserve by computed tomographic angiography-guided diagnostic strategies vs. usual care in patients with suspected coronary artery disease: The prospective longitudinal trial of FFRCT: Outcome and resource impacts study. *Eur Heart J*. 2015;36(47):3359-3367. doi:10.1093/eurheartj/ehv444
64. Jensen JM, Bøtker HE, Mathiassen ON, et al. Computed tomography derived fractional flow reserve testing in stable patients with typical angina pectoris: Influence on downstream rate of invasive coronary angiography. *Eur Heart J Cardiovasc Imaging*. 2018;19(4):405-414. doi:10.1093/ehjci/jex068
65. De Araújo Gonçalves P, Rodríguez-Granillo GA, Spitzer E, et al. Functional evaluation of coronary disease by CT angiography. *JACC Cardiovasc Imaging*. 2015;8(11):1322-1335. doi:10.1016/j.jcmg.2015.09.003
66. Douglas PS, De Bruyne B, Pontone G, et al. 1-Year Outcomes of FFRCT-Guided Care in Patients With Suspected Coronary Disease: The PLATFORM Study. *J Am Coll Cardiol*. 2016;68(5):435-445. doi:10.1016/j.jacc.2016.05.057
67. Nørgaard BL, Terkelsen CJ, Mathiassen ON, et al. Coronary CT Angiographic and Flow Reserve-Guided Management of Patients With Stable Ischemic Heart Disease. *J Am Coll Cardiol*. 2018;72(18):2123-2134. doi:10.1016/j.jacc.2018.07.043

68. Patel MR, Nørgaard BL, Fairbairn TA, et al. 1-Year Impact on Medical Practice and Clinical Outcomes of FFRCT: The ADVANCE Registry. *JACC Cardiovasc Imaging*. 2020;13(1):97-105. doi:10.1016/j.jcmg.2019.03.003
69. Tesche C, Otani K, De Cecco CN, et al. Influence of Coronary Calcium on Diagnostic Performance of Machine Learning CT-FFR: Results From MACHINE Registry. *JACC Cardiovasc Imaging*. 2020;13(3):760-770. doi:10.1016/j.jcmg.2019.06.027
70. Ferencik M, Mayrhofer T, Bittner DO, et al. Use of high-risk coronary atherosclerotic plaque detection for risk stratification of patients with stable chest pain: A secondary analysis of the promise randomized clinical trial. *JAMA Cardiol*. 2018;3(2):144-152. doi:10.1001/jamacardio.2017.4973
71. Cury RC, Abbara S, Achenbach S, et al. CAD-RADS^{TM}: Coronary Artery Disease – Reporting and Data System: An Expert Consensus Document of the Society of Cardiovascular Computed Tomography (SCCT), the American College of Radiology (ACR) and the North American Society for Cardiovascular Imaging (NASCI). Endorsed by the American College of Cardiology. *J Am Coll Radiol*. 2016;13(12):1458-1466.e9. doi:10.1016/j.jacr.2016.04.024
72. Escaned J, Collet C, Ryan N, et al. Clinical outcomes of state-of-the-art percutaneous coronary revascularization in patients with de novo three vessel disease: 1-year results of the SYNTAX II study. *Eur Heart J*. 2017;38(42):3124-3134. doi:10.1093/eurheartj/ehx512
73. Nam CW, Mangiacapra F, Entjes R, et al. Functional SYNTAX score for risk assessment in multivessel coronary artery disease. *J Am Coll Cardiol*. 2011;58(12):1211-1218. doi:10.1016/j.jacc.2011.06.020
74. Yusuf S, Zucker D, Peduzzi P, et al. Effect of coronary artery bypass graft surgery on survival: overview of 10-year results from randomised trials by the Coronary Artery Bypass Graft Surgery Trialists Collaboration. *Lancet (London, England)*. 1994;344(8922):563-570. http://www.ncbi.nlm.nih.gov/pubmed/7914958. Accessed April 4, 2018.
75. Windecker S, Kolh P, Alfonso F, et al. 2014 ESC/EACTS Guidelines on myocardial revascularization: The Task Force on Myocardial Revascularization of the European Society of Cardiology (ESC) and the European Association for Cardio-Thoracic Surgery (EACTS)Developed with the special contribution of the European Association of Percutaneous Cardiovascular Interventions (EAPCI). *Eur Heart J*. 2014;35(37):2541-2619. doi:10.1093/eurheartj/ehu278

76. Miller JM, Rochitte CE, Dewey M, et al. Diagnostic Performance of Coronary Angiography by 64-Row CT. *N Engl J Med*. 2008;359(22):2324-2336. doi:10.1056/nejmoa0806576
77. Papadopoulou SL, Girasis C, Dharampal A, et al. CT-SYNTAX score: A feasibility and reproducibility study. *JACC Cardiovasc Imaging*. 2013;6(3):413-415. doi:10.1016/j.jcmg.2012.09.013
78. Farooq V, Van Klaveren D, Steyerberg EW, et al. Anatomical and clinical characteristics to guide decision making between coronary artery bypass surgery and percutaneous coronary intervention for individual patients: Development and validation of SYNTAX score II. *Lancet*. 2013;381(9867):639-650. doi:10.1016/S0140-6736(13)60108-7
79. Cavalcante R, Sotomi Y, Lee CW, et al. Outcomes After Percutaneous Coronary Intervention or Bypass Surgery in Patients With Unprotected Left Main Disease. *J Am Coll Cardiol*. 2016;68(10):999-1009. doi:10.1016/j.jacc.2016.06.024
80. Collet C, Miyazaki Y, Ryan N, et al. Fractional Flow Reserve Derived From Computed Tomographic Angiography in Patients With Multivessel CAD. *J Am Coll Cardiol*. May 2018. doi:10.1016/j.jacc.2018.02.053
81. Cavalcante R, Onuma Y, Sotomi Y, et al. Non-invasive Heart Team assessment of multivessel coronary disease with coronary computed tomography angiography based on SYNTAX score II treatment recommendations: design and rationale of the randomised SYNTAX III Revolution trial. *EuroIntervention*. 2017;12(16):2001-2008. doi:10.4244/EIJ-D-16-00612
82. Collet C, Onuma Y, Andreini D, et al. Coronary computed tomography angiography for heart team decision-making in multivessel coronary artery disease. *Eur Heart J*. October 2018. doi:10.1093/eurheartj/ehy581
83. Farooq V, van Klaveren D, Steyerberg EW, et al. Anatomical and clinical characteristics to guide decision making between coronary artery bypass surgery and percutaneous coronary intervention for individual patients: development and validation of SYNTAX score II. *Lancet (London, England)*. 2013;381(9867):639-650. doi:10.1016/S0140-6736(13)60108-7
84. Mehanna E, Bezerra HG, Prabhu D, et al. Volumetric characterization of human coronary calcification by frequency-domain optical coherence tomography. *Circ J*. 2013;77(9):2334-2340. doi:10.1253/circj.CJ-12-1458

85. Généreux P, Madhavan M V., Mintz GS, et al. Ischemic outcomes after coronary intervention of calcified vessels in acute coronary syndromes: Pooled analysis from the HORIZONS-AMI (Harmonizing Outcomes with Revascularization and Stents in Acute Myocardial Infarction) and ACUITY (Acute Catheterization and Urgent Intervention Triage Strategy) trials. *J Am Coll Cardiol*. 2014;63(18):1845-1854. doi:10.1016/j.jacc.2014.01.034
86. Kobayashi Y, Okura H, Kume T, et al. Impact of target lesion coronary calcification on stent expansion – An optical coherence tomography study –. *Circ J*. 2014;78(9):2209-2214. doi:10.1253/circj.CJ-14-0108
87. Bourantas C V., Zhang YJ, Garg S, et al. Prognostic implications of coronary calcification in patients with obstructive coronary artery disease treated by percutaneous coronary intervention: A patient-level pooled analysis of 7 contemporary stent trials. *Heart*. 2014;100(15):1158-1164. doi:10.1136/heartjnl-2013-305180
88. Kumbhani DJ, Ingelmo CP, Schoenhagen P, Curtin RJ, Flamm SD, Desai MY. Meta-analysis of diagnostic efficacy of 64-slice computed tomography in the evaluation of coronary in-stent restenosis. *Am J Cardiol*. 2009;103(12):1675-1681. doi:10.1016/j.amjcard.2009.02.024
89. Andreini D, Pontone G, Mushtaq S, Pepi M, Bartorelli AL. Multidetector computed tomography coronary angiography for the assessment of coronary in-stent restenosis. *Am J Cardiol*. 2010;105(5):645-655. doi:10.1016/j.amjcard.2009.10.046
90. Tu S, Barbato E, Köszegi Z, et al. Fractional flow reserve calculation from 3-dimensional quantitative coronary angiography and TIMI frame count: A fast computer model to quantify the functional significance of moderately obstructed coronary arteries. *JACC Cardiovasc Interv*. 2014;7(7):768-777. doi:10.1016/j.jcin.2014.03.004
91. Papafaklis MI, Muramatsu T, Ishibashi Y, et al. Fast virtual functional assessment of intermediate coronary lesions using routine angiographic data and blood flow simulation in humans: Comparison with pressure wire - fractional flow reserve. *EuroIntervention*. 2014;10(5):574-583. doi:10.4244/EIJY14M07_01
92. Asano T, Katagiri Y, Chang CC, et al. Angiography-Derived Fractional Flow Reserve in the SYNTAX II Trial: Feasibility, Diagnostic Performance of Quantitative Flow Ratio, and Clinical Prognostic Value of Functional SYNTAX Score Derived From Quantitative Flow Ratio in Patients With 3-Vessel Disease. *JACC Cardiovasc Interv*. 2019;12(3):259-270. doi:10.1016/j.jcin.2018.09.023

93. Bourassa MG, Enjalbert M, Campeau L, Lesperance J. Progression of atherosclerosis in coronary arteries and bypass grafts: ten years later. *Am J Cardiol*. 1984;53(12):102C-107C. doi:10.1016/0002-9149(84)90759-8
94. Manninen HI, Jaakkola P, Suhonen M, Rehnberg S, Vuorenniemi R, Matsi PJ. Angiographic predictors of graft patency and disease progression after coronary artery bypass grafting with arterial and venous grafts. *Ann Thorac Surg*. 1998;66(4):1289-1294. doi:10.1016/s0003-4975(98)00757-7
95. Mehra MR, Crespo-Leiro MG, Dipchand A, et al. International Society for Heart and Lung Transplantation working formulation of a standardized nomenclature for cardiac allograft vasculopathy-2010. *J Heart Lung Transplant*. 2010;29(7):717-727. doi:10.1016/j.healun.2010.05.017
96. Lee JM, Choi G, Koo B-K, et al. Identification of High-Risk Plaques Destined to Cause Acute Coronary Syndrome Using Coronary Computed Tomographic Angiography and Computational Fluid Dynamics. *JACC Cardiovasc Imaging*. March 2018. doi:10.1016/j.jcmg.2018.01.023
97. Andreini D, Pontone G, Mushtaq S, et al. Atrial fibrillation: Diagnostic accuracy of coronary CT angiography performed with a whole-heart 230-μm spatial resolution CT scanner. *Radiology*. 2017;284(3):676-684. doi:10.1148/radiol.2017161779
98. Pontone G, Andreini D, Guaricci AI, et al. Incremental Diagnostic Value of Stress Computed Tomography Myocardial Perfusion With Whole-Heart Coverage CT Scanner in Intermediate- to High-Risk Symptomatic Patients Suspected of Coronary Artery Disease. *JACC Cardiovasc Imaging*. 2019;12(2):338-349. doi:10.1016/j.jcmg.2017.10.025
99. George RT, Arbab-Zadeh A, Miller JM, et al. Computed tomography myocardial perfusion imaging with 320-row detector computed tomography accurately detects myocardial ischemia in patients with obstructive coronary artery disease. *Circ Cardiovasc Imaging*. 2012;5(3):333-340. doi:10.1161/CIRCIMAGING.111.969303
100. Kim SM, Chang S-A, Shin W, Choe YH. Dual-energy CT perfusion during pharmacologic stress for the assessment of myocardial perfusion defects using a second-generation dual-source CT: a comparison with cardiac magnetic resonance imaging. *J Comput Assist Tomogr*. 2014;38(1):44-52. doi:10.1097/RCT.0b013e3182a77626
101. Rossi A, Dharampal A, Wragg A, et al. Diagnostic performance of hyperaemic myocardial blood flow index obtained by dynamic computed tomography: does it

predict functionally significant coronary lesions? *Eur Hear journal Cardiovasc Imaging*. 2014;15(1):85-94. doi:10.1093/ehjci/jet133

102. Rief M, Zimmermann E, Stenzel F, et al. Computed tomography angiography and myocardial computed tomography perfusion in patients with coronary stents: Prospective intraindividual comparison with conventional coronary angiography. *J Am Coll Cardiol*. 2013;62(16):1476-1485. doi:10.1016/j.jacc.2013.03.088
103. Carrabba N, Schuijf JD, De Graaf FR, et al. Diagnostic accuracy of 64-slice computed tomography coronary angiography for the detection of in-stent restenosis: A meta-analysis. *J Nucl Cardiol*. 2010;17(3):470-478. doi:10.1007/s12350-010-9218-2
104. Greif M, Von Ziegler F, Bamberg F, et al. CT stress perfusion imaging for detection of haemodynamically relevant coronary stenosis as defined by FFR. *Heart*. 2013;99(14):1004-1011. doi:10.1136/heartjnl-2013-303794
105. Tonino PAL, De Bruyne B, Pijls NHJ, et al. Fractional flow reserve versus angiography for guiding percutaneous coronary intervention. *N Engl J Med*. 2009;360(3):213-224. doi:10.1056/NEJMoa0807611
106. Park S-J, Kang S-J, Ahn J-M, et al. Visual-functional mismatch between coronary angiography and fractional flow reserve. *JACC Cardiovasc Interv*. 2012;5(10):1029-1036. doi:10.1016/j.jcin.2012.07.007
107. Windecker S, Kolh P, Alfonso F, et al. 2014 ESC/EACTS Guidelines on myocardial revascularization. *EuroIntervention*. 2015;10(9):1024-1094. doi:10.4244/EIJY14M09_01
108. Fitzgibbon GM, Kafka HP, Leach AJ, Keon WJ, Hooper GD, Burton JR. Coronary bypass graft fate and patient outcome: angiographic follow-up of 5,065 grafts related to survival and reoperation in 1,388 patients during 25 years. *J Am Coll Cardiol*. 1996;28(3):616-626. http://www.ncbi.nlm.nih.gov/pubmed/8772748. Accessed March 19, 2016.
109. Sabik JF, Lytle BW, Blackstone EH, Houghtaling PL, Cosgrove DM. Comparison of saphenous vein and internal thoracic artery graft patency by coronary system. *Ann Thorac Surg*. 2005;79(2):544-551; discussion 544-51. doi:10.1016/j.athoracsur.2004.07.047
110. Berger PB, Alderman EL, Nadel A, Schaff H V. Frequency of early occlusion and stenosis in a left internal mammary artery to left anterior descending artery bypass graft after surgery through a median sternotomy on conventional bypass: benchmark for minimally invasive direct coronary artery bypass. *Circulation*. 1999;100(23):2353-

2358. http://www.ncbi.nlm.nih.gov/pubmed/10587340. Accessed June 2, 2016.

111. Nasu M, Akasaka T, Okazaki T, et al. Postoperative flow characteristics of left internal thoracic artery grafts. *Ann Thorac Surg*. 1995;59(1):154-162. doi:10.1016/0003-4975(94)00795-9

112. Sabik JF, Lytle BW, Blackstone EH, et al. Does Competitive Flow Reduce Internal Thoracic Artery Graft Patency? *Ann Thorac Surg*. 2003;76(5):1490-1497. doi:10.1016/S0003-4975(03)01022-1

113. Collet C, Onuma Y, Sonck J, et al. Diagnostic performance of angiography-derived fractional flow reserve: A systematic review and Bayesian meta-analysis. *Eur Heart J*. 2018;39(35):3314-3321. doi:10.1093/eurheartj/ehy445

114. Collet C, Katagiri Y, Miyazaki Y, et al. Impact of Coronary Remodeling on Fractional Flow Reserve. *Circulation*. 2018;137(7):747-749. doi:10.1161/CIRCULATIONAHA.117.031478

115. Pijls NH, van Son JA, Kirkeeide RL, De Bruyne B, Gould KL. Experimental basis of determining maximum coronary, myocardial, and collateral blood flow by pressure measurements for assessing functional stenosis severity before and after percutaneous transluminal coronary angioplasty. *Circulation*. 1993;87(4):1354-1367. doi:10.1161/01.cir.87.4.1354

116. Pijls NHJ, Klauss V, Siebert U, et al. Coronary pressure measurement after stenting predicts adverse events at follow-up: a multicenter registry. *Circulation*. 2002;105(25):2950-2954. http://www.ncbi.nlm.nih.gov/pubmed/12081986. Accessed August 17, 2016.

117. Hakeem A, Uretsky BF. Role of Postintervention Fractional Flow Reserve to Improve Procedural and Clinical Outcomes. *Circulation*. 2019;139(5):694-706. doi:10.1161/CIRCULATIONAHA.118.035837

118. Glagov S, Weisenberg E, Zarins CK, Stankunavicius R, Kolettis GJ. Compensatory enlargement of human atherosclerotic coronary arteries. *N Engl J Med*. 1987;316(22):1371-1375. doi:10.1056/NEJM198705283162204

119. Sipahi I, Tuzcu EM, Schoenhagen P, et al. Paradoxical increase in lumen size during progression of coronary atherosclerosis: observations from the REVERSAL trial. *Atherosclerosis*. 2006;189(1):229-235. doi:10.1016/j.atherosclerosis.2005.12.006

120. Papadopoulou S-L, Neefjes LA, Garcia-Garcia HM, et al. Natural history of coronary atherosclerosis by multislice computed tomography. *JACC Cardiovasc Imaging*. 2012;5(3 Suppl):S28-37. doi:10.1016/j.jcmg.2012.01.009

121. Serruys PW, Girasis C, Papadopoulou S-L, Onuma Y. Non-invasive fractional flow reserve: scientific basis, methods and perspectives. *EuroIntervention*. 2012;8(4):511-519. doi:10.4244/EIJV8I4A79
122. Collet C, Katagiri Y, Miyazaki Y, et al. Impact of coronary remodeling on fractional flow reserve. *Circulation*. 2018;137(7). doi:10.1161/CIRCULATIONAHA.117.031478
123. Collet C, Sonck J, Vandeloo B, et al. Measurement of Hyperemic Pullback Pressure Gradients to Characterize Patterns of Coronary Atherosclerosis. *J Am Coll Cardiol*. 2019;74(14):1772-1784. doi:10.1016/j.jacc.2019.07.072
124. Wilson RF, White CW. Intracoronary papaverine: an ideal coronary vasodilator for studies of the coronary circulation in conscious humans. *Circulation*. 1986;73(3):444-451. doi:10.1161/01.cir.73.3.444
125. De Bruyne B, Pijls NHJ, Barbato E, et al. Intracoronary and intravenous adenosine 5'-triphosphate, adenosine, papaverine, and contrast medium to assess fractional flow reserve in humans. *Circulation*. 2003;107(14):1877-1883. doi:10.1161/01.CIR.0000061950.24940.88
126. Okabe Y, Otowa K, Mitamura Y, et al. Evaluation of the risk factors for ventricular arrhythmias secondary to QT prolongation induced by papaverine injection during coronary flow reserve studies using a 4 Fr angio-catheter. *Heart Vessels*. 2018;33(11):1358-1364. doi:10.1007/s00380-018-1175-8
127. Collet C, Onuma Y, Grundeken M, et al. In vitro validation of coronary CT angiography for the evaluation of complex lesions. *EuroIntervention*. 2018;13(15):e1823-e1830. doi:10.4244/EIJ-D-17-00326
128. Collet C, Chevalier B, Cequier A, et al. Diagnostic Accuracy of Coronary CT Angiography for the Evaluation of Bioresorbable Vascular Scaffolds. *JACC Cardiovasc Imaging*. 2018;11(5):722-732. doi:10.1016/j.jcmg.2017.04.013
129. Gaur S, Øvrehus KA, Dey D, et al. Coronary plaque quantification and fractional flow reserve by coronary computed tomography angiography identify ischaemia-causing lesions. *Eur Heart J*. 2016;37(15):1220-1227. doi:10.1093/eurheartj/ehv690
130. Maehara A, Matsumura M, Ali ZA, Mintz GS, Stone GW. IVUS-Guided Versus OCT-Guided Coronary Stent Implantation: A Critical Appraisal. *JACC Cardiovasc Imaging*. 2017;10(12):1487-1503. doi:10.1016/j.jcmg.2017.09.008
131. Collet C, Miyazaki Y, Ryan N, et al. Fractional Flow Reserve Derived From Computed Tomographic Angiography in Patients With Multivessel CAD. *J Am Coll Cardiol*. 2018. doi:10.1016/j.jacc.2018.02.053

132. Mizukami T, Tanaka K, Sonck J, et al. Evaluation of epicardial coronary resistance using computed tomography angiography: A Proof Concept. *J Cardiovasc Comput Tomogr*. September 2019. doi:10.1016/j.jcct.2019.09.004
133. Opolski MP, Achenbach S, Schuhbäck A, et al. Coronary computed tomographic prediction rule for time-efficient guidewire crossing through chronic total occlusion: Insights from the CT-RECTOR multicenter registry (computed tomography registry of chronic total occlusion revascularization). *JACC Cardiovasc Interv*. 2015;8(2):257-267. doi:10.1016/j.jcin.2014.07.031
134. Sheth T, Amlani S, Lou Ellins M, et al. Computed tomographic coronary angiographic assessment of high-risk coronary anatomy in patients with suspected coronary artery disease and intermediate pretest probability. *Am Heart J*. 2008;155(5):918-923. doi:10.1016/j.ahj.2007.11.035
135. Monizzi G, Sonck J, Nagumo S, et al. Quantification of calcium burden by coronary CT angiography compared to optical coherence tomography. *Int J Cardiovasc Imaging*. 2020;36(12). doi:10.1007/s10554-020-01839-z
136. Park K-H, Lee HY, Lim C, et al. Clinical impact of computerised tomographic angiography performed for preoperative evaluation before coronary artery bypass grafting. *Eur J Cardiothorac Surg*. 2010;37(6):1346-1352. doi:10.1016/j.ejcts.2009.12.040
137. Mizukami T, Tanaka K, Sonck J, et al. Evaluation of epicardial coronary resistance using computed tomography angiography: A Proof Concept. *J Cardiovasc Comput Tomogr*. September 2019. doi:10.1016/j.jcct.2019.09.004
138. Botman CJ, Schonberger J, Koolen S, et al. Does stenosis severity of native vessels influence bypass graft patency? A prospective fractional flow reserve-guided study. *Ann Thorac Surg*. 2007;83(6):2093-2097. doi:10.1016/j.athoracsur.2007.01.027
139. Gigante C, Mizukami T, Sonck J, et al. Graft patency and progression of coronary artery disease after CABG assessed by angiography-derived fractional flow reserve. *Int J Cardiol*. 2020;316:19-25. doi:10.1016/j.ijcard.2020.04.083
140. Kawashima H, Pompilio G, Andreini D, et al. Safety and feasibility evaluation of planning and execution of surgical revascularisation solely based on coronary CTA and FFRCT in patients with complex coronary artery disease: study protocol of the FASTTRACK CABG study. *BMJ Open*. 2020;10(12):e038152. doi:10.1136/bmjopen-2020-038152

141. Nykonenko A, Feuchtner G, Nykonenko O, et al. Feasibility of coronary CT angiography for guidance of CABG. *J Cardiovasc Comput Tomogr*. September 2020. doi:10.1016/j.jcct.2020.09.005
142. Maron DJ, Hochman JS, Reynolds HR, et al. Initial Invasive or Conservative Strategy for Stable Coronary Disease. *N Engl J Med*. March 2020. doi:10.1056/NEJMoa1915922

List of publications

Pre-procedural Planning of Coronary Revascularization by Cardiac-CT: An Expert Consensus Document of the Society of Cardiovascular Computed Tomography
Andreini D, Collet C, Leipsic J, Nieman K, Bittencurt M, De Mey J, Buls N, Onuma Y, Mushtaq S, Conte E, Bartorelli A, Stefanini G, ***Sonck J****, Knaapen P, Ghoshhajra B, Serruys PW.*
Under review JCCT and EuroIntervention

Clinical Validation of a Virtual Planner for Coronary Interventions Based on Coronary CT Angiography and Blood Flow Simulations
Sonck J*, Nagumo S, Norgaard BN, Otake H, Ko B, Zhang J, Mizukami T, Maeng M, Andreini D, Takahashi Y, Jensen JM, hdayhid A, Heggermont W, Barbato E, Mileva N, Munhoz D, Bartunek J, Updegrove A, Collinsworth A, Penicka M, Van Hoe L, Leipsic J, Koo BK, De Bruyne B, Collet C.*
Under review JACC Imaging

Fractional Flow Reserve After Percutaneous Coronary Intervention: A Pooled, Individual-Patient Analysis and Expert Recommendations
Collet C, Johnson N, Mizukami T, Fearon WF, Berry C, ***Sonck J****, Collison D, Koo BK, Meneveau N, Agarwal SK, Uretsky B, Hakeem A, Doh JH, de Sousa B, Oldroyd K, Leipsic J, Morbiducci U, Taylor C, Ko B, Tonino P, Perera D, Shinke S, Chiastra C, Sposito A, Maria Leone A, Muller O, Fournier S, Matsuo2 H, Adjedj J, Amabile N, Piroth Z, Alfonso F, Rivero F, Ahn JM, Toth G, Ihdayhid A, Rogers C, West W, Amano T, Mileva N, Nagumo S, Wyffels E, Munhoz D, Gallinoro E, Barbato E, Engstrøm T, Escaned J, Ali ZA, Kern MJ, Pijls N, Jüni P and De Bruyne B.*
Under review European Heart Journal

Development, Validation, and Reproducibility of the Pullback Pressure Gradient (PPG) derived from Manual Fractional Flow Reserve Pullbacks
Sonck J*, Mizukami T, Johnson NP, Nagumo S, Gallinoro E, Candreva A, Munhoz D, Shinke T, Svanerud J, Barbato E, De Bruyne B, Collet C.*
Accepted for publication Catheterization and Cardiovascular Interventions

Candreva A, Pagnoni M, Rizzini ML, Mizukami T, Gallinoro E, Mazzi V, Gallo D, Meier D, Shinke T, Aben JP, Nagumo S, Sonck J, Munhoz D, Fournier S, Barbato E, Heggermont W, Cook S, Chiastra C, Morbiducci U, De Bruyne B, Muller O, Collet C.
Risk of myocardial infarction based on endothelial shear stress analysis using coronary angiography.
Atherosclerosis. 2021 Nov 16:S0021-9150(21)01437-4. doi: 10.1016/j.atherosclerosis.2021.11.010. Epub ahead of print. PMID: 34815069.

Gallinoro E, Paolisso P, Candreva A, Bermpeis K, Fabbricatore D, Esposito G, Bertolone D, Fernandez Peregrina E, Munhoz D, Mileva N, Penicka M, Bartunek J, Vanderheyden M, Wyffels E, **Sonck J**, Collet C, De Bruyne B, Barbato E.
Microvascular Dysfunction in Patients With Type II Diabetes Mellitus: Invasive Assessment of Absolute Coronary Blood Flow and Microvascular Resistance Reserve.
Front Cardiovasc Med. 2021 Oct 19;8:765071. doi: 10.3389/fcvm.2021.765071. PMID: 34738020; PMCID: PMC8562107

Mileva N, Nagumo S, Gallinoro E, **Sonck J**, Verstreken S, Dierkcx R, Heggermont W, Bartunek J, Goethals M, Heyse A, Barbato E, De Bruyne B, Collet C, Vanderheyden M.
Validation of Coronary Angiography-Derived Vessel Fractional Flow Reserve in Heart Transplant Patients with Suspected Graft Vasculopathy.
Diagnostics (Basel). 2021 Sep 24;11(10):1750. doi: 10.3390/diagnostics11101750. PMID: 34679451; PMCID: PMC8534544.

De Bruyne B, Pijls NHJ, Gallinoro E, Candreva A, Fournier S, Keulards DCJ, **Sonck J**, Van't Veer M, Barbato E, Bartunek J, Vanderheyden M, Wyffels E, De Vos A, El Farissi M, Tonino PAL, Muller O, Collet C, Fearon WF.
Microvascular Resistance Reserve for Assessment of Coronary Microvascular Function: JACC Technology Corner.
J Am Coll Cardiol. 2021 Oct 12;78(15):1541-1549. doi: 10.1016/j.jacc.2021.08.017. PMID: 34620412.

Impact of Coronary Calcification Assessed by Coronary CT Angiography on Treatment Decision in Three Vessels CAD Patients: Insights from Syntax III trial
Andreini D, Takahashi K, Mushtaq S, Conte E, Modolo R, **Sonck J**, De Mey J, Ravagnani P, Schoors D, Maisano F, Kaufmann P, Lindeboom W, Morel MA, Doenst T, Teichgraber U, Pontone G, Pompilio G, Bartorelli AL, Onuma Y, Serruys PW
mpact of coronary calcification assessed by coronary CT angiography on treatment decision in patients with three-vessel CAD: insights from SYNTAX III trial.
Interact Cardiovasc Thorac Surg. 2021 Sep 20:ivab249. doi: 10.1093/icvts/ivab249. Epub ahead of print. PMID: 34542612.

Trans-lesional fractional flow reserve gradient as derived from coronary CT improves patient management: ADVANCE registry
Takagi H, Leipsic JA, McNamara N, Martin I, Fairbairn TA, Akasaka T, Nørgaard BL, Berman DS, Chinnaiyan K, Hurwitz-Koweek LM, Pontone G, Kawasaki T, Rønnow Sand NP, Jensen JM, Amano T, Poon M, Øvrehus KA, **Sonck J**, Rabbat MG, Mullen S, De Bruyne B, Rogers C, Matsuo H, Bax JJ, Douglas PS, Patel MR, Nieman K, Ihdayhid AR.
J Cardiovasc Comput Tomogr. 2021 Sep 2:S1934-5925(21)00418-4. doi: 10.1016/j.jcct.2021.08.003. Epub ahead of print. PMID: 34518113.

Hyperemic hemodynamic characteristics of serial coronary lesions assessed by pullback pressure gradients.
Candreva A, Mizukami T, **Sonck J**, Munhoz D, Nagumo S, Di Gioia G, Gallinoro E, Mileva N, Bartunek J, Wyffels E, Barbato E, De Bruyne B, Perera D, Collet C.
Catheter Cardiovasc Interv. 2021 Jul 15. doi: 10.1002/ccd.29868. Online ahead of print.PMID: 34264014

Simplified Assessment of the Index of Microvascular Resistance.
Kodeboina M, Nagumo S, Munhoz D, **Sonck J**, Mileva N, Gallinoro E, Candreva A, Mizukami T, Van Durme F, Heyse A, Wyffels E, Vanderheyden M, Barbato E, Bartunek J, De Bruyne B, Collet C.
J Interv Cardiol. 2021 Jun 2;2021:9971874. doi: 10.1155/2021/9971874. eCollection 2021.PMID: 34149324

Mismatch between morphological and functional assessment of the length of coronary artery disease.
Lodi Rizzini M, Nagumo S, Gallo D, **Sonck J**, Mizukami T, D'Ascenzo F, Buytaert D, Morbiducci U, De Bruyne B, Chiastra C, Collet C.
Int J Cardiol. 2021 Jul 1;334:1-9. doi: 10.1016/j.ijcard.2021.04.046. Epub 2021 Apr 30.PMID: 33933514

Basics of Coronary Thermodilution.
Candreva A, Gallinoro E, van 't Veer M, **Sonck J**, Collet C, Di Gioia G, Kodeboina M, Mizukami T, Nagumo S, Keulards D, Fournier S, Pijls NHJ, De Bruyne B.
JACC Cardiovasc Interv. 2021 Mar 22;14(6):595-605. doi: 10.1016/j.jcin.2020.12.037.PMID: 33736767

Rationale and design of the precise percutaneous coronary intervention plan (P3) study: Prospective evaluation of a virtual computed tomography-based percutaneous intervention planner.
Nagumo S, Collet C, Norgaard BL, Otake H, Ko B, Koo BK, Leipsic J, Andreini D, Heggermont W, Jensen JM, Takahashi Y, Ihdayhid A, Zhang Z, Barbato E, Maeng M, Mizukami T, Bartunek J, Updegrove A, Penicka M, Rogers C, Taylor C, De Bruyne B, **Sonck J**.
Clin Cardiol. 2021 Apr;44(4):446-454. doi: 10.1002/clc.23551. Epub 2021 Mar 3.PMID: 33656754

Invasive Coronary Physiology After Stent Implantation: Another Step Toward Precision Medicine.
Biscaglia S, Uretsky B, Barbato E, Collet C, Onuma Y, Jeremias A, Tebaldi M, Hakeem A, Kogame N, **Sonck J**, Escaned J, Serruys PW, Stone GW, Campo G.
JACC Cardiovasc Interv. 2021 Feb 8;14(3):237-246. doi: 10.1016/j.jcin.2020.10.055.PMID: 33541534

Thermodilution-Derived Volumetric Resting Coronary Blood Flow Measurement in Humans.
Gallinoro E, Candreva A, Colaiori I, Kodeboina M, Fournier S, Nelis O, Di Gioia G, **Sonck J**, van 't Veer M, Pijls NHJ, Collet C, De Bruyne B.
EuroIntervention. 2021 Feb 2:EIJ-D-20-01092. doi: 10.4244/EIJ-D-20-01092. Online ahead of print.PMID: 33528358

Duration of Hyperemia With Intracoronary Administration of Papaverine.
Mizukami T, **Sonck J**, Gallinoro E, Kodeboina M, Canvedra A, Nagumo S, Bartunek J, Wyffels E, Vanderheyden M, Shinke T, De Bruyne B, Collet C.
J Am Heart Assoc. 2021 Feb 2;10(3):e018562. doi: 10.1161/JAHA.120.018562. Epub 2021 Jan 17.PMID: 33459027

Implementing Coronary Computed Tomography Angiography in the Catheterization Laboratory.
Collet C, **Sonck J**, Leipsic J, Monizzi G, Buytaert D, Kitslaar P, Andreini D, De Bruyne B.
JACC Cardiovasc Imaging. 2020 Nov 19:S1936-878X(20)30911-6. doi: 10.1016/j.jcmg.2020.07.048. Online ahead of print.PMID: 33248968

Quantification of calcium burden by coronary CT angiography compared to optical coherence tomography.
Monizzi G, **Sonck J**, Nagumo S, Buytaert D, Van Hoe L, Grancini L, Bartorelli AL, Vanhoenacker P, Simons P, Bladt O, Wyffels E, De Bruyne B, Andreini D, Collet C.
Int J Cardiovasc Imaging. 2020 Dec;36(12):2393-2402. doi: 10.1007/s10554-020-01839-z. Epub 2020 Nov 17.PMID: 33205340

Coronary Artery Bypass Grafting or Fractional Flow Reserve-Guided Percutaneous Coronary Intervention in Diabetic Patients With Multivessel Disease.
Di Gioia G, Soto Flores N, Franco D, Colaiori I, **Sonck J**, Gigante C, Kodeboina M, Bartunek J, Vanderheyden M, Van Praet F, Casselman F, Degriek I, Stockman B, Barbato E, Collet C, De Bruyne B.
Circ Cardiovasc Interv. 2020 Oct;13(10):e009157. doi: 10.1161/CIRCINTERVENTIONS.120.009157. Epub 2020 Oct 12.PMID: 33040579

The clinical utility of FFR_{CT} stratified by age.
Anastasius M, Maggiore P, Huang A, Blanke P, Patel MR, Nørgaard BL, Fairbairn TA, Nieman K, Akasaka T, Berman DS, Raff GL, Hurwitz Koweek LM, Pontone G, Kawasaki T, Rønnow Sand NP, Jensen JM, Amano T, Poon M, Øvrehus KA, **Sonck J**, Rabbat MG, Mullen S, De Bruyne B, Rogers C, Matsuo H, Bax JJ, Leipsic J.
J Cardiovasc Comput Tomogr. 2021 Mar-Apr;15(2):121-128. doi: 10.1016/j.jcct.2020.08.006. Epub 2020 Sep 23.PMID: 33032976

Normal Values of Thermodilution-Derived Absolute Coronary Blood Flow and Microvascular Resistance in Humans.
Fournier S, Keulards DCJ, van 't Veer M, Colaiori I, Di Gioia G, Zimmermann FM, Mizukami T, Nagumo S, Kodeboina M, El Farissi M, Zelis JM, **Sonck J**, Collet C, Pijls NHJ, De Bruyne B.
EuroIntervention. 2020 Oct 6:EIJ-D-20-00684. doi: 10.4244/EIJ-D-20-00684. Online ahead of print.PMID: 33016881

Site vs. core laboratory variability in computed tomographic angiography-derived SYNTAX scores in the SYNTAX III trial.
Katagiri Y, Andreini D, Miyazaki Y, Takahashi K, Komiyama H, Mushtaq S, **Sonck J**, Schoors D, Maisano F, Kaufman PA, Leal I, Lindeboom W, Piek JJ, Wykrzykowska JJ, Morel MA, Bartorelli AL, Onuma Y, Serruys PW.
Eur Heart J Cardiovasc Imaging. 2020 Sep 5:jeaa172. doi: 10.1093/ehjci/jeaa172. Online ahead of print.PMID: 32888011

The evolution of the CTO-PCI landscape in Belgium and Luxembourg: a four-year appraisal.
Eertmans W, Kayaert P, Bennett J, Ungureanu C, Bataille Y, Saad G, Haine S, Coussement P, Pereira B, Agostoni P, Janssens L, Vandeloo B, Maréchal P, Cornelis K, de Hemptinne Q, Aminian A, Stammen F, Carlier S, Timmermans P, Vercauteren S, **Sonck J**, De Vroey F, Drieghe B, McCutcheon K, Scott B, Davin L, Gafari C, Dens J; BWGCTO Investigators.
Acta Cardiol. 2020 Aug 5:1-9. doi: 10.1080/00015385.2020.1801197. Online ahead of print.PMID: 32755286

Vessel Fractional Flow Reserve and Graft Vasculopathy in Heart Transplant Recipients.
Nagumo S, Gallinoro E, Candreva A, Mizukami T, Monizzi G, Kodeboina M, Verstreken S, Dierckx R, Heggermont W, Bartunek J, Goethals M, Buytaert D, De Bruyne B, **Sonck J**, Collet C, Vanderheyden M.
J Interv Cardiol. 2020 Jul 12;2020:9835151. doi: 10.1155/2020/9835151. eCollection 2020.PMID: 32733172

Clinical Outcomes Following Coronary Bifurcation PCI Techniques: A Systematic Review and Network Meta-Analysis Comprising 5,711 Patients.
Di Gioia G, **Sonck J**, Ferenc M, Chen SL, Colaiori I, Gallinoro E, Mizukami T, Kodeboina M, Nagumo S, Franco D, Bartunek J, Vanderheyden M, Wyffels E, De Bruyne B, Lassen JF, Bennett J, Vassilev D, Serruys PW, Stankovic G, Louvard Y, Barbato E, Collet C. JACC Cardiovasc Interv. 2020 Jun 22;13(12):1432-1444. doi: 10.1016/j.jcin.2020.03.054.PMID: 32553331

Temporal changes in FFRCT-Guided Management of Coronary Artery Disease - Lessons from the ADVANCE Registry.
Nous F, Budde RPJ, Fairbairn TA, Akasaka T, Nørgaard BL, Berman DS, Raff G, Hurwitz-Koweek LM, Pontone G, Kawasaki T, Sand NPR, Jensen JM, Amano T, Poon M, Øvrehus KA, **Sonck J**, Rabbat MG, Mullen S, De Bruyne B, Rogers C, Matsuo H, Bax JJ, Leipsic J, Patel MR, Nieman K.
J Cardiovasc Comput Tomogr. 2021 Jan-Feb;15(1):48-55. doi: 10.1016/j.jcct.2020.04.011. Epub 2020 May 1.PMID: 32418861

Graft patency and progression of coronary artery disease after CABG assessed by angiography-derived fractional flow reserve.
Gigante C, Mizukami T, **Sonck J**, Nagumo S, Tanzilli A, Bartunek J, Vanderheyden M, Wyffels E, Barbato E, Pompilio G, Mushtaq S, Bartorelli A, De Bruyne B, Andreini D, Collet C.
Int J Cardiol. 2020 Oct 1;316:19-25. doi: 10.1016/j.ijcard.2020.04.083. Epub 2020 Apr 30.PMID: 32360649

Motorized fractional flow reserve pullback: Accuracy and reproducibility.
Sonck J, Collet C, Mizukami T, Vandeloo B, Argacha JF, Barbato E, Andreini D, Bartorelli A, Cosyns B, De Bruyne B.
Catheter Cardiovasc Interv. 2020 Sep 1;96(3):E230-E237. doi: 10.1002/ccd.28733. Epub 2020 Jan 22.PMID: 31967389

Impact of Fractional Flow Reserve Derived From Coronary Computed Tomography Angiography on Heart Team Treatment Decision-Making in Patients With Multivessel Coronary Artery Disease: Insights From the SYNTAX III REVOLUTION Trial.
Andreini D, Modolo R, Katagiri Y, Mushtaq S, **Sonck J**, Collet C, De Martini S, Roberto M, Tanaka K, Miyazaki Y, Czapla J, Schoors D, Plass A, Maisano F, Kaufmann P, Orry X, Metzdorf PA, Folliguet T, Färber G, Diamantis I, Schönweiß M, Bonalumi G, Guglielmo M, Ferrari C, Olivares P, Cavallotti L, Leal I, Lindeboom W, Onuma Y, Serruys PW, Bartorelli AL; SYNTAX III REVOLUTION Investigators.
Circ Cardiovasc Interv. 2019 Dec;12(12):e007607. doi: 10.1161/CIRCINTERVENTIONS.118.007607. Epub 2019 Dec 13.PMID: 31833413

Evaluation of epicardial coronary resistance using computed tomography angiography: A Proof Concept.
Mizukami T, Tanaka K, **Sonck J**, Vandeloo B, Roosens B, Lochy S, Argacha JF, Schoors D, Suzuki H, Belsack D, Andreini D, Barbato E, De Mey J, De Bruyne B, Cosyns B, Collet C. J Cardiovasc Comput Tomogr. 2020 Mar-Apr;14(2):177-184. doi: 10.1016/j.jcct.2019.09.004. Epub 2019 Sep 24.PMID: 31812460

Measurement of Hyperemic Pullback Pressure Gradients to Characterize Patterns of Coronary Atherosclerosis.
Collet C, Sonck J, Vandeloo B, Mizukami T, Roosens B, Lochy S, Argacha JF, Schoors D, Colaiori I, Di Gioia G, Kodeboina M, Suzuki H, Van 't Veer M, Bartunek J, Barbato E, Cosyns B, De Bruyne B.
J Am Coll Cardiol. 2019 Oct 8;74(14):1772-1784. doi: 10.1016/j.jacc.2019.07.072.PMID: 31582137

FFR_{CT} and CT perfusion: A review on the evaluation of functional impact of coronary artery stenosis by cardiac CT.
Conte E, Sonck J, Mushtaq S, Collet C, Mizukami T, Barbato E, Tanzilli A, Nicoli F, De Bruyne B, Andreini D.
Int J Cardiol. 2020 Feb 1;300:289-296. doi: 10.1016/j.ijcard.2019.08.018. Epub 2019 Aug 9.PMID: 31466886

CT Perfusion Versus Coronary CT Angiography in Patients With Suspected In-Stent Restenosis or CAD Progression.
Andreini D, Mushtaq S, Pontone G, Conte E, Collet C, **Sonck J**, D'Errico A, Di Odoardo L, Guglielmo M, Baggiano A, Trabattoni D, Ravagnani P, Montorsi P, Teruzzi G, Olivares P, Fabbiocchi F, De Martini S, Calligaris G, Annoni A, Mancini ME, Formenti A, Magatelli M, Consiglio E, Muscogiuri G, Lombardi F, Fiorentini C, Bartorelli AL, Pepi M.
JACC Cardiovasc Imaging. 2020 Mar;13(3):732-742. doi: 10.1016/j.jcmg.2019.05.031. Epub 2019 Aug 14.PMID: 31422127

Impact of non-invasive anatomical testing on optimal medical prescription in patients with suspected coronary artery disease.
Devuyst S, Gigase A, Spapen J, Brouwers S, Couck T, **Sonck J**, Mizukami T, Gigante C, de Raedt H, Schelfaut D, Heggermont W, De Bruyne B, Penicka M, Van Camp G, Collet C.
Cardiovasc Diagn Ther. 2019 Jun;9(3):221-228. doi: 10.21037/cdt.2019.04.10.PMID: 31275812

Plaque quantification by coronary computed tomography angiography using intravascular ultrasound as a reference standard: a comparison between standard and last generation computed tomography scanners.
Conte E, Mushtaq S, Pontone G, Li Piani L, Ravagnani P, Galli S, Collet C, **Sonck J**, Di Odoardo L, Guglielmo M, Baggiano A, Trabattoni D, Annoni A, Mancini ME, Formenti A, Muscogiuri G, Magatelli M, Nicoli F, Poggi C, Fiorentini C, Bartorelli AL, Pepi M, Montorsi P, Andreini D.
Eur Heart J Cardiovasc Imaging. 2020 Feb 1;21(2):191-201. doi: 10.1093/ehjci/jez089.PMID: 31093656

1-Year Impact on Medical Practice and Clinical Outcomes of FFR_{CT}: The ADVANCE Registry.
Patel MR, Nørgaard BL, Fairbairn TA, Nieman K, Akasaka T, Berman DS, Raff GL, Hurwitz Koweek LM, Pontone G, Kawasaki T, Sand NPR, Jensen JM, Amano T, Poon M, Øvrehus KA, **Sonck J**, Rabbat MG, Mullen S, De Bruyne B, Rogers C, Matsuo H, Bax JJ, Leipsic J.
JACC Cardiovasc Imaging. 2020 Jan;13(1 Pt 1):97-105. doi: 10.1016/j.jcmg.2019.03.003. Epub 2019 Mar 17.

Feasibility of planning coronary artery bypass grafting based only on coronary computed tomography angiography and CT-derived fractional flow reserve: a pilot survey of the surgeons involved in the randomized SYNTAX III Revolution trial.
Sonck J, Miyazaki Y, Collet C, Onuma Y, Asano T, Takahashi K, Kogame N, Katagiri Y, Modolo R, Serruys PW, Bartorelli AL, Andreini D, Doenst T, Maureira JP, Plass A, La Meir M, Pompillio G.
Interact Cardiovasc Thorac Surg. 2019 Mar 18:ivz046. doi: 10.1093/icvts/ivz046. Online ahead of print.PMID: 30887024

Coronary computed tomography angiography for heart team decision-making in multivessel coronary artery disease.
Collet C, Onuma Y, Andreini D, **Sonck J**, Pompilio G, Mushtaq S, La Meir M, Miyazaki Y, de Mey J, Gaemperli O, Ouda A, Maureira JP, Mandry D, Camenzind E, Macron L, Doenst T, Teichgräber U, Sigusch H, Asano T, Katagiri Y, Morel MA, Lindeboom W, Pontone G, Lüscher TF, Bartorelli AL, Serruys PW.
Eur Heart J. 2018 Nov 1;39(41):3689-3698. doi: 10.1093/eurheartj/ehy581.PMID: 30312411

Real-world clinical utility and impact on clinical decision-making of coronary computed tomography angiography-derived fractional flow reserve: lessons from the ADVANCE Registry.
Fairbairn TA, Nieman K, Akasaka T, Nørgaard BL, Berman DS, Raff G, Hurwitz-Koweek LM, Pontone G, Kawasaki T, Sand NP, Jensen JM, Amano T, Poon M, Øvrehus K, **Sonck J**, Rabbat M, Mullen S, De Bruyne B, Rogers C, Matsuo H, Bax JJ, Leipsic J, Patel MR.
Eur Heart J. 2018 Nov 1;39(41):3701-3711. doi: 10.1093/eurheartj/ehy530.PMID: 30165613

Diagnostic performance of angiography-derived fractional flow reserve: a systematic review and Bayesian meta-analysis.
Collet C, Onuma Y, **Sonck J**, Asano T, Vandeloo B, Kornowski R, Tu S, Westra J, Holm NR, Xu B, de Winter RJ, Tijssen JG, Miyazaki Y, Katagiri Y, Tenekecioglu E, Modolo R, Chichareon P, Cosyns B, Schoors D, Roosens B, Lochy S, Argacha JF, van Rosendael A, Bax J, Reiber JHC, Escaned J, De Bruyne B, Wijns W, Serruys PW.
Eur Heart J. 2018 Sep 14;39(35):3314-3321. doi: 10.1093/eurheartj/ehy445.PMID: 30137305

The Tryton® dedicated bifurcation stent: Five-year clinical outcomes.
Green PG, Stella PR, Kumsārs I, Dens J, **Sonck J**, Bennett J, Bethencourt A, López BR, Dudek D, van Geuns RJ, Ramcharitar S.
Cardiovasc Revasc Med. 2019 Apr;20(4):316-323. doi: 10.1016/j.carrev.2018.06.023. Epub 2018 Jul 4.PMID: 30037716

Rationale and design of advantage (additional diagnostic value of CT perfusion over coronary CT angiography in stented patients with suspected in-stent restenosis or coronary artery disease progression) prospective study.

Andreini D, Mushtaq S, Pontone G, Conte E, **Sonck J**, Collet C, Guglielmo M, Baggiano A, Trabattoni D, Galli S, Montorsi P, Ferrari C, Fabbiocchi F, De Martini S, Annoni A, Mancini ME, Formenti A, Magatelli M, Resta M, Consiglio E, Muscogiuri G, Fiorentini C, Bartorelli AL, Pepi M.
J Cardiovasc Comput Tomogr. 2018 Sep-Oct;12(5):411-417. doi: 10.1016/j.jcct.2018.06.003. Epub 2018 Jun 18.PMID: 29933938

Fractional Flow Reserve Derived From Computed Tomographic Angiography in Patients With Multivessel CAD.
Collet C, Miyazaki Y, Ryan N, Asano T, Tenekecioglu E, **Sonck J**, Andreini D, Sabate M, Brugaletta S, Stables RH, Bartorelli A, de Winter RJ, Katagiri Y, Chichareon P, De Maria GL, Suwannasom P, Cavalcante R, Jonker H, Morel MA, Cosyns B, Kappetein AP, Taggart DT, Farooq V, Escaned J, Banning A, Onuma Y, Serruys PW.
J Am Coll Cardiol. 2018 Jun 19;71(24):2756-2769. doi: 10.1016/j.jacc.2018.02.053. Epub 2018 May 22.PMID: 29802016

Thoracoscopic off-pump closure of a large left circumflex coronary artery fistula: A novel minimally invasive approach.
Van Loo I, **Sonck J**, Tanaka K, La Meir M.
J Thorac Cardiovasc Surg. 2018 Oct;156(4):e159-e161. doi: 10.1016/j.jtcvs.2018.04.041. Epub 2018 Apr 17.PMID: 29759732

Impact of Coronary Remodeling on Fractional Flow Reserve.
Collet C, Katagiri Y, Miyazaki Y, Asano T, **Sonck J**, van Geuns RJ, Andreini D, Bittencourt MS, Kitslaar P, Tenekeciouglu E, Tijssen JGP, Piek JJ, de Winter RJ, Cosyns B, Rogers C, Zarins CK, Taylor C, Onuma Y, Serruys PW.
Circulation. 2018 Feb 13;137(7):747-749. doi: 10.1161/CIRCULATIONAHA.117.031478.PMID: 29440200

Assessing the landscape of percutaneous coronary chronic total occlusion treatment in Belgium and Luxembourg: the Belgian Working Group on Chronic Total Occlusions (BWGCTO) registry.
Maeremans J, Kayaert P, Bataille Y, Bennett J, Ungureanu C, Haine S, Vandendriessche T, **Sonck J**, Scott B, Coussement P, Dendooven D, Pereira B, Frambach P, Janssens L, Debruyne P, Van Mieghem C, Barbato E, Cornelis K, Stammen F, De Vroey F, Vercauteren S, Drieghe B, Aminian A, Debrauwere J, Carlier S, Coosemans M, Van Reet B, Vandergoten P, Dens JA; (On behalf of the BWGCTO Investigators).
Acta Cardiol. 2018 Oct;73(5):427-436. doi: 10.1080/00015385.2017.1408891. Epub 2017 Nov 28.PMID: 29183248

Non-invasive treatment planning of tandem coronary artery lesions using an interactive planner for PCI.
Sonck J, Miyazaki Y, Mandry D, Andreini D.
EuroIntervention. 2018 Oct 20;14(8):924-925. doi: 10.4244/EIJ-D-17-00815.PMID: 28994658

Platypnea-orthodeoxia syndrome: an unusual presentation of a complex disease.
Van Meerhaeghe T, Droogmans S, Hanon S, **Sonck J**.
Acta Clin Belg. 2018 Jun;73(3):224-228. doi: 10.1080/17843286.2017.1356635. Epub 2017 Aug 17.PMID: 28816631

Anomalous right coronary artery in a middle-aged patient: A case report and review of the literature.
Rosseel L, Bonnier H, **Sonck J**.
Medicine (Baltimore). 2016 Dec;95(49):e5508. doi: 10.1097/MD.0000000000005508.PMID: 27930539

Air pollution and ST-elevation myocardial infarction: A case-crossover study of the Belgian STEMI registry 2009-2013.
Argacha JF, Collart P, Wauters A, Kayaert P, Lochy S, Schoors D, **Sonck J**, de Vos T, Forton M, Brasseur O, Beauloye C, Gevaert S, Evrard P, Coppieters Y, Sinnaeve P, Claeys MJ.
Int J Cardiol. 2016 Nov 15;223:300-305. doi: 10.1016/j.ijcard.2016.07.191. Epub 2016 Jul 30.PMID: 27541680

How to measure quality of care in patients presenting with STEMI? A single-centre experience.
Wilgenhof A, Droogmans S, **Sonck J**, Lochy S, Kayaert P, Schoors D.
Acta Cardiol. 2015 Feb;70(1):1-11. doi: 10.1080/ac.70.1.3064588.PMID: 26137798

A new method for real-time co-registration of 3D coronary angiography and intravascular ultrasound or optical coherence tomography.
Carlier S, Didday R, Slots T, Kayaert P, **Sonck J**, El-Mourad M, Preumont N, Schoors D, Van Camp G.
Cardiovasc Revasc Med. 2014 Jun;15(4):226-32. doi: 10.1016/j.carrev.2014.03.008. Epub 2014 Mar 19.PMID: 24746102

Multi-modality imaging in an exceptional case of aborted sudden cardiac death.
Sonck J, Tanaka K, Czapla J, Vanderhasselt T, Kayaert P, Scott B, Sutherland G, Van Camp G.
Int J Cardiol. 2014 Feb 1;171(2):e57-8. doi: 10.1016/j.ijcard.2013.11.109. Epub 2013 Dec 10.PMID: 24365616

Acute procedural and six-month clinical outcome in patients treated with a dedicated bifurcation stent for left main stem disease: the TRYTON LM multicentre registry.
Magro M, Girasis C, Bartorelli AL, Tarantini G, Russo F, Trabattoni D, D'Amico G, Galli M, Gómez Juame A, de Sousa Almeida M, Simsek C, Foley D, **Sonck J**, Lesiak M, Kayaert P, Serruys PW, van Geuns RJ.
EuroIntervention. 2013 Mar;8(11):1259-69. doi: 10.4244/EIJV8I11A194.PMID: 23538155

Loss and retrieval of a coronary angioplasty stent balloon.
Kayaert P, **Sonck J**, Semeraro O, Lochy S, Bonnier H, Schoors D.
Cardiovasc Revasc Med. 2013 Jul-Aug;14(4):248-50. doi: 10.1016/j.carrev.2013.01.003. Epub 2013 Feb 19.PMID: 23433829

Clinical relevance of laparoscopically diagnosed hiatal hernia.
Van Nieuwenhove Y, **Sonck J**, De Waele B, Potvlieghe P, Delvaux G, Haentjens P.
Surg Endosc. 2009 May;23(5):1093-8. doi: 10.1007/s00464-008-9970-4. Epub 2008 May 20.PMID: 18491190

The neurotoxicity and safety of treatment with cefepime in patients with renal failure.
Sonck J, Laureys G, Verbeelen D.
Nephrol Dial Transplant. 2008 Mar;23(3):966-70. doi: 10.1093/ndt/gfm713. Epub 2008 Jan 5.PMID: 18175786

Book chapters

Coronary CT Angiography in the Emergency Department
Jeroen Sonck, Takuya Mizukami and Carlos Collet Bortone
Edizione Minerva Medica, 2019 ISBN 8877119675, 9788877119674

Fractional flow reserve derived from computed tomography angiography in clinical practice
Carlos Collet, Takuya Mizukami and **Jeroen Sonck**.
Edizione Minerva Medica, 2019 ISBN 8877119675, 9788877119674

Abstracts presented on congresses

Clinical Use of FFR_{CT} in the Evaluation of Symptomatic Patients with Intermediate Coronary Artery Stenosis - Can it improve diagnosis and reduce radiation risk and cost?
Sonck J
EuroPCR 2017

CT-FFR Made Easy
Sonck J
EuroEcho 2017

HeartFlow Planner - A Game Changer in Coronary Interventions
Sonck J
TCT 2017

Validation of an interactive planner to predict post-PCI FFR and aid in treatment planning
Sonck J, Miyazaki Y, Mandry D, Andreini D, Collet C
EuroPCR 2018

Graft Patency and Progression of Coronary Artery Disease after CABG Assessed by Angiography-Derived Fractional Flow Reserve.
Sonck J, Gigante C, Mizukami T, Nagumo S, Andreini D, Bartorelli A, De Bruyne B, Collet C
Belgian Society of Cardiology 2019

Motorised FFR pullback: Accuracy and reproducibility
Sonck J, Mizukami T, Vandeloo B, Barbato E, Andreini D, Colaiori I, Di Gioia G, Kodeboina M, De Bruyne B, Collet C
EuroPCR 2019

Evaluation of Epicardial Coronary Resistance Using Computed Tomography Angiography
Sonck J, Mizukami T, Tanaka K, Vandeloo B, Lochy S, Argacha JF,
De Mey J, De Bruyne B, Cosyns B, Collet C
EuroPCR 2019

Impact of Physiological Evaluation on the Identification of the Pattern of Coronary Artery Disease
Sonck J, Mizukami T, Vandeloo B, Di Gioia G, Lochy S, Colaiori I, Argacha JF, Kodeboina M, de Bruyne B, Collet C
EuroPCR 2019

Impact of the PPG index on PCI Results
Sonck J, Mizukami T, Nagumo S, Vandeloo B, Argacha JF, Cosyns B, Suzuki H, Shinke T, De Bruyne B, Collet C
Late Breaking Trials, EuroPCR 2020

Clinical validation of a virtual planner of coronary interventions based on coronary CT angiography and blood flow simulations
Sonck J, Nagumo S, Norgaard B, Ko B, Otake H, Koo BK, Mizukami T, Leipsic J, Andreini D, Barbato E, Van Hoe L, Penicka M, De Bruyne B, Collet C
Late Breaking Trials, EuroPCR 2021

Accuracy of the FFRCT Planner in Coronary Calcific Lesions: A Sub-study of the Precise PCI Plan (P3) Study
Accepted TCT 2021

Curriculum Vitae

Jeroen Sonck
Cardiologist

PERSONALIA

Jeroen Sonck, M.D.
Cardiovascular Center
O.L.V. Ziekenhuis - Campus Aalst
Mooreselbaan 164
9300 Aalst
Belgium

CURRENT POSITION

July 2018 -	Interventional Cardiologist and Co-director Cardiovascular Center Aalst, Cardiovascular Center, OLV Hospital, Aalst, Belgium

PROFESSIONAL EXPERIENCE

Sept 2010 - July 2018	Interventional Cardiologist UZ Brussel, Brussels, Belgium
Sept 2011- Feb 2013	Clinical fellowship Catharina Ziekenhuis, Eindhoven, The Netherlands.
Mar 2014 - June 2018	Part-time cardiologist at Heysel Heart Center, Strombeek-Bever, Belgium.

EDUCATION

1997 - 2004	Medicine, Vrije Universiteit Brussel (VUB) - Summa cum laude
2004	Inter-university radio-active radioprotection course
2004	Inter-university ECG course
2005	Acute Medicine: The Belgian Society of Disaster and Emergency Medicine

POST-UNIVERSITY CARDIOLOGY TRAINING

2004-2005	Heilig Hart Ziekenhuis, Lier – Departments of cardiology-CCU, pneumology, gastro-enterology and nephrology
2005-2006	AZ-VUB Jette, Vrije Universiteit Brussel, Brussels – Departments of nephrology, endocrinology, emergency medicine and MUG-SMUR
2006-2007	AZ Middelheim, Antwerp – Departments of gastro-enterology, pneumology, cardiology and intensive care
2007-2008	Onze-Lieve-Vrouw Ziekenhuis Aalst, Aalst – Cardiology department: clinical cardiology – heart failure, emergency-CCU
2008-2009	UZ Brussel, Brussels – Cardiology department: clinical cardiology, echocardiography and cathlab
2009-2010	ZNA Middelheim, Antwerp – Cardiology department: poly-clinical activities (including Heart Rhythm Management), echocardiography and cathlab

CLINICAL TRIALS GCP AND CRA TRAINING

GCP October 2019
JUNIOR CRA September 2020

CLINICAL TRIALS AS PRINCIPAL INVESTIGATOR

Co-investigator Tryton LM study 2012

Local PI Rewinder study 2015

Co-investigator Pfizer Spire trial 2015

Co-investigator Re-DUAL PCI trial 2015

Local PI Advance Trial 2016

Local PI SYNTAX III Revolution trial 2016

PI Acute FFR CT trial 2016

PI FFR CT ACS Trial 2016

Local PI BWGCTO study 2016

PI Precise PCI Plan Study P3 2018

Local PI Refine Registry

PI Corphys Registry 2018

Local PI Advance Extended Trial 2018

Local PI BLIMP study 2019

Local PI DISRUPT CAD II study 2018

PI iPull and MOMA registry 2019

PUBLICATIONS PEER REVIEWED ARTICLES

www.pubmed.com

MEMBERSHIP SCIENTIFIC ORGANISATIONS

Member of the Belgian Society of Cardiology (BSC)
Member of the Belgian Working group on Interventional Cardiology (BWGIC)
Member of the European Society of Cardiology (ESC)
Member of the European Association of PCI (EAPCI)
National Representative for the EURO4C initiative
2020-2022 EAPCI Training & Certification Committee Member

Acknowledgements

I sincerely wish to thank my colleague and friend Carlos Collet for this journey throughout science and innovation. Having met twice, during a coffee break in Brussels we understood that we shared the same vision on interventional cardiology and a close collaboration announced. This has triggered a mutual quest for a refinement of current available technologies aiming at an improvement of patient outcomes. The friendship that developed will endure all future challenges. Our journey would never have become as succesful without the inspiration, ideation, scientific guidance and critical appraisals of Prof. Emanuele Barbato, esteemed promotor of this thesis, and Prof. Bernard De Bruyne. The support of a promoter throughout a thesis cannot be described in brief. The mentorship of Emanuele and Bernard, both scientifically and on a personal level, has allowed me to complete this thesis and has transformed me from a clinical cardiologist into a clinical researcher. Also, the support of my colleagues and friends of the Cardiovascular Center Aalst proved critically important to shape this thesis and chase all innovative ideas transforming the field of interventional cardiology. A specific warm thank you for Jozef Bartunek, willing to streamline our wildest scientific expeditions into feasible projects, aligning colleagues, shaping structures and facilitating our research activities. The support of all colleagues and friends, Eric, Dan, Guy, Jan, Tom and many others of the Cardiovascular Center was instrumental. Also, a special thanks to the cathlab team. Without the support of our excellent nursing team driven by Els, engineer Dimitri, the study nurses team and technicians, none of the projects of this thesis would have become viable.

A dedicated alinea is devoted to our fellows team. The clinical fellows endured many procedures of long and challenging protocols till late evenings. I sincerely tried to teach them all the tricks of the trade but might also have jogged on their nerves while investigating another concept. Sorry for this! A warm thank you and deepest respect to Giuseppe, Iginio, Monika, Carlo and Giovanni, Estefania, Alessandro and Emanuele. Konstantinos, Giuseppe, Dario and all recent and future fellows will hopefully enjoy as much our future scientific efforts and my “cath coaching”. The scientific fellows, filling out eCRF’s, making (again) new slides or graphs and keeping up with all prompts, facilitated all scientific endeavours. Four of them deserve a specific and wholehearted thank you. Grateful forever for the so much appreciated and extensive help in the work on the PPG by our stats and programming wizard Sensei Takuya Mizukami. His help was unequalled. Sakura, at first Japanese shy, but ending

as the “ceremony master” of the weekly P3 investigators meetings. The P3 trial was not executed without her continuous efforts and support. Thank you! Niya Mileva: Your detailed work in our CT ventures was unrivalled. Daniel Munhoz, “the PPG man”, readily available, humbly and benevolently supporting our lab activities and scientific meetings. Thank you all!

In would also like to thank Prof. Daniele Andreini and Prof. Jonathon Leipsic. I really enjoyed every single TC. Hearing weekly your never-ending enthousiasm and endorsements helped me trough the difficult moments. Prof. Charles Taylor supported our efforts with the HeartFlow Planner following a beer and discussion in Helsingborg in January 2017. Without this meeting and his help my carreer would have looked differently. I would also like to express my deepest appreciation for Prof. John Stevens, Ir. Adam Updegrove, Mrs Sarah Mullen and Mrs Amy Collinsworth of the HeartFlow team. Prof. Patrick Serruys and Prof. Yoshinobu Onuma were crucial during my first steps in science with our collaborations in SYNTAX III. Thank you all.

At least as important: My family. My parents for believing in me when I had the “strange idea” to study medicine without any scientific training before. Mama, papa en ook onze oma: bedankt voor alles. De mooie jeugd, de kansen, de steun, de hulp tijdens de moeilijke momenten, de opvoeding van mezelf maar ook alle hulp voor jullie twee oogappels. De eeuwige steun ook al heb ik ongetwijfeld ook foute beslissingen genomen of gemaakt.

Not to be forgotten at all: My children, Helena en Matthias. Lieve kindjes, waar elke papa enkel van kan dromen. Ik moet misschien starten met excuses. Deze thesis is één van de redenen waarom papa soms afwezig was. Of fysiek aanwezig maar opnieuw eens in gedachten verzonken. Een thesis is een lange weg. De combinatie met werken is een grote uitdaging die ook een inspanning van jullie vergde. Jullie lach en kritische opmerkingen waren elke dag opnieuw een stimulans om te groeien als mens, papa, vriend en ook arts. Ondertussen zag papa 2 fantastische, mooie en lieve mensen opgroeien tot jong volwassenen. Ik ben de meest gelukkige papa ter wereld en hoop dat we samen nog vele prachtige momenten mogen delen!

Not to be underestimated: Helen, William, Robin and Olivia. “The 50% of the blend”. A coffee, once more, brought me to you in neighbouring Merchtem. It was an encounter that changed my life and carreer. We became a perfectly blended family travelling the world,

enjoying gastronomy and raising 5 great children. And your continuous “pita behaviour”, critically appraising every step in my life, pushed me forward. You challenged all steps and turned me into an entrepreneur both in family and in professional life. All wrapped with love and support, unceisingly encouraging, caring, reassuring, understanding and nurturing. Thank you for being who you are and hoping to share all future together!

Without any doubt I will have overlooked somebody. Indeed, many more people deserve respect for their valuable contribution making this thesis possible. Dank u!

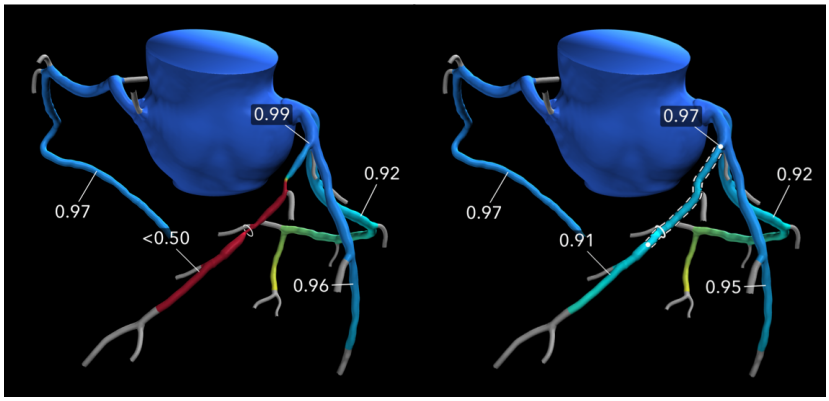
0.99
0.92
0.97
<0.50
0.96
0.97
0.92
0.97
0.91
0.95